

*Dissertation zur Erlangung des Doktorgrades der
Fakultät für Chemie und Pharmazie der
Ludwig-Maximilians-Universität München*



CYCLODEXTRINS AS EXCIPIENTS IN DRYING OF PROTEINS AND CONTROLLED ICE NUCLEATION IN FREEZE-DRYING

Raimund Michael Geidobler

Aus Rosenheim, Deutschland

2014

Erklärung

Diese Dissertation wurde im Sinne von § 7 der Promotionsordnung vom 28. November 2011 von Herrn Prof. Dr. Gerhard Winter betreut.

Eidesstattliche Versicherung

Diese Dissertation wurde eigenständig und ohne unerlaubte Hilfe erarbeitet.

München, den 03.03.2014

Raimund Michael Geidobler

Dissertation eingereicht am: 28.01.2014

1. Gutachter: Prof. Dr. G. Winter

2. Gutachter: Prof. Dr. W. Frieß

Mündliche Prüfung am: 27.02.2014

FOR MY PARENTS

ACKNOWLEDGEMENTS

Finally, after three and a half year, uncounted number of vials analyzed and buffers prepared, it is time to say thank you.

First and foremost, I want to thank Prof. Dr. Gerhard Winter for accepting me into his research group and for his continuous guidance and encouragement throughout the years in which this thesis was created. Thanks also for creating a constructive atmosphere, for challenging tasks and questions and for providing a perfect workspace and an overall good atmosphere. I am most grateful for his idea to look into controlled ice nucleation, which, in my opinion, became a quite successful story. Under his supervision, I did not only improve as a scientist but I could learn a lot for my personal development.

Special thanks go to Prof. Dr. Wolfgang Frieß, not only for being part of my thesis committee but also for his interest in my research work. Thanks also for sharing scientific expertise, especially the little tweaks for the spray drier. He is also responsible for the warm atmosphere in the research groups I was always happy to be part of.

With Yibin Deng, I shared a nice atmosphere in our lab during the time we spent together. You did not only always participate in football together with me, but you broadened my mind by sharing the Chinese culture with me. I also like the time when we were skiing and you really impressed me with your fast advance in skiing and for completing a thesis without consuming coffee.

Furthermore, I want to say thanks to all the nice people in both research groups, for also creating a nice atmosphere and for always finding a solution when problems occurred. It is difficult to mention someone in particular, but I am most grateful for all the (scientific) discussions with Thomas Bosch, Angelika Freitag, Sebastian Hertel, Markus Hofer, Elsa Etzl and Gerhard Sax, you gave me the feeling of being a part of the team from the first day on.

Special thanks go to my students, who supported this work with a Bachelor's thesis or internships, namely Sabrina Nesslinger, Stefanie Mannschedel, Elena Ilyukhina, Verena Seitz, Katharina Geh, Lucia Auchtör, Michaela Breitsamer and Martin Schubert. You all did a very good job, I really liked to work with you.

Sarah Coultas from Kratos analytical, Christian Minke and Mona Calik from the LMU are kindly acknowledged for helping me with measurements of certain samples.

When caring for science all the time, someone needs some balance off work. Here I want to say thanks to Cihad Anamur, who had to listen to all the roadbike-stuff I told him until finally, he bought his own bike. Since then, we have shared a lot of kilometres together. I am looking forward to even more!

Acknowledgements

To all my friends from the studies of pharmacy also goes a warm thank you. Without you and the fun we had together, the time with exams and practical work would have been a lot less endurable. Thank you for becoming and still staying friends, Christian Behrens, Michael Hornburger, Anja Müller, Geoffrey Grünwald, Orhan Causevic, Peter Schweiberger, Florian Schmid, Maren Ketterle, Veronika Schmitt, Martin Bubik, Benjamin Schwenk and Christiane Pauli.

I really appreciate the support from my friends from school, thank you Christoph Traunsteiner, Franz Angerer, Martin Höchstetter, Florian Wimmer and Mark Read.

Of course I want to deeply thank my parents Maria and Raimund for supporting me through all the years until the first job. Without you, I even couldn't have started this work. Hence, this thesis is devoted to you. Of course I want to thank my sister Carolin and my brother Maximilian.

Finally, I want to say thanks to Verena for her support during the last phase of the thesis, for her love and patience and for having become such an important person in my life in the last year.

TABLE OF CONTENTS

I.	Objectives of the thesis	11
II.	Cyclodextrins in freeze-drying and spray-drying of proteins.....	13
II.1	Introduction.....	13
II.1.1	General mechanisms of stabilization by excipients during freezing, drying and in the dried state	13
II.1.2	Possible mechanisms of stabilization provided by cyclodextrins	14
II.1.3	Tabular overview of cyclodextrins used as excipients for drying of proteins	15
II.1.4	Protein stabilization by cyclodextrins at low CD-concentrations – non-ionic surfactant-like behaviour	18
II.1.5	Protein stabilization by cyclodextrins used at high concentrations – water replacement and vitrification.....	20
II.1.6	Protein stabilization by cyclodextrins during storage of lyophilizates.....	21
II.1.7	Conclusions	22
II.1.8	Rational use Of cyclodextrins in parenteral protein formulations	22
II.1.9	Aim of the study	24
II.2	Material and methods.....	25
II.2.1	Materials	25
II.2.2	Preparation of formulations	25
II.2.3	Lyophilization processes	25
II.2.4	Sample preparation for freeze-thaw studies.....	26
II.2.5	Spray-drying process.....	26
II.2.6	Preparation of atomization-control samples	27
II.2.7	Reconstitution of dried products	27
II.2.8	Turbidity	27
II.2.9	Light obscuration	27
II.2.10	Size exclusion chromatography (SE-HPLC)	28
II.2.11	Asymmetrical flow-field-flow separation (AF4)	28
II.2.12	Fourier-transform infrared spectroscopy (FTIR).....	29
II.2.13	Residual moisture content (headspace method).....	29
II.2.14	Residual moisture content (direct injection method)	29
II.2.15	Dynamic scanning calorimetry (T_g').....	29
II.2.16	Dynamic scanning calorimetry (T_g).....	30
II.2.17	Specific surface area	30
II.2.18	X-ray powder diffraction.....	30
II.2.19	Electron spectroscopy for chemical analysis (ESCA)	31
II.3	Results.....	32
II.3.1	Cyclodextrins as replacement for polysorbates - Formulation development for the model protein MabR1	32
II.3.2	Further screening of formulations for the model protein MabR1	41
II.3.3	Collapse freeze-drying of MabR1	50
II.3.4	Controlled nucleation freeze-drying of MabR1	58
II.3.5	Storage stability of MabR1 formulated with 1 % sucrose	63
II.3.6	Controlled nucleation freeze-drying of MabR1 formulated with 5 % sucrose	72
II.3.7	Collapse freeze-drying of 5 % sucrose.....	78

II.3.8	Storage stability of collapse freeze-dried MabR1 formulated with 5 % sucrose	82
II.3.9	The situation at the interface - results from ESCA-studies	90
II.3.10	Storage stability of h-GH	93
II.3.11	Storage stability of GCSF	102
II.3.12	HP β CD employed in spray drying of MabR1.....	110
II.3.13	HP β CD as bulking agent in freeze-drying	120
II.3.14	Subvisible particle formation by placebo HP β CD.....	133
II.3.15	Final discussion	149
II.3.16	Summary	153
II.4	References	154
III.	Controlled ice nucleation in pharmaceutical freeze-drying	159
III.1	Introduction.....	159
III.2	Controlled ice nucleation in the field of freeze-drying: fundamentals and technology review 160	
III.2.1	Introduction	160
III.2.2	Fundamentals of ice nucleation and impact on the freeze-drying process	160
III.2.3	Methods to induce and control ice nucleation	167
III.2.4	Summary and outlook.....	176
III.2.5	References	177
III.3	A new approach to achieve controlled ice nucleation of super-cooled solutions during the freezing step in freeze-drying	181
III.3.1	Introduction	181
III.3.2	Materials and methods	182
III.3.3	Results.....	183
III.3.4	Discussion	186
III.3.5	Outlook	187
III.3.6	References	187
III.4	Transferability to a pilot-scale freeze-dryer	188
III.4.1	Introduction	188
III.4.2	Materials and methods	188
III.4.3	Results.....	189
III.4.4	Discussion and outlook.....	193
III.5	Freeze-thaw studies of a monoclonal antibody	194
III.5.1	Introduction	194
III.5.2	Materials and methods	194
III.5.3	Results.....	196
III.5.4	Discussion	197
III.5.5	References	198
III.6	Influence of the freezing step on the properties of two placebo model formulations 199	
III.6.1	Introduction	199
III.6.2	Materials and methods	199
III.6.3	Results.....	202
III.6.4	Discussion	208
III.6.5	Conclusion	208
III.6.6	References	208

III.7	Can controlled ice nucleation improve freeze-drying of highly-concentrated protein formulations?.....	208
III.7.1	Introduction	209
III.7.2	Materials and methods	209
III.7.3	Results	212
III.7.4	Discussion and outlook.....	215
III.7.5	References	216
III.8	The Mpemba effect is not applicable to vial freeze-drying	217
III.8.1	Introduction	217
III.8.2	Materials and methods	218
III.8.3	Results	219
III.8.4	Discussion	221
III.8.5	References	223
III.9	Summary of chapter III.....	224
IV.	Final summary	225
V.	Appendix	230
V.1	Publications	230
V.2	Poster presentations	230
V.3	Oral presentations	231
V.4	Curriculum Vitae	232

I. OBJECTIVES OF THE THESIS

The objective of this thesis is to evaluate the potential use of cyclodextrins as replacement for polysorbates in the field of freeze-drying for pharmaceutical relevant proteins. Stable freeze-dried formulations of therapeutic proteins shall be developed and the mechanism by which cyclodextrins stabilize proteins will be elucidated. The focus of this study clearly lies on the hydroxypropylated derivative HP β CD, because of its toxicological safety and interfacial activity. Furthermore, the use of cyclodextrins in spray-drying will be investigated. State-of-the-art analytics will be performed to investigate protein stability immediately after the drying process and after storage stability studies.

Furthermore, a second focus of this thesis is to evaluate the impact of controlled nucleation in pharmaceutical freeze-drying. Although knowledge of the impact of ice nucleation temperature on the freeze-drying process is available, controlled nucleation has been hyped recently with the development of commercially available methods. In this thesis, we developed and applied an own, new method to study ice nucleation effects on pharmaceutically relevant formulations as well as on highly-concentrated protein formulations.

II. CYCLODEXTRINS IN FREEZE-DRYING AND SPRAY-DRYING OF PROTEINS

II.1 INTRODUCTION¹

II.1.1 GENERAL MECHANISMS OF STABILIZATION BY EXCIPIENTS DURING FREEZING, DRYING AND IN THE DRIED STATE

Excellent reviews have been published summarizing the stabilization of proteins during drying and in the dried state [1-4]. Commonly used excipients which can counteract the aforementioned stresses and their mechanisms of stabilization are presented briefly in the following section.

To prevent unfolding of proteins at high and low temperature stresses, disaccharides like sucrose or trehalose or polyols like sorbitol or mannitol are commonly employed, acting via the preferential hydration / exclusion mechanism [5]. In the field of freeze-drying, those excipients are employed to stabilize the protein drug during the freezing step and are referred to as cryoprotectants. Polymers, like dextran, polyvinylpyrrolidone and polyethylenglycol (PEG) are commonly used as cryoprotectants as well [4].

Unfolding of proteins at interfaces can be prevented by surfactants. Surfactants, primarily the non-ionic polysorbate 20 and 80 are frequently added to the bulk solution to inhibit unfolding of proteins at interfaces, for example at the air-liquid interface present during spray-drying and at the ice-water interface, occurring during the freezing step in freeze-drying [6-8]. As mentioned in a preceding paragraph, surfactants are known to compete with proteins for the adsorption to interfaces and hence reduce unfolding and subsequent aggregation at the interface [9, 10].

To preserve the activity of proteins during dehydration, two commonly accepted hypotheses are discussed: the water replacement [11-14] and the vitrification [15-19] hypotheses. Excipients stabilizing the protein during the drying stage and in the dried state are referred to as lyoprotectants [1].

¹ The section II.1 is part of the publication Serno, T., R. Geidobler, and G. Winter, Protein stabilization by cyclodextrins in the liquid and dried state. *Advanced Drug Delivery Reviews*, 2011. 63(13): p. 1086-1106. The text present in the thesis is the same as in the publication and was written by R. Geidobler and corrected for publication by G. Winter.

During dehydration, the hydration shell surrounding the protein is lost, and the loss of hydrogen bonds can be compensated by excipients able to interact with the protein by hydrogen-bonding, thus serving as a water substitute. Disaccharides like sucrose and trehalose and polyols like sorbitol are commonly used lyoprotectants. By acting as a water substitute, the native protein structure is preserved and the protein is thermodynamically stabilized with an increase in free energy of the unfolded state [3, 20]. Usually, direct interaction of the stabilizer and the protein and defined minimum ratios of stabilizer to protein are needed [21, 22].

The vitrification (or glassy dynamics) hypotheses refers to a kinetic mechanism of stabilization in the dried state. A steady increase in viscosity of the amorphous phase, during the freezing and dehydration steps in freeze-drying or during the evaporation stage in spray-drying leads to the formation of an amorphous glass [23]. An adequate glass forming excipient needs to be present. Commonly used excipients are disaccharides and polymers like dextran and PEG [23]. In the rigid environment below the glass transition temperature, featuring a high viscosity, the protein is immobilized and hence kinetically stabilized. In contrast to the water replacement hypothesis, not a molar ratio of stabilizer to protein but a certain volume of stabilizer is required for dilution of the protein into the amorphous matrix [20].

II.1.2 POSSIBLE MECHANISMS OF STABILIZATION PROVIDED BY CYCLODEXTRINS

Due to their particular structural properties, cyclodextrins are valuable excipients for drying of protein pharmaceuticals. A CD-derivative frequently used as stabilizer in freeze-drying and spray-drying of formulations is the substituted derivative hydroxypropyl-beta-cyclodextrin (HP β CD), which in contrast to the parent α -, β - and γ -cyclodextrin shows interfacial activity at concentrations of 0.1 % (w/v). [24]. This amphiphilic quality of HP β CD may stabilize proteins during the cooling and freezing step and upon rehydration of lyophilizates as well as during the atomization step in spray drying, possibly inhibiting protein unfolding and aggregation at interfaces, as discussed above.

Due to their carbohydrate nature all CDs are in principle able to interact with proteins by hydrogen bonding fulfilling the needs for water replacement during dehydration. However, it is known that especially the parent cyclodextrins form an intramolecular hydrogen bond ring [25]. Therefore, parent cyclodextrins should be less able to provide intermolecular hydrogen bonds to proteins and this mechanism of stabilization must be expected to be operative mainly for the substituted derivatives, especially hydroxypropylated derivatives.

In literature, the nomenclature and the assignment to an assumed stabilizing mechanism of cyclodextrins is not consistent. CDs are referred to as surfactants [26, 27], polymers [28] or sugars [29, 30], indicating that the stabilization mechanism is not yet fully understood.

II.1.3 TABULAR OVERVIEW OF CYCLODEXTRINS USED AS EXCIPIENTS FOR DRYING OF PROTEINS

There are several reports on the use of cyclodextrins with different drying techniques. An overview of these studies is presented in Table 5 and Table 6. In the nineteen-nineties, several studies were performed using enzymes as model proteins assessing the stabilizing potential of CDs by determining their enzymatic activity after drying and reconstitution [26, 30-34]. Besides those model proteins, also reports on drying on therapeutic proteins, such as a mouse IgG antibody [35], IL-2 and tumor necrosis factor (TNF) [36] in the presence of CD derivatives were published. Cyclodextrins were investigated in a wide range of concentrations, ranging from 0.0001 % (w/v) up to 10 % (w/v) [30, 37]. From these numbers it can already be deduced that CDs presumably fulfilled very different roles in these formulations. The following chapter gives an overview on the available studies and elucidates the different molecular mechanisms by which CDs can provide stabilization during the drying of proteins as well as during storage of dried protein formulations.

Table II-1: Overview of studies using CD-derivatives as excipients in freeze-drying (FD) of protein formulations.

*: abbr. for (3-[(3-Cholamidopropyl)-dimethylammonio]-1-propanesulfonate)

Protein(s)	CDs	Further excipients used	Analytical methods used for characterization of protein stability	Key results	Proposed protein stabilizing mechanism by cyclodextrins	Reference
Invertase (0.064 mg/ml)	β -CD (10% w/v), β -CD-Alginate (10%), β -CD + Trehalose (1:1, 10%)	Alginate, Dextran, Trehalose	Invertase assay with sucrose	β -CD and β -CD-A inferior to trehalose during FD, β -CD + trehalose showed best results during storage over 25 h at 43% controlled humidity; inhibition of trehalose crystallization	complexation of hydrophobic residues for β -CD and β -CD-A	Santagapita et al [28]
CYP3A4 (0.4 μ M)	M β CD, HP β CD (different molar ratios (50:1 – 600:1 (~0.003 - ~0.034 % w/v))	2 Crown ethers, Sucrose, Trehalose, Mannitol	CYP3A4-Activity with testosterone	CDs inferior to sugars, slight effect at very low concentrations	water replacement	Chefson et al [29]
LDH (0.25 mg/ml)	HP β CD (0.005 %, 0.02 %, 0.1 %)	Sucrose, Trehalose, Glucose, Dextran, PEG, Ficoll, Polysorbate 80, Brij 35	LDH assay, PAGE	CDs inferior to sugars but better than no excipient and polysorbate 80	surface activity	Anchordoquy et al [27]
LDH (2 μ g/ml)	HP β CD, M β CD, α -CD, β -CD, γ -CD (0.005 mM – 100 mM)	PEG 3350, CHAPS*, Sucrose fatty acid monoester, Polidocanol, SDS, Glucose, Trehalose, Sodium glutamate	LDH assay	HP β CD and M β CD preserved enzymatic activity during FD at concentrations of 0.1 mM to 10 mM, no effect of parent CDs; HP β CD stabilization independent of phosphate-buffer concentration	surface activity, interaction with hydrophobic residues	Izutsu et al [33]

Protein(s)	CDs	Further excipients used	Analytical methods used for characterization of protein stability	Key results	Proposed protein stabilizing mechanism by cyclodextrins	Reference
LDH (12.8 µg/ml)	α-CD, HPαCD, β-CD, HPβCD, SBEβCD, MβCD, γ-CD, HPγCD (1% w/w) and 0.0001% to 1 % (w/w) for HPβCD	Glucose, Maltose, Trehalose, Sucrose, Raffinose (1% w/w)	LDH assay	HPαCD, HPβCD, MβCD, and HPγCD superior to trehalose; other derivatives provide stability similar to trehalose and sucrose; Increasing degree of substitution (DS) correlated with increase in relative activity	No clear statement: water replacement / amorphous glass forming / complexation	Iwai et al [37]
TNF (0.25 mg/ml)	HPβCD (0.5% w/v) + Mannitol 1.5 %	PEG 6000, Dextran, Sucrose, Trehalose	TNF assay (cell killing), SDS-Page	HPβCD + Mannitol resulted in less dimer formation than lyophilization without excipient; bioactivity was preserved	Amorphous glass forming	Hora et al [36]
Mouse IgG2a mAb (1.0 mg/ml)	HPβCD (5% w/v)	Sucrose, Dextran	SDS-Page, SE-HPLC, ELISA, IEF	HPβCD comparable to sucrose and dextran after lyophilization but superior during storage at 56 °C; HPβCD inhibited aggregate formation at 4 °C for 32 days.	Amorphous glass with high Tg, complexation	Ressing et al [35]
BSA (0.1%), Trypsin (0.1%)	α-CD (9.9% w/w)	Lactose, Sucrose, Mannitol, Dextrin, Tween 80, some others	Trypsin assay, SEM, DSC, ESCA (Electron spectroscopy for chemical analysis)	α-CD showed highest Trypsin activities and low Trypsin surface coverage but high BSA surface coverage after annealing; no correlation of surface coverage and activity	no clear statement; carbohydrate-like behaviour (water replacement, amorphous glass forming)	Millqvist-Fureby et al [30]
β-Galactosidase (0.1 mg/ml)	HPβCD, MβCD, α-CD, β-CD, γ-CD (0.01 mM – 10 mM)	Glucose, Trehalose, Proline, Polidocanol, SDS, CHAPS*, sucrose fatty acid monoester, PEG 400, 3350	β-Galactosidase assay with Galactopyranoside-derivative, SE-HPLC, SDS-Page,	HPβCD and MβCD showed stabilizing effects at concentrations above 0.1 mM, α-CD, β-CD and γ-CD not; HPβCD and DM-β-CD showed positive effect in reconstitution medium	surface activity	Izutsu et al [32]
IL-2 (0.8 mg/ml)	β-CD (5 mg / ml)	Mannitol, Sucrose, Trehalose, Raffinose, Stachyose	FTIR, Turbidity, activity assay, SE-HPLC, SDS-Page	Stabilization by β-CD	high Tg of dried product and water replacement	Prestrelski et al [38]
LDH (2 µg/ml)	HPβCD 0.01 mg/ml – 10 mg/ml (+ Mannitol 400 mM / Sucrose 200 mM)	CHAPS, PEG 400, 3000, 20000, Polidocanol, Triton X-100, Brij 58, sodium cholate, sucrose monolaurate	LDH Assay	HPβCD showed best stabilizing effect used alone and intermediate effects when used in combination with mannitol and sucrose	surface activity, formation of an amorphous glass	Izutsu et al [26]

Protein(s)	CDs	Further excipients used	Analytical methods used for characterization of protein stability	Key results	Proposed protein stabilizing mechanism by cyclodextrins	Reference
IL-2 (1 mg/ml)	HP β CD (0- 25 % w/v) and 0.2 % - 2 % in combination with sucrose (1% - 2 %, all w/w); β -CD (concentration not stated)	-	Visual inspection, Turbidity, Western blot, centrifugation, 4D UV, Bioactivity (HT-2 cell proliferation assay)	HP β CD reduced turbidity in concentrations of > 0.5 % in combination with sucrose (1 %) during storage, no turbidity was observed with HP β CD but with β -CD, both in combination with sucrose (1-2 %)	complexation	Brewster et al [39]
IL-2 (1 mg / ml)	HP β CD (0.5 %) in combination with sucrose (2 %)	Polysorbate 80, HSA, Arginine, Carnitine, Betaine	SE-HPLC, RP-HPLC, Western blot, Fluorimetric light scattering, bioactivity (HT-2 cell proliferation assay), ELISA	Fully bioactive IL-2, negligible dimer formation but significant amount of oxidized IL-2 detected during storage	unclear: hydrophobic / hydrophilic character of HP β CD	Hora [40]

Table II-2: Overview of studies using cyclodextrins as excipients for spray-drying (SD) or supercritical fluid drying (SCFD) of protein formulations.

Protein(s) used	CD(s) used	Other excipients used	Analytical methods used for characterization of protein stability	Outcome of test	Proposed protein stabilizing mechanism of cyclodextrins	References
β -Galactosidase (4% w/v)	HP β CD (1% w/v) alone and in combination with Sucrose 1%	Sucrose	μ DSC, SE-HPLC, SDS-Page, Galactosidase assay.	HP β CD superior to sucrose	inhibition of denaturation at liquid/air interface	Branchu et al [34]
Trypsin (0.02 %, 0.1 %, 0.5 % w/w)	α -CD (9.5 % - 9.98 % w/w)	Lactose, Sucrose, Mannitol, Dextrin, Tween 80	ESCA, DSC, Surface tension, Trypsin assay	α -CD showed good results in residual activity and was best excipient in FD	no clear statement; carbohydrate-like behaviour (water replacement, amorphous glass forming)	Millqvist-Fureby et al [31]
rhGH (2 mg/ml)	M β CD (10, 100, 1000:1 Molar ratio, 0.12 %, 1.2 % and 12 % w/v), 100:1 M β CD also in combination with Polysorbate 20 (0.01%), Zinc (2:1 molar ratio) and lactose (4 mg / ml)	Polysorbate 20, Lactose, Zinc	SE-HPLC	M β CD stabilizes in molar ratio of 1000:1 and 100:1 (SE-HPLC) and in combination with Zinc, Lactose and Polysorbate 20 at 100:1 molar ratio	surface activity	Jalalipour et al [41]
IgG monoclonal antibody (20 mg / ml)	HP β CD (80 mg / ml)	Trehalose (80 mg / ml)	FTIR, CD, Fluorescence, UV spectroscopy, SE-HPLC, SDS-PAGE	HP β CD as efficient as trehalose	no clear statement; use of HP β CD as a sugar	Jovanovic et al [42]

II.1.4 PROTEIN STABILIZATION BY CYCLODEXTRINS AT LOW CD-CONCENTRATIONS – NON-IONIC SURFACTANT-LIKE BEHAVIOUR

Evidence for surfactant-like effects of cyclodextrins was found for freeze-dried LDH at a concentration of 0.25 mg/ml in the presence of HP β CD at different concentrations (0.005 %, 0.02 % and 0.1 %) [27]. HP β CD showed a slightly positive effect on remaining enzyme activity after reconstitution of lyophilizates and in freeze-thawing experiments at concentrations of 0.1 %, and it was found to be superior to polysorbate 80. However, enzymatic activity was much better preserved by employing glucose, trehalose or sucrose. Slightly different results were observed in another study with freeze-dried LDH at much lower concentrations (2 μ g /ml protein) [33]. HP β CD and M β CD turned out to be effective in preserving enzymatic activity. The protective effect of HP β CD, as measured by LDH activity, was most pronounced at concentrations above 1 mM (approx. 0.14 % w/v). M β CD showed best stabilization at 0.2 mM (approx. 0.026 % w/v), while the parent cyclodextrins as well as sucrose and trehalose showed

almost no remaining LDH activity after lyophilization and reconstitution. A third study using LDH as model protein achieves similar results. A wide concentration range of HP β CD from 0.0001 % to 1 % (w/w) was investigated and could clearly show that HP β CD was able to preserve the enzymatic activity already at very low concentrations (0.01 %) with a maximum stabilization between 0.1 % and 1 % [37].

In addition to the concentration-dependent stabilization by HP β CD, the degree of substitution (DS) of the CD-derivatives was also found to have a significant influence on recovery of LDH activity. The higher the degree of substitution, the better was the recovery of activity of LDH. It is known that an increase in the degree of substitution of the CD correlates with a decrease in surface tension of water – therefore the surfactant-like effects of CDs must be expected to become more pronounced with increasing DS [24, 43].

HP β CD was also studied by Izutsu et al with the same model protein, LDH, in a concentration of 2 μ g/mL as single excipient and in combination with 200 mM sucrose and 400 mM mannitol [26]. At concentrations of around 0.01 % (w/v) and 0.1 % (w/v), HP β CD showed best results when used alone and comparable results were obtained in combination with sucrose whereas the combination with mannitol resulted in slightly lower activity at the same concentrations. The authors state that the amphiphilic character of HP β CD and its ability to remain amorphous is protecting LDH during freeze-drying, which is in agreement with results obtained on another enzyme, β -galactosidase [32]. Parent cyclodextrins formed an amorphous glass, but failed to stabilize β -galactosidase during freeze-drying whereas M β CD and HP β CD were effective at maintaining the enzymatic activity at concentrations of 0.014 % (w/v), indicating surfactant-like behavior of the CD-derivatives.

Further evidence for interfacial stabilization by CDs is given by a study on spray-dried β -galactosidase at a concentration of 40 mg / ml [34]. The enzyme was spray-dried along with 1 % (w/v) HP β CD, a mixture of 1 % (w/v) HP β CD and 1 % (w/v) sucrose and sucrose alone. HP β CD as single excipient yields almost 100 % remaining activity whereas sucrose alone even had a negative impact on the relative activity of the enzyme. The combination of HP β CD and sucrose was inferior to HP β CD alone. No alterations of the enzyme as compared to before drying were detected by DSC, SE-HPLC, SDS-PAGE and IEF patterns in all formulations. The authors speculate that the mechanism of protein degradation consisted of subtle changes in protein structure at the air-water interface and they concluded that HP β CD successfully protected β -galactosidase from surface denaturation. This was also observed for M β CD, which protected rh-GH during spray-drying at concentrations above 1.2 % (w/v) [41]. The addition of polysorbate 20, lactose and zinc further reduced aggregate levels, as determined by SE-HPLC. The authors conclude that surfactant-like behaviour of M β CD is protecting rh-GH from denaturation at the air-water interface.

However, there are also reports on amphiphilic cyclodextrin derivatives failing to stabilize proteins at low excipient concentrations. For instance, M β CD and HP β CD failed to stabilize the enzyme CYP3A4 [29]. Both derivatives showed no significant increase in activity recovery of CYP3A4 at very low protein concentrations and a 50:1 molar ratio excess of the CDs (approximately 0.003 % (w/v)). Disaccharides like sucrose or trehalose performed better than both cyclodextrin derivatives; however, they were used at much higher molar ratios up to 30000:1. This indicates that dehydration could have been the predominant stress for CYP3A4 and disaccharides are able to compensate for the loss of the hydration shell. The concentrations for the cyclodextrins employed in this study are probably too low to serve as sufficient lyoprotectants whereas their quality as surfactant-like excipients did not alter protein stability in this case.

II.1.5 PROTEIN STABILIZATION BY CYCLODEXTRINS USED AT HIGH CONCENTRATIONS – WATER REPLACEMENT AND VITRIFICATION

Besides their effect on stabilization at the air-water, ice-water and solid-void interface, cyclodextrins are also reported to stabilize by both water-replacement and vitrification. However, the clear attribution of the mechanism of stabilization to one particular effect might be difficult, since several modes of action often contribute to the protein stabilization observed. For the purpose of employing CDs as lyoprotectants, much higher weight ratios are needed compared to the use as surfactant like excipients; typical weight ratios of sugar to protein range from at least 1:1 to approx. 5:1 [2]. However, these ratios are greatly dependent on the type of protein. Concentrations of bulking agents prior to freeze-drying are typically in a range between 1 % and 10 % (w/v) [1]. Cyclodextrins usually yield amorphous glasses.

As discussed above, parent cyclodextrins, which are known to form intramolecular hydrogen bonds, hindering them to form hydrogen bonds with other molecules, are likely to exhibit little degree of water-replacement but should still be able to form amorphous glasses and stabilize according to the vitrification hypothesis. Proof for this can be found in a study on LDH, in which various cyclodextrins, including parent-CDs and derivatives (HP α CD, HP β CD, SBE β CD, M β CD, HP γ CD) as well as disaccharides were investigated, all in concentrations of 1 % (w/w) [37]. All hydroxypropylated derivatives as well as M β CD yielded higher relative activities than the parent cyclodextrins and SBE β CD. The relative activity of LDH freeze-dried with the parent cyclodextrins was on the same level as LDH freeze-dried with trehalose and sucrose. The authors found that a concentration of 1 % is too low for water replacement by disaccharides and that the increased activity observed for hydroxypropylated CD derivatives is due to their additional hydroxyl moieties, possibly contributing to hydrogen-bonding. There are numerous further reports of failure or at least of inferiority of parent cyclodextrins as compared to

hydroxypropylated derivatives with regard to protein stabilization, but in turn this could also be attributed to their lack of surface activity [28, 32, 33, 39].

In contrast, in cases in which the formation of amorphous glasses was shown to be sufficient to preserve protein stability, parent cyclodextrins can well fulfill this task, as demonstrated in a study on spray- and freeze-drying of trypsin and BSA [31]. Relative activity for spray-dried trypsin in the presence of amorphous α -CD was 95 % and 92 % for freeze-dried trypsin, respectively. The authors stated that the mechanism of stabilization is unclear, but glass forming excipients seemed to have a higher ability to preserve the enzyme's activity, compared to partly crystalline sucrose and mannitol.

II.1.6 PROTEIN STABILIZATION BY CYCLODEXTRINS DURING STORAGE OF LYOPHILIZATES

Besides the aforementioned protein-stabilizing mechanisms during freezing and drying, there are some additional factors influencing storage stability of lyophilizates. These are for example high glass transition temperatures (T_g) of the lyophilized cake [44, 45] and an optimal residual water content (usually < 1 % w/w) [46]. Furthermore, crystallization of initially amorphous excipients might be harmful to the dried protein [47]. Little is known about glass transition temperatures of freeze-dried cyclodextrins with only some published values available. Due to its high molecular weight, parent β -CD possesses a rather high glass transition temperature. Reported T_g -values of freeze-dried β -CD are 55 °C at a water content of 2.5 % (w/w) in combination with invertase and 108 °C at a water content of 2.5 % – 3.5 % (w/w) in combination with IL-2 [28, 38].

There are some hints available in literature that storage stability of CD-containing lyophilizates can be attributed to the high glass transition temperatures of cyclodextrins. In an early study on an antibody, HP β CD at a concentration of 5 % (w/v) was employed to freeze-dry an IgG monoclonal mouse antibody [35]. Recovery of the antibody immediately after lyophilization as measured by ELISA was above 80 % even without any excipients and was not improved by the addition of HP β CD, sucrose or dextran. However, during subsequent storage for 18 days at 56°C, the HP β CD-containing formulation yielded higher levels of antigen binding than the sucrose- and dextran-formulation. Residual moisture levels of the freeze-dried cakes were 1-2 % (w/w), probably resulting in storage close to or above the T_g of sucrose but most likely below the T_g of HP β CD and dextran [38, 48].

The high glass transition temperature of β -CD was probably also beneficial in a study on freeze-dried formulations of the cytokine IL-2. During storage at 45 °C for 36 weeks, β -CD prevented protein aggregation more effectively than sucrose and dextran but slightly less than

trehalose. In addition to their high T_g -values, cyclodextrins, remaining amorphous can inhibit crystallization of other excipients during storage of lyophilizates. This was the case with β -CD at a concentration of 10 % (w/v) in combination with trehalose [28]. In another study, HP β CD was used at a concentration of 0.5 % in combination with mannitol (1.5 %) for freeze-drying of TNF [36]. After storage for one month at 37° C, HP β CD-containing formulations showed intermediate levels of non-reducible dimers and well preserved bioactivity. The stabilizing effect of HP β CD during storage of the lyophilizates was attributed to vitrification.

II.1.7 CONCLUSIONS

Summarizing the different studies on the use of CDs in lyophilized protein formulations, it can be stated that cyclodextrins, especially the substituted derivatives, are valuable excipients. Different mechanisms of stabilization seem to be exerted simultaneously. From the fact that protein stabilization can already be achieved at low concentrations of cyclodextrins and that surface active cyclodextrins (hydroxypropylated and methylated derivatives) seem to be most effective at inhibiting aggregation it can be deduced that surfactant-like effects of CDs seem to play an important role in the mechanism of stabilization. In addition there is evidence that sugar-like effects, most importantly water replacement, play an important role. The formation of an amorphous glass alone (vitrification), as provided by parent CDs, can be insufficient to ensure adequate protein stability. However, the high glass transition temperatures observed in protein formulations containing cyclodextrins can contribute to the physical stability of freeze-dried products, for example by preventing crystallization of amorphous stabilizers.

II.1.8 RATIONAL USE OF CYCLODEXTRINS IN PARENTERAL PROTEIN FORMULATIONS

We gave an overview on studies investigating cyclodextrins as excipients in dried protein formulations. Based on these studies some practical guidance on how to rationally apply cyclodextrins for the design of dried protein formulations is given in the following: First, it has to be determined which purpose the cyclodextrin-derivative should serve in the formulation. The purpose will determine the choice of derivatives as well as the concentration range to be tested. If a surfactant-like effect is desired, the choice will be on surface active-derivatives at comparably low concentrations; if CDs are supposed to serve as lyoprotectants, higher concentrations of amorphous, hydrogen-bond forming derivatives shall be selected.

Another aspect takes into account the acceptance of CDs as excipients in parenteral products. If only CD-derivatives should be selected that are already used in approved parenteral products, HP β CD is without doubt the excipient of choice. Because of its surfactant-like and amorphous carbohydrate-like properties and toxicological safety, it perfectly meets the

requirements to stabilize proteins during all process steps in freeze- and spray-drying as discussed in section II.1.2. Figure II-1 shows a decision chart on how to select the proper cyclodextrin derivative.

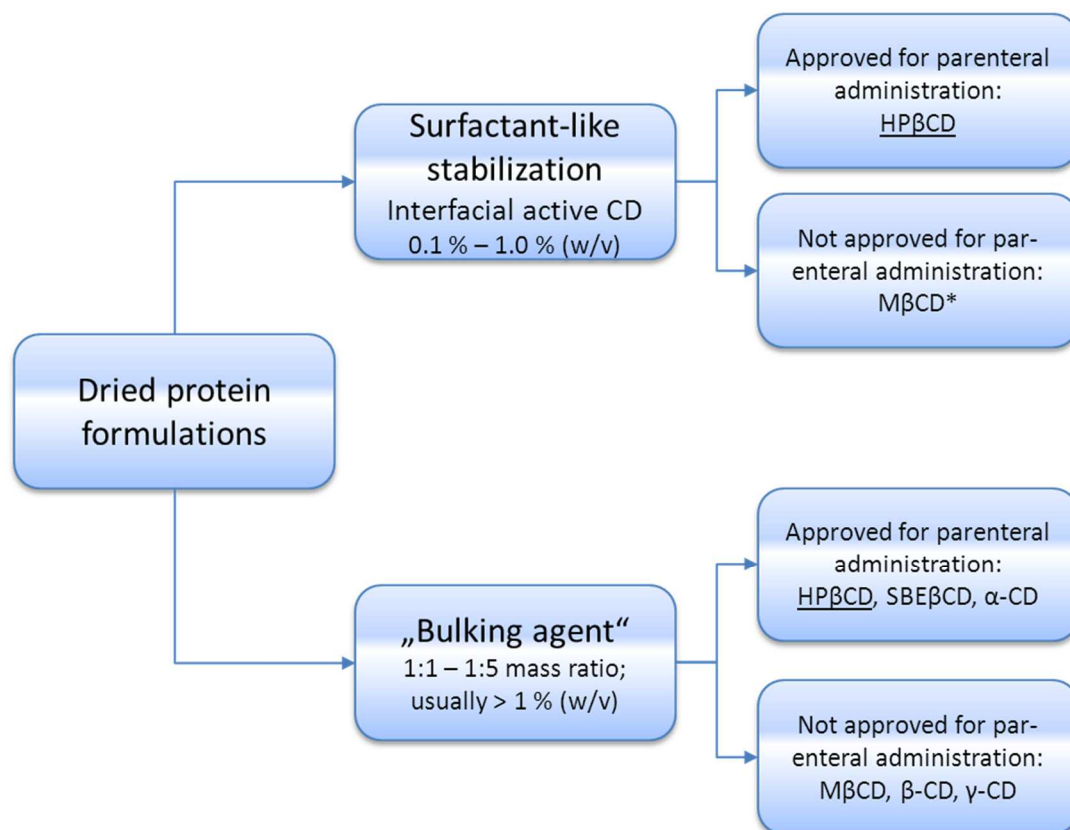


Figure II-1: Guidance to cyclodextrin type and concentration selection for dried protein formulations.

The most prominent characteristic of HPβCD is its interfacial activity, which renders it a valuable replacement for surfactants, such as polysorbates. The concentration of CD needed for adequate stabilization of proteins during freeze-drying is rather low when surfactant-like effects are desired. From section II.1.4 it can be deduced that for HPβCD concentrations of approximately 0.1 % (w/v) up to 1 % (w/v) of HPβCD were most effective and further increase does not provide further stabilization against interfacially-induced stress conditions.

If cyclodextrins are supposed to act as lyoprotectants, higher concentrations (larger than 1 % (w/v)) should be applied. However, the positive effects of CDs in this function are not as clear from the current literature as their impact on the suppression of interfacially-induced degradation pathways. In some cases it might be beneficial to add CDs to protein formulations, because high glass transition temperatures can be achieved allowing for good physical stability of the lyophilized cakes at elevated temperatures. The possibility to increase T_g' in liquid formulations allows for a higher storage temperature of bulk solutions.

II.1.9 AIM OF THE STUDY

The aim of this study was to evaluate the potential use of cyclodextrins as replacement for surfactants, mainly polysorbates in the field of freeze-drying of pharmaceutical relevant proteins. The focus clearly lies on the hydroxypropylated derivative HP β CD, because of its safety and interfacial activity. If stable formulations can be achieved, they will be analysed with state-of-the-art analytics and storage stability of the lyophilizates will be evaluated. If possible, the stabilization mechanism of HP β CD will be evaluated.

II.2 MATERIAL AND METHODS

II.2.1 MATERIALS

A monoclonal antibody MabR1 was used as a model protein because it is sensitive to freezing- and drying associated stresses. The antibody was formulated in a 10.5 mM sodium-phosphate buffer at pH = 6.4. Human growth hormone (hGH) was formulated in a 10 mM sodium-phosphate buffer at pH = 7.00. Granulocyte-colony stimulating factor (GCSF) was formulated at pH = 4.00 in a 10 mM citrate buffer. Both proteins are known to be sensitive to interfacial stresses [49, 50]. Sodium phosphate monobasic and dibasic were bought from Merck, Darmstadt, Germany or Applichem, Darmstadt, Germany; Sodium chloride and Trehalose was purchased from BDH Prolabo, (VWR, Ismaning, Germany) or Merck (Darmstadt, Germany). Sucrose was kindly provided from Suedzucker (Plattling, Germany). Polysorbate 80 was obtained from Sigma Aldrich Chemicals. Hydroxypropyl-beta-cyclodextrin (Cavasol HP Pharma) and methyl-beta-cyclodextrin (Cavasol M Pharma) were kindly provided by Wacker Chemie AG, München, Germany. All chemicals were of analytical grade.

II.2.2 PREPARATION OF FORMULATIONS

Formulations were prepared by mixing concentrated stock solutions of excipients and protein and final dilution with buffer. For Sucrose, Trehalose, HP β CD and M β CD, usually 10 % or 20 % (w/v) solutions were prepared and for polysorbate 80, a 1 % (w/v) solution was used. The final solutions were filtered through 0.22 μ m PVDF filters (Pall Acrodisc or Millipore Millex) which were pre-rinsed with at least 5 ml of buffer to remove extractables, particularly surfactant residuals. 2.3 ml of filtered solutions were pipetted into DIN 6R vials which were semi-stoppered and transferred to the freeze-dryer.

II.2.3 LYOPHILIZATION PROCESSES

II.2.3.1 CONVENTIONAL FREEZE-DRYING PROCESS

Lyophilization of the samples in a conventional process was performed using a Martin Christ Epsilon 2-6D freeze-dryer (Martin Christ, Osterode, Germany) equipped with a pirani pressure sensor. The samples were equilibrated at -3 °C for 1 hour and subsequently frozen to -50 °C using a ramp of 0.3 °C/min. After a 2 h isothermal hold, the pressure in the chamber was reduced to 0.09 mbar and the shelf temperature was increased to -20 °C with 0.5 °C/min. Primary drying with these settings was carried out for 35 h. After primary drying, the shelf temperature was increased to 5 °C with 0.1 °C/min and to 25 °C with 0.2 °C/min. Secondary

drying was carried out for 7 h at 25 °C. The samples were stoppered at approximately 800 mbar with dry nitrogen gas and crimped after unloading.

II.2.3.2 CONTROLLED NUCLEATION FREEZE-DRYING PROCESS

To decrease specific surface area compared to the conventional freeze-drying process, controlled ice nucleation was performed with our published method [51]. Ice nucleation of the samples was induced at a product temperature of approximately -5 °C by lowering the pressure to approximately 3.7 mbar followed by re-pressurization of the chamber via the cold condenser. The shelf temperature was held at -8 °C for 2 h post-nucleation to allow for slow ice crystal growth and Ostwald ripening. Complete solidification was obtained by lowering the shelf temperature to -50 °C with 1 °C/min. Primary drying and secondary drying ramps were the same as with the conventional freeze-drying process with a final shelf temperature of 25 °C (1% Sucrose) or 35 °C (5% Sucrose) which was held for 7 h. The samples were stoppered at approximately 800 mbar with dry nitrogen gas and crimped after unloading.

II.2.3.3 COLLAPSE FREEZE-DRYING PROCESS

Collapse lyophilization, which is freeze-drying above T_c , was performed to intentionally reduce specific surface area. Freezing of samples was performed using the same protocol as with conventional freeze-drying cycle. After freezing, the chamber pressure was reduced to 1.03 or 2.56 mbar and the shelf temperature was increased to 45 °C with 0.5 °C/min and held for 24 h. The samples were stoppered at approximately 800 mbar with dry nitrogen gas and crimped after unloading.

II.2.4 SAMPLE PREPARATION FOR FREEZE-THAW STUDIES

Samples which were subjected to the freeze-thawing stress were placed in the lyophilizer and frozen in the same way as the samples which were freeze-dried. After equilibration at the final freeze-temperature of -50 °C, samples were unloaded and stored at -80 °C until further analysis. Thawing of samples was performed in a 25 °C water bath.

II.2.5 SPRAY-DRYING PROCESS

Spray drying was performed using a B-290 spray dryer (Büchi Labortechnik AG, Flawil, Switzerland) equipped with the two-fluid nozzle which was water-cooled throughout the process. The liquid was atomized with nitrogen at fluid flow rate of approximately 4.4 ml / min and atomizing gas flow rate of 667 l / h. Inlet temperature was set to 160 °C and the aspirator was set to 100 % or approximately 38 m³/h, resulting in an outlet temperature of 76 °C ± 3. A LT Mini dehumidifier (Deltatherm, Much, Germany) was used to lower relative humidity of inlet

air. A high efficiency cyclone with grounding was used to collect the spray-dried powder in a 50 ml falcon tube. Samples were then weighed and aliquoted into DIN 6R vials in a glove box with a humidity of less than 10 % r.h.

II.2.6 PREPARATION OF ATOMIZATION-CONTROL SAMPLES

The same hardware setup as for spray drying was used. To check for interfacial stress exerted on MabR1 by atomization and baseline particle concentrations, the protein solution as well as placebos were pumped through the two-fluid nozzle and atomization was performed as in the spray drying process. The liquid was collected using a 50 ml falcon tube directly placed under the nozzle.

II.2.7 RECONSTITUTION OF DRIED PRODUCTS

Reconstitution of dried samples was performed by adding the amount of water which was removed by the corresponding drying process. The density of the solutions prepared was determined in a pycnometer. The mass of protein and excipients was subtracted and the result is the mass of water which needs to be added for rehydration. Reconstitution times were determined and the time until a clear solution was obtained was recorded as reconstitution time.

II.2.8 TURBIDITY

The turbidity of samples was measured using a Hach Lange Nephla nephelometer (Hach Lange GmbH, Düsseldorf, Germany). Scattered light of $\lambda = 860$ nm laser is detected at an angle of 90° and the result is given in FNU (Formazine nephelometric units). 1.9 ml were pipetted in pre-rinsed turbidity glass cuvettes with a flat bottom and placed into the device. Measurement was performed twice with a 90° turn between measurements.

II.2.9 LIGHT OBSCURATION

Subvisible particles were determined using a PAMAS SVSS-35 particle counter (PAMAS - Partikelmess- und Analysesysteme GmbH, Rutesheim, Germany) equipped with an HCB-LD-25/25 sensor which has a detection limit of approximately 120,000 particles $> 1 \mu\text{m}$ per ml. The rinsing volume was 0.5 ml and was followed by three measurements of 0.3 ml. Before each measurement, the system was rinsed with highly purified water until the total particle concentration was less than 100 per ml and no particles larger than $10 \mu\text{m}$ were present in the measurement cell. The samples were analyzed in the turbidity cuvettes. Data collection was

done using PAMAS PMA software and particle diameters in the range of $>1 \mu\text{m}$ to $200 \mu\text{m}$ were determined. All results are given in cumulative particles per milliliter.

II.2.10 SIZE EXCLUSION CHROMATOGRAPHY (SE-HPLC)

To determine protein monomer, dimer, fragment and high molecular weight soluble aggregates, size exclusion chromatography was performed using a Gynkotek HPLC system equipped with a M480 and a M300 pump, a coolable Gina 50T autosampler and an UVD 170U UV/VIS detector (Dionex, Idstein, Germany). For MabR1, a 50 mM sodium phosphate buffer with 300 mM sodium chloride at pH = 7.00 was used with a Tosoh SWXL 3000 column (Tosoh Bioscience, Stuttgart, Germany), because this buffer was found to be optimal for the Tosoh column [52]. For both h-GH and GCSF, a Sephadex 75 (GE Healthcare, Freiburg, Germany) column was used. Elution of h-GH was performed using a 50 mM sodium-phosphate buffer with 150 mM sodium chloride at pH = 7.00 and elution of GCSF was performed in a 100 mM sodium phosphate buffer, pH = 7.00. In all cases, sodium azide was added in a concentration of 0.05 % (w/v).

II.2.11 ASYMMETRICAL FLOW-FIELD-FLOW SEPARATION (AF4)

An orthogonal method to size exclusion chromatography is asymmetrical flow-field-flow fractionation. Protein fragments, monomer as well as higher molecular aggregates are separated by a liquid cross flow combined with a parabolic channel flow. A Postnova AF2000 system (Postnova GmbH, Landsberg am Lech, Germany) was used for separation equipped with a PN 1122 pump, a PN 5300 autosampler. A Shimadzu SPD 10 UV detector was used to monitor protein absorption at $\lambda = 280 \text{ nm}$. Furthermore, the system is equipped with a PN 3150 refractive index detector and a PN 3620 or a Wyatt miniDawn MALLS detector. A spacer of $500 \mu\text{m}$ was used. For Mab R1, A buffer with 10 mM sodium phosphate and 150 mM sodium chloride was used. Approximately $30 \mu\text{g}$ were injected into the separation channel equipped with a regenerated cellulose membrane (RC) with a cut off of 10 kDa and focused for 4 min with an injection flow of 0.2 ml/min and a cross flow of 2.0 ml/min. Subsequently, protein species were separated with a constant cross-flow of 2.0 ml/min and a detector flow of 1.0 ml/min for 25 minutes. The cross flow is reduced to 0 ml/min within 5 minutes and elution is continued for additional 20 minutes at a detector flow of 1.0 ml/min. hGH was separated in the same manner except the the cross flow was changed to 2.5 ml/min, the detector flow was set to 0.5 ml/min and a 5 kDa RC membrane was used. The buffer was the same as for size-exclusion chromatography of hGH.

II.2.12 FOURIER-TRANSFORM INFRARED SPECTROSCOPY (FTIR)

To determine protein secondary structure, a Bruker Tensor 27 FTIR spectrometer (Bruker Optics, Ettlingen, Germany) was used. Samples were either measured in the BIO ATR II cell or in a calcium fluoride flow-through cell. The mercury cadmium telluride detector was cooled with liquid nitrogen and the beam path was purged with nitrogen. Each spectrum was recorded in 120 scans between 850 to 4000 cm^{-1} with a 4 cm^{-1} resolution and a corresponding blank spectrum was subtracted. The second derivative spectrum in the range between 1720 to 1480 cm^{-1} was calculated using the Savitzky-Golay smoothing algorithm with 17 smoothing points by the Opus 6.5 software after vector normalization of the spectra and a correlation coefficient according to Prestrelski and coworkers [53] was calculated in Microsoft Excel.

II.2.13 RESIDUAL MOISTURE CONTENT (HEADSPACE METHOD)

To determine residual water content after freeze-drying, Karl Fischer titration was used. Between 10 and 50 mg of sample aliquots were prepared in a glove box with a relative humidity of less than 10 %, filled into DIN 2R Vials and crimped. The samples were then placed in an oven with 90 °C to enable fast extraction of water and the headspace gas is transported into a coulometric Karl Fischer titrator (Aqua 40.00, Elektrochemie Halle). The results are calculated in relative water content (m/m).

II.2.14 RESIDUAL MOISTURE CONTENT (DIRECT INJECTION METHOD)

To determine residual moisture of collapsed freeze-dried and spray-dried samples, the Karl-Fischer direct injection method with methanol was used. Between 10 and 50 mg of sample aliquots were prepared in a glove box with a relative humidity of less than 10 %, filled into DIN 2R Vials and crimped. Approximately 2.5 ml of methanol with very low water content was added to the sample for extraction of water. Subsequently, the sample was placed in an ultrasonic bath for 10 minutes. An aliquot of 1 ml was injected into a coulometric Karl Fischer titrator (737 KF Coulometer, Metrohm, Filderstadt, Germany). The results are calculated in relative water content (m/m).

II.2.15 DYNAMIC SCANNING CALORIMETRY (T_g)

The glass transition temperature of the maximally freeze-concentrated samples was determined using either a Netzsch DSC 204 (Selb, Germany) or a Mettler Toledo DSC 821e (Gießen, Germany) dynamic scanning calorimeter. Approximately 25 μl of the liquid samples were weighed into aluminium crucibles and crimped. The samples were cooled to -70 °C with a cooling rate of 10 K/min with the Netzsch system which was equipped with a liquid nitrogen

cooler. With the Mettler system, the samples were cooled to -40 °C with a cooling rate of -10 K/min and to -50 °C with a cooling rate of 2 K/min. T_g' was determined by heating the samples with a heating rate of 10 K/min and the inflection point of the glass transition was evaluated.

II.2.16 DYNAMIC SCANNING CALORIMETRY (T_g)

The glass transition of the dried lyophilizates was measured using either a Netzsch DSC 204 (Selb, Germany) or a Mettler Toledo DSC 821e (Gießen, Germany) dynamic scanning calorimeter. Aliquots of 5 to 20 mg of dried lyophilized cake were compacted in an aluminium crucible and crimped in a glove box with a relative humidity of less than 10 %. Both devices cannot work in modulating mode, so the samples were cooled to -10 °C with a cooling rate of 10 K/min, heated to 110 °C with a heating rate of 10 K/min to allow for relaxation of the samples and sample was heated again from -10 °C to 180 °C with 10 K/min. For samples which were based on 1 % HP β CD, no glass transition could be detected using a heating rate of 10 K/min, so those samples were heated with 50 K/min. The glass transition temperature was evaluated from the inflection point of the glass transition using the Netzsch Proteus software or the Mettler StarE Software.

II.2.17 SPECIFIC SURFACE AREA

Specific surface area of lyophilizates was determined using Brunauer-Emmet-Teller krypton gas adsorption in a liquid nitrogen bath at 77.3 K (Autosorb 1, Quantachrome, Odelzhausen, Germany). Samples were gently crushed with a spatula and weighed into glass tubes. Outgassing was performed at least for 2 h at room temperature and an outgassing test was performed before every measurement. An eleven point gas adsorption curve was measured, covering a p/p_0 ratio of appr. 0.05 to 0.30. Data evaluation was performed according to the multipoint BET method fit of the Autosorb 1 software.

II.2.18 X-RAY POWDER DIFFRACTION

XRD was used to determine the solid state of the lyophilized product with an XRD 3000 TT diffractometer (Seifert, Ahrensburg, Germany). The device is equipped with a copper anode (40 kV, 30 mA) and has a wavelength of 0.154178 nm. The scintillation detector voltage was 1000 V. The samples were placed on the sample holder and analysed in the range of 5-45 ° 2-theta with steps of 0.05° 2-theta.

II.2.19 ELECTRON SPECTROSCOPY FOR CHEMICAL ANALYSIS (ESCA)

The dried product was analysed using an AXIS Ultra DLD X-ray photoelectron spectrometer (Kratos Analytical, Manchester, England) to determine atom concentration at the interface (approximately 5 – 10 nm deep) of the lyophilizates. Where necessary the automatic charge neutraliser system was used. When used, the spectra were calibrated to 285.0 eV binding energy for the hydrocarbon C 1s peak post acquisition. Analysis times typically were 3 minutes with a XRAY power of 300 W and a large area of approximately 300 x 700 μm was measured. Data reduction and processing was performed using the Vision 2 processing software.

II.3 RESULTS

II.3.1 CYCLODEXTRINS AS REPLACEMENT FOR POLYSORBATES - FORMULATION DEVELOPMENT FOR THE MODEL PROTEIN MABR1

II.3.1.1 FORMULATION SCREENING

In a first screening, various concentrations and combinations of the excipients sucrose, HP β CD, M β CD and polysorbate 80 were conventional freeze-dried with the model antibody MabR1 and analysis of the protein was performed after preparation (t0), after freeze-thaw studies (t1) and after freeze-drying (t2) for each of the formulations shown in Table II-3. Sucrose was used in a concentration of 1 %, which results in a protein-to-sugar mass ratio of 1:1 or a molar ratio of 1:438, which is on the lower limit of sugar concentrations to create challenging conditions. This limit usually is around 60 mM [3]. 60 mM equals approximately 2 % Sucrose and a molar ratio of protein:disaccharide of 1:900 for the 10 mg/ml of antibody used in this study.

Table II-3: Concentrations and combination of excipients for the screening of the model antibody MabR1.

Form #	Mab R1 [mg/ml]	Sucrose [%]	HP β CD [%]	M β CD [%]	Polysorbate 80 [%]
1	10	-	-	-	-
2	10	-	-	-	0.04
3	10	0.1	-	-	-
4	10	1	-	-	-
5	10	1	-	-	0.04
6	10	1	1	-	-
7	10	-	0.1	-	-
8	10	-	1	-	-
9	10	-	1	-	0.04
10	10	-	-	0.1	-
11	10	-	-	1	-
12	10	-	-	1	0.04

II.3.1.2 PROTEIN STABILITY DETERMINATION – SUBVISIBLE PARTICLES AND TURBIDITY

Light obscuration and turbidity showed a high sensitivity of detecting protein instability by formation of subvisible particles. The model protein MabR1 proved to be a good model because it showed sensitivity to freezing as well as drying and rehydration, which is illustrated in Figure II-2. The addition of polysorbate 80 (PS80) reduced subvisible particle formation after freeze-thawing stress (t1 FT) but was not successful in stabilization during dehydration in the freeze-drying process and reconstitution (t2 FD). The addition of sucrose in combination with PS80 showed the lowest number of subvisible particles after the freeze-drying process and rehydration and turbidity values remained unchanged. For some formulations, the coincidence limit of the PAMAS SVSS system was exceeded; however, since the goal was to obtain stable formulations with acceptable particle numbers of appr. < 30.000 per ml, it was not important if actual numbers of particles are 120,000 or 200,000 per ml.

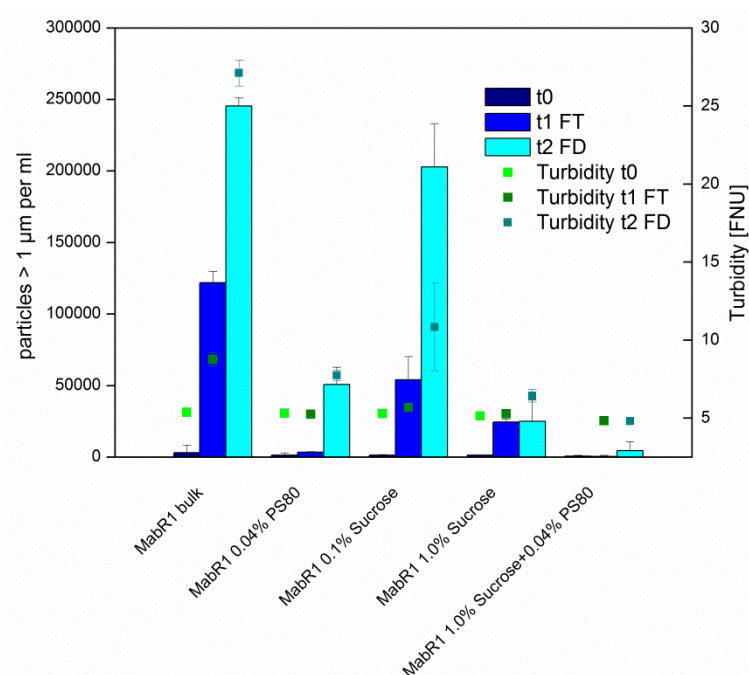


Figure II-2: Results from light obscuration and turbidity for the model protein MabR1. t0=analysis after preparation, t1 FT = analysis after freeze-thaw stress, t2 FD: analysis after freeze-drying and rehydration.

When both cyclodextrins derivatives, HP β CD and M β CD, were added as excipients, the concentrations of 1.0 % (w/v) showed the best results with respect to subvisible particle formation after freeze-thawing as well as after freeze-drying and rehydration, as shown in Figure II-3. However, turbidity was slightly increased in those formulations. The combinations of cyclodextrins with polysorbate 80 and sucrose with polysorbate 80 showed acceptable subvisible particle concentrations and almost unchanged turbidity values. HP β CD in

combination with sucrose was slightly inferior with respect to subvisible particles and turbidity to those combinations, as shown in Figure II-4. With respect to results from light obscuration, the formulations can be ranked as following: Formulation 5, 9 and 12 with low particle concentrations < 10,000 per ml and formulation 4, 6, 8, and 11 with acceptable particle concentrations of < 30,000.

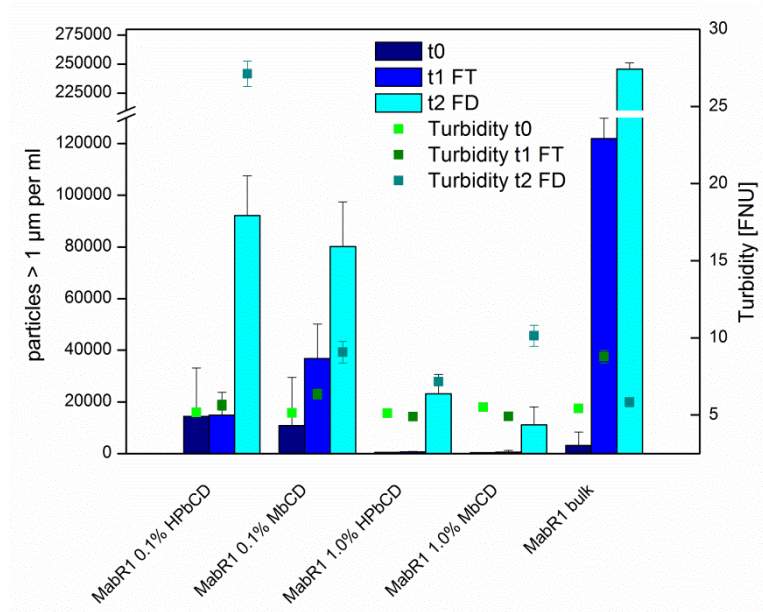


Figure II-3: Results from light obscuration and turbidity for formulations containing cyclodextrins in two concentrations in comparison to the bulk antibody formulation. t0=analysis after preparation, t1 FT = analysis after freeze-thaw stress, t2 FD: analysis after freeze-drying and rehydration.

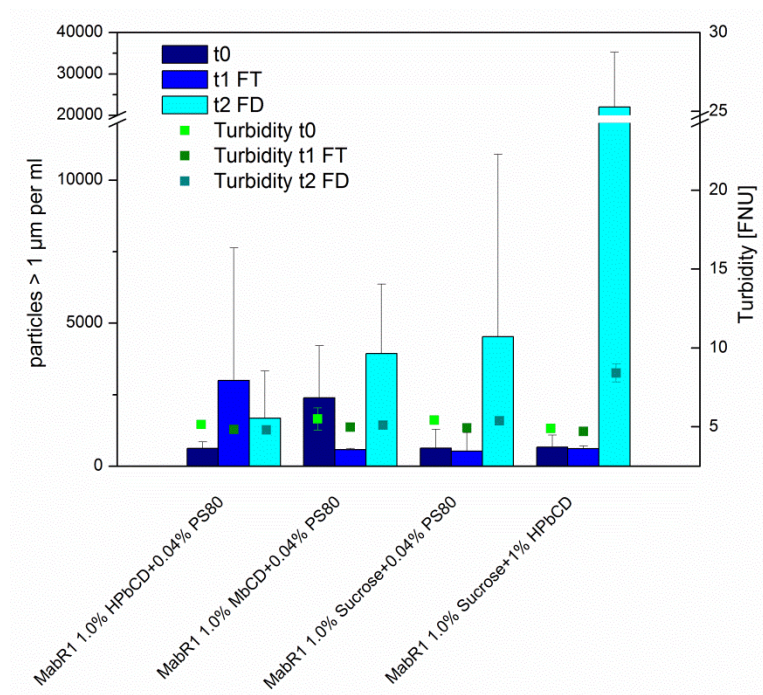


Figure II-4: Results from light obscuration and turbidity for various combinations of CDs, sucrose and PS80. t0=analysis after preparation, t1 FT = analysis after freeze-thaw stress, t2 FD: analysis after freeze-drying and rehydration.

As more extensively discussed in section II.3.14, HP β CD placebo particle formation was also investigated and it was found that 1.0 % HP β CD showed the highest amount of particles and turbidity whereas the combination of sucrose and HP β CD showed less subvisible particles but almost the same turbidity value, as displayed in Figure II-5.

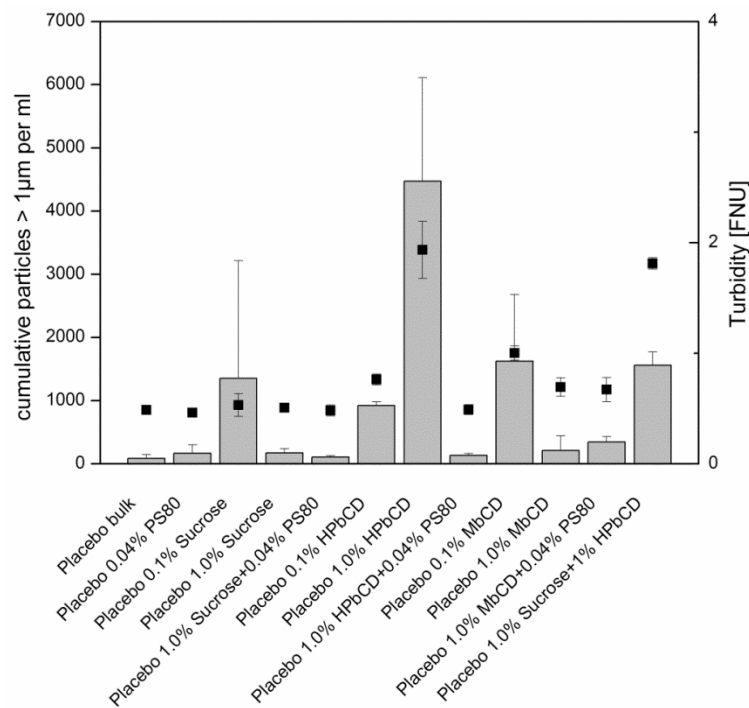


Figure II-5: Results from light obscuration and turbidity for formulations freeze-dried and rehydrated without protein.

II.3.1.3 SIZE-EXCLUSION CHROMATOGRAPHY

A slight decrease in MabR1 monomer content was observed for all formulations after freeze-drying and rehydration which is accompanied with a slight increase in dimer content (see Figure II-6) and high-molecular-weight aggregates (HMWA) (see Figure II-7). This trend was most pronounced for the formulation without excipients and less pronounced for the formulations containing sucrose or HP β CD at a concentration of 1.0 % independent of the presence of polysorbate 80. Total protein AUC remained more or less unchanged, indicating that only a small fraction of protein formed aggregates (Figure II-7, B).

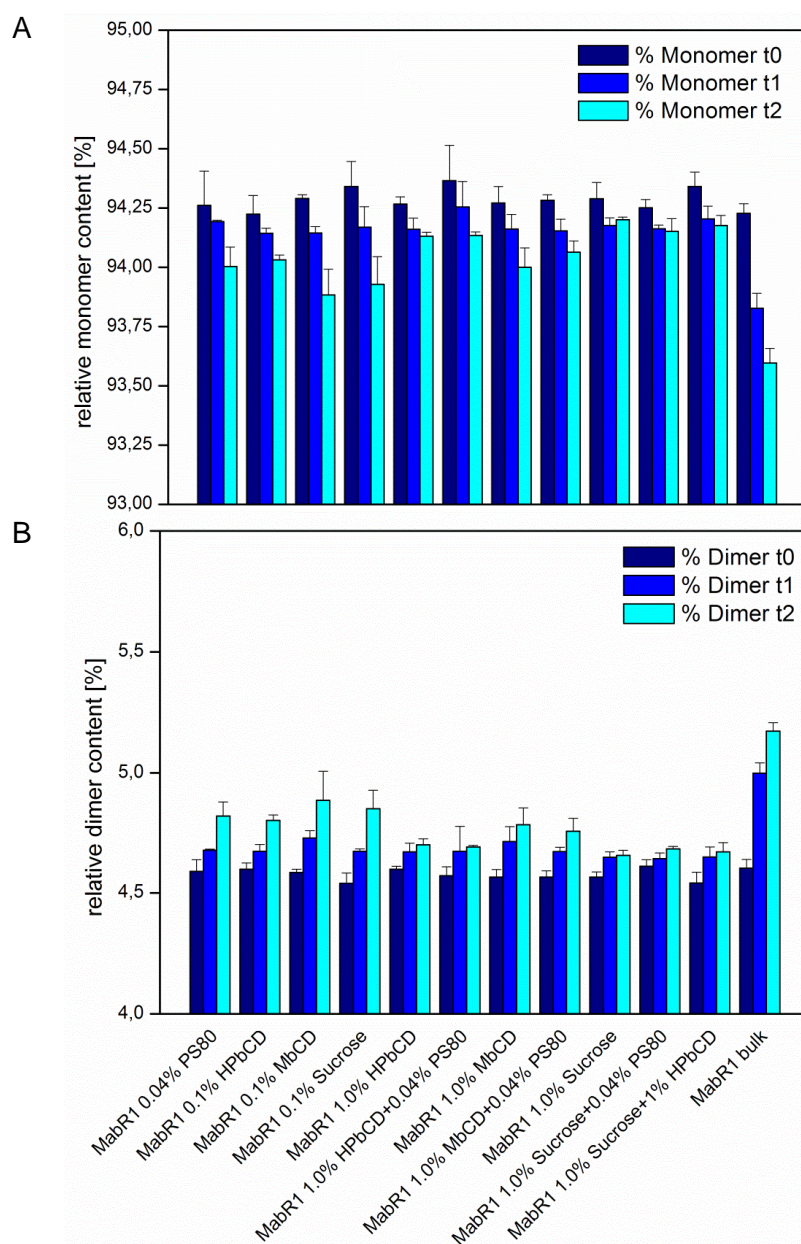


Figure II-6: Relative monomer (A) and dimer (B) content of MabR1 as determined with SE-HPLC. t0=analysis after preparation; t1=analysis after freeze-thawing; t2=analysis after freeze-drying and rehydration.

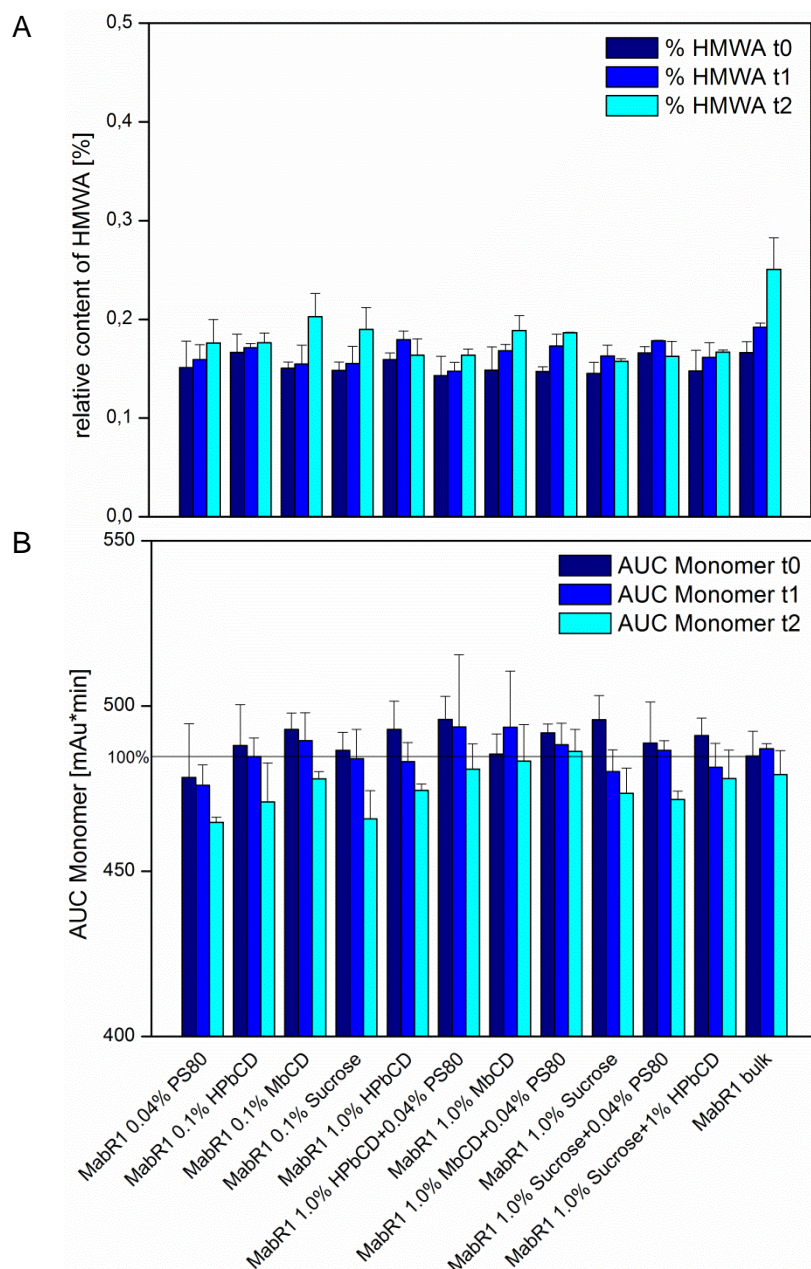


Figure II-7: Relative high molecular weight aggregates (A) and total protein area under the curve (AUC) (B) of MabR1 as determined with SE-HPLC. t0=analysis after preparation; t1=analysis after freeze-thawing; t2=analysis after freeze-drying and rehydration. The 100% border refers to the AUC of bulk t0.

II.3.1.4 FOURIER-TRANSFORM INFRARED SPECTROSCOPY

Results from FTIR showed that correlation coefficients were over 0.9 for all formulations and showed no differences by visual comparison, including the bulk formulation without excipient (spectra are not shown). These findings indicate that no changes in secondary structure lead to aggregation of MabR1 or the amount of aggregates, which is often less than 1 % of total protein amount [54], is not enough to be detectable by FTIR spectroscopy.

Table II-4: Calculated correlation coefficients according to Prestrelski for all formulations after freeze-thawing (FT) and freeze-drying (FD).

Formulation	r_{t1} (FT)	r_{t2} (FD)
MabR1 bulk	0.9954	0.9900
MabR1 + 0.04 % PS80	0.9805	0.9771
MabR1 + 0.1 % Sucrose	0.9756	0.9934
MabR1 + 1.0 % Sucrose	0.9954	0.9965
MabR1 + 1.0 % Sucrose + 0.04 % PS80	0.9969	0.9943
MabR1 + 0.1 % HP β CD	0.9964	0.9957
MabR1 + 1.0 % HP β CD	0.9588	0.9853
MabR1 + 1.0 % HP β CD + 0.04 % PS80	0.9908	0.9696
MabR1 + 0.1 % M β CD	0.9876	0.9915
MabR1 + 1.0 % M β CD	0.9645	0.9815
MabR1 + 1.0 % M β CD + 0.04 % PS80	0.9954	0.9900
MabR1 + 1.0 % Sucrose + 1 % HP β CD	0.9763	0.9849

II.3.1.5 PHYSICO-CHEMICAL CHARACTERIZATION OF THE FREEZE-DRIED CAKES

Residual moistures of all formulations were below 2.0 %, and for all formulations containing at least 1.0 % of sucrose, HP β CD or M β CD, residual moisture values were between 0.5 % and 1.0 % (w/w), as illustrated in Figure II-8. Glass transition temperatures could only be detected for the formulations which contain 1.0 % sucrose as excipient. Specific surface areas for selected formulations were in the range from 1.1 m²/g to 1.73 m²/g for MabR1-containing samples and higher for placebo samples, as shown in Table II-5.

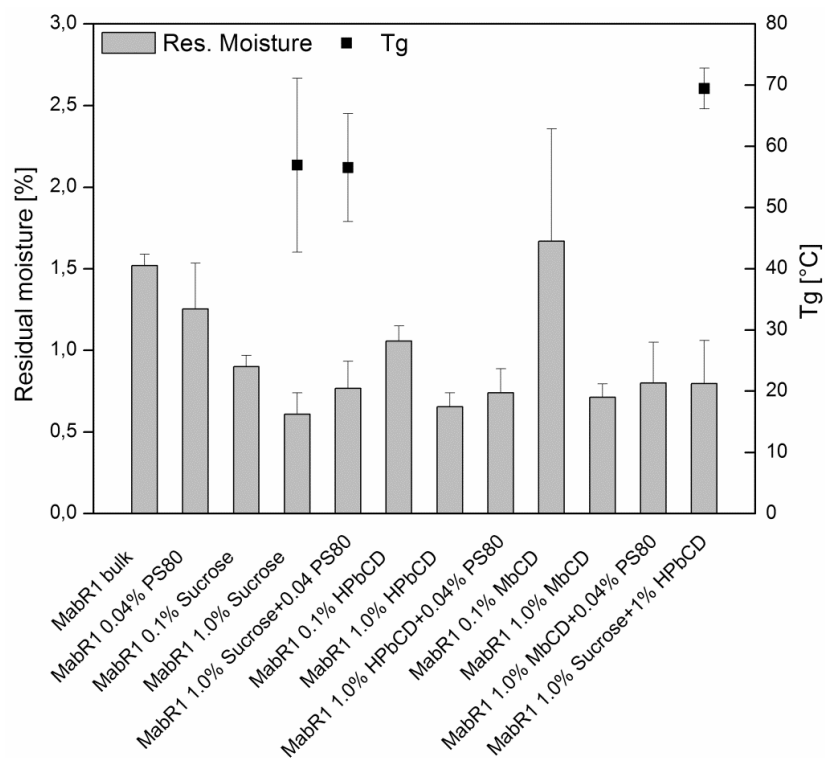


Figure II-8: Residual moisture and glass transition temperature (T_g) for all formulations.

Table II-5: Specific surface area of selected formulations of MabR1 or placebo.

Formulation	SSA [m ² /g]
MabR1 bulk	1.73
MabR1 + 0.04 % PS80	1.16
MabR1 + 1.0 % Sucrose	1.33
MabR1 + 1.0 % HPβCD	1.40
MabR1 + 1.0 % HPβCD + 0.04 % PS80	1.65
Placebo 1.0 % Sucrose	1.95
Placebo 1.0 % Sucrose + 1 % HPβCD	1.63

II.3.1.6 DISCUSSION AND SUMMARY

Overlooking the results from the first screening experiment, it could be observed that MabR1 is sensitive to freezing and freeze-drying followed by rehydration. Degradation of MabR1 was mainly observed with subvisible particle counting, which is a sensitive method to detect small fractions of degraded protein, since even a high number of particles (e.g. 10,000 particles > 2 μm per ml) represents only a small fraction of protein, (e.g. < 20 $\mu\text{g/ml}$) [54]. Consequently, small changes in aggregated protein mass result in large deviation in particle numbers. Based on results from light obscuration, the best formulations contained polysorbate 80 which was combined with a cryo/lyoprotectant such as sucrose or both cyclodextrin derivatives employed in this study, HP β CD and M β CD. The combination of sucrose and HP β CD also lead to acceptable but higher particle concentrations. Consequently, polysorbate 80 was superior to HP β CD in this study. In the presence of a cryo- and lyoprotectant such as sucrose, only minor changes in relative monomer content and dimer content were observable immediately after freeze-drying and rehydration and protein recovery. Furthermore, this small amount of aggregated protein also poses a challenge for spectroscopic methods like FTIR and results did not show any significant changes in the amide I and II region. These results suggest that even if a small percentage of total protein is degraded, these fractions may not be detected by FTIR or aggregated species do not show differences in secondary structure.

The buffer employed in this study was a sodium-phosphate buffer at pH=6.4 in a concentration of 10 mM. It has long been known that sodium phosphate buffers tend to crystallize during freezing with an accompanying pH-shift [55], and this crystallization can be reduced by adding amorphous stabilizers such as disaccharides or polymers [56] and by keeping buffer concentration as low as possible [2]. However, in the study presented, buffer concentration was very low and if sucrose was added, crystallization of sodium phosphate dibasic is unlikely. Moreover, addition of polysorbate 80 in a very low concentration lead to low numbers of subvisible particle numbers during freeze-thawing, indicating that interfacial denaturation of the antibody is the main degradation pathway and buffer crystallization as well as cold denaturation, that is unfolding of proteins at low temperatures, are probably no issue in this study.

II.3.2 FURTHER SCREENING OF FORMULATIONS FOR THE MODEL PROTEIN MABR1

After the results for the formulation screening, further screening and fine-tuning of the formulation with MabR1 at 10 mg/ml was performed with different concentrations of HP β CD (0.1 %, 0.35 % and 0.60 %), all in combination with 1.0 % sucrose. Analysis was performed after preparation (t0), after freeze-thawing (t1 FT) and after freeze-drying and rehydration (t2 FD). Two different lots of MabR1 were used to check for robustness of the formulations.

II.3.2.1 PROTEIN STABILITY DETERMINATION – SUBVISIBLE PARTICLES AND TURBIDITY

Similar to the first study, light obscuration and turbidity showed greatest sensitivity to detect protein instabilities due to aggregation. For both lots of MabR1, subvisible particles after freeze-thaw (t1) and freeze-drying and rehydration (t2) were almost identical and therefore average values were calculated for both lots. However, the results from the initial screening of MabR1 could not be reproduced and the subvisible particles for the formulation containing sucrose only was much higher; also the combination of sucrose with HP β CD, almost independent of concentration, resulted in large amounts of subvisible particle numbers, as shown in Figure II-9, A. For the concentrations of 0.35 % and 0.60% HP β CD, the number of particles larger 10 μ m was slightly reduced (Figure II-9, B), indicating that 0.1 % HP β CD is most probably not enough for stabilization of the protein after freeze-drying and rehydration.

After reconstitution of the formulations with a solution of 0.04 % polysorbate 80, a reduction in subvisible particles > 1 μ m and turbidity was observed for all formulations except the formulation which contains 0.1 % HP β CD, as shown in Figure II-11. This result suggests that either fewer particles formed during the rehydration step or particles were “dissolved” or refolded in the presence of a surfactant. No significant differences between the HP β CD concentrations were observed after freeze-thawing and no increase in subvisible particles compared to t0 analysis was observed. Similar to the first screening study in section II.3.1, placebo particles and an increase of turbidity were observed with the formulation which contained HP β CD and the amount correlated with the concentration, as shown in Figure II-10.

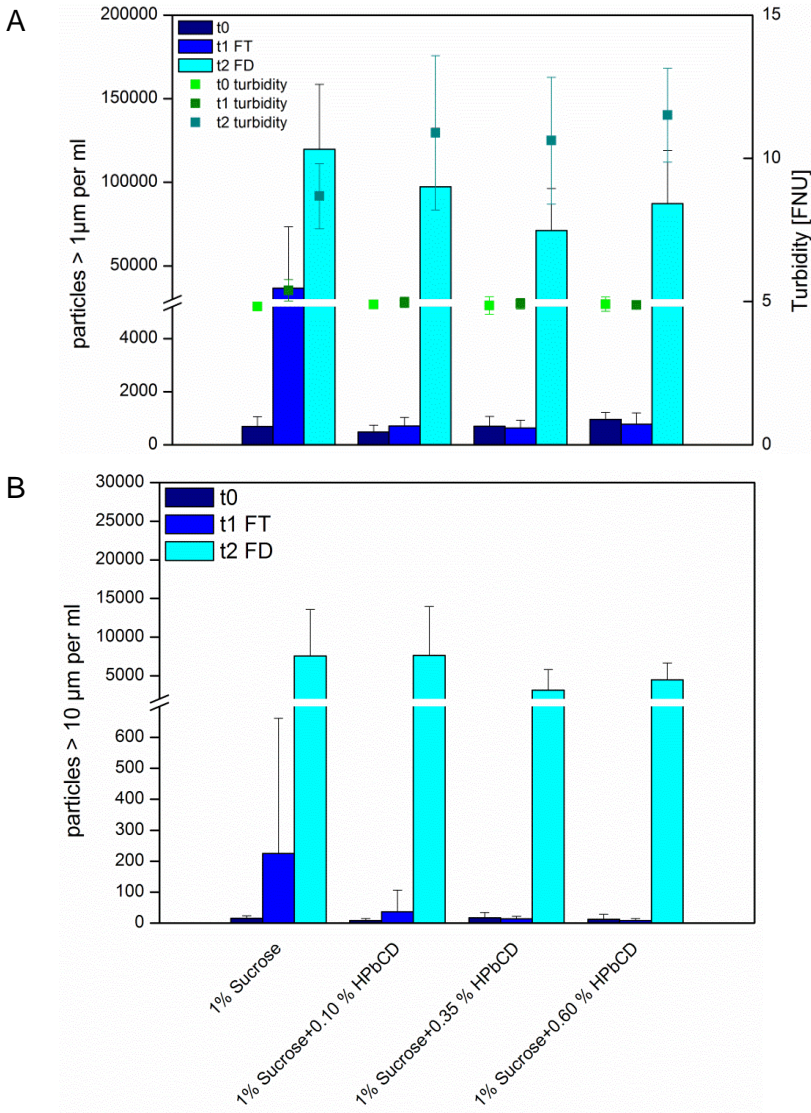


Figure II-9: Results from light obscuration for particles > 1µm and turbidity (A) and particles > 10 µm (B) for the combinations of sucrose and HPβCD. t0=analysis after preparation; t1=analysis after freeze-thawing; t2=analysis after freeze-drying and rehydration.

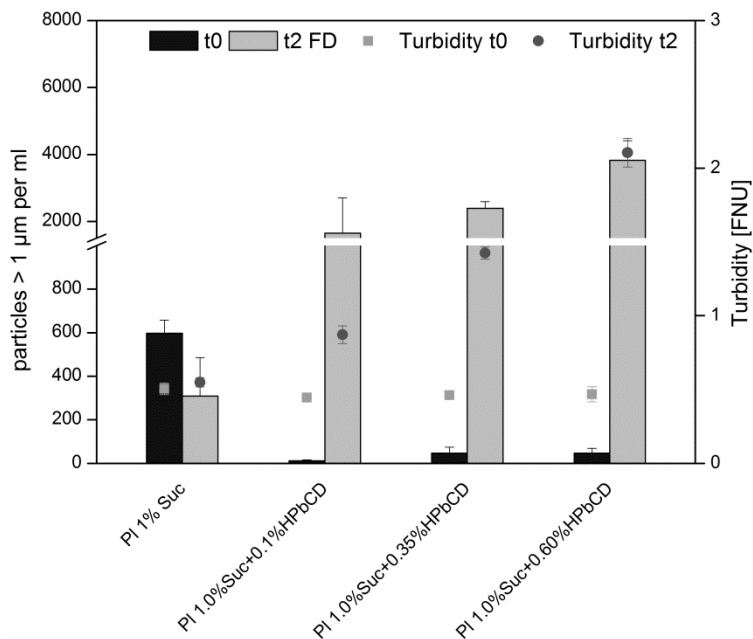


Figure II-10: Subvisible particles and turbidity for placebo formulations containing only sucrose and variable amounts of HPβCD. t0=after preparation; t2=after freeze-drying and rehydration.

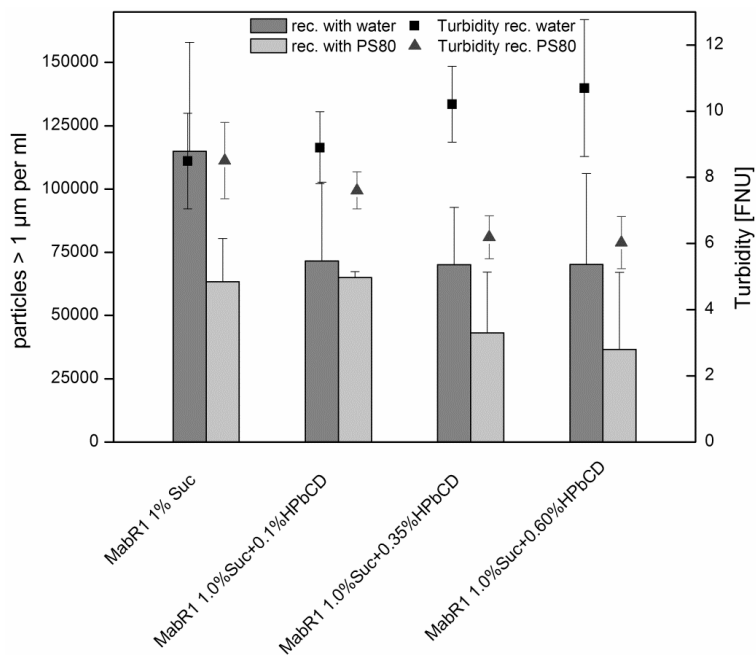


Figure II-11: Results from light obscuration and turbidity for MabR1 formulations which were freeze-dried and either reconstituted with water (rec. with water) or with a solution of 0.04 % PS80 (rec. with PS80).

II.3.2.2 SIZE-EXCLUSION CHROMATOGRAPHY

No significant differences in soluble protein species as well as total protein recovery (AUC) as determined with size-exclusion chromatography were observed for all formulations and both lots of MabR1 at all analytical time points, as shown in Figure II-12 and Figure II-13.

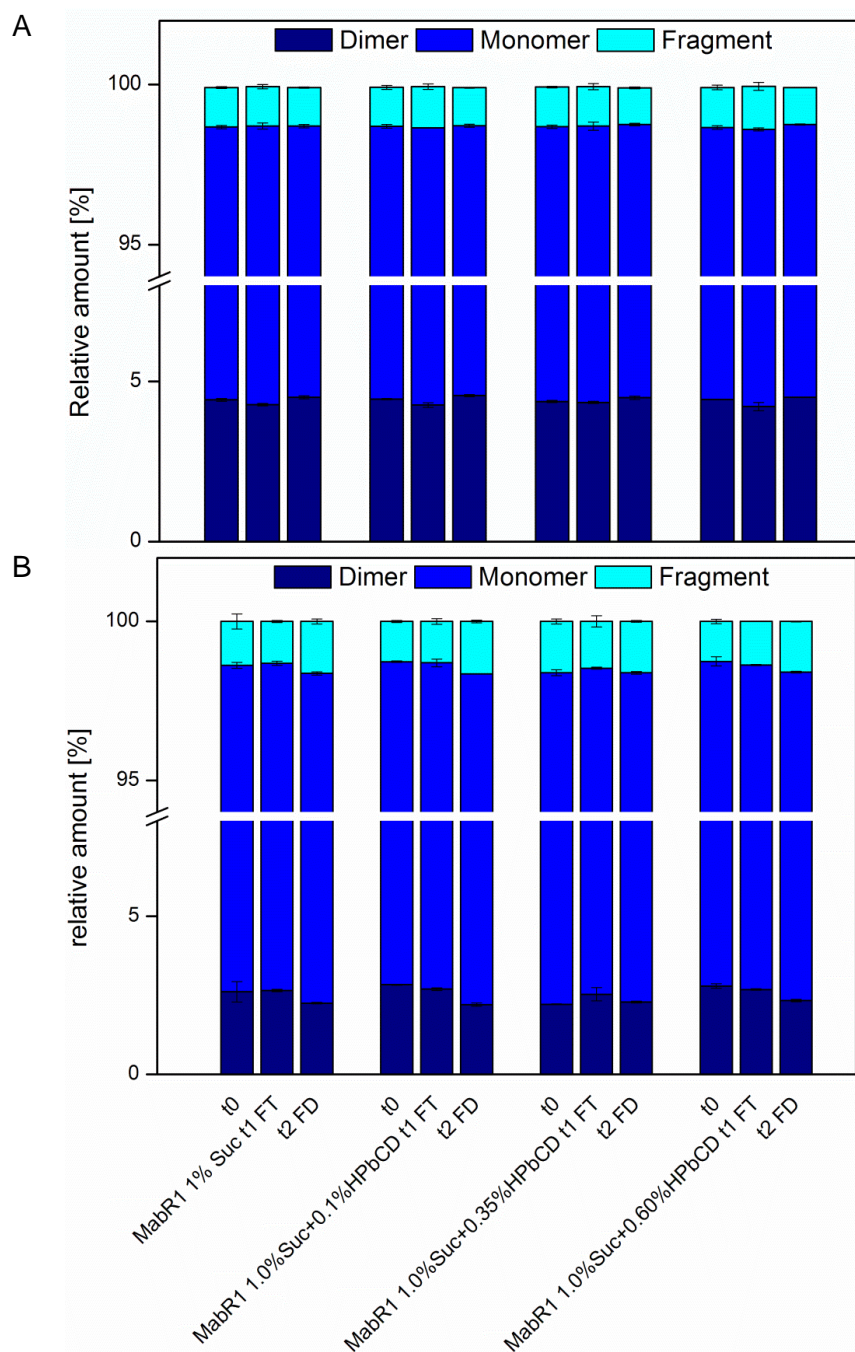


Figure II-12: Relative amounts of MabR1 protein species as determined by SE-HPLC for Lot 1 (A) and Lot 2 (B). t0=analysis after preparation; t1=analysis after freeze-thawing; t2=analysis after freeze-drying and rehydration.

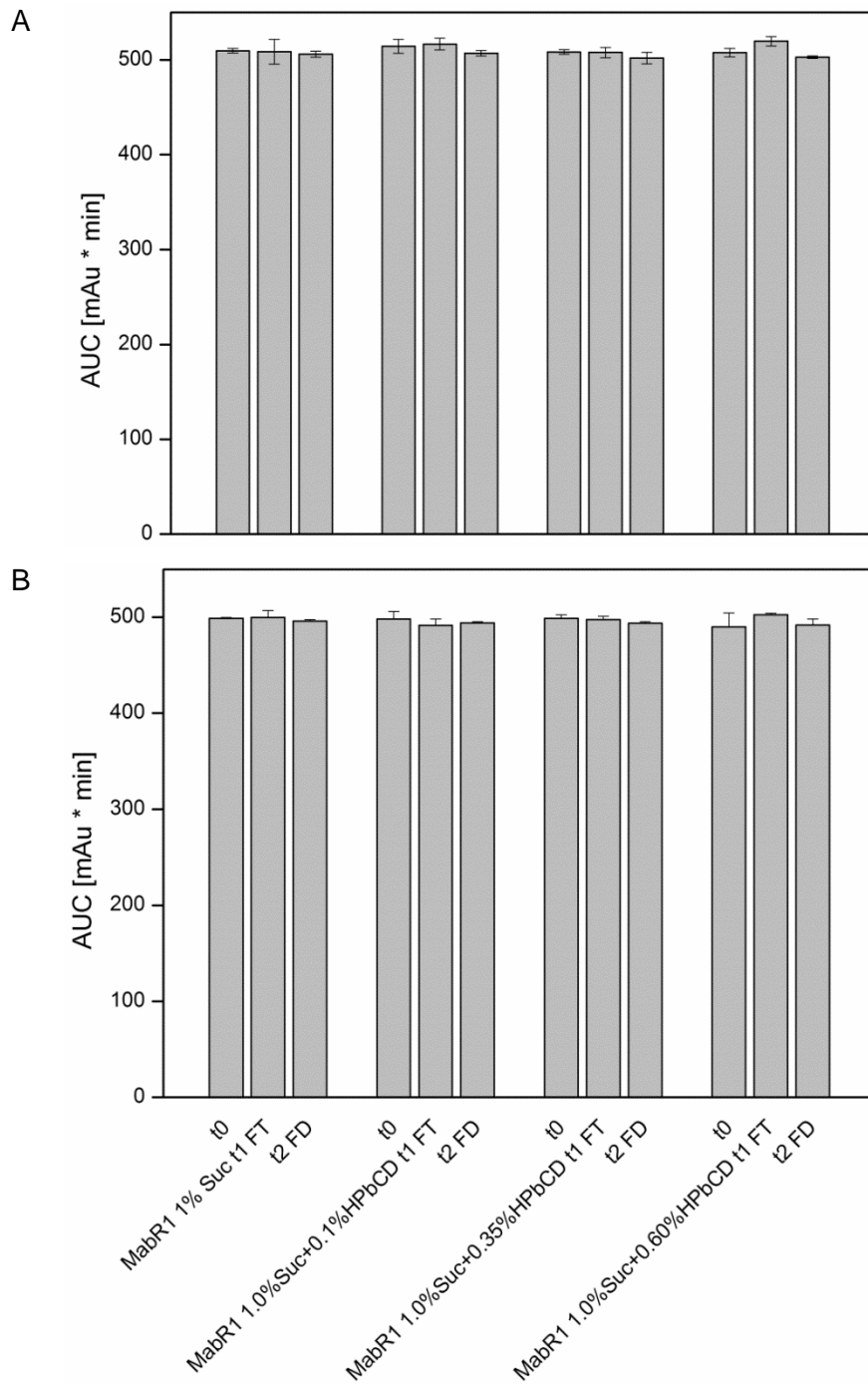


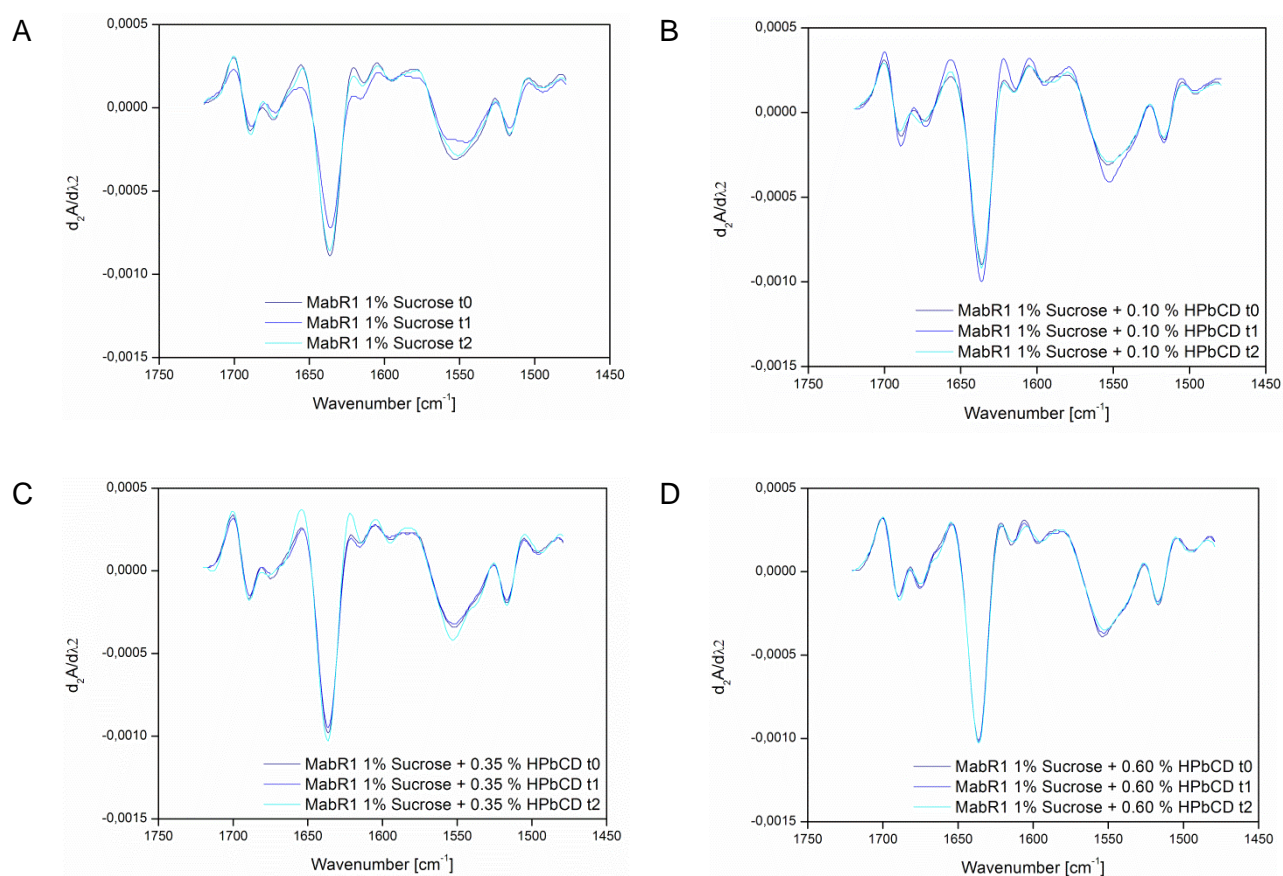
Figure II-13: Total protein recovery for Lot 1 (A) and Lot 2 (B) as determined by SE-HPLC. t0=analysis after preparation; t1=analysis after freeze-thawing; t2=analysis after freeze-drying and rehydration.

II.3.2.3 FTIR SPECTROSCOPY

No major differences were observed with FTIR-spectroscopy as correlation coefficients are all > 0.98 , as indicated in Table II-6 and spectra were almost perfectly superimposing each other, as shown in Figure II-14 for Lot 1 and Figure II-15 for Lot 2. However, correlation coefficients were highest for the formulation which contains 0.35% and 0.6 % HP β CD, which was most pronounced with Lot 1.

Table II-6: Correlation coefficients (r) as determined with FTIR for both Lots and timepoints t1 and t2 compared to t0.

Formulation	Lot 1		Lot 2	
	rt1 (FT)	rt2 (FD)	rt1 (FT)	rt2 (FD)
MabR1 1% Sucrose	0.9852	0.9887	0.9972	0.9939
MabR1 1% Sucrose + 0.10 % HP β CD	0.9934	0.9916	0.9973	0.9987
MabR1 1% Sucrose + 0.35 % HP β CD	0.9986	0.9910	0.9950	0.9934
MabR1 1% Sucrose + 0.60 % HP β CD	0.9989	0.9982	0.9953	0.9989

Figure II-14: 2nd derivative FTIR spectra of the amide I (1600-1700 cm^{-1}) and amide II band (1600 – 1500 cm^{-1}) for all formulations of MabR1, Lot 1 with 0 % (A), 0.10 % (B), 0.35 % (C) and 0.60 % (D) and all timepoints.

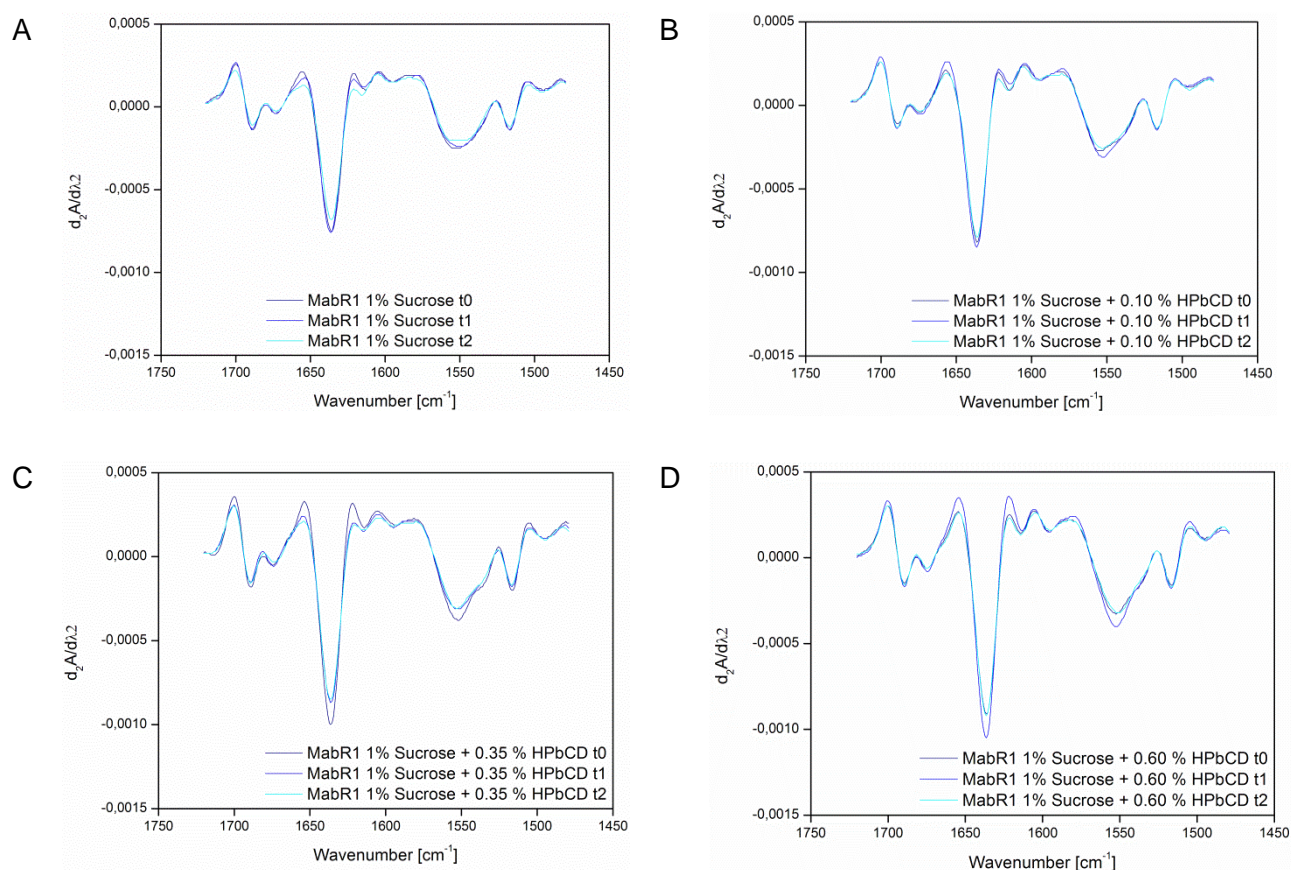


Figure II-15: 2nd derivative FTIR spectra of the amide I (1600-1700 cm⁻¹) and amide II band (1600 – 1500 cm⁻¹) for all formulations of MabR1, Lot 2 with 0 % (A), 0.10 % (B), 0.35 % (C) and 0.60 % (D) and timepoints.

II.3.2.4 PHYSICO-CHEMICAL ANALYSIS OF THE FREEZE-DRIED CAKES

Acceptable glass transition temperatures of the freeze-dried cakes were obtained for both lots with T_g s > 60 °C as shown in Figure II-16. In addition, residual moisture levels were quite low at a level of around 0.2 % (w/w), and were slightly lower than in the first screening study. Table II-7 shows the results for specific surface area of these formulations.

Table II-7: Specific surface area (SSA) for all formulations of Lot 2.

Formulation	BET SSA [m ² /g]
MabR1 1% Sucrose	1.45
MabR1 1% Sucrose + 0.10 % HPβCD	1.62
MabR1 1% Sucrose + 0.35 % HPβCD	1.56
MabR1 1% Sucrose + 0.60 % HPβCD	1.45

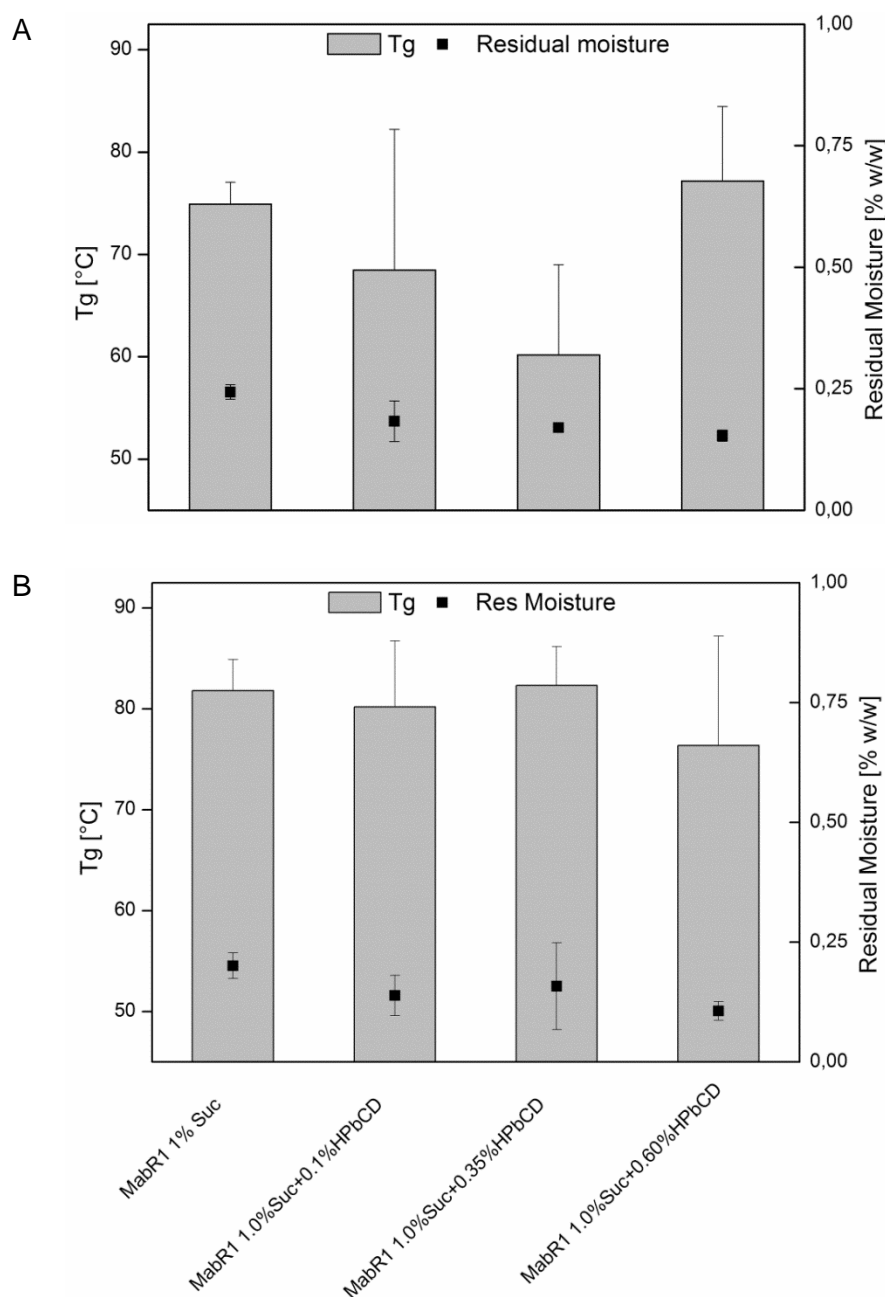


Figure II-16: Glass transition temperatures of the freeze-dried cakes and corresponding residual moistures for Lot 1 (A) and Lot 2 (B).

II.3.2.5 DISCUSSION AND SUMMARY

The combination of sucrose with increasing concentrations of HP β CD (0.10, 0.35 and 0.60 %) lead to unacceptable high numbers of subvisible particles. In addition, the control with 1 % sucrose only showed slightly higher subvisible particle numbers, especially for the size class of > 10 μ m. For this formulation, the results from the first screening study (section II.3.1) could not be reproduced. These batch-to-batch variations may originate due to different ice nucleation temperatures, which can lead to different interfacial areas, such as the ice-water interface and the liquid-air interface encountered during rehydration. This was the case for the

formulation of MabR1 formulated with 1 % sucrose with a SSA of 1.46 m²/g in this study and 1.34 m²/g in the previous study in section II.3.1. Another hint that the SSA plays a major role in degradation of MabR1 is the experiment with reconstitution of the lyophilizates with a solution of PS80. This result suggests that HP β CD is not able to protect the antibody to the same extent or by the same mechanism as PS80. Interestingly, this is only true for the reconstituted but not for the freeze-thawed samples, which showed no significant increase in subvisible particles compared to the initial numbers prior to lyophilization. Here, a concentration of HP β CD as low as 0.1 %, was very effective in protecting the antibody during freeze-thawing. This observation is true for both lots of MabR1 investigated in this study. Reconstitution of protein lyophilizates with different qualities of degraded polysorbate could also help to identify the impact of those oxidized species on protein stability.

II.3.3 COLLAPSE FREEZE-DRYING OF MABR1

With conventional freeze-drying, stabilization of the model antibody MabR1 with HP β CD was not successful because unacceptable subvisible particle levels were obtained. Collapse freeze-drying has been shown to effectively stabilize proteins in the freeze-dried state despite the unusual cake appearance [57, 58]. Moreover, with collapse freeze-drying, specific surface area is excessively reduced and residual moistures are somewhat higher. In this study, we want to investigate if the model protein MabR1 profits from collapse freeze-drying and the accompanying changed product quality attributes.

II.3.3.1 FREEZE-DRYING PROCESS

Aggressive freeze-drying results in a process which is very fast comparable to conventional freeze-drying process and collapse results from viscous flow if T_c is exceeded. An aggressive freeze-drying cycle is characterized by a high shelf temperature and a high pressure set-point. The product temperature during steady state sublimation, as measured with a temperature probe, was approximately $-13\text{ }^\circ\text{C}$, which results in a high sublimation rate. Sublimation is finished after 12.5 hours process time and is indicated by the convergence of the product temperature with shelf temperature. After this time point, desorption of unfrozen water takes place and residual moisture is further decreased.

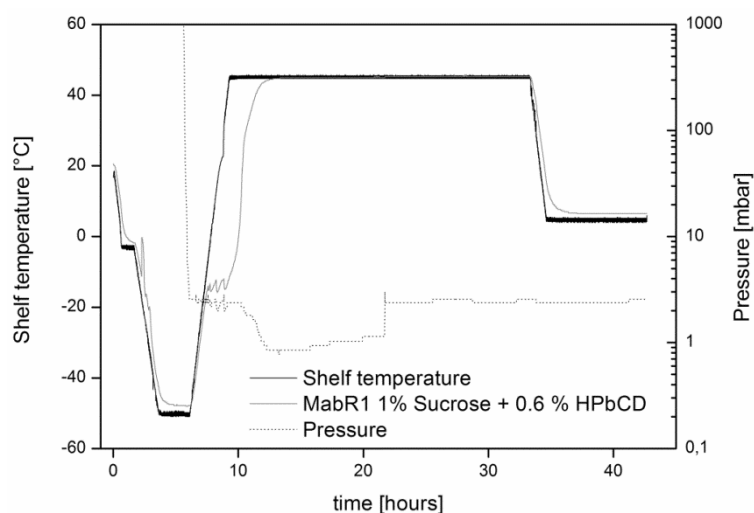


Figure II-17: Shelf temperature and pressure traces of the collapse freeze-drying run. A temperature sensor was placed in the formulation of MabR1 with 1% Sucrose and 0.6 % HP β CD. The pressure set-point was 2.56 mbar (Pirani manometer).

II.3.3.2 PROTEIN STABILITY ANALYSIS – SUBVISIBLE PARTICLES AND TURBIDITY

As in the previous studies, light obscuration and turbidity were quite sensitive to degradation of small amounts of protein. With collapse freeze-drying of MabR1, the formulation containing Sucrose and 0.6% HP β CD showed very acceptable particle levels and turbidity values after freeze-drying and rehydration which were even lower than the polysorbate containing

formulations, as illustrated in Figure II-18 and despite macroscopic collapse of the freeze-dried cake. Sucrose alone or in combination with only 0.1 % HP β CD both showed slightly less subvisible particles compared to conventional freeze-drying (section II.3.2.1) but still, subvisible particle levels were unacceptable high for those formulations. PS80 and HP β CD, independent of concentration, both inhibited formation of subvisible particles in freeze-thawing (t1 FT). The formulations containing 0.6 % HP β CD and PS80 resulted in very few particles > 10 μ m, with 17 and 80 particles per ml, respectively.

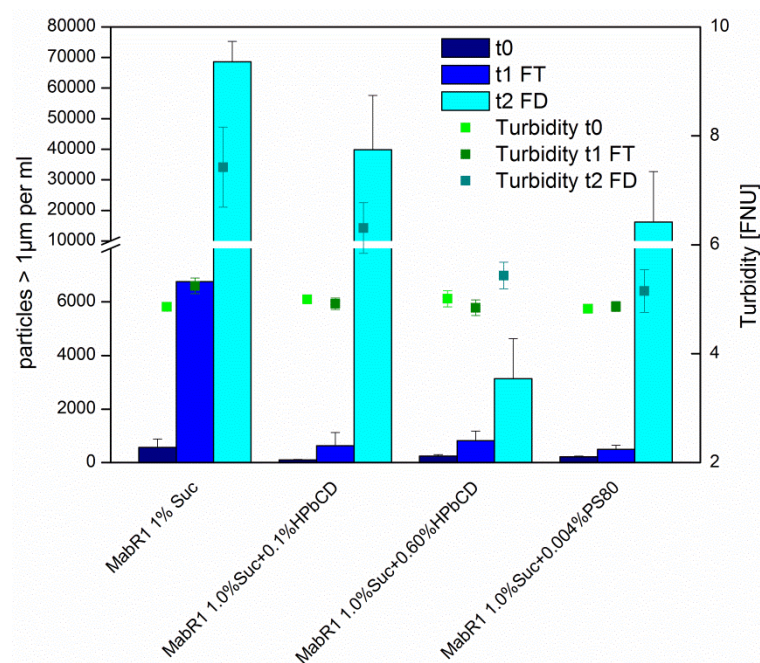


Figure II-18: Results from light obscuration and turbidity for collapse freeze-dried and rehydrated MabR1. t0=analysis after preparation; t1=analysis after freeze-thawing; t2=analysis after freeze-drying and rehydration.

Furthermore, with collapse freeze-drying, placebo particles of HP β CD could be reduced and were not significantly higher than the control of 1 % Sucrose, as shown in Figure II-19. Turbidity values were at baseline levels for all placebo formulations and unchanged compared to values after preparation which are usually around 0.5 FNU (data not shown).

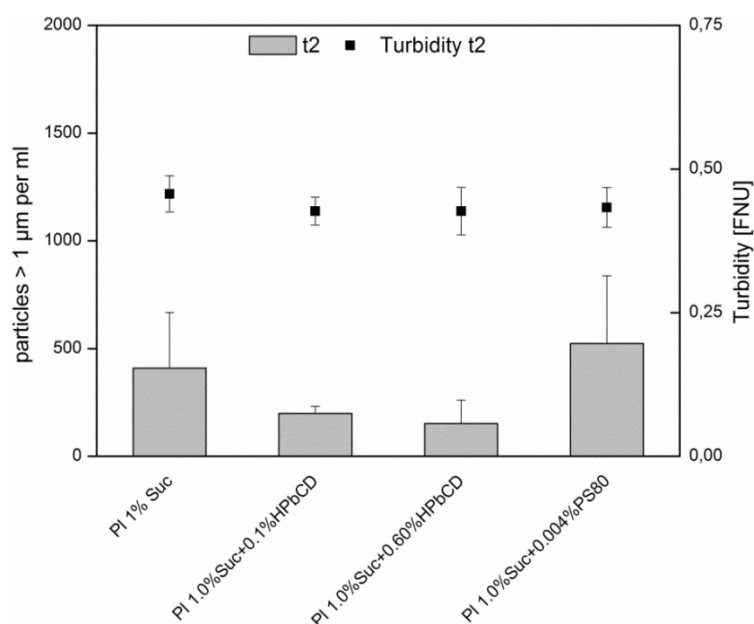


Figure II-19: Results from light obscuration and turbidity for collapsed freeze-dried and rehydrated placebo formulations.

II.3.3.3 SIZE-EXCLUSION CHROMATOGRAPHY

No changes in relative protein species were observed for all time points, indicating that the subvisible particles formed for all formulations were only a very small fraction of the total protein content, as suggested by Figure II-20 and Figure II-21.

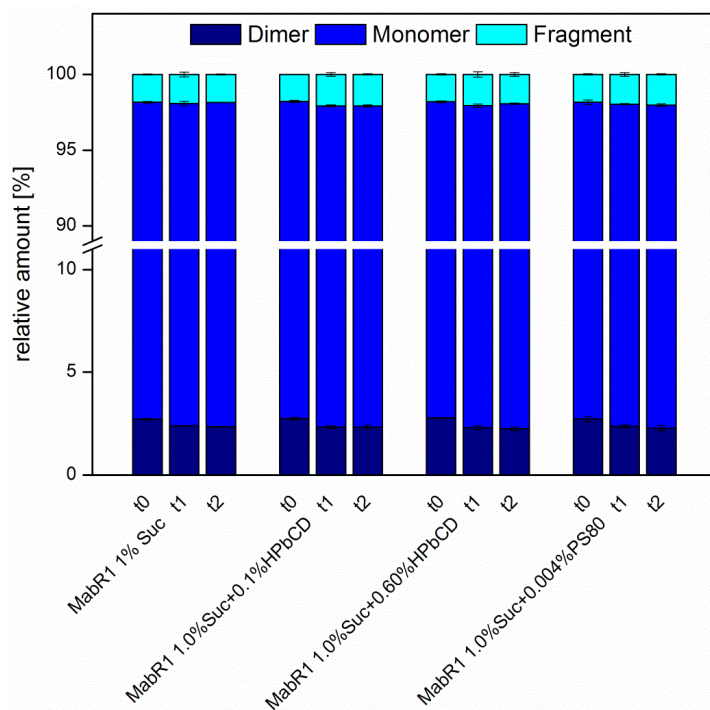


Figure II-20: Relative amounts of MabR1 protein species as determined by SE-HPLC. t0=analysis after preparation; t1=analysis after freeze-thawing; t2=analysis after freeze-drying and rehydration.

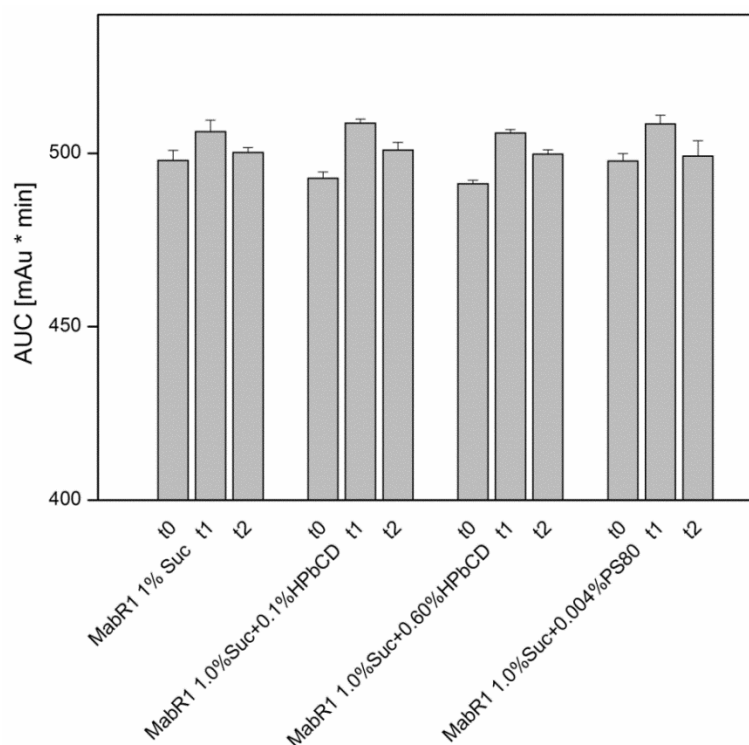


Figure II-21: Total protein recovery (AUC) of MabR1 as determined with size-exclusion chromatography. t0=analysis after preparation; t1=analysis after freeze-thawing; t2=analysis after freeze-drying and rehydration.

II.3.3.4 FTIR SPECTROSCOPY

FTIR was not able to detect small changes in protein stability and all correlation coefficients were close to 1.0 as displayed in Table II-8. Visual comparison of spectra also showed almost perfectly superimposing curves with no major differences for all formulations and time points, as suggested in Figure II-22.

Table II-8: Correlation coefficients of FTIR spectra calculated for both timepoints t1 and t2 compared to t0.

Formulation	rt1 (FT)	rt2 (FD)
MabR1 1 % Sucrose	0.999	0.998
MabR1 1 % Sucrose + 0.10 % HPβCD	1.000	1.000
MabR1 1 % Sucrose + 0.60 % HPβCD	1.000	1.000
MabR1 1 % Sucrose + 0.004 % PS80	0.998	0.998

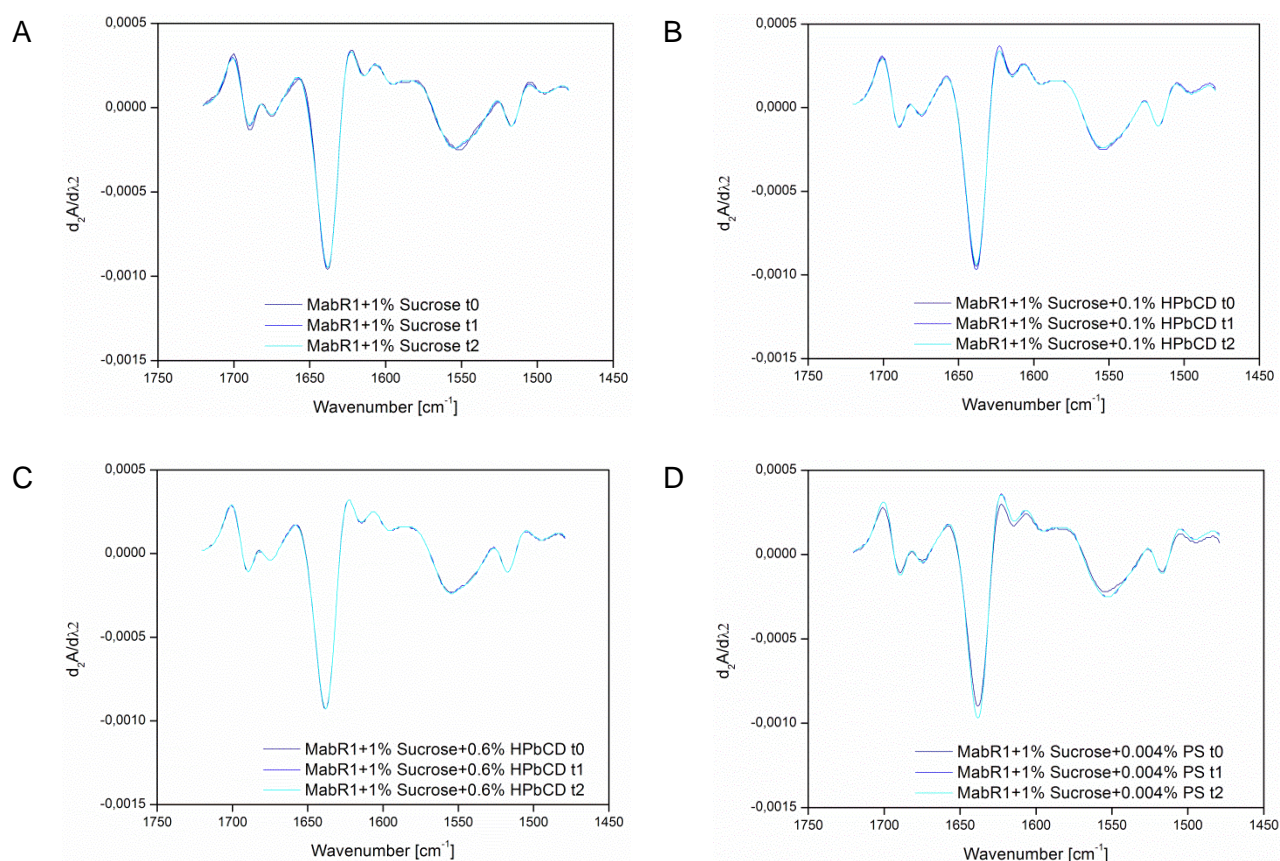


Figure II-22: 2nd derivative FTIR spectra of the amide I (1600-1700 cm^{-1}) and amide II band (1600 – 1500 cm^{-1}) for all formulations of MabR1, with 0 % (A), 0.10 % (B) and 0.60 % HP β CD (C) and 0.004 % PS80 (D) and all timepoints.

II.3.3.5 PHYSICO-CHEMICAL CHARACTERIZATION OF FREEZE-DRIED SAMPLES

As expected, drying above T_c lead to macroscopic collapse of the freeze-dried cakes; Figure II-23 shows the macroscopic appearance of the lyophilized cakes. Collapse of the lyophilized samples can be quantified by specific surface area (SSA) measurements. Table II-9 shows the SSA of the freeze-dried samples. All values were between 0.1 and 0.2 m^2/g and very low compared to conventional freeze-drying, which were between 1.3 to 1.7 m^2/g . However, residual moistures and glass transition temperatures were acceptable with T_g s of above 70 $^{\circ}\text{C}$ and residual moistures below 2 %. Also reconstitution times were not significantly prolonged compared to conventional freeze-drying with a dissolution time of around 10 seconds with some schlieren present for approximately 60 sec, independent of formulation composition.

Table II-9: Specific surface area for all formulations as determined by krypton gas adsorption.

Formulation	BET SSA [m ² /g]
MabR1 1 % Sucrose	0.14
MabR1 1 % Sucrose + 0.10 % HP β CD	0.21
MabR1 1 % Sucrose + 0.60 % HP β CD	0.15
MabR1 1 % Sucrose + 0.004 % PS80	0.12

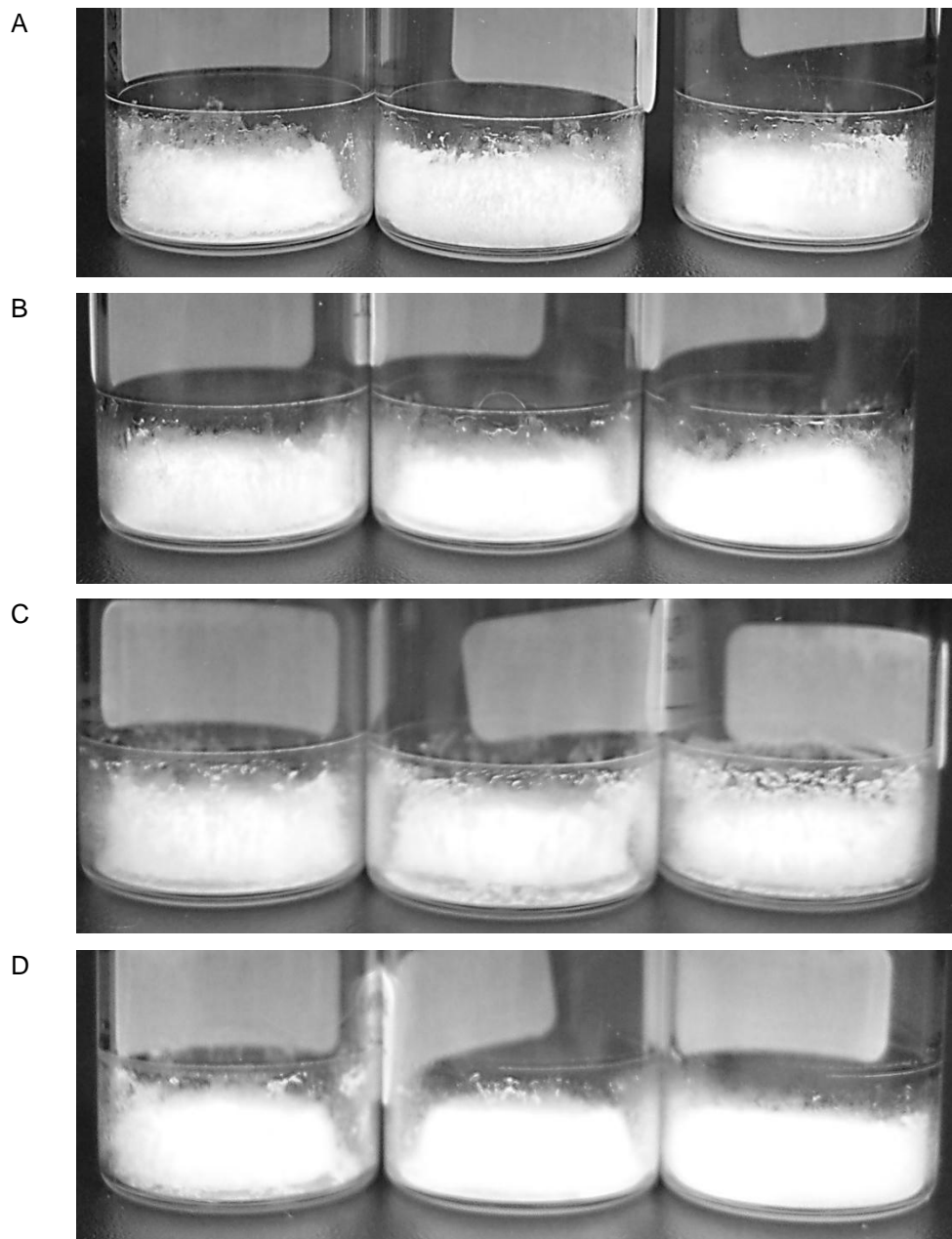


Figure II-23: Macroscopic appearance of collapse freeze-dried cakes. A: MabR1 + 1 % Sucrose; B: MabR1 + 1 % Sucrose + 0.1 % HP β CD; C: MabR1 + 1 % Sucrose + 0.6 % HP β CD; D: MabR1 + 1 % Sucrose + 0.004 % PS80.

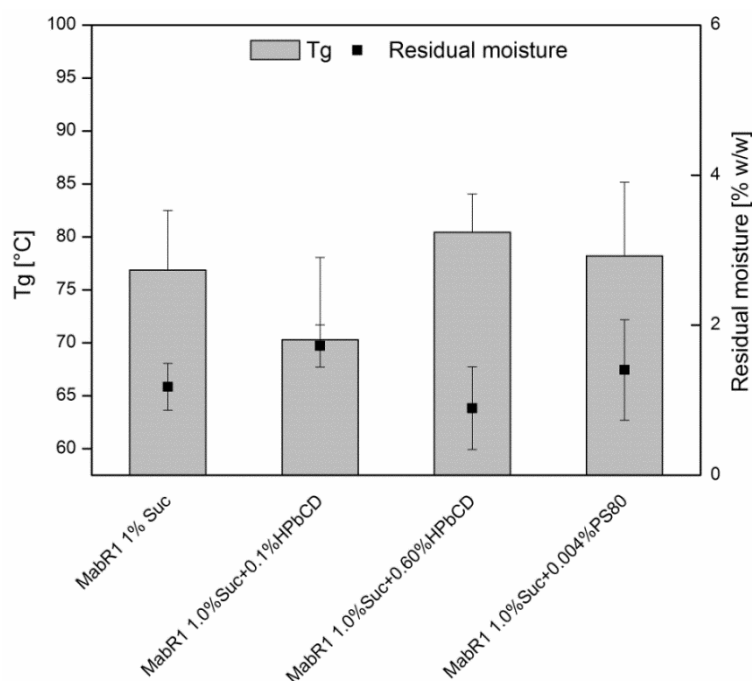


Figure II-24: Glass transition temperatures and residual moisture of collapse freeze-dried lyophilizates.

II.3.3.6 SUMMARY AND DISCUSSION

Most interestingly, it could be shown in this study that the freeze-drying process has a positive impact on protein stability despite or even due to collapse of the cake. As suggested in the previous chapter II.3.2, HPβCD was not able to stabilize the antibody at the liquid-air interface in a similar mechanism as PS80. However, if this interface is being decreased, as performed in this study by collapse of the lyophilized cake, successful stabilization of the antibody can be obtained, at least immediately after drying. By decreasing specific surface area of the freeze-dried product, the fraction of protein located at this interface is also decreased and upon reconstitution, the amount of protein prone to aggregation is reduced. This was not only true for the formulation containing HPβCD but also for the formulation containing sucrose, which also showed less particles than with conventional freeze-drying. Aggregation of the interface-sensitive MabR1 can be effectively mitigated by HPβCD during freeze-thawing as well as during reconstitution, if the interface is not too large. The concentration of 0.6 % (w/v) showed best subvisible particle concentrations compared to the lower concentration of 0.1 %. The mechanism by which HPβCD stabilizes must be different than that provided by polysorbates. Furthermore, placebo particles of HPβCD, which were present in the conventional freeze-dried samples, were eliminated by the collapse freeze-drying process. By decreasing specific surface area, one may expect longer reconstitution times, since the wetted area of the lyophilized cake becomes smaller. At least in this study, reconstitution times were not much prolonged and also residual moisture as well as glass transition temperatures both were in acceptable ranges. However, the reconstitution time may be responsible also for the improved

stability of MabR1 in collapsed samples, which has been shown in another study with interferon- γ to be beneficial for protein refolding. When reconstitution time was slowed by reconstitution with a solution of polysorbate 20 [59] or by a different way of preparation, spray-freeze-drying, less aggregation of interferon- γ was observed [60]. The authors speculate that, by slower dissolution, less air is entrapped in the liquid, thus creating a less large air-liquid interface, at which the protein can adsorb and degrade. In addition, a prolonged dissolution time decreases maximum protein concentration of intermediate-state, aggregate-competent protein, thus allowing these proteins species to refold [59].

II.3.4 CONTROLLED NUCLEATION FREEZE-DRYING OF MABR1

In the collapse freeze-drying experiments, we observed that the formulations of 1 % Sucrose as well as the combinations of 1 % Sucrose and HP β CD, especially in concentrations of 0.6 %, profited from a low specific surface area. Another possibility to create a low specific surface area is ice nucleation at high product temperatures and a low degree of super-cooling. We found that inducing ice nucleation at a high product temperature of around -4 °C followed by a long isothermal hold time results in the lowest achievable SSA (see section III.6). In this study, we wanted to find out, if MabR1 formulations also profit from controlled ice nucleation and intermediate to low SSAs.

II.3.4.1 LYOPHILIZATION PROCESS

Ice nucleation was induced at a product temperature of approximately -3.5 °C and was followed by a 2h isothermal hold post-nucleation to allow slow crystallization and Ostwald ripening to create a SSA as low as possible. Ice nucleation was induced within several seconds and 100 % of vials were nucleated. After approximately 90 minutes, phase transformation from water to ice was finished, as indicated by convergence of the product temperature sensors with the shelf temperature. Temperature probes were placed into water to only monitor the product temperature during the ice nucleation process; hence drying steps were excluded from Figure II-25.

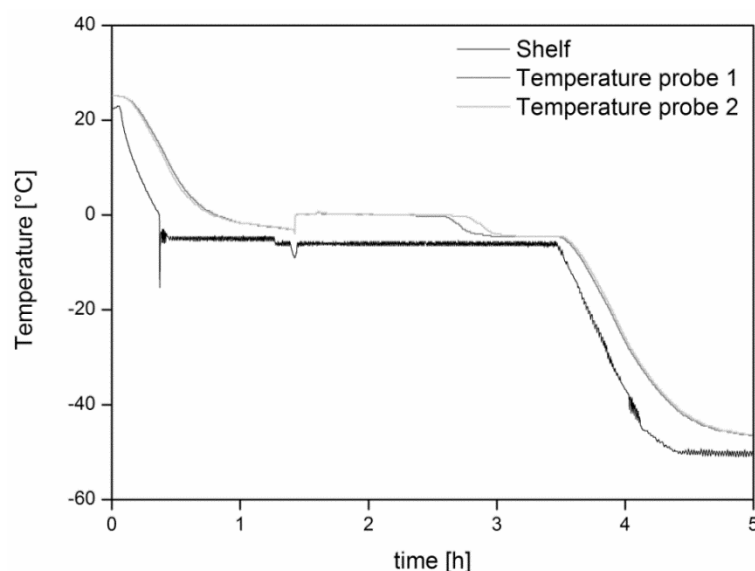


Figure II-25: Magnification of the freezing step of the controlled nucleation lyophilization run. Both temperature probes were placed in water to monitor product temperature before induction of ice nucleation.

II.3.4.2 PROTEIN STABILITY– SUBVISIBLE PARTICLES AND TURBIDITY

Controlled ice nucleation leads to a reduction in specific surface area to intermediate values between conventional and collapse freeze-drying. Both formulations investigated in this study

profited from the decrease in SSA, which is shown in Figure II-26. As SSA could not be decreased as low as with collapse drying ($\sim 0.15 \text{ m}^2/\text{g}$, section II.3.3.5) but was significantly lower than with conventional freeze-drying ($\sim 1.5 \text{ m}^2/\text{g}$, section II.3.1.5), controlled nucleation also lead to intermediate particle levels for both formulations. The formulation with 0.6 % HP β CD profited more from lowering of SSA and also subvisible particles formed by HP β CD in the placebo formulation were reduced, as displayed in Figure II-27.

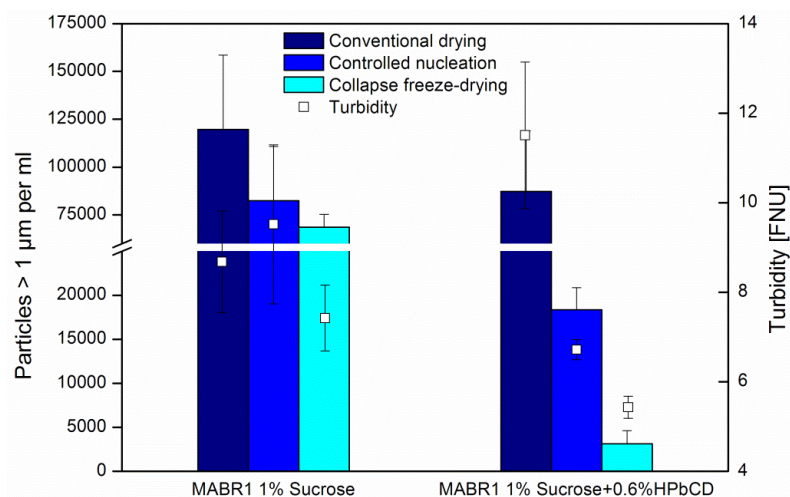


Figure II-26: Overview of subvisible particles > 1 µm and turbidity for different drying processes for the formulations of MabR1 and 1 % Sucrose with and without the addition of 0.6 % HP β CD.

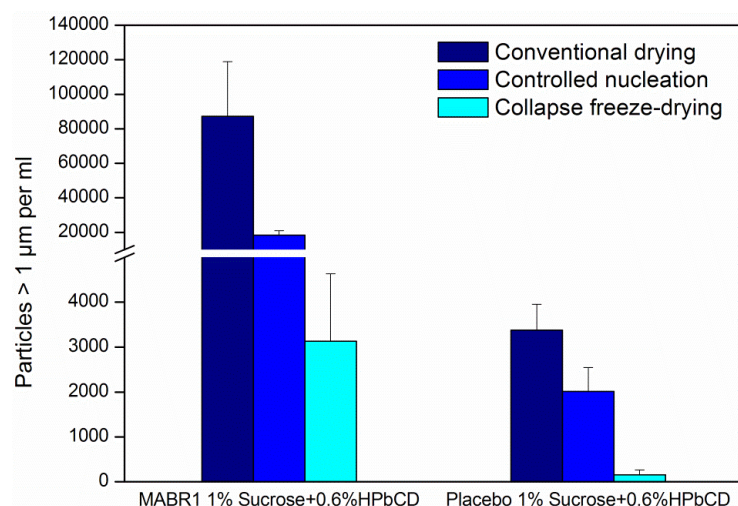


Figure II-27: Comparison of subvisible particles > 1 µm of the Formulations 1 % Sucrose and 0.6 % HP β CD with MabR1 and without MabR1 (Placebo).

II.3.4.3 SIZE-EXCLUSION CHROMATOGRAPHY

In agreement with the previous studies on MabR1, only minor changes in dimer or monomer content were observed in size-exclusion chromatography after lyophilisation and rehydration (t2), as shown in Table II-10. However, a small increase of relative amount of high-molecular-

weight aggregates as well as dimer was observed after freeze-drying and rehydration compared to samples after preparation (t₀) for both formulations studied.

Table II-10: Relative amount of protein species as determined with SE-HPLC for several freeze-drying processes of MabR1. t₀ = after preparation, t₂: after freeze-drying and rehydration.

		HMWA	Dimer	Monomer	Fragment
Controlled nucleation FD (with 2h post-nucleation hold)					
MabR1 + 1 % Sucrose	t ₀	0.09 ± 0.01	4.43 ± 0.04	94.24 ± 0.05	1.23 ± 0.03
	t ₂	0.22 ± 0.01	4.60 ± 0.02	94.31 ± 0.07	0.87 ± 0.04
MabR1 + 1 % Sucrose + 0.6 % HPβCD	t ₀	0.09 ± 0.01	4.44 ± 0.01	94.22 ± 0.06	1.25 ± 0.07
	t ₂	0.22 ± 0.01	4.57 ± 0.03	94.29 ± 0.09	0.93 ± 0.06
Collapse FD					
MabR1 + 1 % Sucrose	t ₀	- -	2.71 ± 0.04	95.45 ± 0.07	1.84 ± 0.04
	t ₂	- -	2.36 ± 0.02	95.79 ± 0.02	1.86 ± 0.04
MabR1 + 1 % Sucrose + 0.6 % HPβCD	t ₀	- -	2.77 ± 0.02	95.42 ± 0.06	1.81 ± 0.04
	t ₂	- -	2.25 ± 0.08	95.82 ± 0.05	1.93 ± 0.12
Conventional FD					
MabR1 + 1 % Sucrose	t ₀	- -	2.60 ± 0.32	96.02 ± 0.09	1.38 ± 0.23
	t ₂	- -	2.24 ± 0.02	96.12 ± 0.05	1.64 ± 0.07
MabR1 + 1 % Sucrose + 0.6 % HPβCD	t ₀	- -	2.78 ± 0.07	95.97 ± 0.14	1.26 ± 0.07
	t ₂	- -	2.32 ± 0.04	96.09 ± 0.03	1.59 ± 0.01

II.3.4.4 PHYSICO-CHEMICAL CHARACTERIZATION OF LYOPHILIZATES

Freeze-drying with controlled nucleation resulted in a decrease of specific surface area compared to conventional freeze-drying. As there is an inverse correlation between SSA and residual moisture [61], a low SSA leads to increased residual moistures if secondary drying is not adjusted, which was also the case here. Nevertheless, residual moistures were around 1 % and also glass transition temperatures were acceptable with T_gs of > 60 °C. Reconstitution times were less than 10 s for all formulations.

Table II-11: Glass transition temperatures, residual moisture and specific surface area for both formulations in the controlled nucleation freeze-drying run.

Formulation	T _g [°C]	Residual moisture [% w/w]	SSA [m ² /g]
MabR1 + 1% Sucrose	66.00 ± 4.063	1.186 ± 0.121	0.531
MabR1 + 1 % Sucrose + 0.6 % HPβCD	74.73 ± 4.539	0.952 ± 0.056	0.588 ± 0.188

Lyophilizate cakes appeared different than conventional freeze-dried ones with some crack formation and shiny surfaces as shown in Figure II-28. However, both formulations as well as placebo controls were fully amorphous with no detectable peaks in the x-ray powder diffraction patterns (see Figure II-29).



Figure II-28: Macroscopic appearance of lyophilizate cakes of formulation MabR1 + 1 % Sucrose (A) and MabR1 + 1 % Sucrose + 0.6 % HPβCD (B).

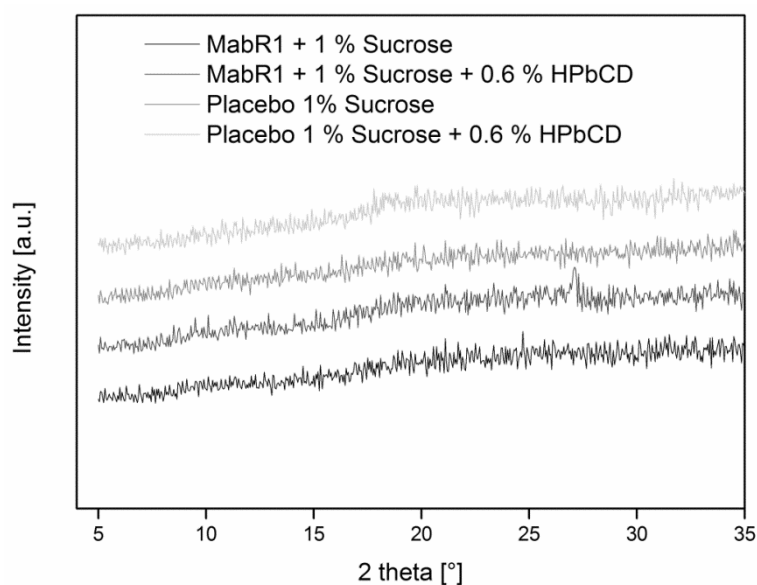


Figure II-29: Results from XRD for controlled nucleation freeze-drying samples.

II.3.4.5 SUMMARY AND DISCUSSION

Controlled nucleation at a relatively high product temperature of $-3.5\text{ }^{\circ}\text{C}$ lead to intermediate specific surface areas and also intermediate particle levels compared to collapse freeze-drying and conventional freeze-drying. At least for MabR1, a good correlation of the SSA and the subvisible particle number could be observed for the formulations without a surfactant and 0.6 % HP β CD and this correlation could also be established for the placebo particles formed by HP β CD. Currently, controlled nucleation is the easiest possibility to create lyophilizates with a low SSA and a freeze-dried cake featuring “elegance”. However, at least with the freezing protocol applied here to achieve the lowest possible specific surface area, a slight increase of high-molecular weight aggregates was observed. With this result in mind, it is not reasonable to use a thermal treatment step, also called annealing, to decrease SSA. Annealing is known to foster ice crystal growth by keeping the product temperature at a value above T_g' and smaller ice crystals melt in favour of larger ones, an interfacially driven process. However, during the hold step at $T_p > T_g'$, freeze-concentration-associated stress is exerted on the product. In this study, this was possibly the case when crystallization proceeds post-nucleation and the fraction of HMWAs was slightly increased. This would have most likely also been observed with a thermal treatment step but was not observed in the other studies of MabR1 without controlled nucleation. Of course, the long isothermal hold post-nucleation can be shortened or completely left out, if a product is sensitive towards freeze-concentration associated stresses.

II.3.5 STORAGE STABILITY OF MABR1 FORMULATED WITH 1 % SUCROSE

The previous chapters showed that a stable freeze-dried formulation of MabR1 in combination with HP β CD with acceptable subvisible particle levels, similar to the addition of polysorbate, can be obtained by collapse freeze-drying of those formulations. The next step is to investigate isothermal storage stability of those lyophilizates. Due to the high T_g s obtained for both formulations, high temperatures for storage stability were chosen for accelerated stability studies, 60 °C, 40 °C and 25 °C for the formulation of MabR1 with 1 % Sucrose and 0.004 % PS80 or 0.6 % HP β CD, respectively.

II.3.5.1 PROTEIN STABILITY – SUBVISIBLE PARTICLES AND TURBIDITY

After the freeze-drying process at t_0 , subvisible particles and turbidity were somewhat higher for both formulations than in the previous experiment in section II.3.3.2. For both formulations and temperatures of 60 °C and 40 °C, large standard deviations and an increase in subvisible particles were observed, especially for the formulation which contained 0.6 % HP β CD, which is displayed in Figure II-30 and Figure II-31. Only the formulation with PS80 which was stored at 25 °C showed almost unchanged particle levels and turbidity (see Figure II-32), which points to a general instability of both formulations at the chosen storage conditions. For the size class > 10 μ m, a similar picture was obtained with many particles and high standard deviations for the formulation which contained HP β CD, stored at 60 °C, as displayed in Figure II-33. For the PS80 formulation and the lower storage temperatures of the HP β CD formulation, particle concentrations were around 2000 per ml over storage time. Despite the huge standard deviations, the large amount of particles and the non-linearity of the particle concentrations, no visible particles could be detected by visual inspection. However, the results suggest that larger aggregates were formed by continuous degradation of the protein and may have been unnoticed due to the high turbidity observed.

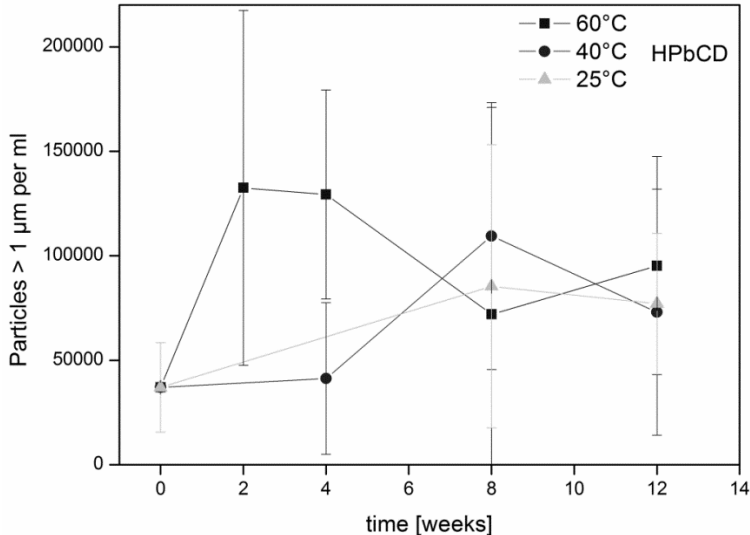


Figure II-30: Subvisible particles > 1 µm per ml for the formulation MabR1 + 1 % Sucrose + 0.6 % HPβCD stored at three different temperatures for 12 weeks.

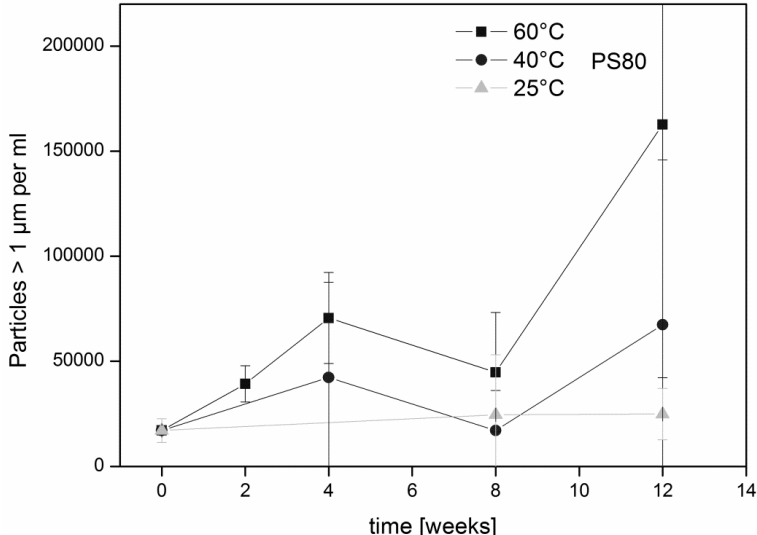


Figure II-31: Subvisible particles > 1 µm per ml for the formulation MabR1 + 1 % Sucrose + 0.004 % PS80 stored at three different temperatures for 12 weeks.

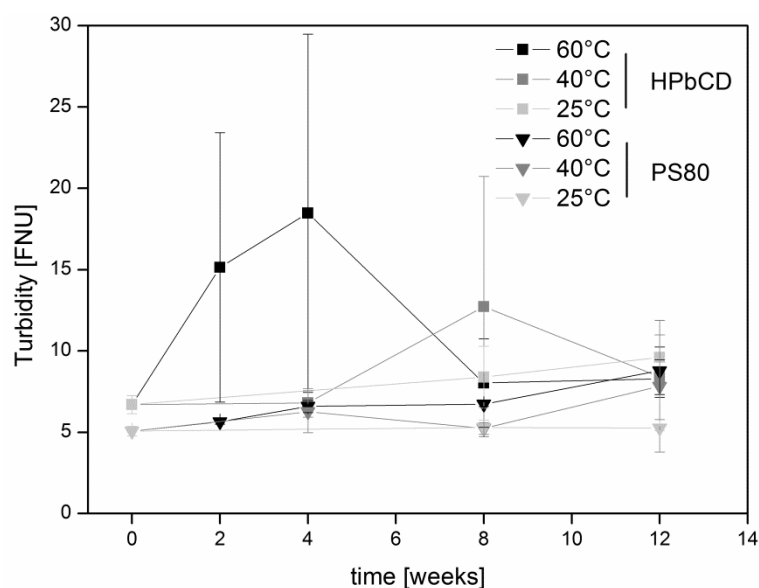


Figure II-32: Results from turbidity for both formulations at all timepoints and storage temperatures.

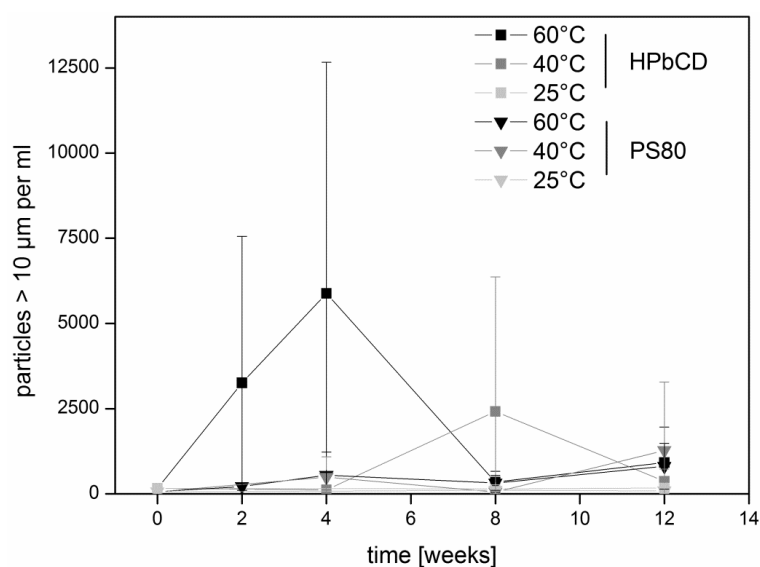


Figure II-33: Subvisible particles > 10 µm per ml for both formulations of MabR1 stored at three different temperatures for 12 weeks.

II.3.5.2 SIZE-EXCLUSION CHROMATOGRAPHY AND ASYMMETRICAL FLOW-FIELD-FLOW FRACTIONATION

Size-exclusion chromatography as well as asymmetrical flow-field-flow fractionation (AF4) showed a loss in relative monomer content for both formulations. The decrease in monomer content was most exaggerated at higher temperatures, especially at 60 °C. The formulation containing HPβCD showed a somewhat faster degradation than the Polysorbate 80 containing formulation as measured with SE-HPLC (Figure II-34). This trend was not observable in AF4 (Figure II-36). However, the formulation containing PS80 showed significantly more dimer formation in SE-HPLC and this trend was observable with both orthogonal methods, as shown in Figure II-35 and Figure II-37. At 40 °C, no significant difference between the formulations

was observed although both formulations showed an increase in dimer and a loss of monomer. At 25 °C, only minor changes in monomer content and dimer content could be detected with both methods. Total protein recovery as shown in Figure II-38 did not show significant differences between formulations, time points and storage temperatures, suggesting that the minor changes in AUC which were observed are method artefacts.

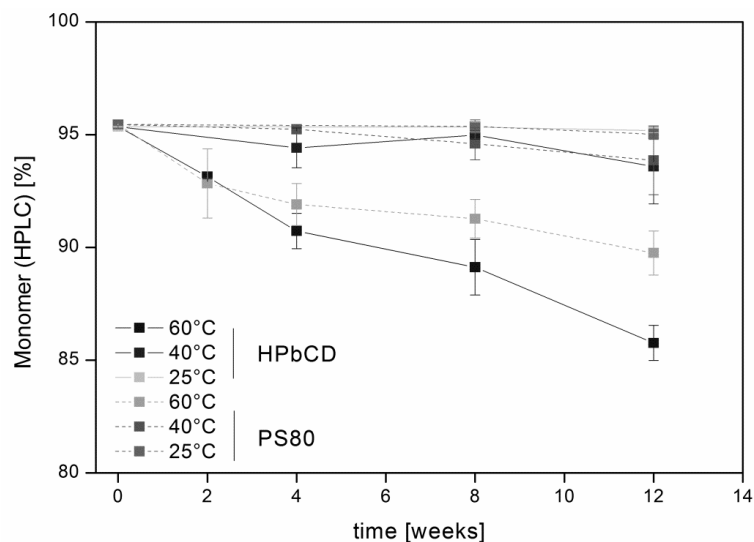


Figure II-34: Relative MabR1 monomer content as determined by SE-HPLC for both formulations stored at three different temperatures for 12 weeks.

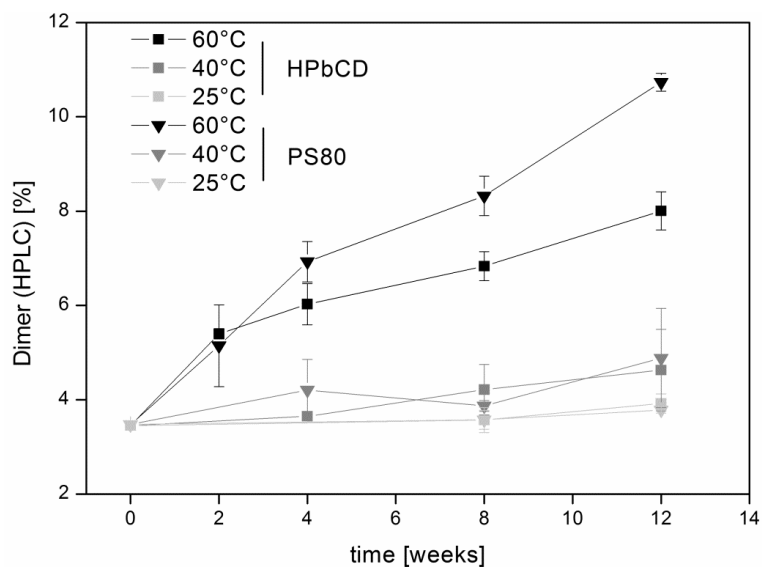


Figure II-35: Relative MabR1 dimer content as determined by SE-HPLC for both formulations stored at three different temperatures for 12 weeks.

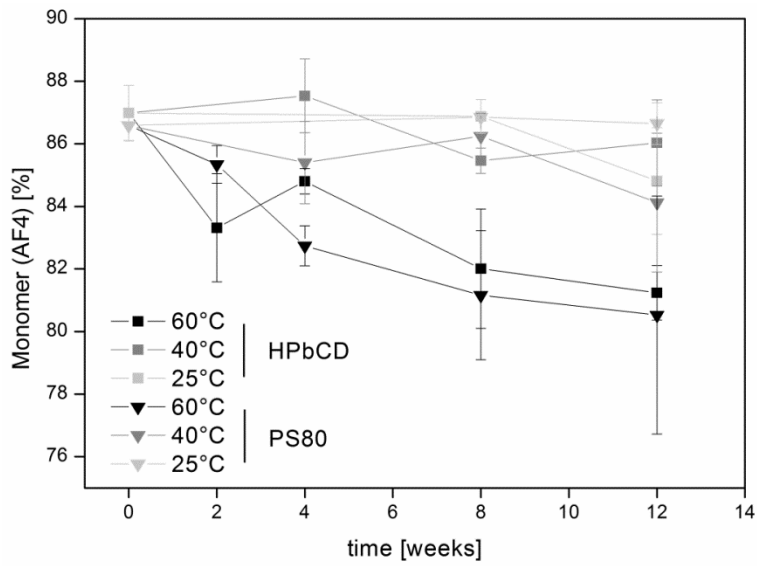


Figure II-36: Relative MabR1 monomer content as determined by AF4 for both formulations stored at three different temperatures for 12 weeks.

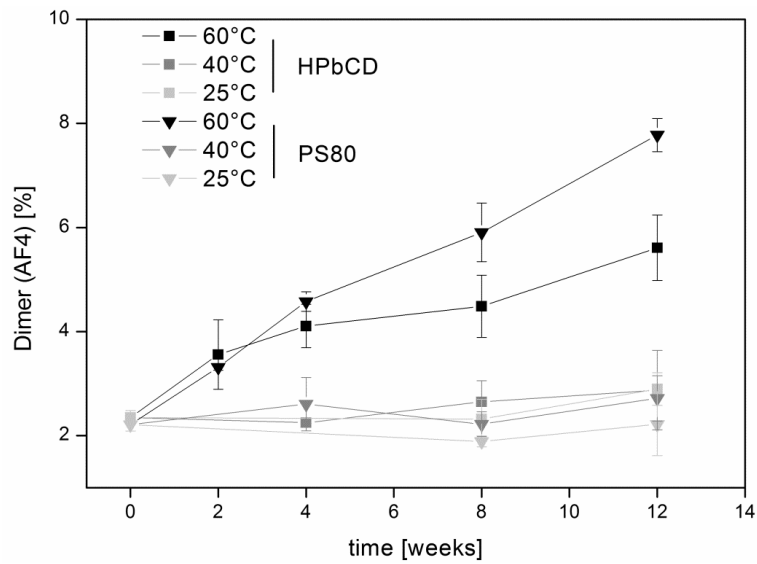


Figure II-37: Relative MabR1 dimer content as determined by AF4 for both formulations stored at three different temperatures for 12 weeks.

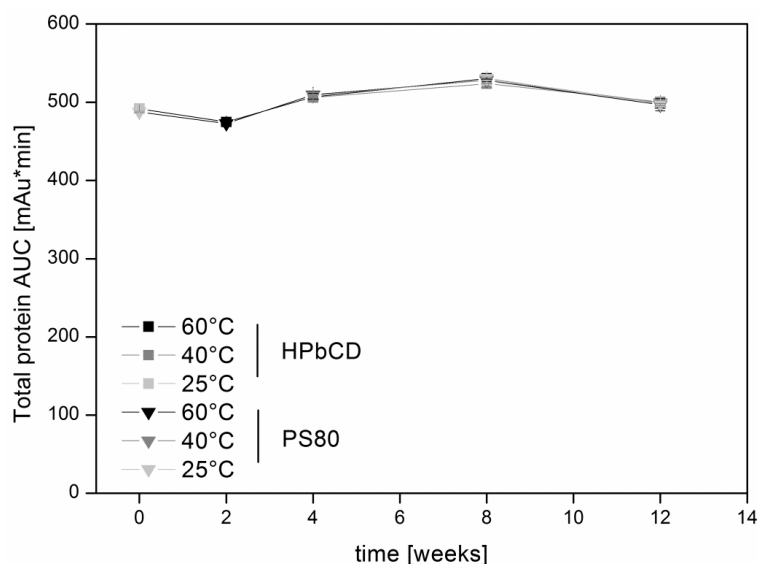


Figure II-38: Total protein recovery as determined with SE-HPLC for both formulations at all timepoints at three different storage temperatures.

II.3.5.3 FTIR SPECTROSCOPY

Although a lot of subvisible particles were formed and SE-HPLC as well as AF4 indicate substantial dimer formation with accompanying loss of monomer, no changes in FTIR spectra could be observed and correlation coefficients remained unchanged, as shown in Figure II-40. These findings suggest that no changes in protein secondary structure were occurred in degradation of MabR1 and no intermolecular β -sheets have been formed during storage in the dried state. Also, visible comparison of spectra showed no significant differences, as shown for representative spectra of t0 (after freeze-drying) and stored for 12 weeks at 60 °C (t4) in Figure II-39.

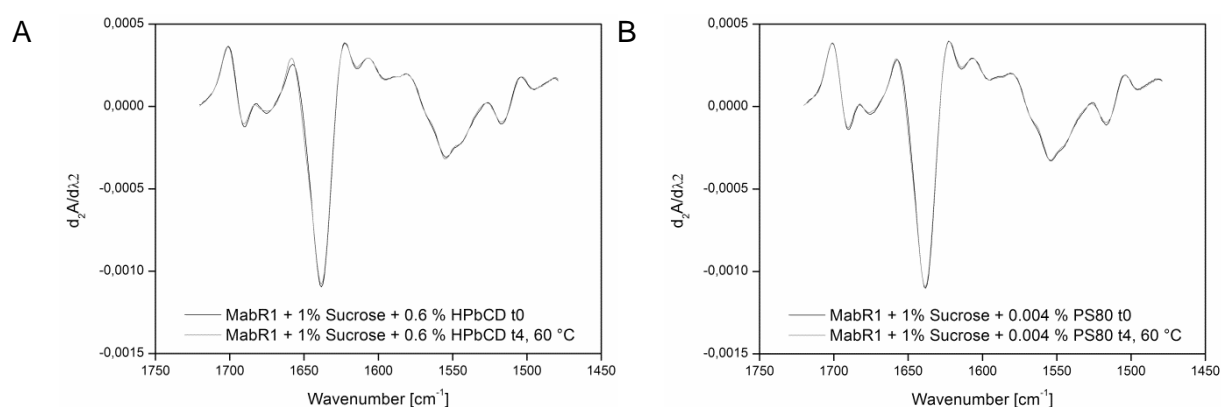


Figure II-39: Representative 2nd derivative FTIR spectra for HPβCD-containing formulations (A) and PS80-containing formulations (B) at t0 (after freeze-drying) and stored for 12 weeks at 60 °C (t4).

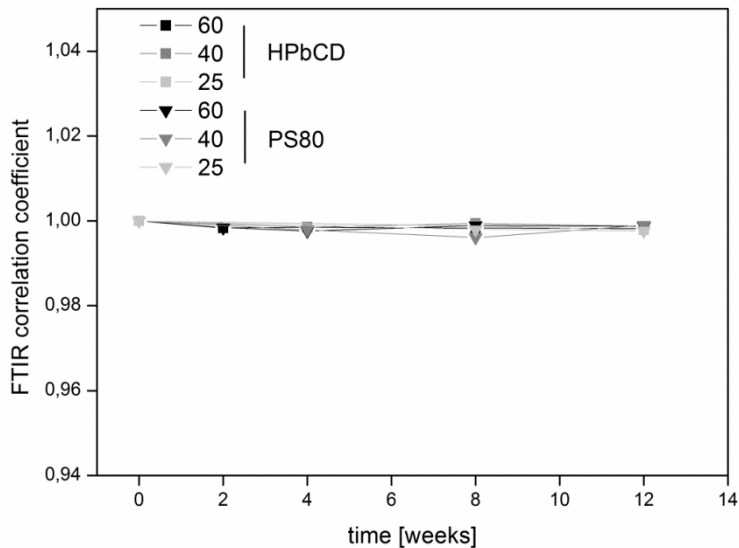


Figure II-40: FTIR correlation coefficients for both formulations at all timepoints at three different storage temperatures.

II.3.5.4 PHYSICO-CHEMICAL CHARACTERIZATION OF LYOPHILIZED CAKES

During storage, residual moisture slightly increased within all samples, as shown in Figure II-41, especially with higher temperatures from 0.4 % to approximately 1.0 % to 1.5 %. Although stoppers were dried after steam-sterilization, a certain uptake of water vapour cannot be completely avoided and for these formulations with a low concentration of solutes, already an uptake of some μg results in an increase in residual moisture, which is stated as relative mass of water per total mass. However, the uptake of water did neither result in a significant decrease of the glass transition temperature which were all above $70\text{ }^{\circ}\text{C}$ nor in a change in specific surface area, as shown in Figure II-42 and Figure II-43. Reconstitution times were approximately 10 seconds followed by schlieren for around 60 seconds and were unchanged over storage time.

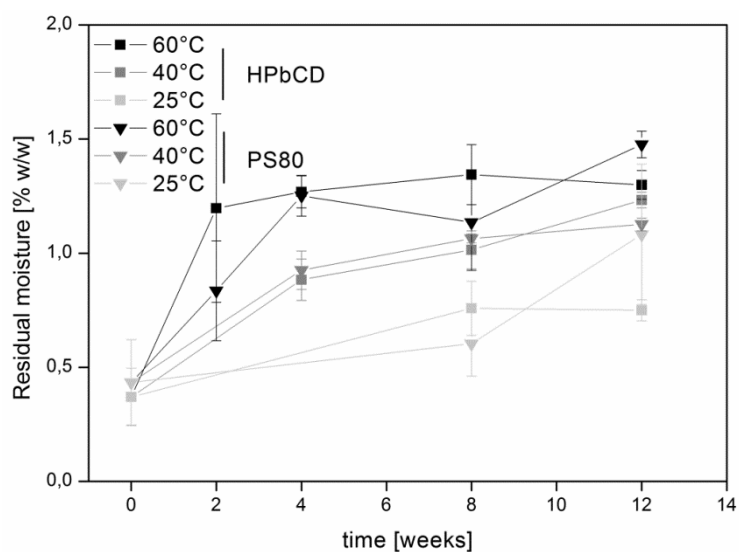


Figure II-41: Residual moisture for both formulations stored at three different temperatures for 12 weeks.

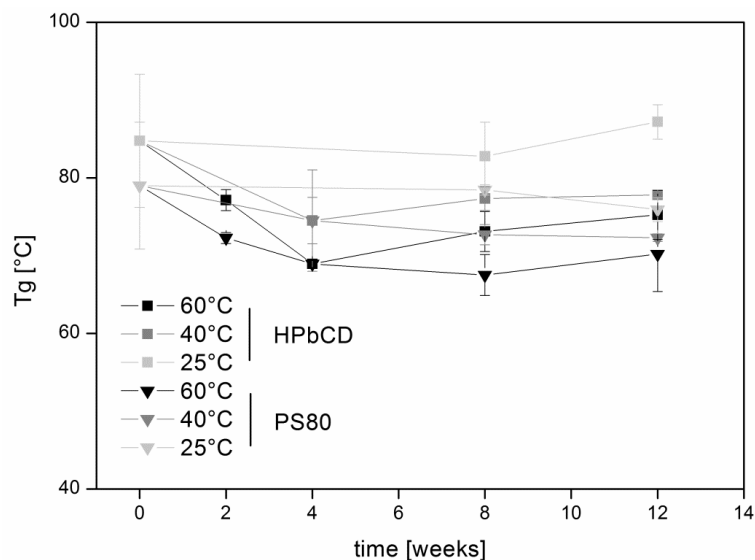


Figure II-42: Glass transition temperatures of both formulations stored at three different temperatures over storage time.

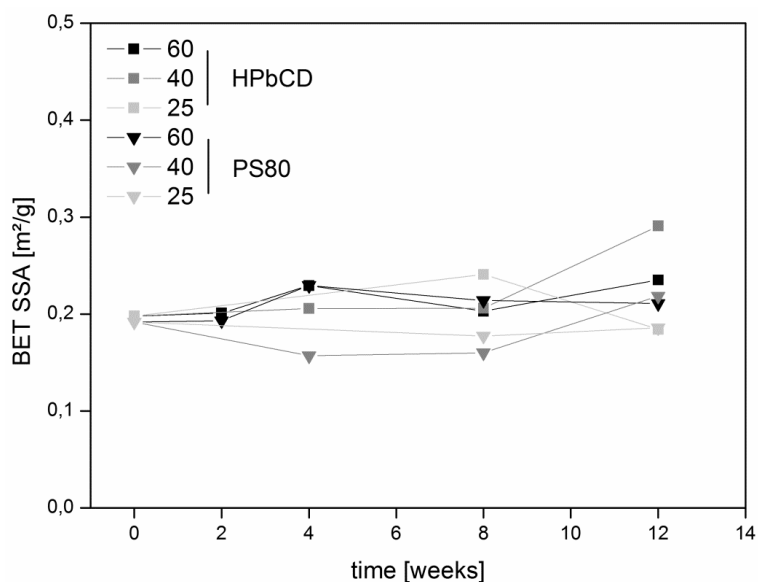


Figure II-43: Specific surface area for both formulations stored at three different temperatures for 12 weeks.

II.3.5.5 DISCUSSION AND SUMMARY

During storage of the two formulations employed in this study, degradation of the antibody MabR1 was observed, especially at the storage temperatures of 60 °C and 40 °C. At these temperatures, degradation of the antibody was also confirmed by size-exclusion chromatography and asymmetrical flow-field-flow fractionation. The formation of dimer during storage of lyophilizates is usually prevented by a lyoprotectant such as sucrose or trehalose and is less dependent on interface areas which were very low due to the collapse freeze-drying process. In this study, as already mentioned, a very low amount of sucrose was used to create challenging conditions for the formulation study; however, during storage of the lyophilizates,

the concentration of sucrose was possibly too low to achieve sufficient stabilization of the protein. In the next studies, the concentration of sucrose will be increased to create storage stable lyophilizates.

II.3.6 CONTROLLED NUCLEATION FREEZE-DRYING OF MABR1 FORMULATED WITH 5 % SUCROSE

The stability study of MabR1 formulated with 1 % sucrose in combination with 0.6 % HP β CD or 0.004 % PS80 had shown that only poor stability of the lyophilizates was obtained, especially at 60 °C, but also at 40 °C an increase in dimer formation was observed. These findings indicate that the protein-to-sugar mass ratio of 1:1 was not enough and as a next step, we increased this ratio to 1:5 (m/m) and employed controlled ice nucleation at low degrees of super-cooling to reduce SSA. MabR1 was formulated at 10 mg/ml with 5 % Sucrose and 0 %, 0.35 % and 0.60 % of HP β CD was added. 0.004 % polysorbate 80 instead of HP β CD served as positive control. Protein stability was assessed directly after the freeze-drying process and rehydration (t₂) and compared to pre-process formulations (t₀).

II.3.6.1 FREEZE-DRYING PROCESS

Ice nucleation was induced at a product temperature of approximately -5 °C followed by an isothermal hold post-nucleation of -8 °C for 2 hours, as shown in Figure II-44. Secondary drying temperature was increased to 35 °C, to achieve residual moisture levels of around 1 % (w/w) as obtained for the formulations based on 1 % sucrose similar as in chapter 0. Table II-12 shows product temperatures during steady-state primary drying of the formulations containing HP β CD. Primary drying is finished for all formulations after approximately 26 hours.

Table II-12: Product temperatures (T_p) of 4 formulations during steady-state freeze-drying (5 h after constant shelf temperature of -20 °C).

Formulation	T_p after 5h of primary drying [°C]	Primary drying duration [h]
MabR1 + 5 % Sucrose + 0.6 % HP β CD	-39.0	24.6
MabR1 + 5 % Sucrose + 0.35 % HP β CD	-39.3	24.9
5 % Sucrose + 0.6 % HP β CD	-39.8	21.6
5 % Sucrose + 0.35 % HP β CD	-40.0	25.7

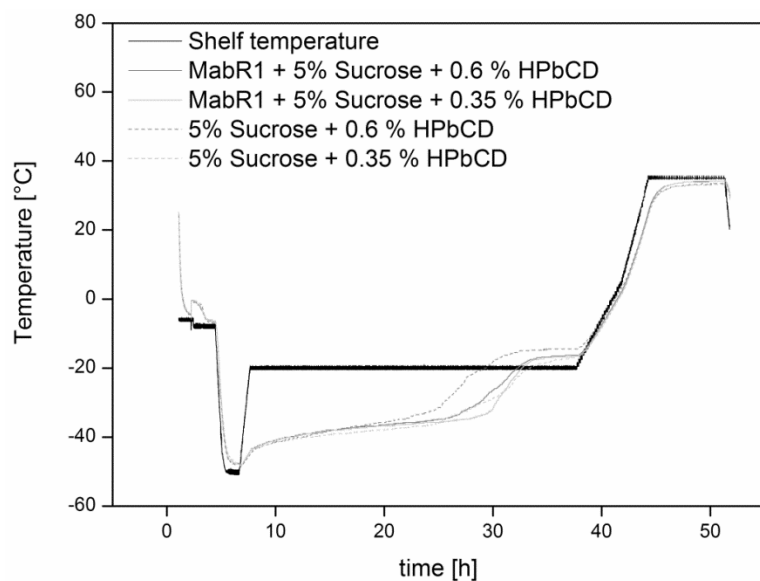


Figure II-44: Controlled nucleation freeze-drying run of MabR1 formulated with 5 % Sucrose. Thermocouples were placed in formulations of 5 % Sucrose with 0.35 % or 0.6 % HP β CD and with MabR1 or with placebos only.

II.3.6.2 PROTEIN STABILITY IMMEDIATELY AFTER FREEZE-DRYING – SUBVISIBLE PARTICLES AND TURBIDITY

After freeze-drying and rehydration the formulation containing 5 % Sucrose in combination with 0.004 % PS80 showed lowest particulate concentrations and turbidity as shown in Figure II-45. Further, the formulation containing no surfactant showed slightly less particles than both formulations containing HP β CD. Having a closer look on placebo particles, it was observed that both HP β CD formulations showed significantly higher concentrations of subvisible particles than the formulations without HP β CD. Interestingly, the placebo formulation showed higher particle levels than the corresponding antibody formulation. It is difficult to compare antibody formulations with the placebo formulation, since the situation at the interface is probably completely different. However, placebo particles formed by HP β CD probably contribute to the total amount of particles in the antibody formulation. The number of placebo particles formed in the antibody formulation is probably a lot lower, as it is suggested by Figure II-45. Besides that, the increase in sucrose concentration also leads to a great reduction in subvisible particles compared to the formulation with 1 %, as shown in section II.3.4. Particle concentrations > 10 μm were higher with 5 % sucrose only compared to the formulations containing HP β CD or PS80, as displayed in Table II-13. The formulation with PS80 showed the lowest amount of subvisible particles also in the size class > 10 μm .

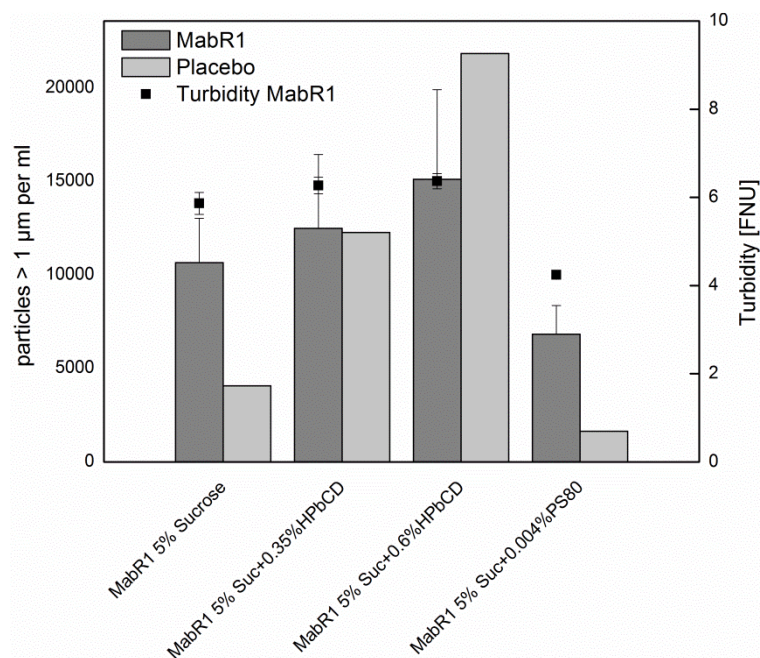


Figure II-45: Subvisible particles and turbidity after rehydration for controlled-nucleation freeze-drying of MabR1. The light grey bars show particles of formulations without protein.

Table II-13: Subvisible particles > 10 µm for all formulations.

Formulation	Subvisible particles > 10 µm per ml
MabR1 + 5 % Sucrose	190 ± 77
MabR1 + 5 % Sucrose + 0.35 %HPβCD	104 ± 31
MabR1 + 5 % Sucrose + 0.6 % HPβCD	103 ± 47
MabR1 + 5 % Sucrose + 0.004 % PS80	22 ± 4

II.3.6.3 SIZE-EXCLUSION CHROMATOGRAPHY

As already observed in the other studies, no significant changes in relative protein amounts and no major changes in total AUC were detected after lyophilization and rehydration, as shown in Figure II-46 and Figure II-47.

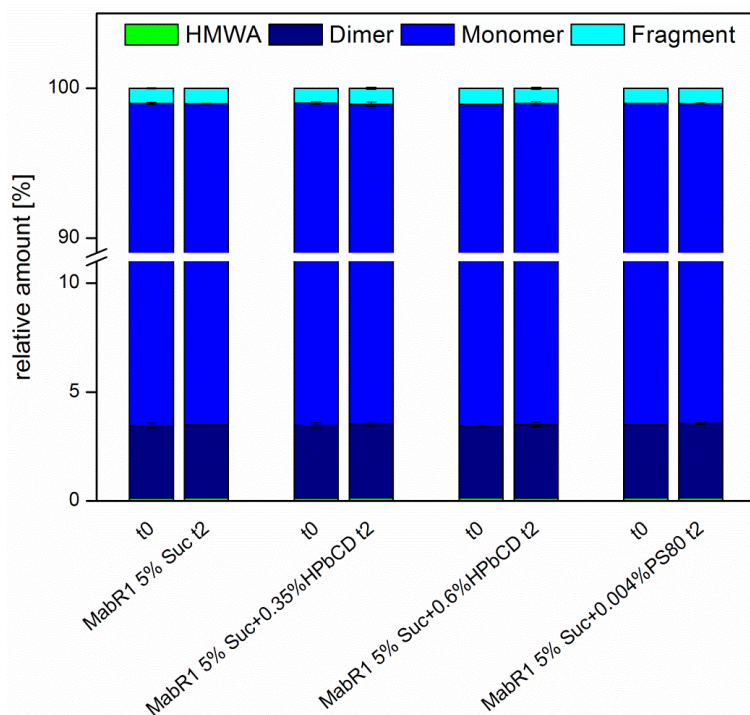


Figure II-46: Relative amount of high-molecular weight aggregates (HMWA), dimer, monomer and fragment for all formulations after preparation (t0) and after freeze-drying and rehydration (t2).

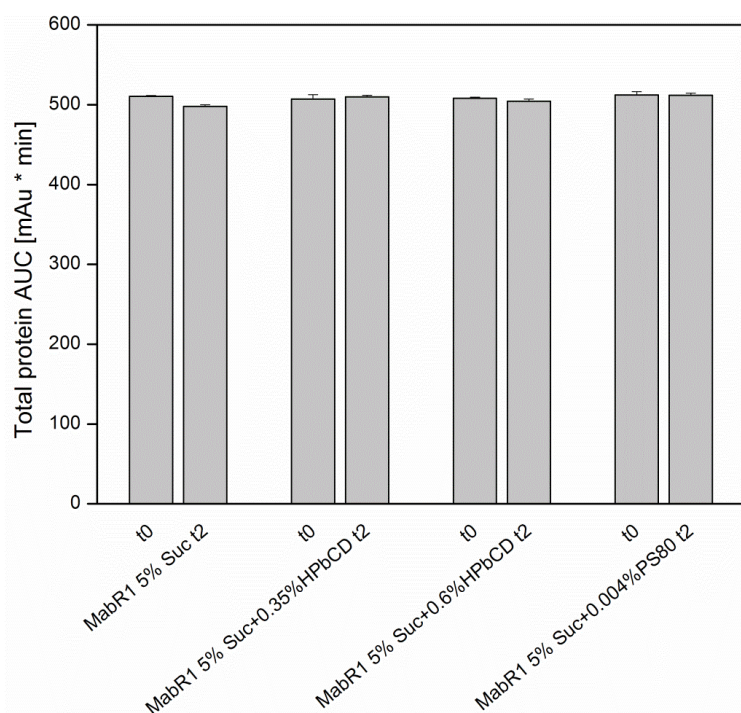


Figure II-47: Total protein AUC for all formulations after preparation (t0) and after freeze-drying and rehydration (t2).

II.3.6.4 PHYSICO-CHEMICAL CHARACTERIZATION OF LYOPHILIZATES

Residual moisture for freeze-dried MabR1 with 5 % Sucrose was between 1.0 and 1.25 % and specific surface area was between 0.4 and 0.5 m²/g, as shown in Table II-14. Glass transition temperatures were approximately 60 °C. Although these values were quite similar to those for the formulations with 1 % sucrose (see section II.3.4), it should be stated that specific surface area is mass normalized. Due to the higher amount of solids in the 5 % Sucrose formulations, the absolute surface area is increased in those formulations compared to the 1 % Sucrose based formulations.

Table II-14: Residual moisture, glass transition temperatures (T_g) and specific surface area (SSA) for all formulations after lyophilization.

	Residual moisture [% w/w]	BET SSA [m ² /g]	T _g [°C]
MabR1 + 5 % Sucrose	1.22 ± 0.01	0.44 ± 0.08	64.0
MabR1 + 5 % Sucrose + 0.35 % HPβCD	1.12 ± 0.06	0.42 ± 0.02	58.2
MabR1 + 5 % Sucrose + 0.6 % HPβCD	1.04 ± 0.04	0.415	-
MabR1 + 5 % Sucrose + 0.004 % PS80	1.16 ± 0.15	0.50 ± 0.01	63.2

II.3.6.5 SUMMARY AND DISCUSSION

By increasing the amount of sucrose to 5 % w/v, an interesting observation could be made. While the formulation containing polysorbate was the best formulation with regard to subvisible particles after freeze-drying, the results for the HPβCD formulations were somewhat unexpected with similar amounts of subvisible particles than the control formulation containing 5 % sucrose. However, it is very difficult to distinguish between proteinaceous and HPβCD particles, which would have been very helpful in this study because a significant amount of placebo particles of HPβCD was observed in the formulations without MabR1. Although controlled nucleation was able to significantly reduce the specific surface area of the freeze-dried formulations compared to conventional freeze-drying, the absolute surface areas become higher by increasing the mass of solutes. Hence, compared to the studies with controlled nucleation from section II.3.4, the total surface area for the formulations in this study is approximately 2.5-fold higher. As observed in the previous chapters, HPβCD is able to stabilize the model antibody if the surface area is very small as with collapse freeze-drying. Generally, the increase in sucrose concentration from 1 % to 5 % was beneficial for MabR1 stability. After ice nucleation, freeze-concentration takes place and the protein is diluted in an amorphous matrix formed by sucrose. By increasing the amount of amorphous stabilizer, the protein gets more diluted and aggregation is therefore hindered. It has been found that 0.3 M,

which equals approximately 10 % (w/v) for disaccharides, is the minimum needed concentration [4]. For LDH, it has been shown that increasing concentrations of sucrose can increase recovery of the enzyme and best recovery was obtained with a sucrose concentration as high as 34 % [62]. More examples are summarized in the review by Wang [1]. While these results may not be true for any protein, an increase in sucrose concentration was also beneficial in this study; however, the addition of PS80 could further decrease subvisible particles indicating that interfacial degradation of MabR1 still is a major degradation pathway.

II.3.7 COLLAPSE FREEZE-DRYING OF 5 % SUCROSE

After the controlled nucleation experiment with the formulations containing 5 % sucrose in section II.3.6, the effect of the increased concentration of the disaccharide was already visible with regard to subvisible particles and a positive impact of PS80 was observed. Placebo particles formed by HP β CD dominated the results for the controlled nucleation study. Thus, a collapse freeze-drying run is expected to eliminate placebo particle formation and the effect of HP β CD is expected to be more reliably observed.

II.3.7.1 LYOPHILIZATION PROCESS

The collapse freeze-drying process was carried out at a pressure of 2.53 mbar (pirani sensor controlled) and product temperatures were approximately -13 °C for investigated formulations at a shelf temperature of 45 °C.

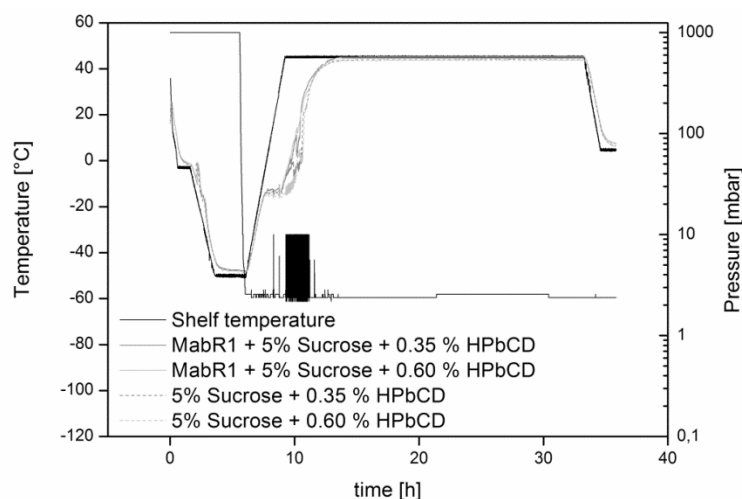


Figure II-48: Lyophilization process for collapse freeze-dried MabR1 with 5% Sucrose.

II.3.7.2 PROTEIN STABILITY – SUBVISIBLE PARTICLES AND TURBIDITY

After collapse freeze-drying of formulations of MabR1 with 5 % Sucrose, a similar picture was obtained as with the formulations containing 1 % Sucrose, as described in section II.3.3. All formulations profited from the collapse freeze-drying procedure with regard to total subvisible particle formation, however, formulations containing HP β CD and PS80 contained significantly less particles than the formulations without surfactant, as displayed in Figure II-49. Turbidity values were almost the same for all formulations. Furthermore, as expected, collapse freeze-drying eliminated particle formation also in placebo samples. Subvisible particles > 10 μ m were less than 55 per ml for all formulations as shown in Table II-15.

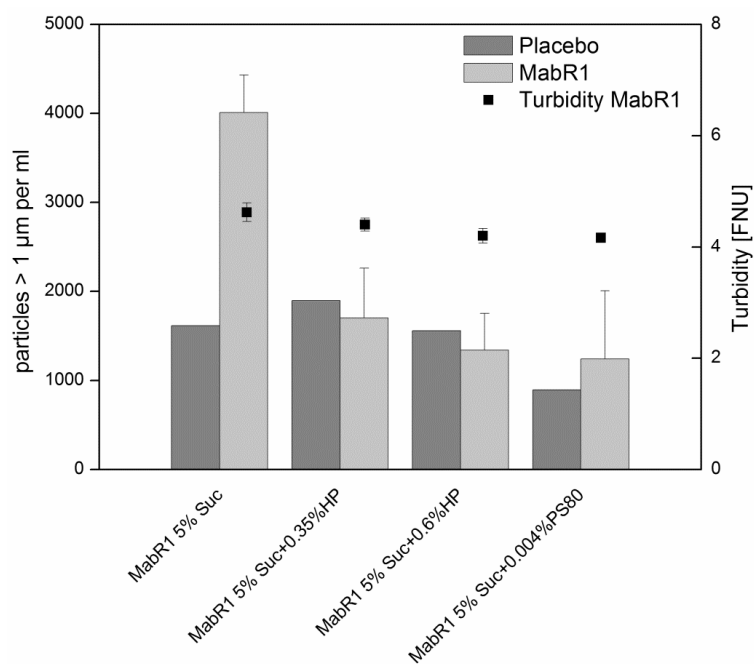


Figure II-49: Subvisible particles and turbidity after rehydration for collapse freeze-dried MabR1. The light grey bars show particles of formulations without protein.

Table II-15: Subvisible particles > 10 µm per ml for collapse freeze-dried MabR1.

Formulation	Subvisible particles > 10 µm per ml
MabR1 + 5 % Sucrose	23 ± 15
MabR1 + 5 % Sucrose + 0.35 % HPβCD	52 ± 57
MabR1 + 5 % Sucrose + 0.6 % HPβCD	10 ± 8
MabR1 + 5 % Sucrose + 0.004 % PS80	28 ± 27

II.3.7.3 SIZE-EXCLUSION CHROMATOGRAPHY

No changes in relative amounts of protein species could be observed, as shown in Figure II-50 and also, no change in total protein AUC was detected, as displayed in Figure II-51.

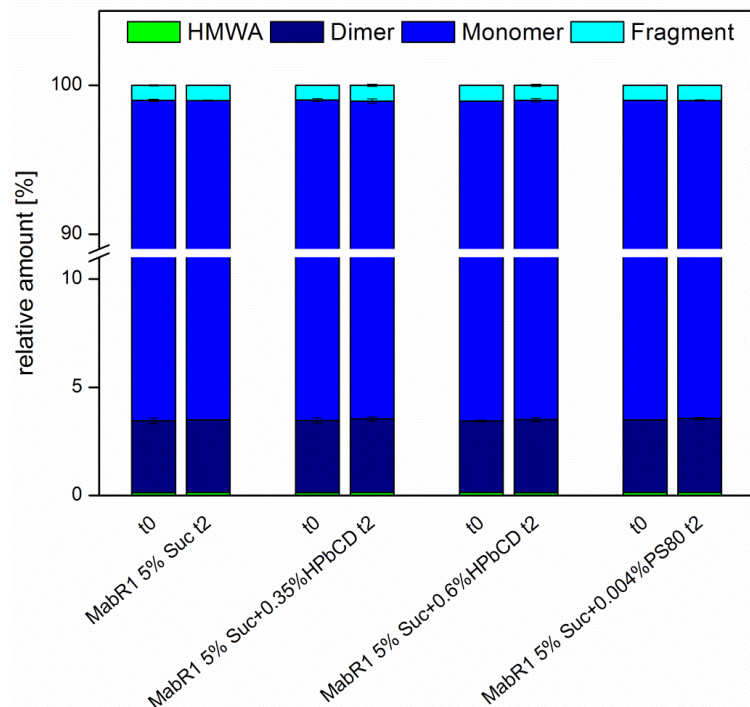


Figure II-50: Relative amount of protein species of MabR1 after preparation (t0) and collapse-freeze-drying and rehydration (t2).

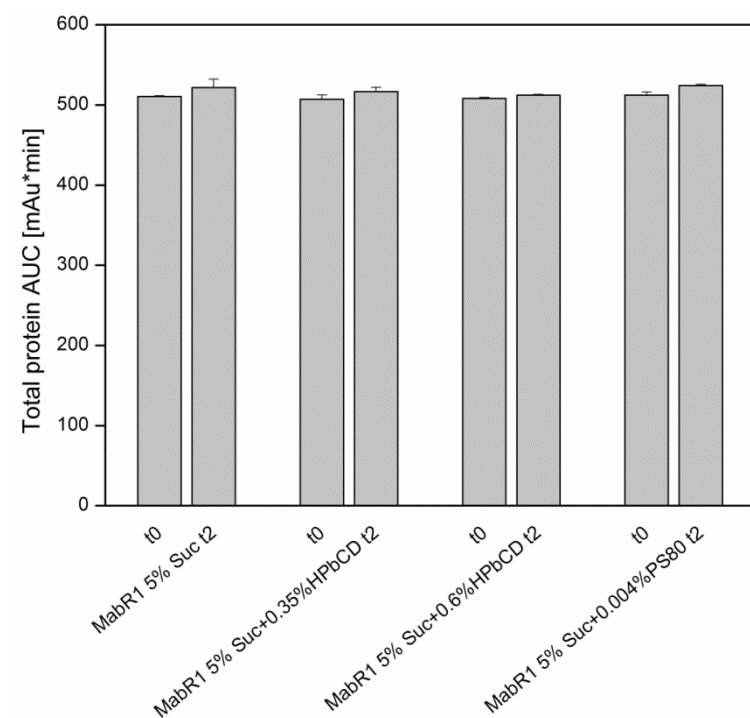


Figure II-51: Total protein AUC for collapse freeze-dried MabR1 after preparation (t0) and freeze-drying and rehydration (t2).

II.3.7.4 PHYSICO-CHEMICAL CHARACTERIZATION OF LYOPHILIZATES

Freeze-drying above T_c in this case resulted in very low specific surface areas of approximately $0.1 \text{ m}^2/\text{g}$. This very low SSA resulted in residual moistures of around 2 % [w/w] and in glass transition temperatures of $50 \text{ }^\circ\text{C}$ to $55 \text{ }^\circ\text{C}$, as displayed in Table II-16.

Table II-16: Residual moisture, SSA and glass transition temperatures (T_g) for all formulations of collapse freeze-dried MabR1.

	Residual moisture [% w/w]	BET SSA [m^2/g]	T_g [$^\circ\text{C}$]
MabR1 + 5 % Sucrose	2.21 ± 0.16	0.09	51.3 ± 1.5
MabR1 + 5 % Sucrose + 0.35 % HP β CD	1.84 ± 0.02	-	54.8 ± 2.0
MabR1 + 5 % Sucrose + 0.6 % HP β CD	1.96 ± 0.37	0.093	54.8 ± 2.1
MabR1 + 5% Sucrose + 0.004 % PS80	2.10 ± 0.06	0.104	54.3 ± 2.3

II.3.7.5 SUMMARY AND DISCUSSION

In comparison to the samples which were freeze-dried using controlled ice-nucleation (see section II.3.6), the specific surface area was reduced to approximately one fifth by viscous flow of the freeze-dried cake. The reduction of SSA lead to fewer particles than in the previous chapter for all formulations investigated and the formulations containing HP β CD or PS80 showed fewer particles than the formulation without surfactant. By employing collapse freeze-drying to intentionally keep the surface area as low as possible, stable protein formulations with HP β CD could be obtained with similar subvisible particle counts as with polysorbate and both formulations are subjected to storage stability studies in the next chapter.

II.3.8 STORAGE STABILITY OF COLLAPSE FREEZE-DRIED MABR1 FORMULATED WITH 5 % SUCROSE

After the promising and successful collapse freeze-drying run with the formulations containing MabR1 at 10 mg/ml, 5% Sucrose; two formulations containing 0.6 % HP β CD or 0.004 % polysorbate 80 were again collapse freeze-dried and stored at 40 °C, 25 °C and at 2-8 °C (KS).

II.3.8.1 FREEZE-DRYING PROCESS

In order to reduce residual moisture in comparison to the pre-test, the pressure during freeze-drying was 1.03 mbar (pirani sensor controlled) in contrast to 2.53 mbar in the pre-test. This resulted in a product temperature of around -24 °C during steady-state sublimation. The thermocouple was placed in a 5 % Sucrose shielding vial.

II.3.8.2 PROTEIN STABILITY– SUBVISIBLE PARTICLES AND TURBIDITY

Collapse freeze-drying of both formulations of MabR1 based on 5 % Sucrose showed unchanged turbidity values, as shown in Figure II-52, acceptable particle levels > 1 μ m and 10 μ m, as displayed in Figure II-53 and Figure II-54 for all storage temperatures. The formulation containing 0.004 % PS80 showed slightly higher particle levels for both size classes than the formulation with 0.6 % HP β CD.

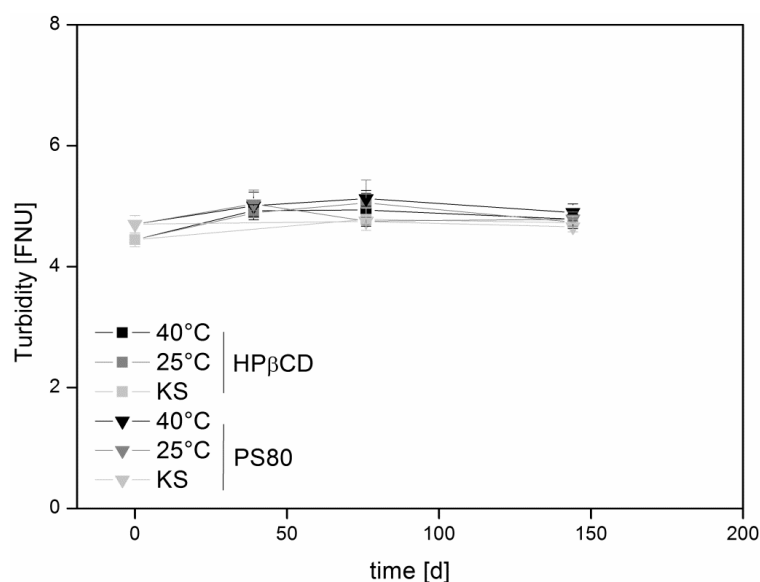


Figure II-52: Turbidity of both formulations stored at 40 °C, 25 °C and 2-8 °C (KS) versus storage time.

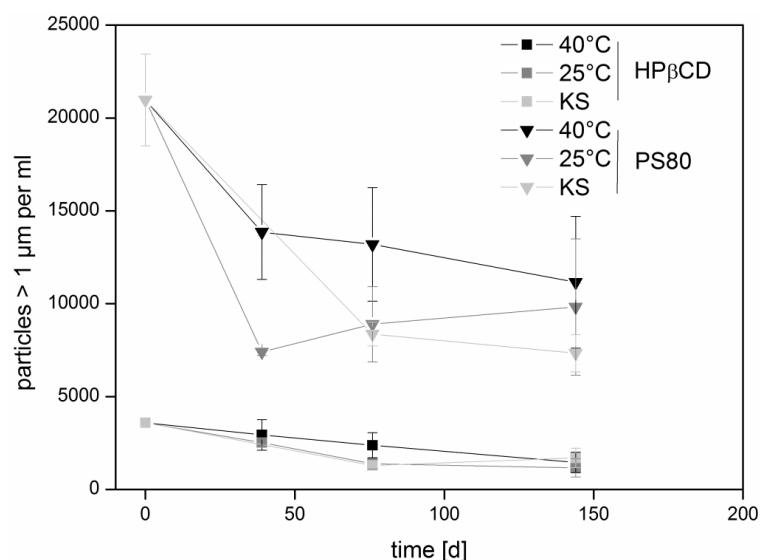


Figure II-53: Particles > 1 µm of both formulations stored at 40 °C, 25 °C and 2-8 °C (KS) versus storage time.

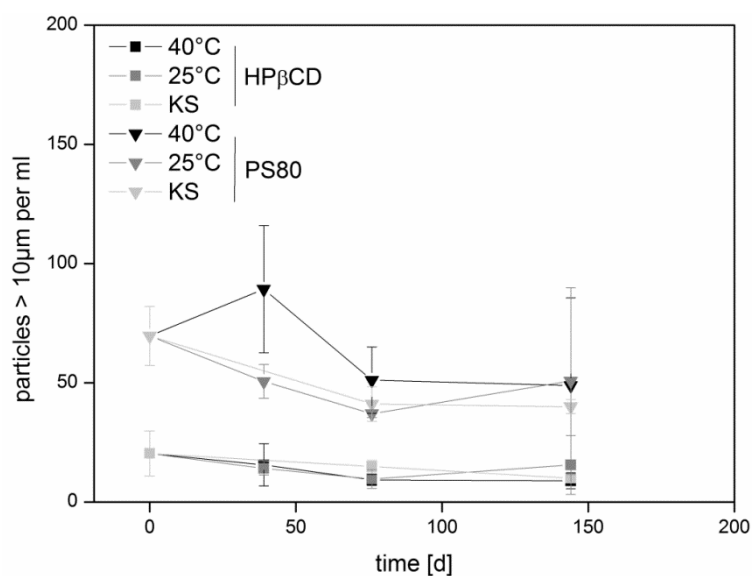


Figure II-54: Particles > 10 µm of both formulations stored at 40 °C, 25 °C and 2-8 °C (KS) versus storage time.

II.3.8.3 SIZE-EXCLUSION CHROMATOGRAPHY AND AF4

No change in monomer and dimer content was observed with SE-HPLC and these findings were confirmed by AF4. However, higher standard deviations were observed with AF4. Furthermore, relative amounts of monomer and dimer species are slightly lower with AF4 than SE-HPLC, because a larger fraction of high-molecular-weight aggregates was observed with MabR1 after end of cross-flow, as shown in a sample chromatogram in Figure II-59.

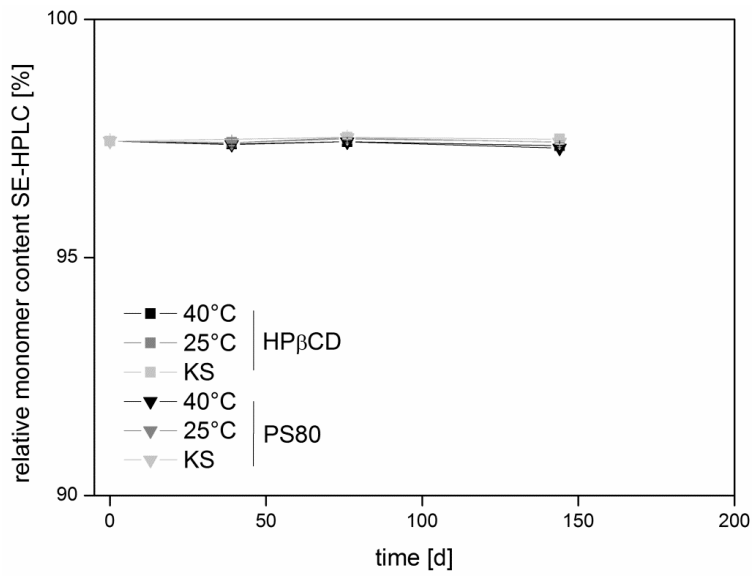


Figure II-55: Relative monomer content of MabR1 as determined with SE-HPLC for both formulations stored at three different temperatures.

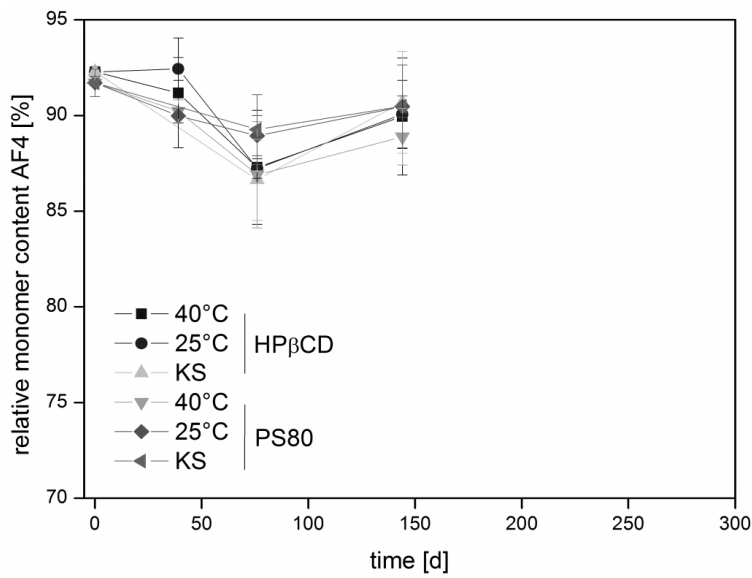


Figure II-56: Relative monomer content of MabR1 as determined with AF4 for both formulations stored at three different temperatures.

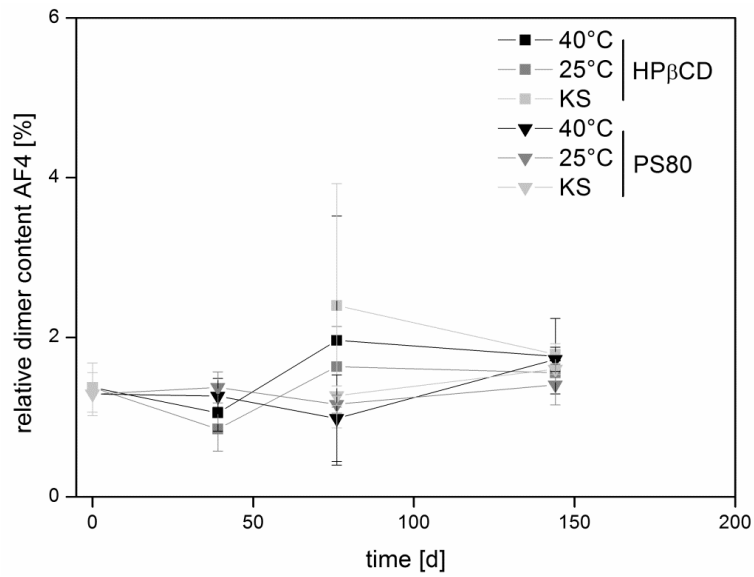


Figure II-57: Relative dimer content of MabR1 as determined with SE-HPLC for both formulations stored at three different temperatures.

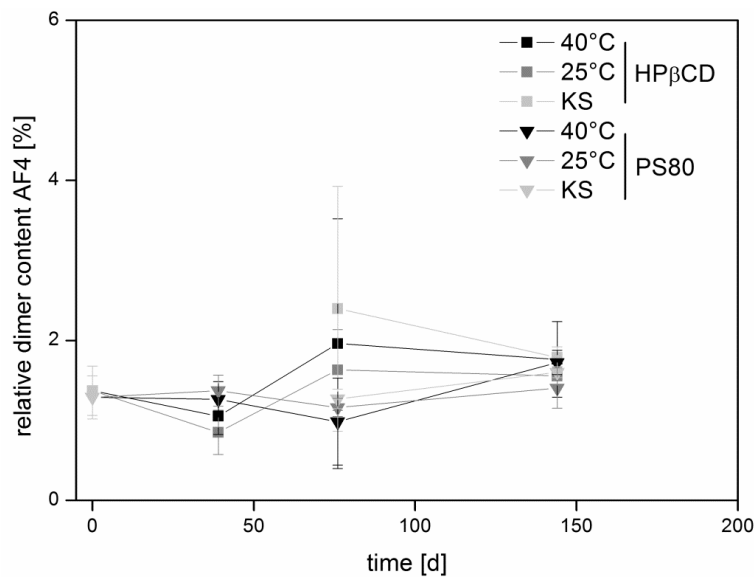


Figure II-58: Relative dimer content of MabR1 as determined with AF4 for both formulations stored at three different temperatures.

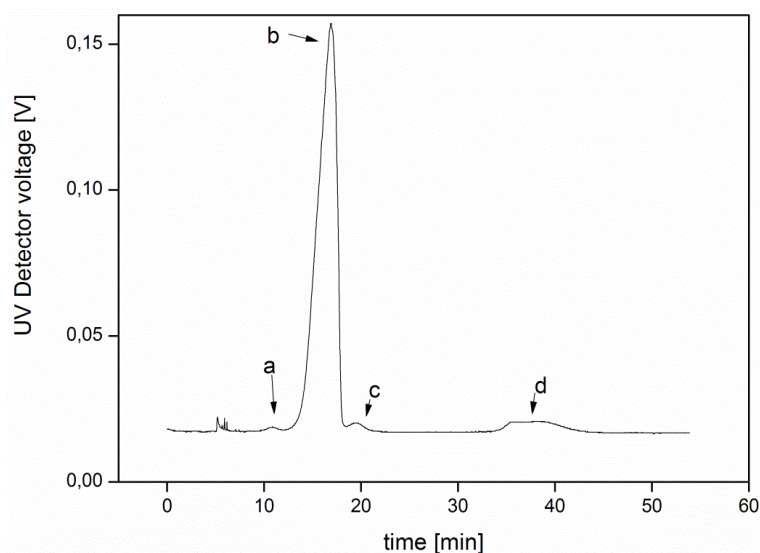


Figure II-59: Sample chromatogram for MabR1 in AF4 separation. Fragment (a), Monomer (b) and dimer (c) are separated from high-molecular-weight aggregates (d), which are not eluting in SEC, because of their size of approximately ~ 50 nm.

II.3.8.4 PHYSICO-CHEMICAL CHARACTERIZATION

All lyophilizate cakes were macroscopically collapsed without visible solid “bubbles”, as depicted in Figure II-60. No changes in cake appearance were observed during storage and no browning was visible. Residual moistures were between 2.0 and 3.0 %, as shown in Figure II-61 and were slightly higher than in the freeze-drying process in section II.3.7. Interestingly, the reduction of the freeze-drying pressure from 2.56 mbar to 1.03 mbar with the accompanying product temperature drop lead to an increase in residual moisture. However, glass transition temperatures were acceptable with around 45 °C and both product quality attributes did not change significantly over storage time, as shown in Figure II-62. Specific surface area was very low with SSAs of less than 0.1 m²/g, as shown in Figure II-63 and did not change over storage time.



Figure II-60: Pictures of lyophilized cakes; A: MabR1 formulated with 5 % Sucrose and 0.6 % HP β CD and stored for 76 days in the fridge at 2-8° B: MabR1 formulated with 5 % Sucrose and 0.004 % PS80 and stored for 76 days in the fridge at 2-8°C.

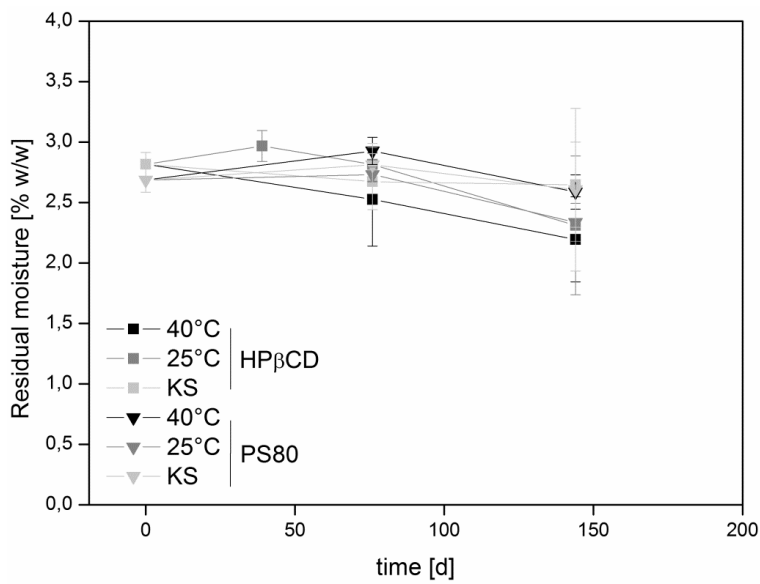


Figure II-61: Residual moisture of lyophilized cakes for both formulations stored at three different temperatures.

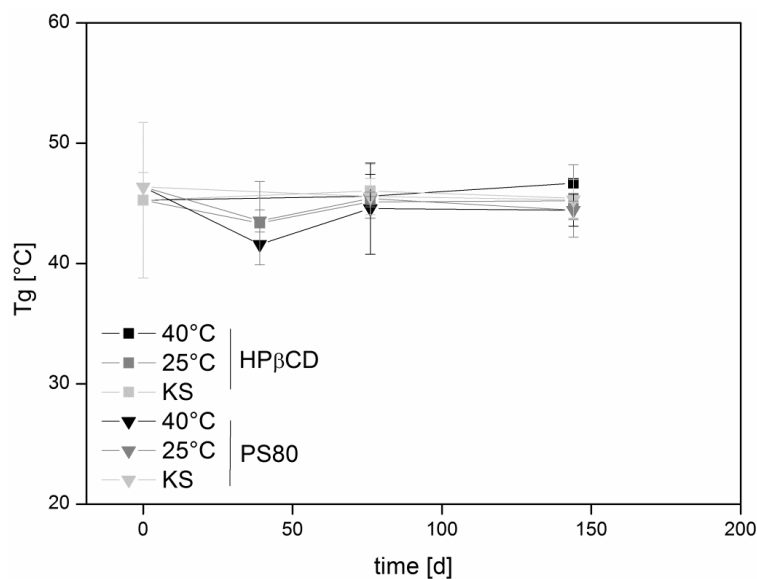


Figure II-62: Glass transition temperatures of lyophilized cakes for both formulations stored at three different temperatures.

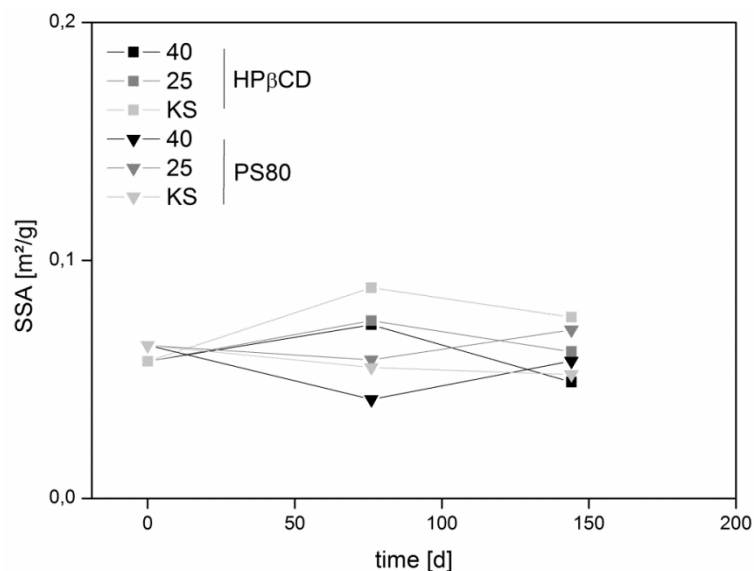


Figure II-63: Specific surface area of lyophilized cakes for both formulations stored at three different temperatures.

II.3.8.5 SUMMARY AND DISCUSSION

In this study, successful storage stability of both formulations of MabR1 with 5 % sucrose and HPβCD or PS80 was obtained compared to the storage study with 1.0 % sucrose in section II.3.5. Increasing sucrose concentration to 5 % decreased the T_g to only 45 °C since fully amorphous systems follow the Gordon-Taylor equation which describes the resulting glass transition temperature of a blend of polymers [63]. Increasing the content of sucrose with a lower T_g compared to that of proteins hence results in a decrease of T_g of the blend, both during dehydration (usually stated as T_g') as well as in the dried product. Consequently, with decrease of T_g' , also T_c is decreased and the amorphous matrix features a lower viscosity which allows for increased viscous flow during sublimation. Macroscopic collapse of higher-concentrated

sucrose formulations thus was more excessive than for the formulations containing 1 % sucrose and MabR1. Hence, lower specific surface areas, higher residual moistures and lower glass transition temperatures of samples based on 5 % Sucrose compared to 1 % Sucrose were obtained. While it is known that $T_g - T_{\text{Storage}}$ is not a good predictor of storage stability [3], storage of lyophilizates above its T_g results in increased mobility and possible faster degradation of proteins [64]. Hence, maximum storage temperature of the lyophilizates containing 5 % sucrose was 40 °C. Although $T_g - T_{\text{Storage}}$ was only ~ 5 °C for the samples stored at 40 °C, remarkable storage stability of MabR1 was observed even at this temperature and despite the relatively high residual moisture of the dried product no loss in monomer was detected. A possible explanation of this remarkable stability can be derived from the theory of glassy dynamics or molecular mobility in lyophilizates. Amorphous glasses are kinetically stable systems, featuring a high viscosity, which greatly slows reaction rates; however, they are not completely ceased [3]. Molecular mobility can be described by α - and β -relaxations which is mobility on a global scale, which is often coupled to viscosity and local, fast dynamics, respectively [65]. When amorphous glasses undergo aging, the enthalpy ΔH and the free volume, ΔV , that is the volume in which a molecule can move [65], are decreased [66, 67]. It is imaginable that, by the onset of collapse during sublimation phase, the glass is annealed and α -relaxations are slowed down, thus enhancing storage stability. Due to technical restrictions, neither α - nor β -relaxations could be measured in this study.

II.3.9 THE SITUATION AT THE INTERFACE - RESULTS FROM ESCA-STUDIES

II.3.9.1 INTRODUCTION

With ESCA, it is possible to study the interface of a lyophilized cake in the first 5 to 10 nm from the surface [68]. This allows quantification of protein surface coverage at the solid/gas interface by the nitrogen atom signal [30]. In addition, the contribution of N-C=O / C=O signals from peptide bonds to total carbon surface coverage is indicating protein presence at the interface. It is expected that the ice/liquid interface during the freezing step is kinetically stable after complete crystallization of water and the amorphous matrix is cooled below T_g' , which leads to a dramatic increase in viscosity of those systems [69]. If viscous flow of the amorphous solid is avoided during primary and secondary drying, data from the dried cake is transferrable also to the ice/liquid interface formed during freezing of the liquids.

II.3.9.2 RESULTS

Results from conventional freeze-drying show that the addition of PS80 decreases the amount of nitrogen surface coverage as well as peptide-bond surface coverage significantly, as shown in Table II-17. This is also true for the combination of Sucrose and PS80 but not for the combination of HP β CD and PS80. In general, the addition of HP β CD did not lead to such a decrease in nitrogen coverage as the addition of PS80 did and is in good agreement to other studies performed with proteins and surfactants for dried proteins [30, 70] and for liquid formulations of proteins [71]. Interestingly, also M β CD showed a significant decrease in nitrogen surface coverage. The M β CD derivative employed in this study had a significantly higher degree of substitution, thus, surface tension of water is lowered compared to HP β CD when employed in the same concentration [24]. It may be concluded that the most surface active component is enriched at a surface [70].

A slightly different picture is observed with collapse freeze-drying when the amorphous matrix undergoes viscous flow. Also the formulations containing either 0.1 % or 0.6 % HP β CD to MabR1 with Sucrose lead to a significant reduction in nitrogen surface coverage, comparable to the combination of sucrose and polysorbate 80, as shown in Table II-18. However, this result is not representative for the ice/liquid interface established during the freezing step. For the spray-dried samples (see section II.3.12), both, HP β CD and PS80, decreased nitrogen surface coverage compared to the formulation with trehalose to a higher extent than conventional freeze-drying, as shown in Table II-19. During spray-drying, evaporation of water at the interface reaches a steady-state phase in the first phase (constant rate period [65]) and a crust of solids is formed when solubility of excipients is exceeded. During concentration increase due to evaporation of water, diffusion of smaller molecules like surfactants might occur and those molecules might then more easily accumulate to the interface than proteins. This

complex, highly dynamic situation then does not reflect the situation right after atomization, with a possible higher protein surface coverage.

Table II-17: Results from ESCA for surface coverage of Carbon, Oxygen and Nitrogen. The percentage of the C=O signal relative to total carbon signal is also shown. All results are from conventional freeze-drying.

Formulation	Surface coverage Carbon [%]	Percent of N-C=O or C=O of total Carbon [%]	Surface coverage of Oxygen	Surface coverage of Nitrogen
MabR1	52.78	22.44	22.46	13.81
MabR1 + 0.04 % PS80	73.17	9.58	21.42	3.70
MabR1 + 1.0 % HP β CD	58.93	20.35	29.70	8.01
MabR1 + 1.0 % Sucrose + 1 % HP β CD	57.84	22.98	33.95	5.94
MabR1 + 1.0 % Sucrose	54.67	21.05	32.78	8.29
MabR1 + 1.0 % Sucrose + 0.04 % PS80	70.72	7.58	24.41	3.49
MabR1 + 1.0 % HP β CD + 0.04 % PS80	61.66	16.66	27.48	7.49
MabR1 + 1.0 % M β CD	59.09	16.57	33.15	3.30

Table II-18: Results from ESCA for surface coverage of Carbon, Oxygen and Nitrogen. The percentage of the C=O signal relative to total carbon signal is also shown. All results are from collapse freeze-drying.

Formulation	Surface coverage Carbon [%]	Percent of N-C=O or C=O of total Carbon [%]	Surface coverage of Oxygen	Surface coverage of Nitrogen
MabR1 + 1.0 % Sucrose	60.30	19.52	25.72	9.98
MabR1 + 1.0 % Sucrose + 0.1 % HP β CD	57.62	16.15	33.52	4.74
MabR1 + 1.0 % Sucrose + 0.60 % HP β CD	59.18	13.66	33.60	2.65
MabR1 + 1.0 % Sucrose + 0.004 % PS80	66.02	7.64	25.55	3.72
MabR1 + 1.0 % HP β CD	59.35	15.30	32.51	4.58
MabR1 + 1.0 % HP β CD + 0.004 % PS80	59.46	12.92	32.04	3.63

Table II-19: Results from ESCA for surface coverage of Carbon, Oxygen and Nitrogen. The percentage of the C=O signal relative to total carbon signal is also shown. All results are from spray-drying. PS80 = polysorbate 80

Formulation	Surface coverage Carbon [%]	Percent of N-C=O or C=O of total Carbon[%]	Surface coverage of Oxygen	Surface coverage of Nitrogen
MabR1 + 5.0 % Trehalose	61.10	18.68	30.81	6.91
MabR1 + 5.0 % Trehalose + 0.35 % HP β CD	58.54	20.65	39.23	1.68
MabR1 + 5.0 % Trehalose + 0.60 % HP β CD	57.81	18.73	39.76	1.79
MabR1 + 5.0 % Trehalose + 0.04 % PS80	69.88	11.30	29.30	1.59

II.3.9.3 SUMMARY AND DISCUSSION

In contrast to PS80, HP β CD seems not to be able to displace the protein from the interface but a co-existence of the cyclodextrin derivative and MabR1 is suggested by the data set. Such a behaviour was also observed for the liquid/air interface for HP β CD and an IgG antibody [71]. The authors of this study state that polysorbate occupies a generated interface and displaces proteins from that interface; this is also true, if a protein monolayer was already present at this interface. In contrast, HP β CD was present at the interface together with the IgG studied when a solution of both was studied and an IgG, already present at a surface, could not be displaced by the addition of HP β CD. The potency to occupy a given interface possibly correlates with the degree of reduction of the surface tension of water and this reduction is far lower for HP β CD than for polysorbate. In addition, polysorbate can faster occupy an interface compared to HP β CD. The stabilization mechanism of HP β CD hence must be different than those provided by non-ionic surfactants. Interestingly, as can be derived from our results, it may be speculated that during the viscous flow of the amorphous matrix during collapse freeze-drying, the nitrogen content at the interface is slightly lowered. This observation, together with the very low surface area obtained in these processes, may both contribute to the overall good stability observed for these samples.

II.3.10 STORAGE STABILITY OF h-GH

After the successful stabilization of MabR1, it was tested, if the formulation of 5 % Sucrose and 0.6 % HP β CD as well as the collapse freeze-drying process could be transferred to another protein, human growth hormone (hGH). hGH is a model protein, which is sensitive towards interfaces and hence a good model to study the impact of surfactants on protein degradation. Although a lot of marketed formulations are lyophilizates, also liquid formulations of hGH are available. hGH was formulated at 1.0 mg/ml in a sodium phosphate buffer, pH = 7.00 and in a first pre-test, hGH was collapse freeze-dried with 5% Sucrose and 0, 0.35 or 0.6 % HP β CD or 0.004 % PS80. Subsequently, formulations with 0.6 % HP β CD and 0.004 % PS80 were stored at 40 °C, 25 °C and at 2-8 °C (KS). Storage stability of the protein was investigated for 118 days.

II.3.10.1 FREEZE-DRYING PROCESS

The collapse freeze-drying process was carried out at the FTS Lyostar 3 at a pressure of 1 mbar (capacitance manometer controlled). Steady-state product temperature, as determined with thermocouples placed in 5 % Sucrose shielding vials was approximately -17 °C.

II.3.10.2 PROTEIN STABILITY – SUBVISIBLE PARTICLES AND TURBIDITY

Figure II-64 shows the results from light obscuration and turbidity for hGH samples and corresponding placebo formulations. The addition of 0.35 % and 0.60 % HP β CD as well as the addition of PS80 significantly reduced subvisible particle formation and turbidity of hGH compared to the formulation without surfactant. The formulation with 0.6 % HP β CD showed lowest turbidity values and subvisible particles. In addition, the combinations of Sucrose with 0.6 % HP β CD or PS80 both also showed the lowest numbers of subvisible particles > 10 μ m, as shown in Table II-20.

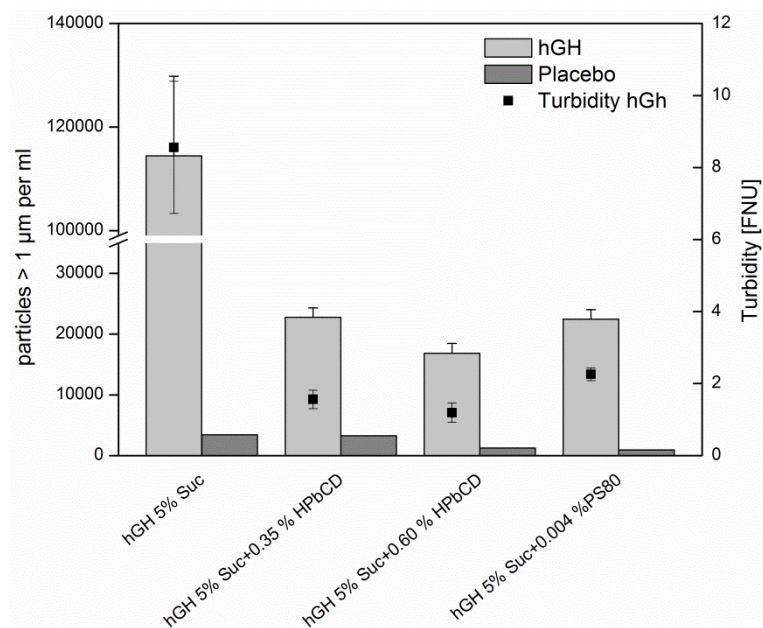


Figure II-64: Subvisible particles > 1 µm and turbidity for hGH formulations and subvisible particles for corresponding formulations without protein (Placebo, dark grey bars).

Table II-20: Subvisible particles > 10 µm per ml for all formulations after freeze-drying and rehydration.

Formulation	Subvisible particles > 10 µm
hGH 5 % Sucrose	1829 ± 603
hGH 5 % Sucrose + 0.35 % HPβCD	175 ± 7
hGH 5 % Sucrose + 0.60 % HPβCD	88 ± 28
hGH 5 % Sucrose + 0.004 % PS80	63 ± 13

II.3.10.3 PROTEIN STABILITY – SIZE-EXCLUSION CHROMATOGRAPHY

A slight increase in dimer formation was visible for all formulations except the formulation containing 5 % Sucrose and 0.6 % HPβCD. The formulation without surfactant showed the highest increase in dimer content after freeze-drying and rehydration, as shown in Figure II-65.

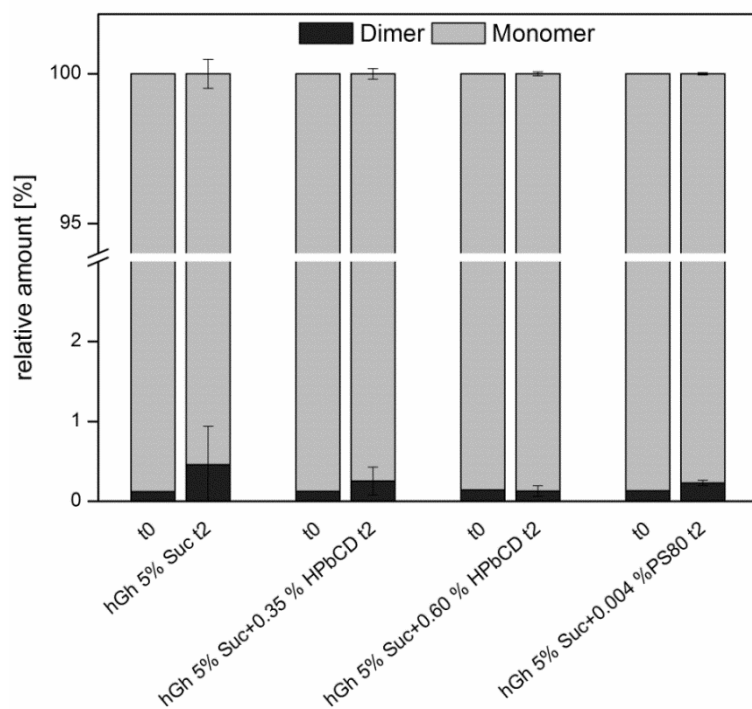


Figure II-65: Relative amount of protein species as determined with SE-HPLC for all formulations after preparation (t0) and collapse freeze-drying and rehydration (t2).

II.3.10.4 PHYSICO-CHEMICAL CHARACTERIZATION OF LYOPHILIZATES

The formulation containing only 5 % sucrose and hGH showed the lowest specific surface area and highest residual moisture, as shown in Table II-21. In addition, as shown in Figure II-66, this formulation also appeared most collapsed whereas the other formulations showed some solid bubble formation, slightly higher SSAs and lower residual moistures. Reconstitution times were 30 seconds followed by 90 seconds of visible schlieren formation.

Table II-21: Residual moisture and SSA for all dried formulations.

Formulation	Residual moisture [% w/w] (n=2)	SSA [m ² /g]
hGH 5 % Sucrose	2.43 ± 0.48	0.06
hGH 5 % Sucrose + 0.35 % HPβCD	1.19 ± 0.16	0.17
hGH 5 % Sucrose + 0.60 % HPβCD	1.23 ± 0.05	0.14
hGH 5% Sucrose + 0.004 % PS80	1.22 ± 0.21	0.14

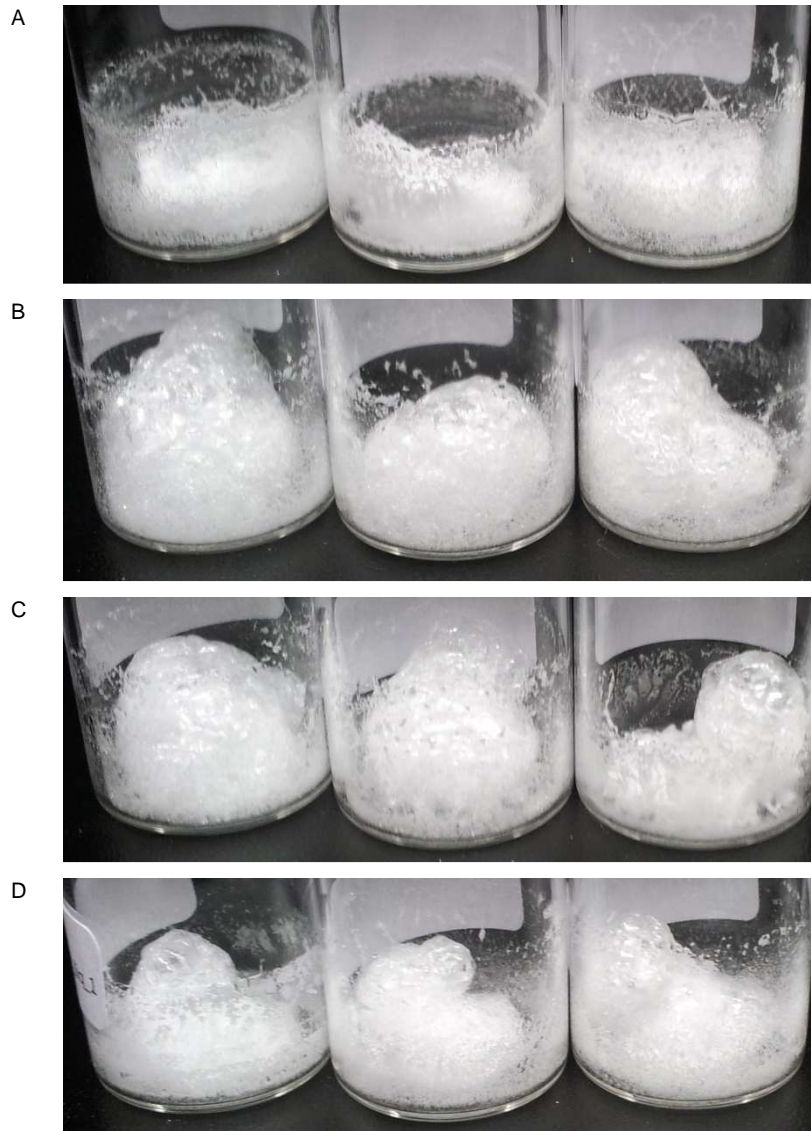


Figure II-66: Macroscopic appearance of lyophilizate cakes. hGH + 5 % Sucrose (A); hGH + 5 % Sucrose + 0.35 % HP β CD (B); hGH + 5 % Sucrose + 0.60 % HP β CD (C), hGH + 5 % Sucrose + 0.004 % PS80 (D).

II.3.10.5 STORAGE STABILITY OF HGH – SUBVISIBLE PARTICLES AND TURBIDITY

Results from the pre-test could very well be reproduced with the samples subjected for storage stability and turbidity as well as particles > 1 μ m and > 10 μ m did not change significantly over the storage period, as shown in Figure II-67, Figure II-68 and Figure II-69. The formulation with 0.6 % HP β CD showed slightly lower turbidity values but comparable subvisible particle levels to the formulation containing 0.004 % PS80.

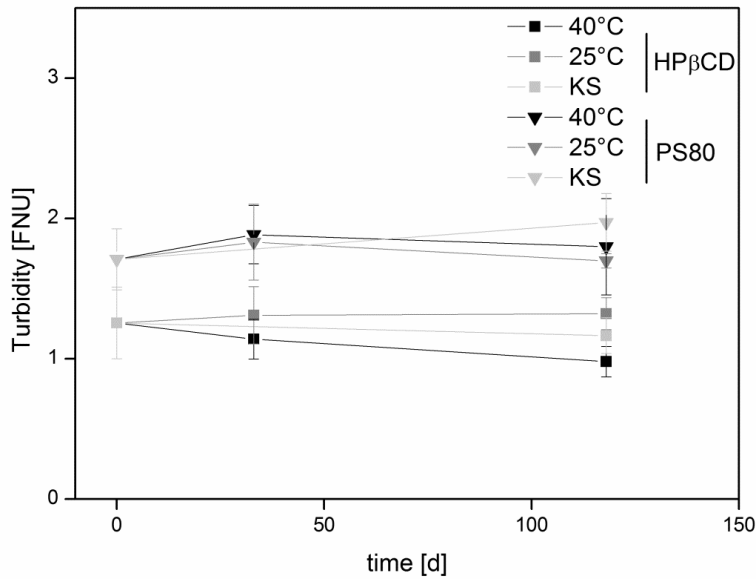


Figure II-67: Turbidity for stored formulations of hGH (5 % Sucrose + 0.6 % HPβCD or 0.004 % PS80) at three different temperatures, 40 °C, 25 °C and 2-8 °C (KS) over storage time.

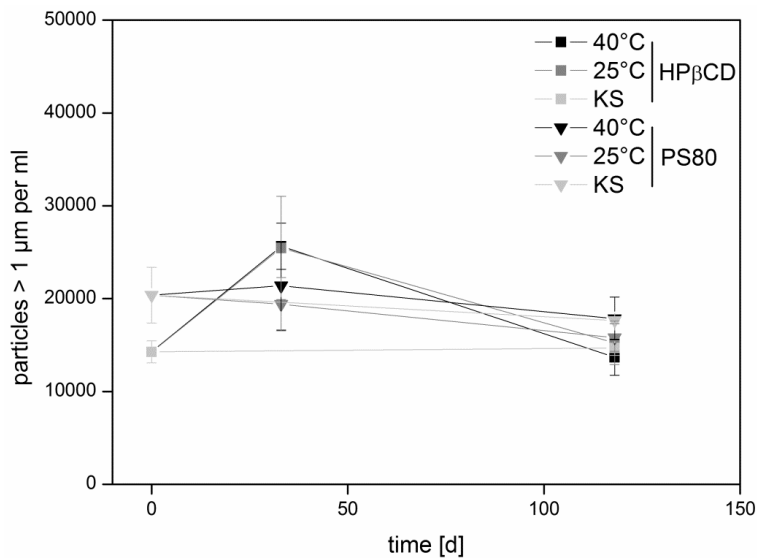


Figure II-68: Subvisible particles > 1 μm for both formulations of hGH stored at 40 °C, 25 °C and 2-8 °C (KS).

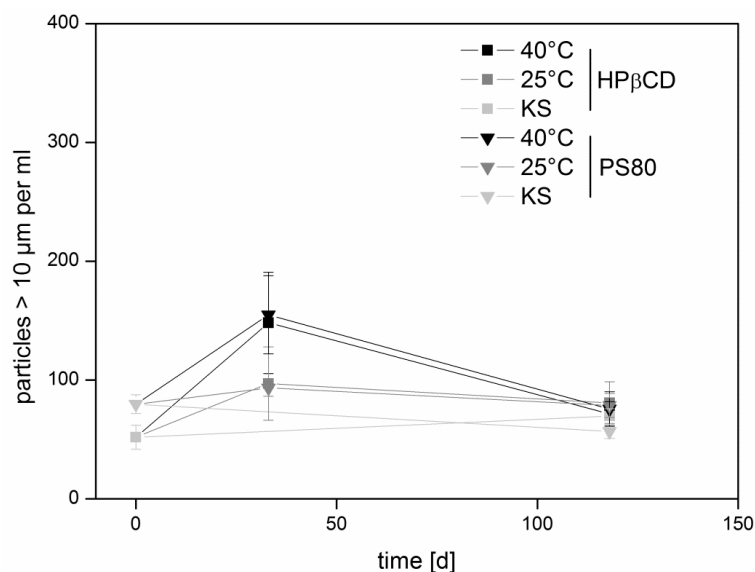


Figure II-69: Subvisible particles > 10 µm for both formulations of hGH stored at 40 °C, 25 °C and 2-8 °C (KS).

II.3.10.6 STORAGE STABILITY OF hGH – SIZE-EXCLUSION CHROMATOGRAPHY AND AF4

During storage period, no changes were observable in monomer and dimer content at all temperatures, as displayed in Figure II-70 and Figure II-71. The formulation with polysorbate 80 showed a little higher dimer content than the formulation with 0.6 % HPβCD. This was also confirmed by AF4, for samples stored for 118 days. The formulation with HPβCD showed slightly higher relative monomer contents and less dimer content than the formulation containing polysorbate 80, as shown in Figure II-72.

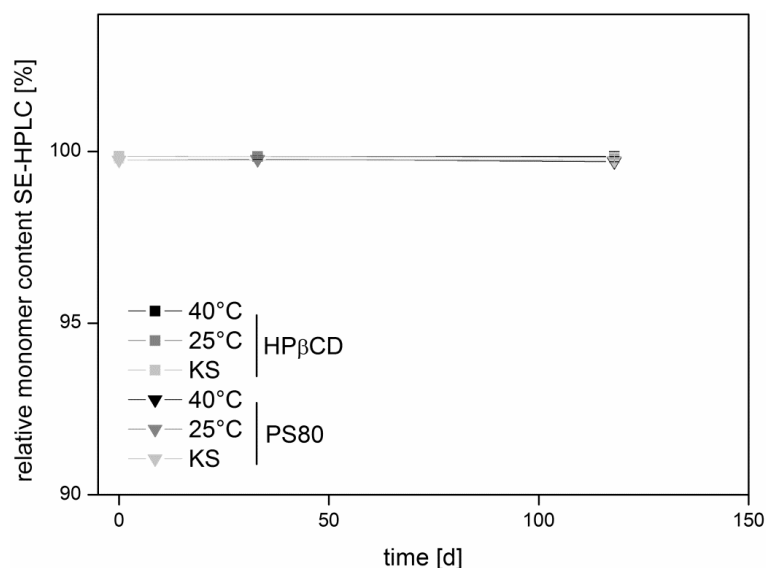


Figure II-70: Relative monomer content of hGH as determined by SE-HPLC for all storage temperatures of both formulations.

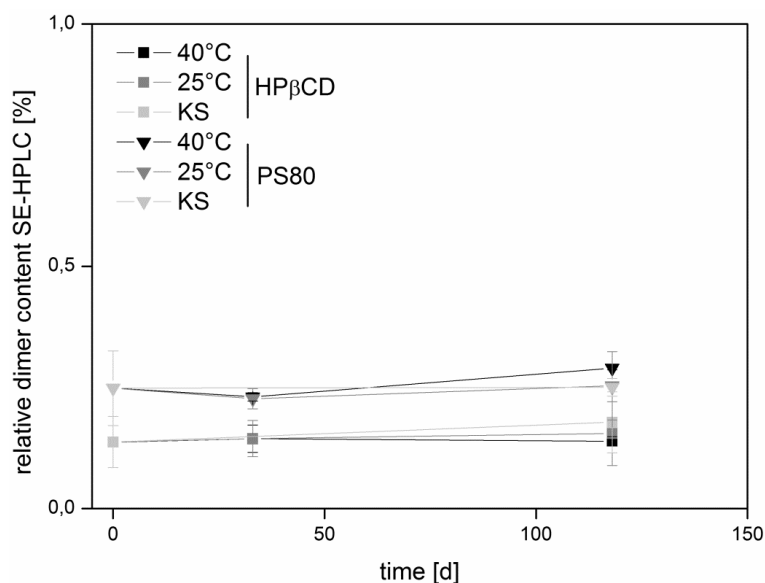


Figure II-71: Relative dimer content of hGH as determined by SE-HPLC for all storage temperatures of both formulations.

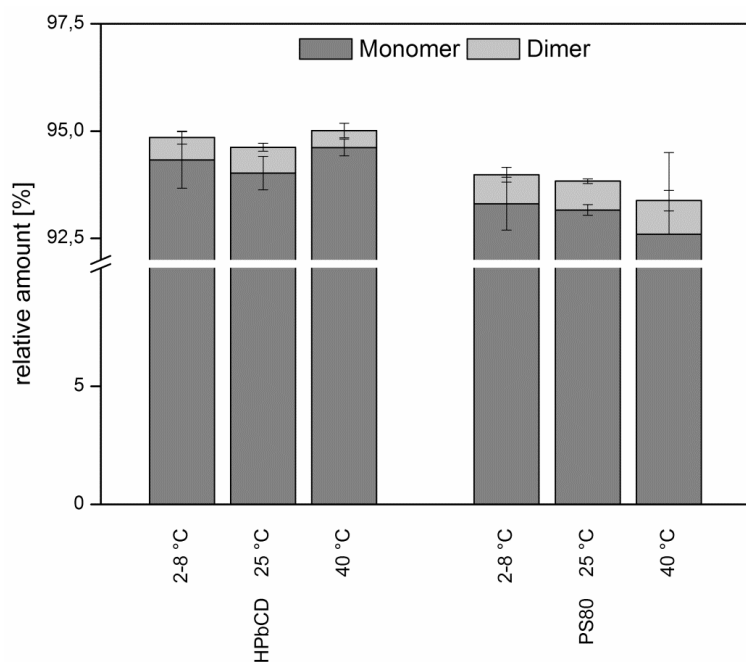


Figure II-72: Results from AF4 for samples of collapse freeze-dried hGH with 0.6 % HPβCD (left) and 0.004 % PS80 (right) stored at three different temperatures for 118 days.

II.3.10.7 PHYSICO-CHEMICAL INVESTIGATION OF FREEZE-DRIED LYOPHILIZATES

Residual moistures were in the range of 1.0 – 1.5 % during the storage study (Figure II-73) and glass transition temperatures were between 60 °C and 70 °C, as shown in Figure II-74. Furthermore, SSA did not change during the storage period (Figure II-75) and reconstitution times were 30 seconds followed by some schlieren for approximately 90 seconds and did not change over observed storage time.

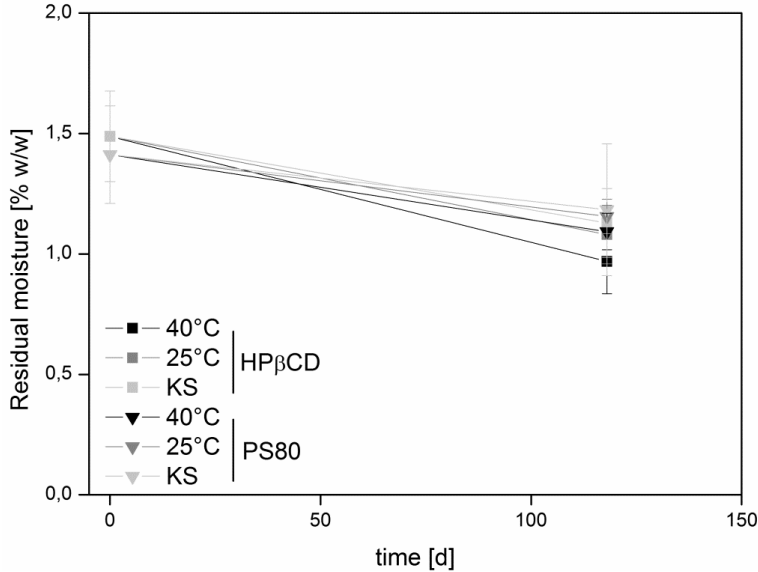


Figure II-73: Residual moisture of both formulations of hGH stored at three different temperatures.

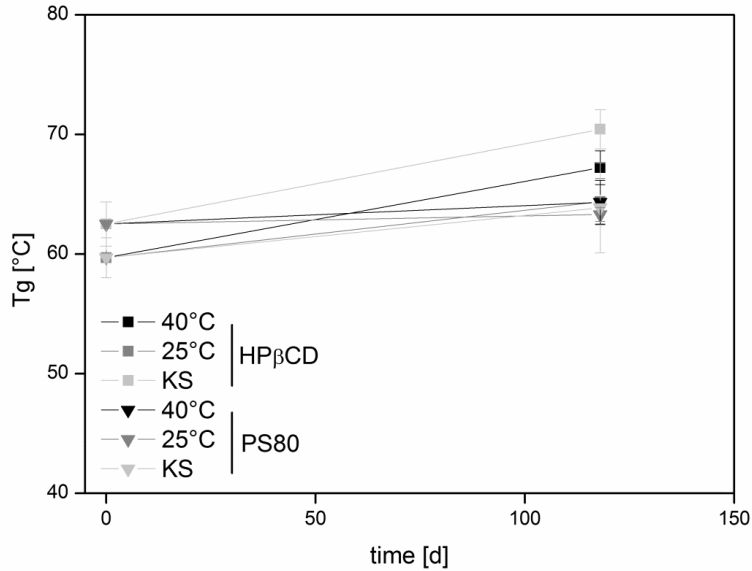


Figure II-74: Glass transition temperatures (T_g) for both formulations of hGH stored at three temperatures.

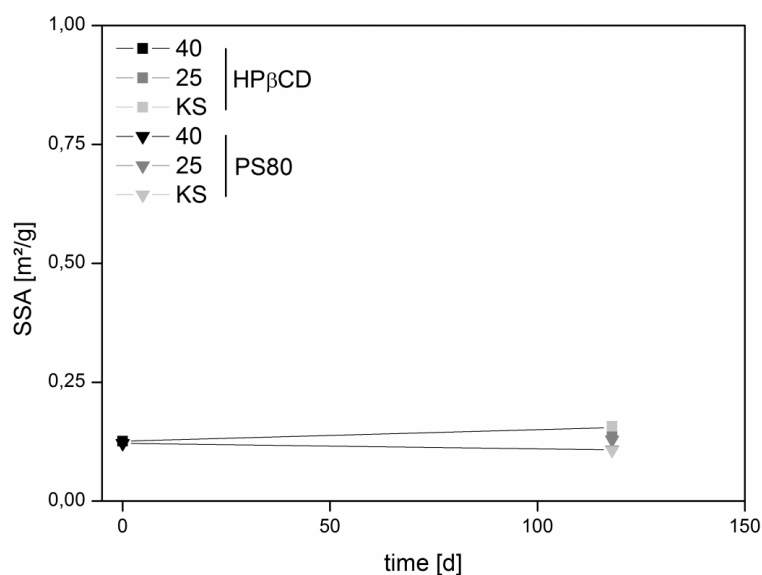


Figure II-75: SSA for both formulations of hGH stored at three temperatures.

II.3.10.8 SUMMARY AND DISCUSSION

While the aforementioned impact of the freeze-drying process and specific surface area are in general applicable to any protein, we intended to show applicability of the combination of formulation (with HP β CD) and the collapse freeze-drying process on hGH. hGH is structurally completely different from antibodies and features a molecular weight of approximately 22 kDa. Further, it is known that hGH is exposing aromatic amino acids and is prone to aggregation [72]. It has been shown that HP β CD is interacting with hGH by possible complexation of amino acid residues and prevents hGH from aggregating [43, 72]. Further, surfactants, like polysorbates, prevent hGH from aggregating during agitation by directly binding to the protein in molar ratios of > 4:1 [49] and help refolding of molten hGH intermediates [73]. hGH has been shown to be stabilized by HP β CD in liquid formulations in very low concentrations (2.5 mM) during agitation and freeze-thaw studies [50], and in this study, storage stable formulations of freeze-dried hGH could be obtained and the formulation containing 0.6 % HP β CD was superior to the formulation which contained polysorbate and an increase in dimer was observed for the polysorbate-containing formulation directly after freeze-drying and remained unchanged during the storage period. These findings suggest that the stabilizing effects found for liquid formulations of hGH and HP β CD can also be transferred to freeze-drying.

II.3.11 STORAGE STABILITY OF GCSF

After the positive results with MabR1 and hGH, another interfacial-sensitive protein, GCSF was investigated. Similar to hGH, GCSF is storage stable in liquid formulations and there is no need to freeze-dry this protein; however, due to its sensitivity towards interfaces, it is a good model protein to study effects of surfactants on protein stability. GCSF was dialyzed into a 10 mM citrate buffer pH = 4.00 and 5 % Sucrose, and either 0.60 % HP β CD or 0.004 % PS80 were added. Serving as a negative control, 5 % Sucrose and GCSF was also freeze-dried but not subjected to storage stability.

II.3.11.1 LYOPHILIZATION PROCESS

Collapse lyophilization was carried out at the FTS Lyostar III with a pressure of 1 mbar. The steady-state product temperature as shown in Figure II-76 was approximately -17 °C.

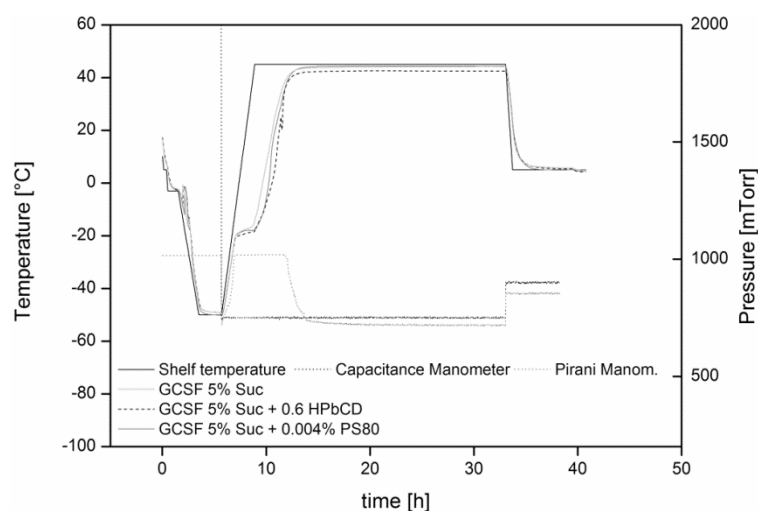


Figure II-76: Lyophilization process for GCSF. Thermocouples were placed in each formulation of GCSF.

II.3.11.2 PROTEIN STABILITY— OVERVIEW AFTER FREEZE-DRYING

After freeze-drying and rehydration, a positive influence of both, HP β CD and PS80 compared to the formulation without surfactant could be observed. PS80 was superior to HP β CD with a lower turbidity and less subvisible particles > 1 μ m, as illustrated in Figure II-77.

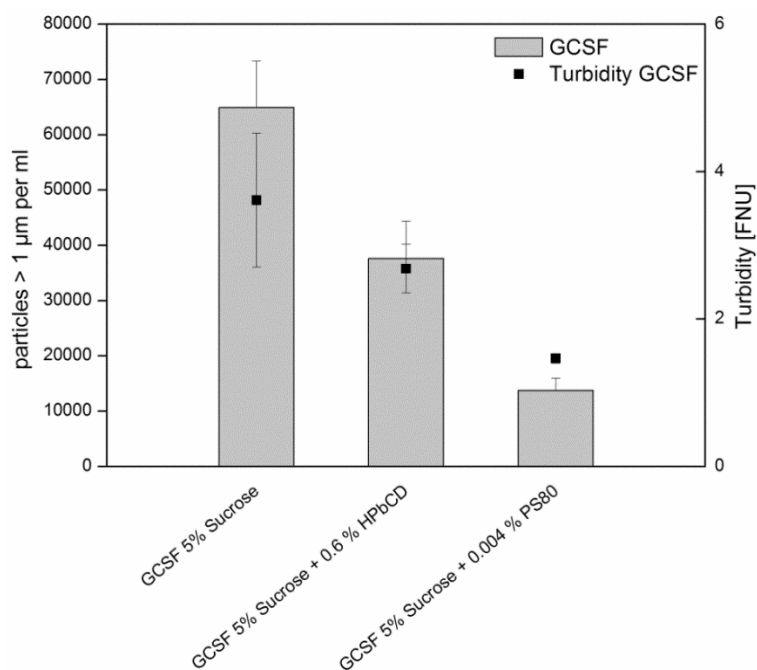


Figure II-77: Subvisible particles and turbidity for all GCSF formulations after freeze-drying and rehydration.

II.3.11.3 PROTEIN STABILITY– STORAGE STABILITY

During storage, no major changes in turbidity or subvisible particles > 1 µm and > 10 µm were observable, as shown in Figure II-78, Figure II-79 and Figure II-80. However, a small trend towards lower total particle numbers is observed and also a trend towards lower turbidity of GCSF formulated with 0.6 % HPβCD. With both formulations, visible particles were observed after 48 and 106 days. The study of GCSF hence was cancelled after 106 days.

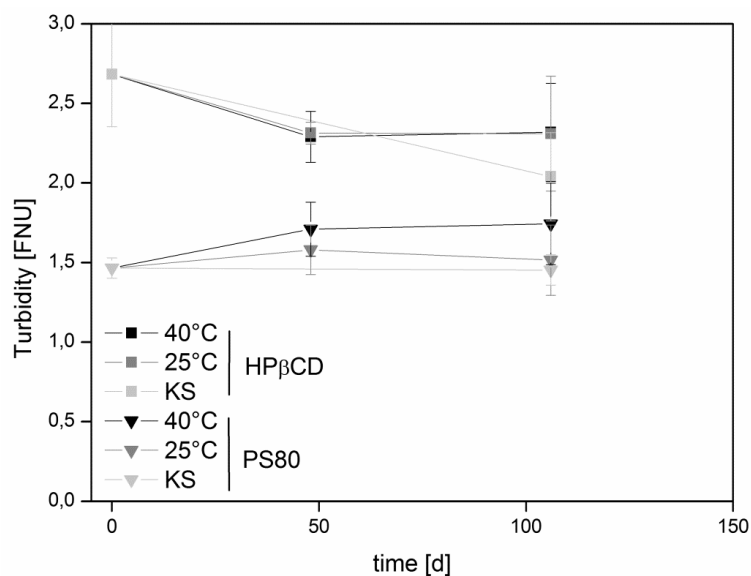


Figure II-78: Turbidity for both formulations stored at three temperatures (40 °C, 25 °C and 2-8 °C (KS)).

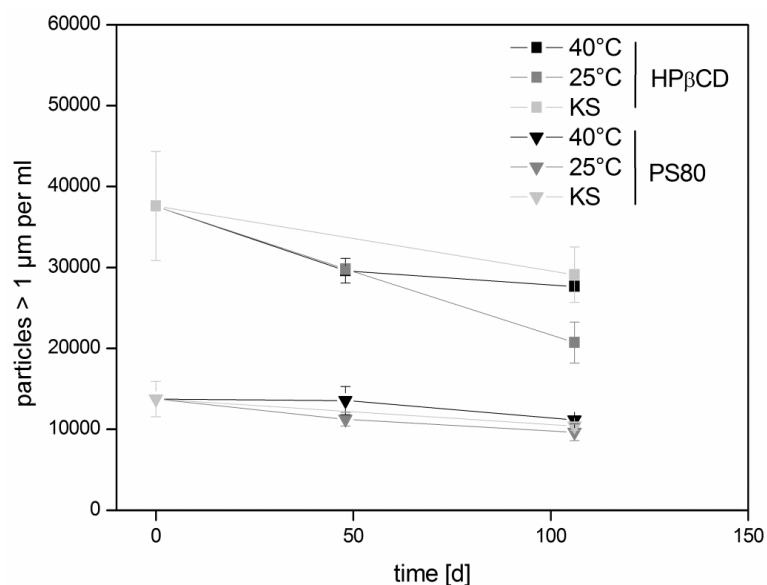


Figure II-79: Subvisible particles > 1 µm for both formulations stored at three temperatures. At time points of 48 and 106 days, visible particles appeared in both formulations.

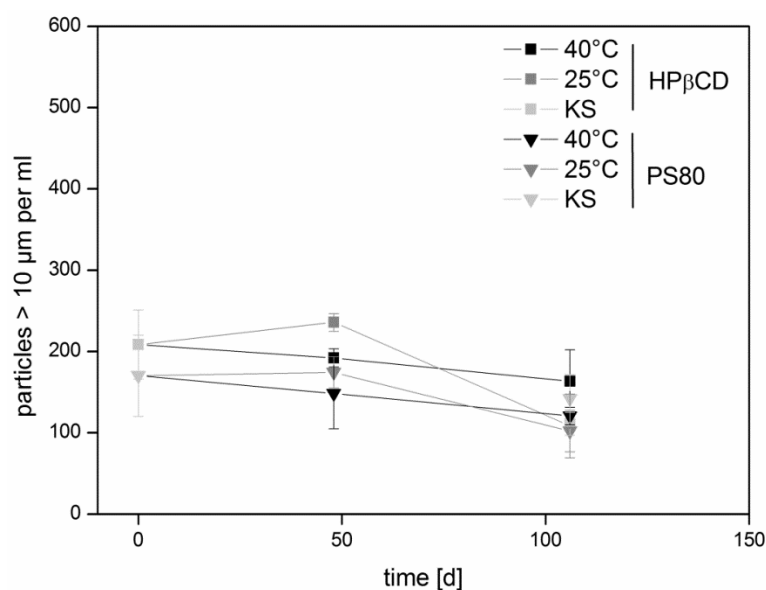


Figure II-80: Subvisible particles > 10 µm for both formulations stored at three temperatures.

II.3.11.4 SIZE-EXCLUSION CHROMATOGRAPHY

After freeze-drying and rehydration, a decrease of monomer content accompanied by an increase of dimer fraction for the formulation of GCSF containing HPβCD was observed, as shown in Figure II-81 and Figure II-82. However, after 104 days, an increase in dimer and a decrease in monomer content could also be observed for the formulation of GCSF formulated with sucrose and PS80 which was stored at 40 °C. A trend to lower protein AUC with high standard deviations could be observed in Figure II-83.

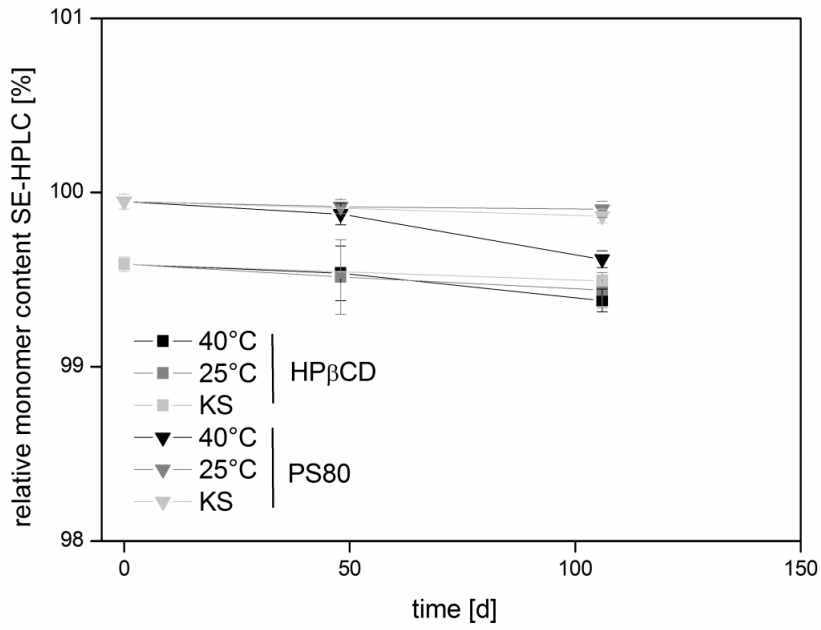


Figure II-81: Relative monomer content as determined by SE-HPLC for both formulations stored at three temperatures.

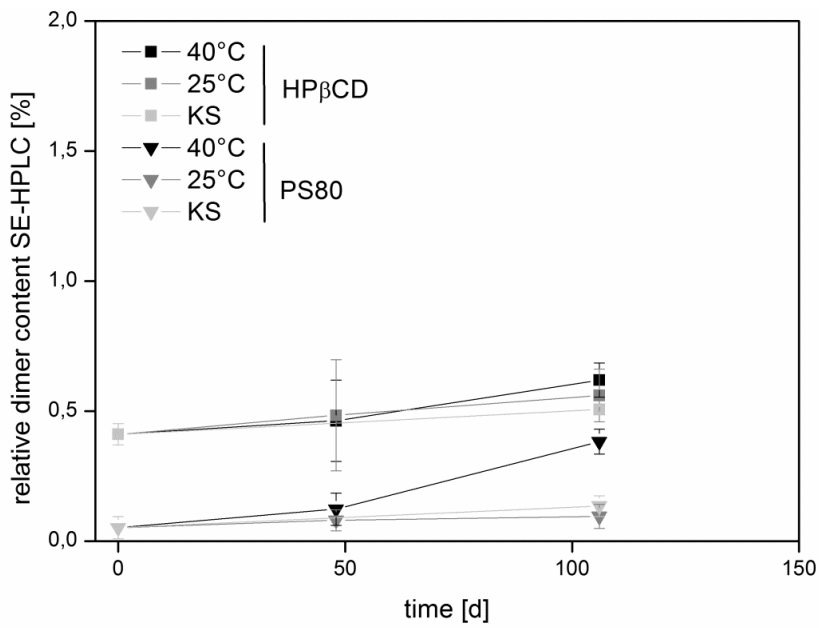


Figure II-82: Relative dimer content as determined by SE-HPLC for both formulations stored at three temperatures.

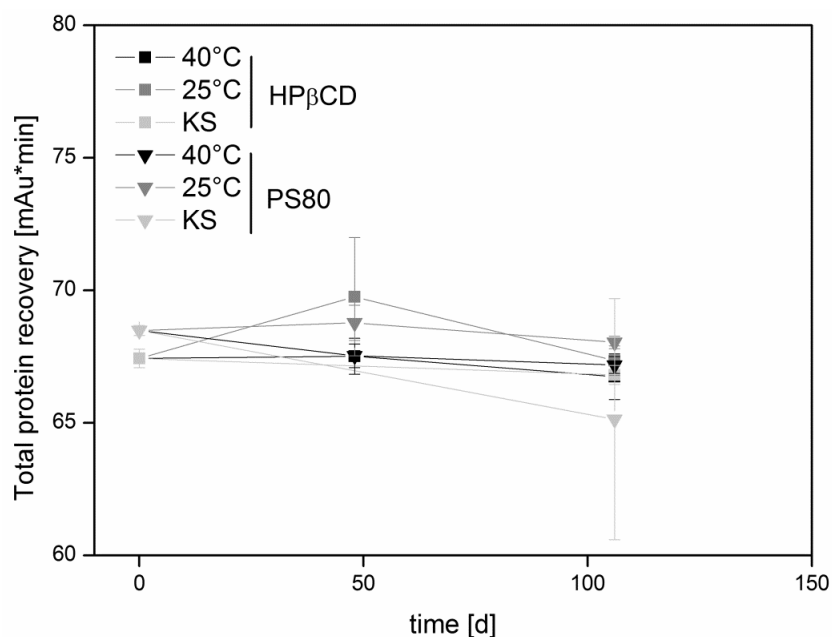


Figure II-83: Total protein recovery (AUC) as determined with SE-HPLC for GCSF stored at three temperatures.

II.3.11.5 PHYSICO-CHEMICAL INVESTIGATION OF LYOPHILIZATE CAKES

All lyophilizate cakes were visibly collapsed, as shown in Figure II-84. However, the formulation which contains HPβCD showed a more solid-bubble-like appearance whereas the formulations containing mainly 5 % sucrose were collapsed and shrunken. This difference was also observable with a lower SSA as depicted in Figure II-87 of the formulation which contains PS80 compared to HPβCD with approximately 0.05 m²/g and 0.15 m²/g, respectively. The SSAs did not change significantly over storage time. This difference in SSA also translated to slightly higher residual moistures of the PS80 formulation and both formulations showed a slight increase in residual moisture over storage time (see Figure II-85). Glass transition temperatures remained over 50 °C for 48 days with a trend to lower T_gs, especially for the samples stored at 40 °C, as depicted in Figure II-86.

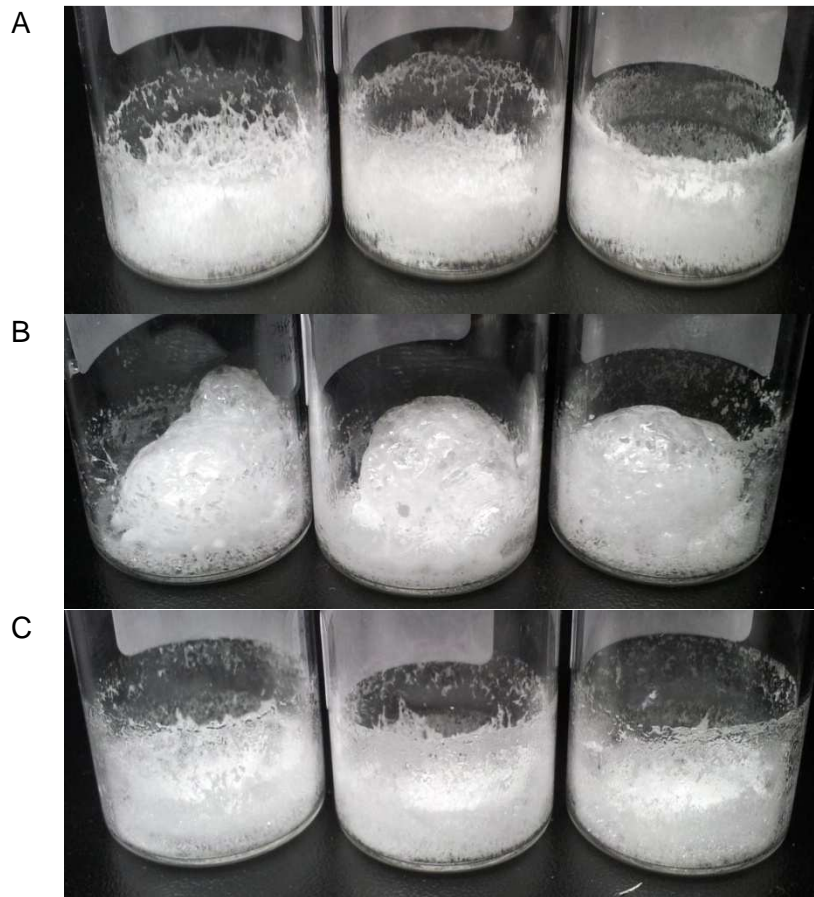


Figure II-84: Macroscopic appearance of collapse freeze-dried lyophilizate cakes. GCSF + 5 % Sucrose (A); GCSF + 5 % Sucrose + 0.6 % HP β CD (B); GCSF + 5 % Sucrose + 0.004 % PS80 (C).

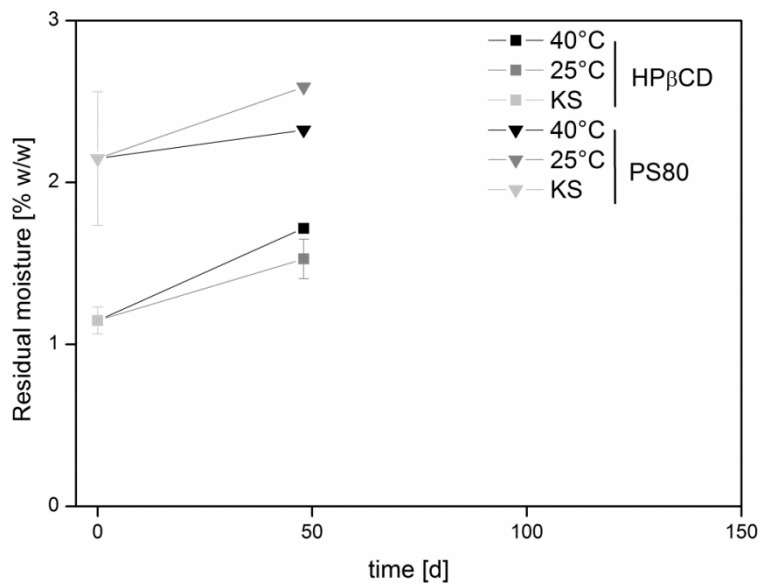


Figure II-85: Residual moisture for stored GCSF formulations.

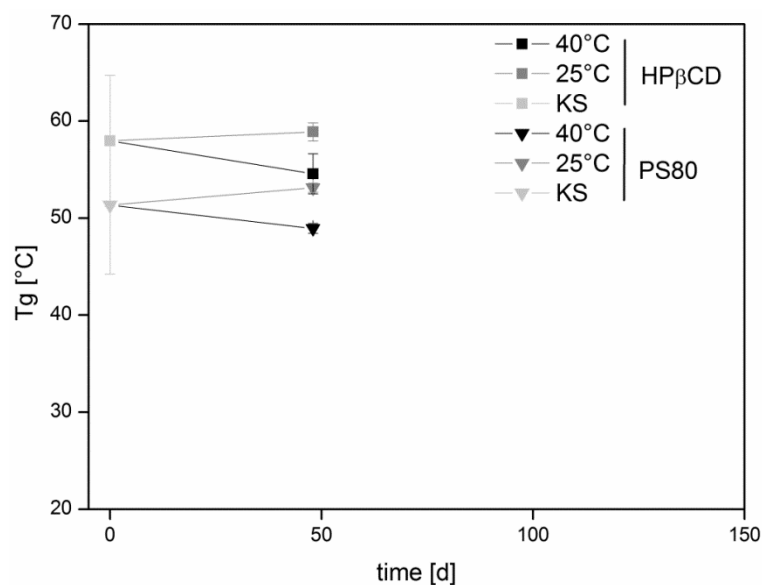


Figure II-86: Glass transition temperatures for stored GCSF formulations.

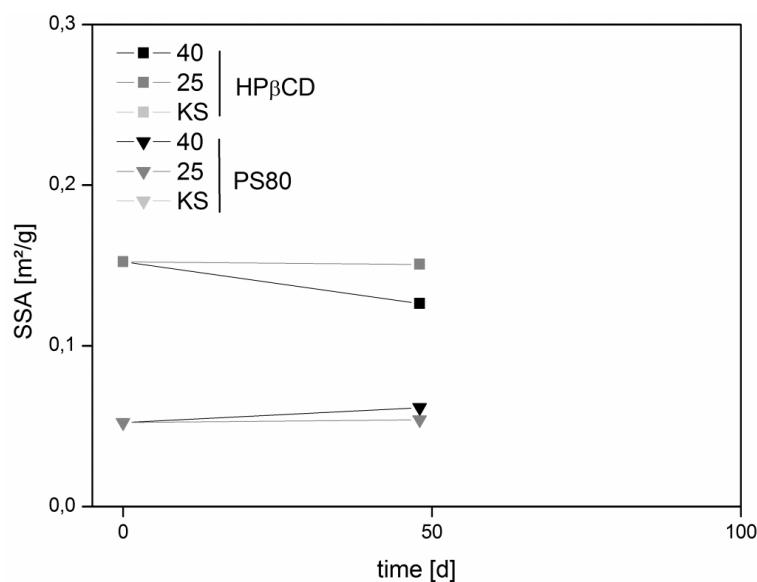


Figure II-87: Specific surface area for stored GCSF formulations.

II.3.11.6 SUMMARY AND DISCUSSION

In contrast to MabR1 and hGH, it was difficult to apply collapse freeze-drying with polysorbate 80 and HPβCD to GCSF. Both surfactants showed a positive impact on subvisible particle formation compared to the formulation containing sucrose only. Polysorbate 80 was superior to HPβCD with less subvisible particles formed after freeze-drying and rehydration. However, during accelerated storage of those samples, visible particles appeared in all formulations, which suggest a general instability of GCSF in the dried state and hence the study was cancelled. In a study using FTIR spectroscopy to detect drying-induced variations in the secondary structure of several proteins including GCSF, it was found that especially G-CSF showed relatively high correlation values (r) between protein in buffer solution and in the dried

state, what is usually associated with superior stability of the protein. However, particulate matter was not a focus of this study and as shown in the previous chapter II.3.5, FTIR is not always able to detect small amounts of degraded protein.

II.3.12 HP β CD EMPLOYED IN SPRAY DRYING OF MABR1

II.3.12.1 INTRODUCTION

After successful freeze-drying of MabR1 with HP β CD and polysorbate and low specific surface areas, spray-drying as a control experiment was performed to elucidate the impact of higher SSAs. In addition to analysis after spray-drying and rehydration, analysis was also performed after atomization without drying. Sucrose was replaced with trehalose in the spray-drying study because of its higher glass transition temperatures. Sucrose is very difficult to spray dry and yields are usually quite low. Furthermore, due to the expected high interfacial area generated by atomization of the liquid, the amount of polysorbate 80 was increased to 0.04 %. Table II-22 shows the formulations investigated in this study. In addition, for each formulation, a placebo formulation was prepared.

Table II-22: Study design for spray drying of MabR1.

Formulation	MabR1 [mg/ml]	Trehalose [%]	HP β CD [%]	PS 80 [%]	Storage stability study
1	10	5	-	-	-
2	10	5	0.35	-	-
3	10	5	0.6	-	40 °C, 25 °C, 2-8 °C
4	10	5	-	0.04	40 °C, 25 °C, 2-8 °C

II.3.12.2 SPRAY DRYING PROCESS AND YIELD

Table II-23 shows the yields of spray-dried MabR1 and placebo formulations. Acceptable yields for MabR1 were obtained with values of > 80 % for the formulations containing Trehalose and HP β CD. However, yields for the polysorbate-containing formulations were slightly lower because unlike the other formulations, the formulation containing polysorbate stuck to the cyclone to some extent and had to be removed by continuous agitation during the spray drying process; separation of powder from the gas stream was probably less effective than with the formulations without PS80 with no product remaining in the cyclone.

Table II-23: Product yield of spray dried placebo and MabR1 formulations.

Formulation	Yield Placebo [%]	Yield MabR1 [%]
5 % Trehalose	40.1	80.4
5 % Trehalose + 0.35 % HP β CD	77.1	81.7
5 % Trehalose + 0.60 % HP β CD	77.7	83.7
5 % Trehalose + 0.04 % PS80	65.8	68.2

II.3.12.3 PROTEIN STABILITY– SUBVISIBLE PARTICLES AND TURBIDITY

Immediately after spray-drying and rehydration, only the formulation of MabR1 which contains 5 % Trehalose and 0.04 % PS80 showed subvisible particle numbers below 50,000 per ml and turbidity values of less than 10 FNU as shown in Figure II-88. With increasing HP β CD concentration up to 0.6 %, a decrease in subvisible particles and turbidity after rehydration was observed compared to the control formulation without surfactant. PS80 also showed better performance in stabilization of the antibody after atomization only. Subvisible particles in the size class > 10 μ m did not significantly differ for the different formulations, as depicted in Figure II-89. Subvisible particles and turbidity in placebo formulations also increased from atomization to spray-drying and rehydration, as shown in Figure II-90. Even the placebo formulations had subvisible particle concentrations of around 20,000 after rehydration.

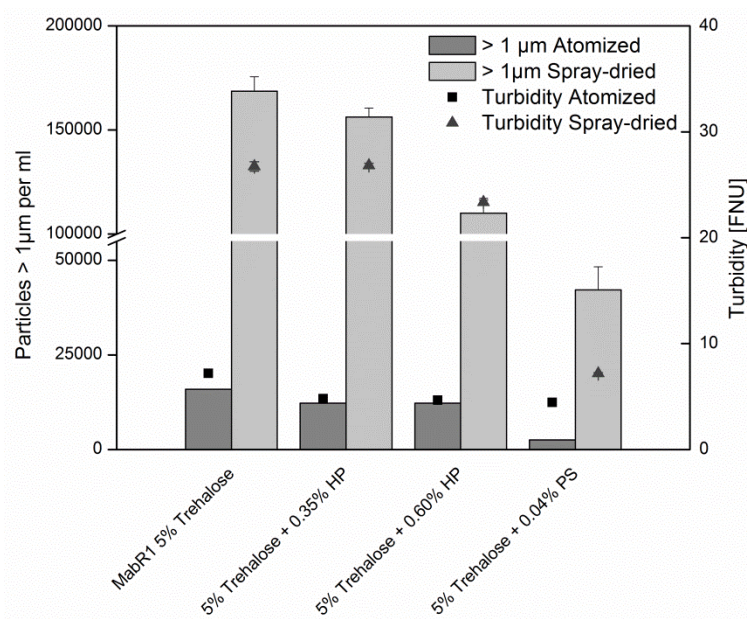


Figure II-88: Turbidity and subvisible particles for atomized and spray-dried and rehydrated formulations of MabR1.

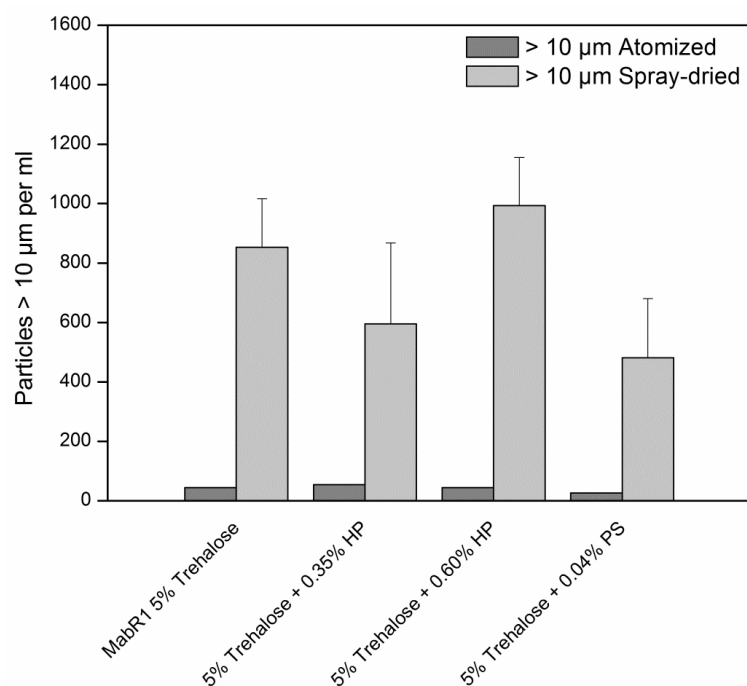


Figure II-89: Subvisible particles > 10 µm for atomized and spray-dried and rehydrated MabR1.

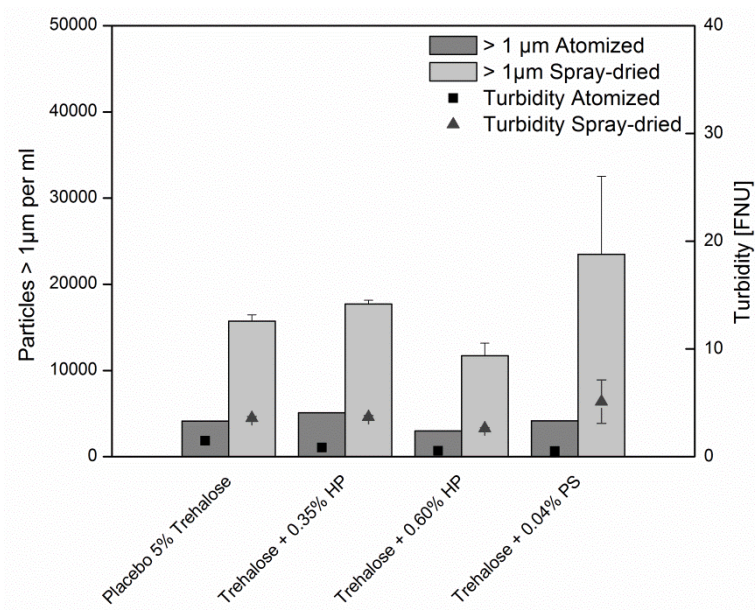


Figure II-90: Turbidity and subvisible particles for atomized and spray-dried and rehydrated placebo formulations without protein.

II.3.12.4 SIZE-EXCLUSION CHROMATOGRAPHY

After spray-drying and rehydration, the relative amount of high-molecular weight aggregates as well as dimer was increased in the formulation of MabR1 which contains 0.04 % polysorbate 80. This was not observed with the other formulations containing no PS80, as shown in Figure II-91 and was also not observed in the previous freeze-drying chapters.

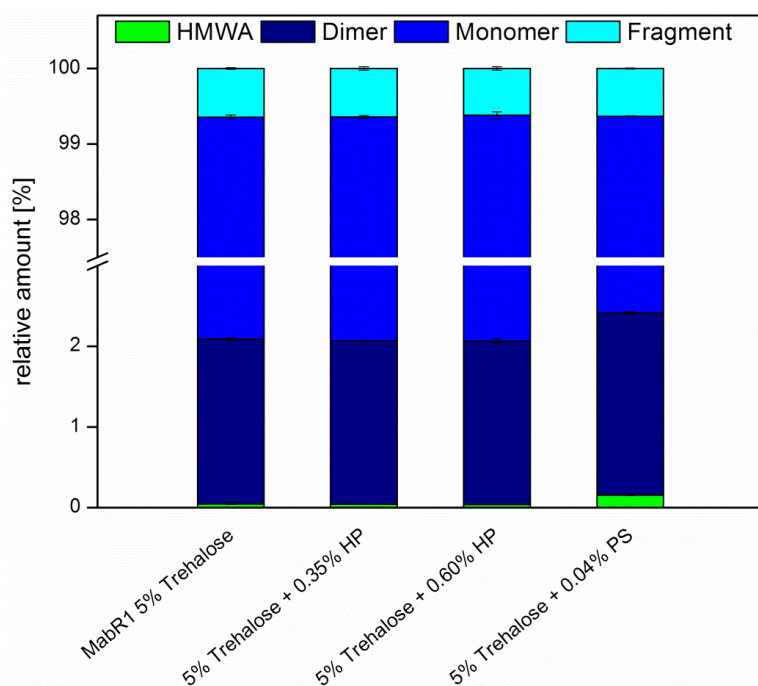


Figure II-91: Relative amount of protein species after spray-drying and rehydration of all formulations of MabR1.

II.3.12.5 PROTEIN STABILITY– STORAGE STABILITY

When stored for 62 days, a slight decrease in turbidity was observed for the formulation containing 0.6 % HP β CD whereas a tendency to higher values was observed for the formulations which contain 0.04 % PS80 (see Figure II-92), independent on storage temperature for both formulations. Subvisible particles > 1 μ m remained almost unchanged in all formulations, which is shown in Figure II-93. The polysorbate containing formulations, which showed a higher amount of dimer immediately after spray-drying, showed a temperature-dependent increase in dimer and a decrease in monomer content as determined with SE-HPLC; this was not observed for HP β CD-containing formulations, as shown in Figure II-94 and Figure II-95. Also in AF4, these trends were only partly visible with a slight decrease of monomer content of PS80-formulations as illustrated in Figure II-96. Large standard deviations for relative monomer and dimer amounts (see Figure II-97) impedes evaluation of these samples.

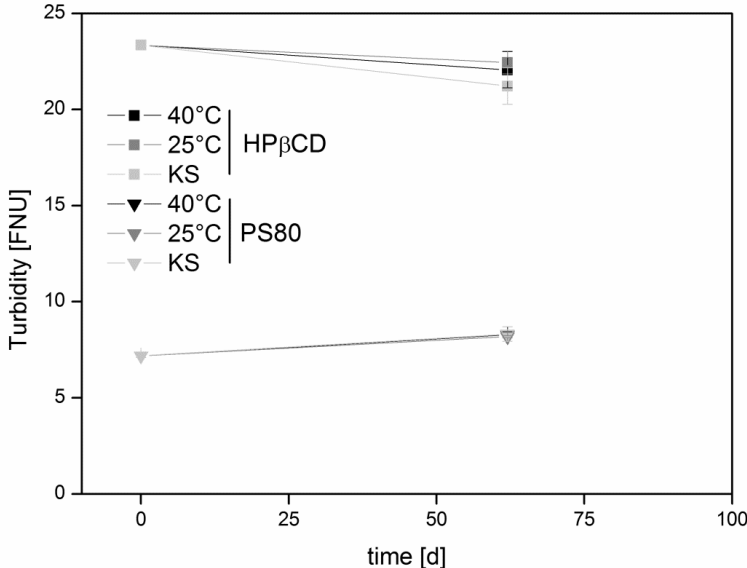


Figure II-92: Turbidity for all formulations of MabR1 with 5 % Trehalose and 0.04 % PS80 or 0.6 % HPβCD stored at three different temperatures.

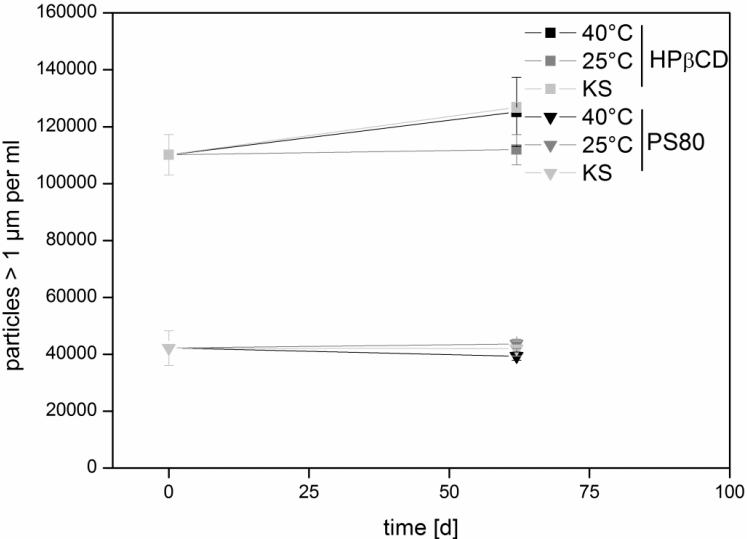


Figure II-93: Subvisible particles > 1 μm for all formulations of MabR1 stored at three different temperatures.

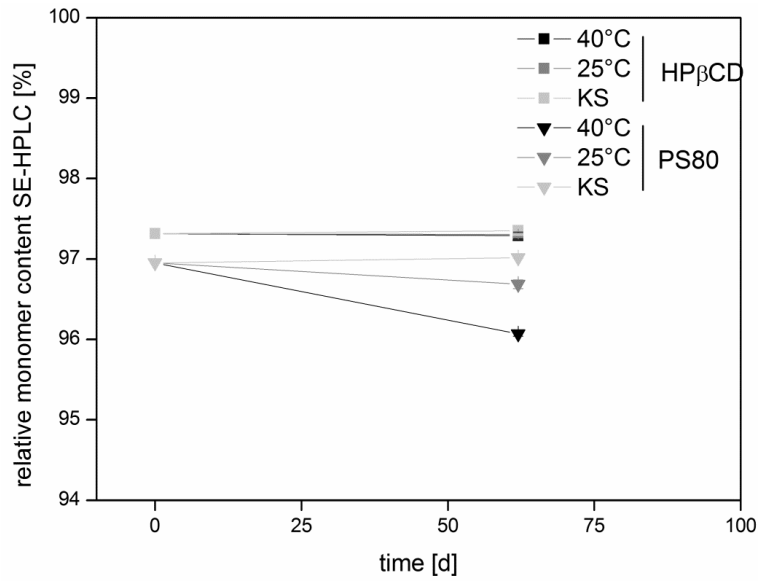


Figure II-94: Relative monomer content as determined with SE-HPLC for all formulations of MabR1 stored at three different temperatures.

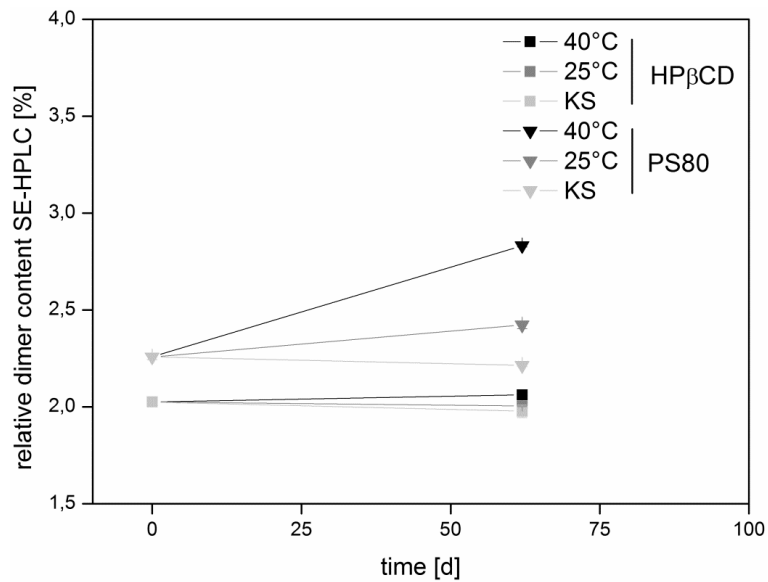


Figure II-95: Relative dimer content as determined with SE-HPLC for all formulations of MabR1 stored at three different temperatures.

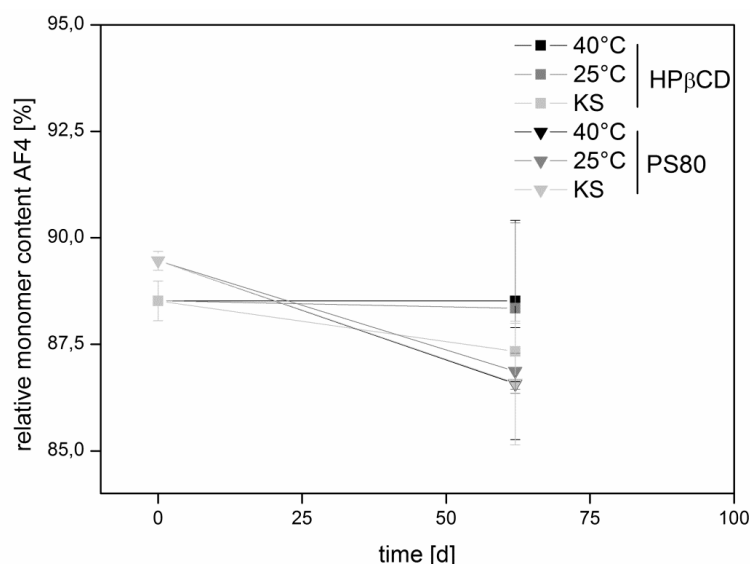


Figure II-96: Relative monomer content as determined with AF4 for all formulations of MabR1 stored at three different temperatures.

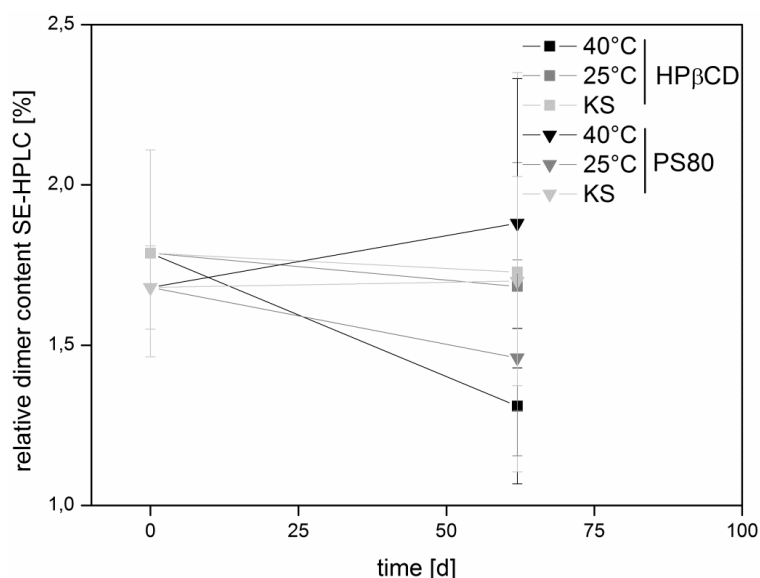


Figure II-97: Relative dimer content as determined with AF4 for all formulations of MabR1 stored at three different temperatures.

II.3.12.6 PHYSICO-CHEMICAL INVESTIGATION OF SPRAY-DRIED SAMPLES - STORAGE STABILITY

The formulation of MabR1 with HPβCD exhibited higher residual moistures than the formulation with PS80 and the differences in residual moistures were also visible in glass transition temperatures, which were consequently higher in PS80 formulations, as shown in Figure II-98 and Figure II-99 while both formulations had approximately the same specific surface areas, as depicted in Figure II-100. Interestingly, the HPβCD formulations showed a small temperature-dependent decrease in residual moisture and an increase in T_g over storage period. These differences may also be attributed to inhomogeneities in the powder. Reconstitution times varied greatly between formulations from 2 to more than 11 minutes.

Especially PS80 containing formulations reconstituted faster (2-3 minutes) because the spray dried powder immersed in the added liquid whereas the powder of the HP β CD-containing formulation was floating on top of the liquid, thus the wetted area was relatively small and dissolution is slow.

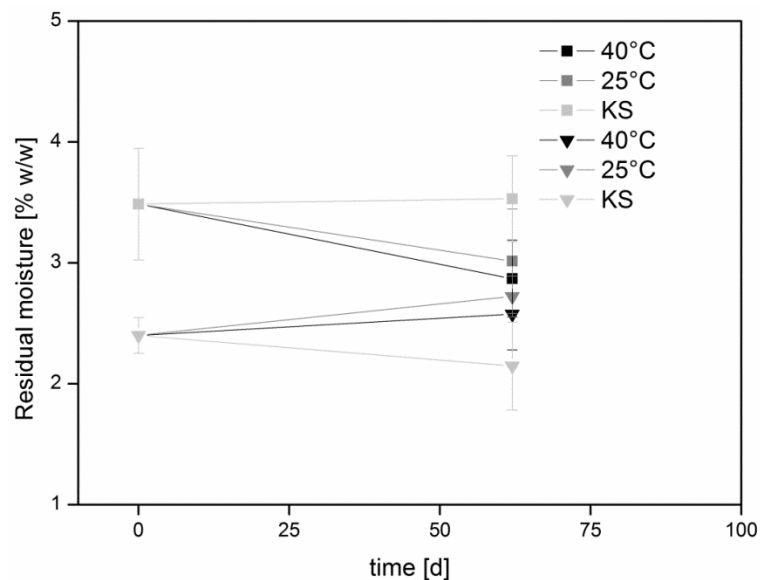


Figure II-98: Residual moisture of all formulations of MabR1 stored at three temperatures.

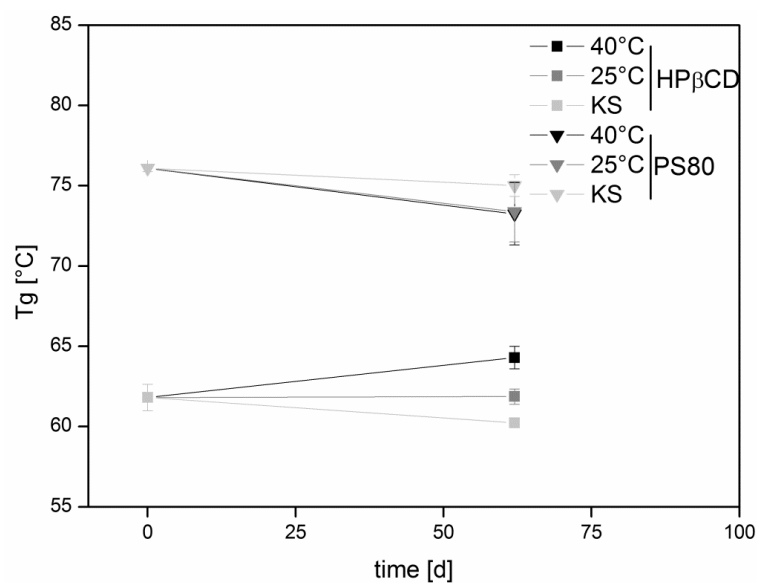


Figure II-99: Glass transition temperatures (T_g) of all formulations stored at three different temperatures.

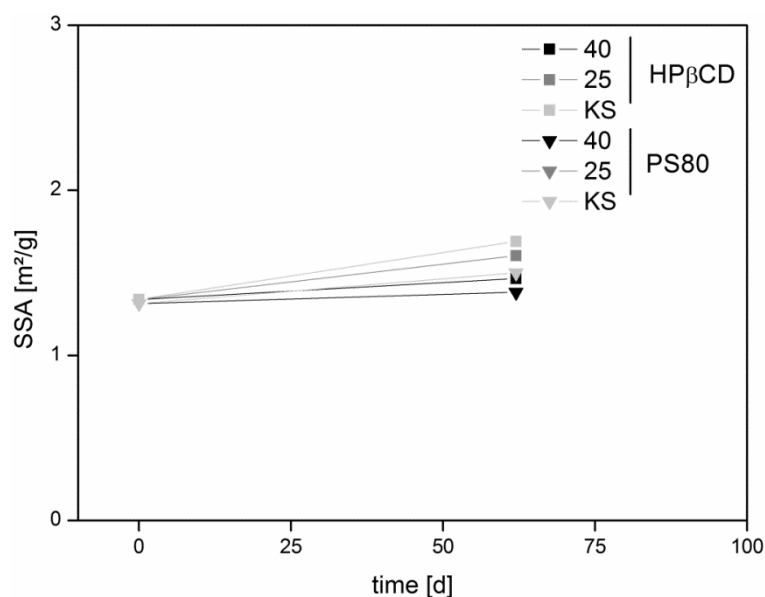


Figure II-100: Specific surface area for all formulations of MabR1 stored at three different temperatures.

II.3.12.7 SUMMARY AND DISCUSSION

Spray-drying of MabR1 was performed as a control experiment to the freeze-drying processes. In the previous chapters, it was found that a low SSA was general beneficial for MabR1 stability with regard to subvisible particles. As spray-drying usually produces higher values of surface areas due to atomization of the liquid prior to drying [65], HPβCD was expected to be inferior to polysorbate in this study. This hypothesis was confirmed by subvisible particle analysis after atomization as well as after rehydration of the dried powder. Atomization and subsequent drying of the liquid droplet is usually finished within less than a second. Fast diffusion to the produced air-water-interface thus is necessary for an excipient to enrich at this interface. It has been shown that polysorbate is more quickly decreasing surface tension and equilibrium is reached faster compared to HPβCD [71]. However, with the formulation containing polysorbate 80, an increase in dimer content and high-molecular weight aggregates was observed in size-exclusion chromatography. This was observed immediately after spray drying and became more pronounced during isothermal storage with a significant reduction in monomer content. This dual effects of polysorbate – stabilization at interfaces, but destabilization due to oxidation has already been reported for IL-2 muterin [74]. Oxidation of especially antibodies is not easy to detect without mass spectroscopy and we could not directly measure oxidized species of antibodies; however in this study, the temperature-dependent reduction of protein monomer may be attributed to oxidation of the antibody by polysorbate 80. Degradation of polysorbates has been extensively studied [75-78] and includes formation of peroxides and fatty-acid release by hydrolyzation [76]. It has been shown that polysorbates can oxidize proteins in liquids as well as in lyophilizates [74, 78]. It is suggested to use the minimum effective concentration of polysorbates to minimize degradation products [76] and also a concentration

dependency in protein degradation was observed [74]. In our studies, we chose a concentration of 0.004 % of PS80 which is only little above the CMC for freeze-drying but a 10-fold higher concentration of 0.04 % for the spray drying experiments because surfaces areas generated by atomization were expected to be higher in spray-drying. This difference in concentrations may be the reason why we did not observe loss of monomer in freeze-drying experiments. In addition, spray drying is performed at high temperatures and in this study air was used as drying gas, which may have fostered degradation of polysorbates already during the drying process.

II.3.13 HP β CD AS BULKING AGENT IN FREEZE-DRYING

II.3.13.1 INTRODUCTION

A potential use of HP β CD, as presented in the introduction, is the ability to serve as a bulking agent, forming an amorphous glass and providing hydrogen bonds to stabilize proteins in the dried state. However, as will be shown in chapter II.3.14, HP β CD needs to be formulated with PS80 to attenuate subvisible placebo particles formed by HP β CD alone. HP β CD, since not used alone, could then be used as a replacement to the commonly employed disaccharides sucrose and trehalose. Benefits of HP β CD compared to the well-established, relatively cheap and efficiency-proven disaccharides would be the possibility to design more economic and faster freeze-drying processes due to the high glass transition temperatures of HP β CD (appr. -13 °C to -14 °C for the pure excipient). HP β CD was formulated at 1.0% (w/v) and polysorbate 80 was added in a concentration of 0.004 %. Storage stability studies were performed with 10 mg/ml MabR1, 1.0 mg/ml hGH and 1.0 mg/ml GCSF. Data from GCSF samples are not presented here because after storage for 48 days, visible particles appeared in all formulations with 1 % HP β CD, similar to the results obtained for sucrose based formulations.

II.3.13.2 LYOPHILIZATION PROCESS CONSIDERATIONS

Due to the relatively high T_g' of pure HP β CD, even aggressive lyophilization of these lyophilizates did not lead to macroscopic collapse of the freeze-dried cake. For this reason, the process is called “aggressive freeze-drying”. As postulated, economic freeze-drying processes are possible with HP β CD as bulking agent.

II.3.13.3 PROTEIN STABILITY IMMEDIATELY AFTER FREEZE-DRYING OF MABR1

When polysorbate was added to lyophilized formulations of MabR1, subvisible particles and turbidity could be significantly reduced compared to formulations without PS80, as shown in Figure II-101. Furthermore, no changes in fragments or dimers could be observed with size exclusion chromatography for the aggressive freeze-drying run, as illustrated in Figure II-102, similar to sucrose-based formulations, as discussed earlier. Based on these results, samples were subjected to storage stability.

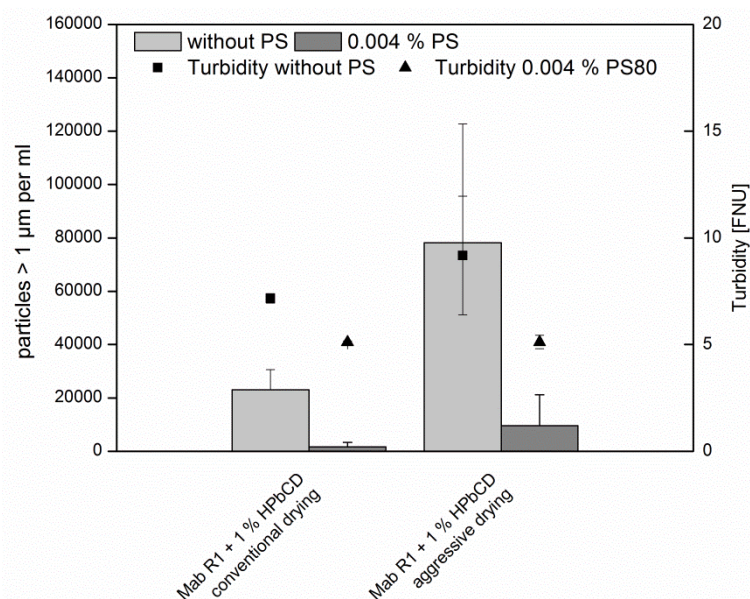


Figure II-101: Subvisible particles > 1 µm and turbidity for HPβCD-based formulations of MabR1.

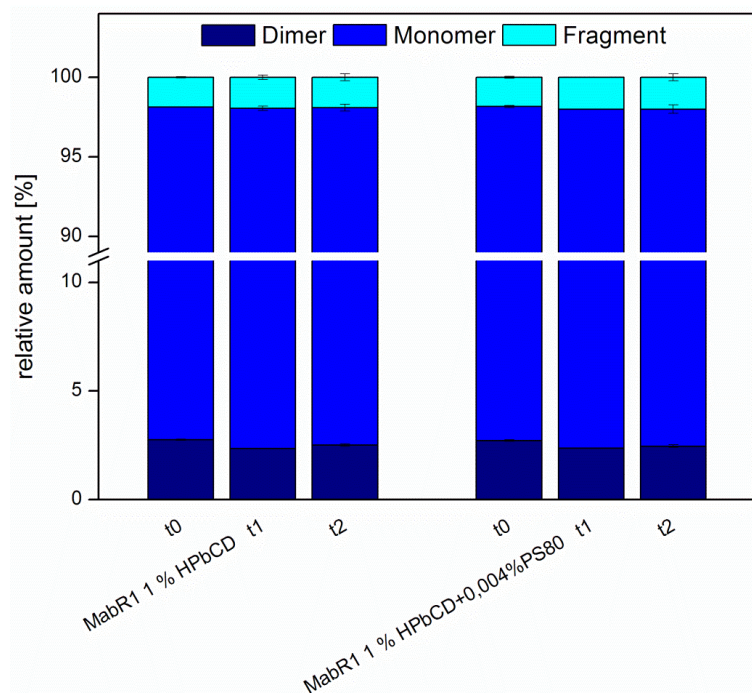


Figure II-102: Relative amount of protein species for HPβCD-based formulations, as determined with SE-HPLC. t0 = analysis after preparation; t1 = analysis after freeze-thawing; t2 = analysis after freeze-drying and rehydration.

II.3.13.4 STORAGE STABILITY STUDY OF MABR1

MabR1 was stored at 60 °C, 40 °C and 25 °C to compare results with the first study of MabR1 stored at the same concentration with sucrose and PS80. Over storage time, a large number of subvisible particles formed, as shown in Figure II-104 and also turbidity increased, as illustrated in Figure II-103. This was most pronounced with the formulation which was stored at 60 °C and formulations based on HPβCD showed higher turbidities and subvisible particles, however, only turbidity can be considered to be linear in this range. The samples which were

stored at 40 °C and 25 °C showed less increase in subvisible particles with appr. 50,000 and 35,000 particles > 1 µm per ml, respectively and were comparable to the sucrose reference formulation. Temperature-dependent degradation of MabR1 was further confirmed by size exclusion chromatography and AF4. Protein monomer content decreased and dimer content increased, as shown in Figure II-105 and Figure II-106 and HPβCD-containing formulations showed slightly faster degradation kinetics than sucrose based formulations. Interestingly, decrease in relative monomer content seemed to level off between the second-last and last analysis time point. The higher the temperature, the higher the reduction of monomer and increase in dimer content was. These results were basically also confirmed by AF4 measurements, as shown in Figure II-107 and Figure II-108. The loss in monomer goes along with a reduction of protein recovery, especially for the samples stored at 60 °C, as shown in Figure II-109. Consequently, protein degradation was more exaggerated with HPβCD-based formulations compared to the collapse freeze-dried sucrose formulations.

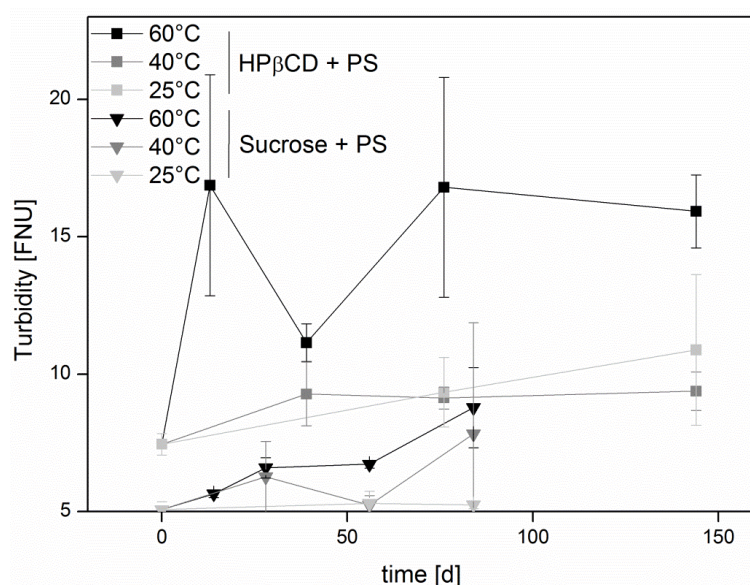


Figure II-103: Turbidity for MabR1 formulated with 1 % HPβCD and 0.004 % PS80 over storage time. Storage stability was performed at 60 °C, 40 °C and 25 °C.

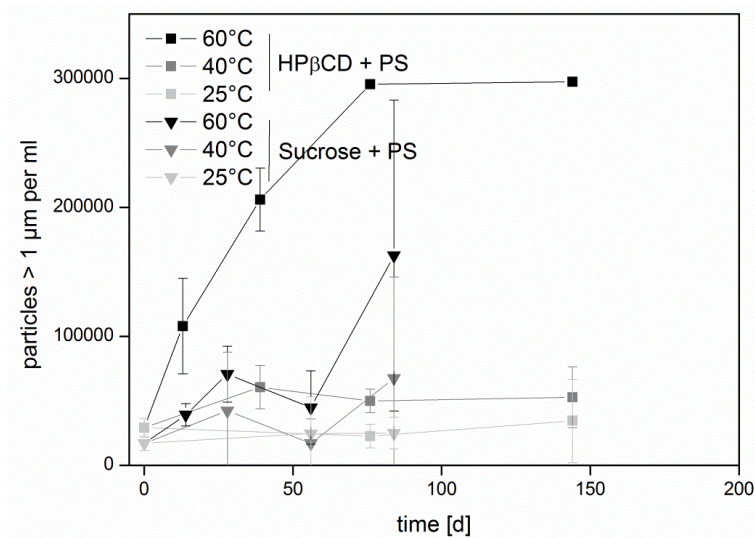


Figure II-104: Results from light obscuration for MabR1, formulated with 1 % HPβCD + 0.004 % PS80 or 1 % Sucrose and 0.004 % PS80.

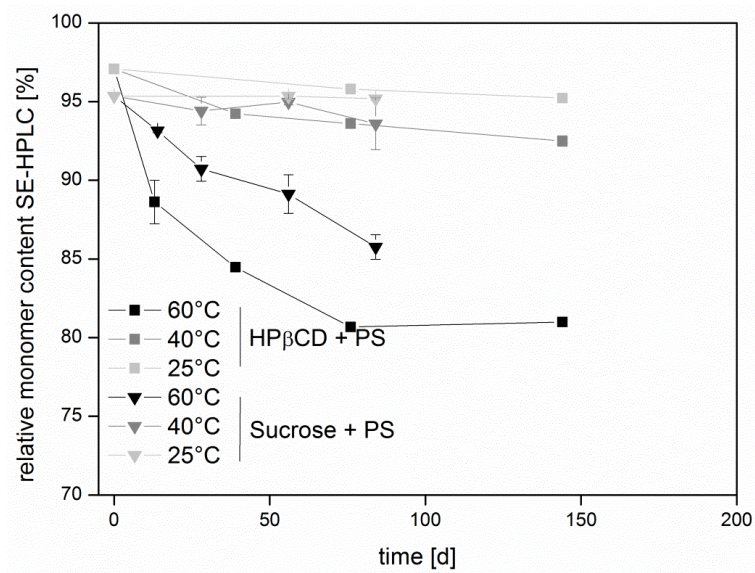


Figure II-105: Relative monomer content as determined by SE-HPLC over storage time for MabR1 and 1 % HPβCD + 0.004 % PS80 or 1 % Sucrose + 0.004 % PS80.

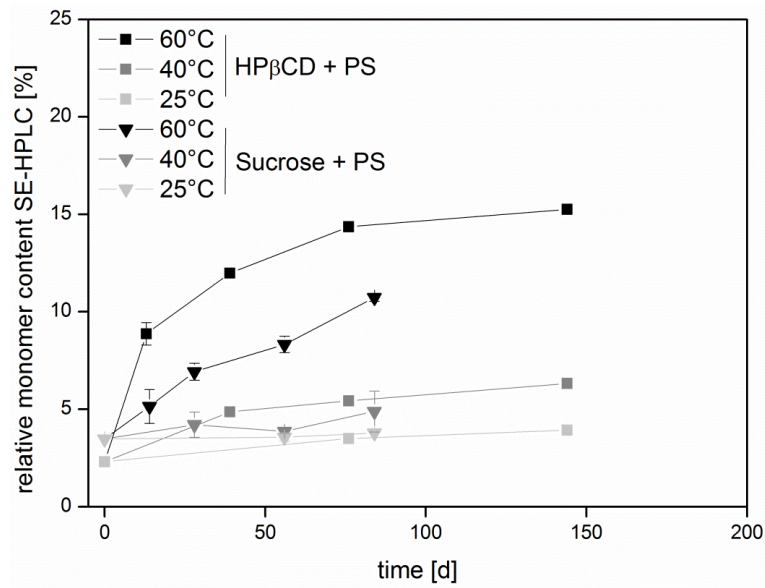


Figure II-106: Relative dimer content as determined by SE-HPLC over storage time for MabR1 and 1 % HPβCD + 0.004 % PS80 or 1 % Sucrose + 0.004 % PS80.

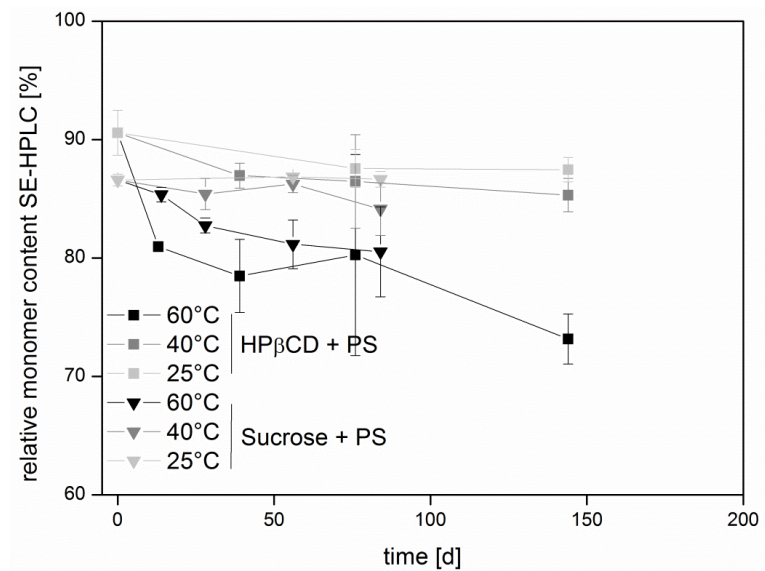


Figure II-107: Relative monomer content as determined by AF4 over storage time for MabR1 and 1 % HPβCD + 0.004 % PS80 or 1 % Sucrose + 0.004 % PS80.

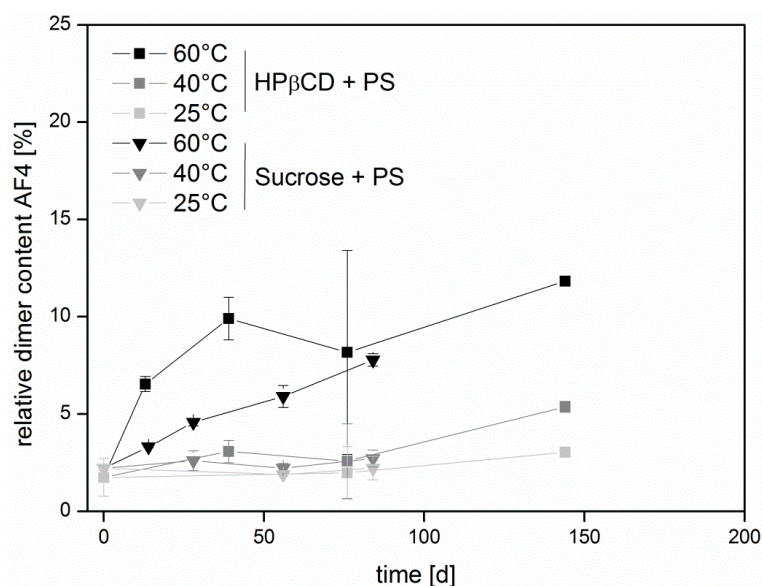


Figure II-108: Relative dimer content as determined by AF4 over storage time for MabR1 and 1 % HPβCD + 0.004 % PS80 or 1 % Sucrose + 0.004 % PS80.

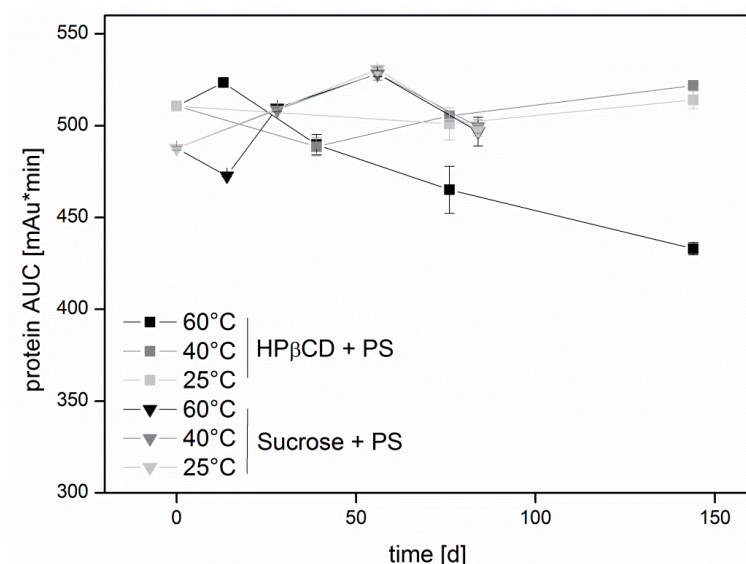


Figure II-109: Protein recovery as determined with SE-HPLC for MabR1 stored at three different temperatures.

II.3.13.5 PHYSICO-CHEMICAL INVESTIGATION ON 1 % HPβCD-BASED FORMULATIONS OF MABR1

Reconstitution of all samples was very fast with less than 10 seconds required for complete dissolution. Residual moistures for samples increased over storage time with increasing temperatures, as shown in Figure II-110. Residual moisture uptake is favoured by the high specific surface area and low amount of solids. Hence, glass transition temperatures slightly decreased. The sample, which was stored at 60 °C was therefore stored at a temperature around its T_g , as shown in Figure II-111. However, specific surface areas for all samples were between $\sim 1.5 \text{ m}^2/\text{g}$ and $\sim 1.7 \text{ m}^2/\text{g}$ over storage time, and no visible collapse or browning was observed during storage, independent of storage temperature. Lyophilized cakes of HPβCD

seem to be quite brittle at a (very low) concentration of approximately 20 mg/ml solids and cakes showed some macroscopic damage with broken-off pieces, as shown in Figure II-112.

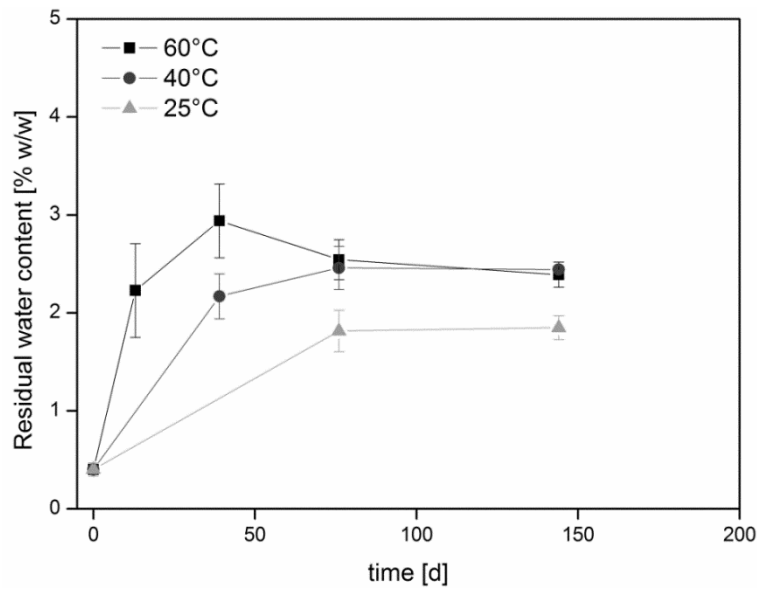


Figure II-110: Residual moisture of lyophilized cakes of MabR1 stored at three different temperatures.

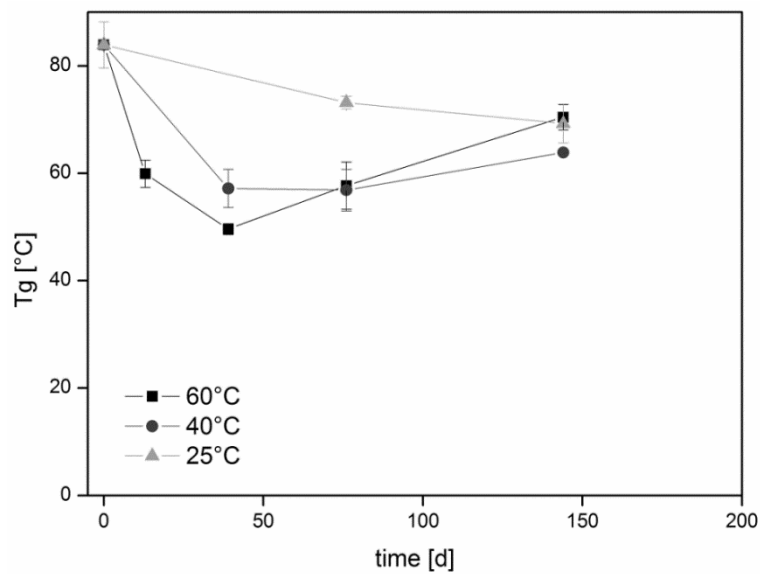


Figure II-111: Glass transition temperatures of lyophilized cakes of MabR1 stored at three different temperatures.



Figure II-112: Macroscopic appearance of lyophilizate cakes based on 1 % HP β CD.

II.3.13.6 STORAGE STABILITY OF HGH FORMULATED WITH 1% HP β CD AND PS80

Storage stability of 1 mg/ml hGH with 1.0 % HP β CD and 0.004 % PS80 was performed, and lyophilizates were stored at 60 °C, 40 °C and 25 °C. Turbidity and subvisible particles > 1 μ m did not change significantly over observed storage time independent of storage temperature as shown in Figure II-113 and Figure II-114. However, hGH monomer content decreased when stored at 60 °C and dimer content increased while total protein AUC remained unchanged (Figure II-115, Figure II-116 and Figure II-117). The increase in dimer content for storage temperatures of 40 °C and 25 °C was only 0.1 %. These results were confirmed by AF4 with a temperature-dependent increase in dimer content of hGH after 118 days, as shown in Figure II-118.

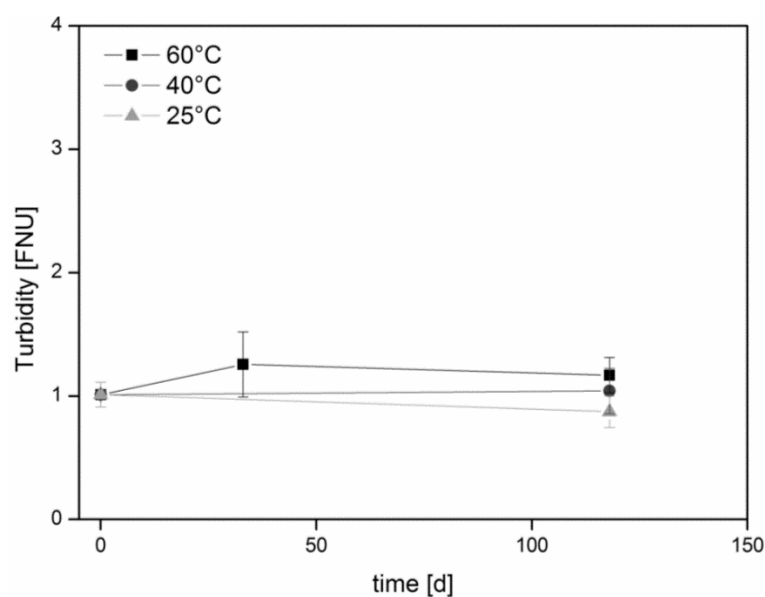


Figure II-113: Turbidity for hGH formulated with 1 % HP β CD and 0.004 % PS80. Storage stability was performed at 60 °C, 40 °C and 25 °C.

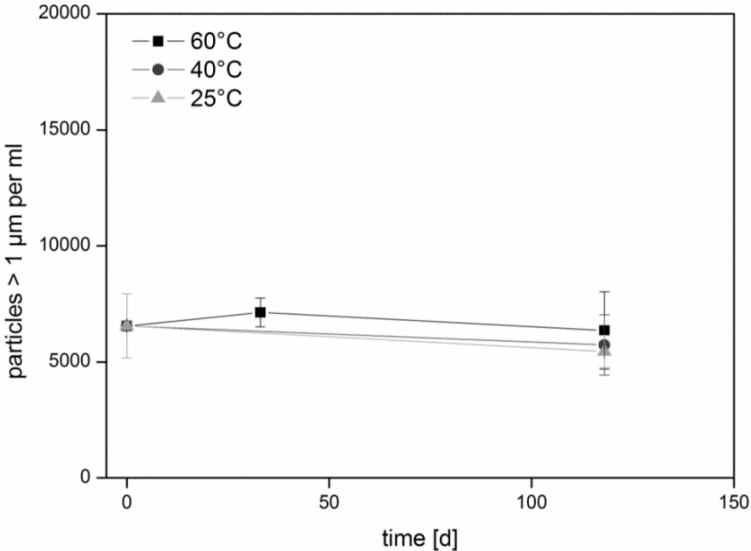


Figure II-114: Subvisible particles > 1 µm for hGH formulated with 1 % HPβCD and 0.004 % PS80. Storage stability was performed at 60 °C, 40 °C and 25 °C.

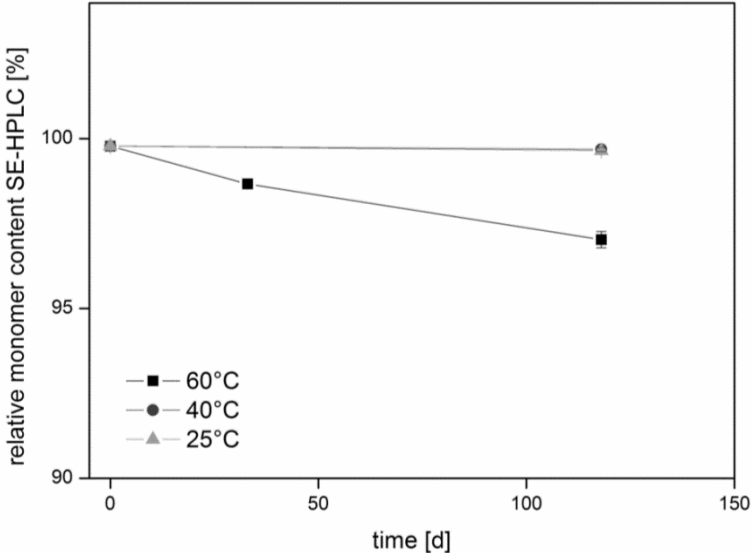


Figure II-115: Relative monomer content as determined by SE-HPLC of hGH stored at three different temperatures.

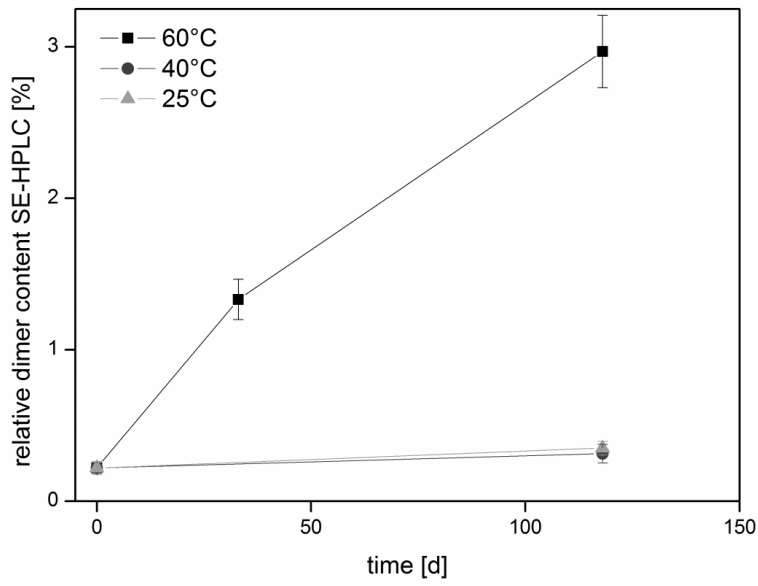


Figure II-116: Relative dimer content as determined by SE-HPLC of hGH stored at three different temperatures.

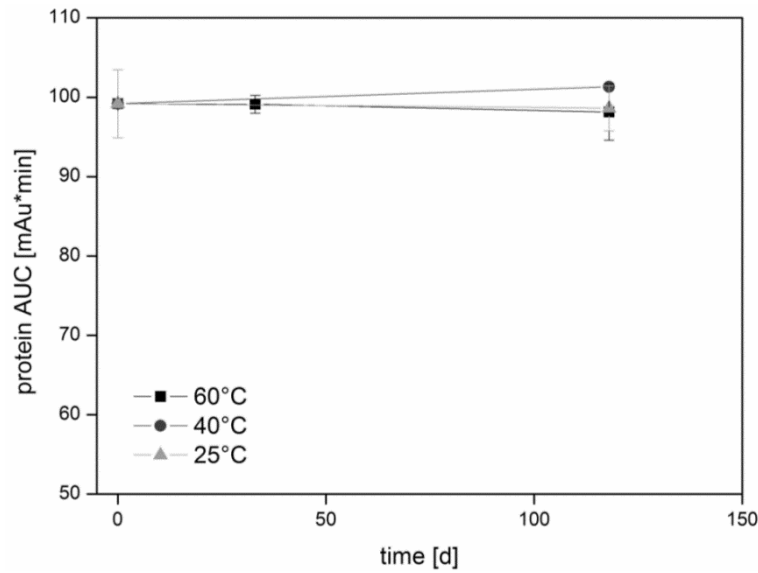


Figure II-117: Total protein recovery as determined by SE-HPLC for hGH stored at three different temperatures.

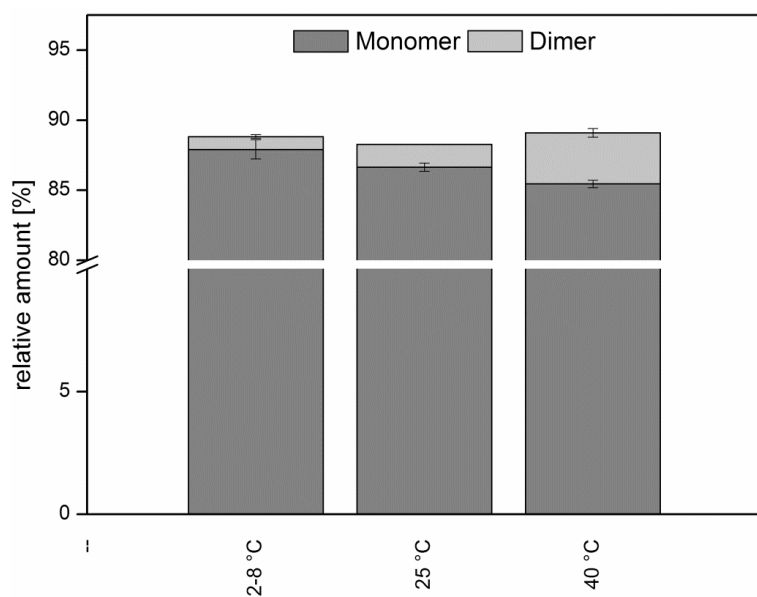


Figure II-118: Relative monomer and dimer content as determined by AF4 of hGH + 1 % HPβCD + 0.004 % PS80 stored at three temperatures for 118 days.

II.3.13.7 PHYSICO-CHEMICAL INVESTIGATION OF STORED hGH SAMPLES

Residual moisture for stored samples increased over storage time, which was most pronounced for samples stored at 60 °C, as depicted in Figure II-119. Glass transition temperatures were quite high with temperatures of around 80 °C and did not change significantly over storage period (see Figure II-120). Reconstitution was very fast and complete dissolution was obtained within less than 10 seconds.

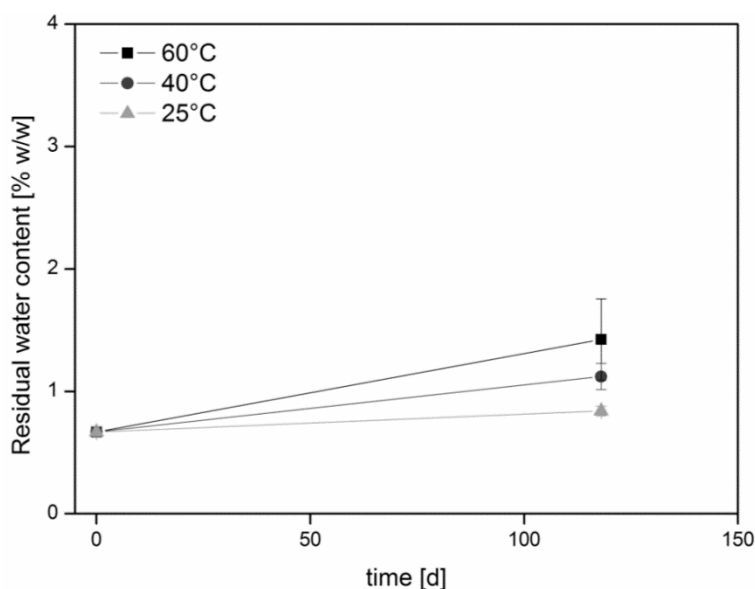


Figure II-119: Residual moistures for stored samples of hGH over storage time.

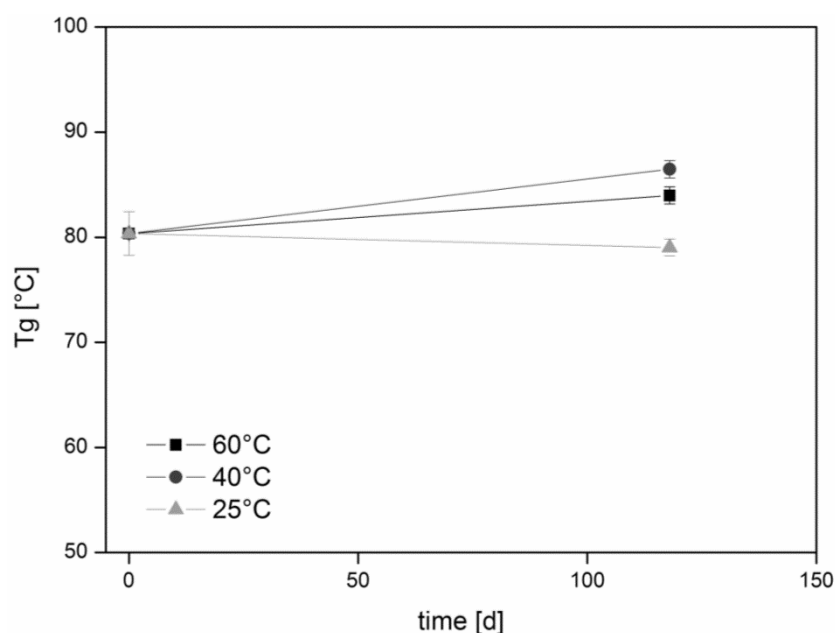


Figure II-120: Glass transition temperatures for stored samples of hGH over storage time.

II.3.13.8 SUMMARY AND DISCUSSION

Different results for HP β CD as bulking agent in combination with 0.004 % PS80 were obtained. When HP β CD was used in a 1:1 mass ratio of excipient:MabR1, poor stability of the antibody was observed and HP β CD was inferior to sucrose. However, it is important to mention that formulations based on HP β CD did not collapse during the collapse freeze-drying conditions but an elegant cake structure was retained whereas sucrose based formulations collapsed during the freeze-drying process. It has been discussed that the high temperatures encountered during the aggressive freeze-drying process may anneal the amorphous glass and thus, increased long-term stability is possible (see discussion in section II.3.8.5). While this is true for both formulations, only the collapsed sucrose formulations can profit from the low SSA generated with a collapse freeze-drying process. Hence, comparison of both formulations is limited considering thermal history and SSA and the different residual moistures and T_g s. However, another hint that HP β CD is probably not a significant better lyoprotectant than sucrose can be found in the data from section II.3.5, where storage stability of MabR1 was investigated formulated with sucrose and both excipients, HP β CD and PS80. HP β CD was added in substantial amounts (6 mg/ml) to sucrose, which was used in a concentration of only 10 mg/ml. At these concentrations, increased storage stability of HP β CD-containing formulations should have been visible compared to the formulation with PS80, which only contains sucrose as lyoprotectant. This was not the case and degradation of the model antibody was equally fast with no clear advantage of the HP β CD formulation. For hGH however, at a excipient:protein ratio of 10:1, at least at storage temperatures of 40 °C and

25 °C, acceptable stabilization of the protein was observed. These findings indicate that there is a potential of HP β CD to act as bulking agent and stabilization of certain proteins can be obtained. From a toxicological aspect, higher concentrations of HP β CD can be employed and up to 3 g/day are tolerated in humans [79]. Economic advantages of HP β CD with its high glass transition temperatures, especially T_g' , enables more efficient freeze-drying cycles if product stability is comparable to commonly used excipients. Employment of HP β CD should therefore be considered, however, from our perspective, combination with polysorbates is necessary if subvisible particles are a major concern.

II.3.14 SUBVISIBLE PARTICLE FORMATION BY PLACEBO HP β CD

II.3.14.1 INTRODUCTION

Freeze-drying is the most important process for drying of temperature-sensitive active pharmaceutical ingredients, especially proteins. The process includes a freezing step followed by primary drying with removal of ice by sublimation. Unfrozen water is removed by diffusion and desorption in the secondary drying step and typical residual moisture levels of 1.0 % (m/m) are obtained. The freeze-drying process is considered gentle and activity-retaining, however, it comprises several stresses to proteins such as cold denaturation, presence of the ice-water interface, freeze-concentration with possible crystallization of excipients and removal of water and hydration shell [1]. Furthermore, upon reconstitution, a large liquid-air interface is formed which can also be detrimental for protein stability [80]. To counteract stresses from the freeze-drying process, excipients are added to formulations of proteins. To protect proteins from interfacial denaturation and aggregation, surfactants like polysorbates currently are the gold standard. However, their tendency to create peroxides with potentially oxidation of proteins is receiving a lot of attention recently [76, 78, 81]. A possible alternative to polysorbates is HP β CD, which is also known to accumulate at the air-water interface [24]. However, we observed that after freeze-drying and rehydration of HP β CD-containing samples, subvisible particles were formed. Particles present in a formulation can originate from various sources, e.g. filters, packaging material or stoppers. However, in protein formulations, subvisible particles are often formed by aggregation of protein monomers and this is considered a serious product quality issue [82]. While quantification of subvisible particles in the range of > 1 μ m is quite easy, the origin of those particles is difficult to determine. Furthermore, situation becomes increasingly difficult if subvisible particles can be formed not only by a protein present but also by excipients in this formulation. The aim of this work was to study the formation of aggregates of HP β CD and to investigate in which process step these particles form. In addition, we wanted to find out, which formulation- and process parameters are influencing subvisible particle formation and how formation of those particles can be avoided.

II.3.14.2 MATERIALS

Sodium phosphate monobasic dihydrate and sodium phosphate dibasic dehydrate were obtained from Merck (Merck, Darmstadt, Germany). Potassium phosphate dibasic, polysorbate 80 and sucrose was obtained by Sigma Aldrich Chemicals (Sigma Aldrich, Munich, Germany). Hydroxypropyl-beta-cyclodextrin, (HP β CD) (Cavasol W7 HP Pharma, molar degree of substitution (mDS) 0.59 – 0.73) was obtained from Wacker (Wacker Chemie AG, Munich, Germany) and was the main employed cyclodextrin derivative in the study; HP β CD (Kleptose HP, Roquette, Frankfurt, Germany) with a different mDS of 0.87 was kindly provided

by Roquette. β -Cyclodextrin (β -CD) was used from Wacker (Cavamax W7 Pharma, Wacker Chemie AG, Munich, Germany). All chemicals were of analytical grade.

II.3.14.3 PREPARATION OF FORMULATIONS (FOR PLACEBO FORMULATIONS ONLY)

Formulations were prepared by mixing concentrated stock solutions of excipients and protein and final dilution with buffer. For Sucrose, Trehalose, Arginine phosphate and HP β CD, usually 10 % (w/v) solutions were prepared. A 10 mM sodium/potassium phosphate buffer pH=7.2 was used to prepare 5.05 % Arginine phosphate, 5 % Sucrose and 5 % Trehalose in combination with 0.0 %, 0.1 % or 1.0 % HP β CD. In addition, a formulation with 1.0 % HP β CD was prepared. All solutions were filtered through 0.22 μ m Celluloseacetate filters (VWR, Ismaning, Germany) which were pre-rinsed with at least 5 ml of water. Either 2.3 ml or 3 ml of each formulation was pipetted into DIN 6R or DIN 20R vials, respectively, semi-stoppered and transferred to the freeze-dryer.

II.3.14.4 CONVENTIONAL FREEZE-DRYING PROCESS (FOR PLACEBO FORMULATIONS ONLY)

For the placebo freeze-drying experiments only, the following freeze-drying process was used: Lyophilization of the samples in a conventional process was performed using a Martin Christ Epsilon 2-6D freeze-dryer (Martin Christ, Osterode am Harz, Germany) or an FTS Lyostar 2 (SP Scientific, Stone Ridge, USA). The samples were cooled to -60 °C within with 0.3 °C minute (slow freezing, SF). In addition, a second set of samples was frozen with liquid nitrogen immersion on the lyophilizer tray (N₂) and placed on the lyophilizer shelves at -60 °C. This temperature was held for 2 hours to ensure complete solidification of the samples. Subsequently, the pressure was reduced to 0.08 mbar and the temperature was raised to -30 °C for primary drying with a heating rate of 0.5 °C per minute. These conditions were held for 45 hours. Secondary drying was performed at three temperatures, 0 °C for 5 hours, 30 °C for 3 h and 40 °C for 10 hours each at a pressure of 0.011 mbar. The heating rates were 0.5 °C/min between the steps. After freeze-drying, re-pressurization of the dryer was performed using dry air to approximately 800 mbar and the vials were stoppered. Samples were analyzed directly after preparation (t₀), after freeze-thawing (t₁, FT), after primary drying (t₂, PD) and secondary drying (t₃, SD)

II.3.14.5 SUBVISIBLE PARTICLE FORMATION DURING THE FREEZE-DRYING PROCESS

After preparation of formulations and filtration as well as after freeze-thawing and the primary drying step, all samples remained clear with almost unchanged subvisible particle counts. However, in the samples with HP β CD, an increase in subvisible particles in the 1-digit micrometer range, as well as in turbidity was detected after the secondary drying step. This increase in subvisible particles and turbidity was observable independent on presence of

amorphous stabilizers sucrose, trehalose or arginine phosphate or when HP β CD was used as single excipient as shown in Figure II-121, Figure II-122, Figure II-123 and Figure II-124. The amount of subvisible particles detected after secondary drying as well as the turbidity value were influenced by the concentration of HP β CD used and the freezing protocol. As expected, the higher the concentration of HP β CD, the more particles are generated, which is true for the formulations based on Sucrose and Trehalose. Surprisingly, the opposite was observed with the formulations based on arginine phosphate and the lower concentration of HP β CD showed higher subvisible particles numbers than the formulation with 1.0 %. The impact of the freezing protocol was quite distinct and nitrogen immersion in general resulted in higher total particle counts than the slow ramp freezing protocol.

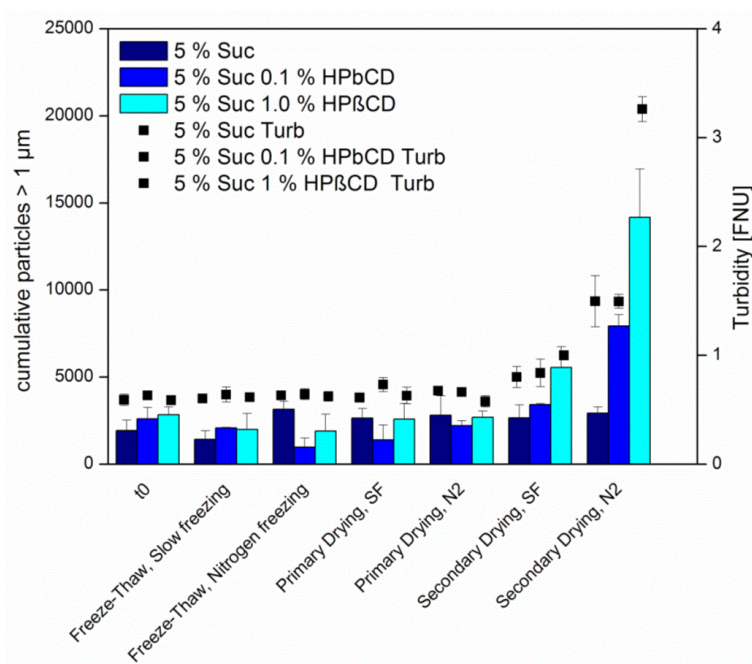


Figure II-121: Subvisible particles and turbidity for sucrose-based formulations without HP β CD, or containing 0.1 % or 1.0 % HP β CD. Samples were analysed after preparation (t0), freeze-thawing, primary drying or secondary drying and were either ramp frozen (SF) or liquid nitrogen immersed (N2).

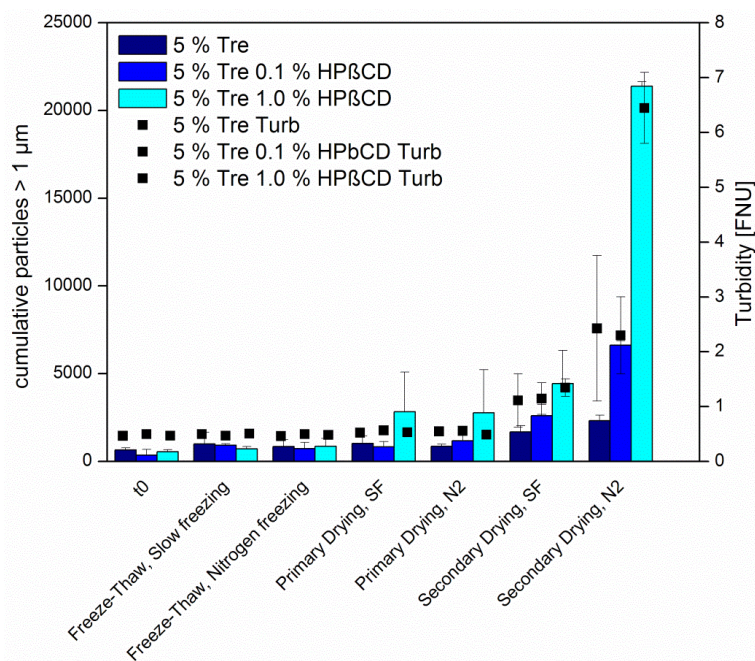


Figure II-122: Subvisible particles and turbidity for trehalose-based formulations without HPβCD, or containing 0.1 % or 1.0 % HPβCD. Samples were analysed after preparation (t0), freeze-thawing, primary drying or secondary drying and were either ramp frozen (SF) or liquid nitrogen immersed (N2).

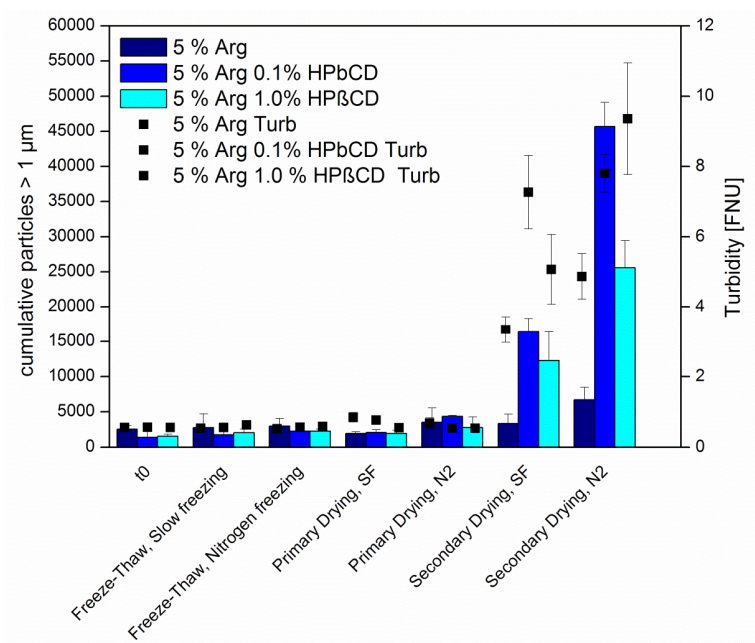


Figure II-123: Subvisible particles and turbidity for arginine phosphate-based formulations without HPβCD, or containing 0.1 % or 1.0 % HPβCD. Samples were analysed after preparation (t0), freeze-thawing, primary drying or secondary drying and were either ramp frozen (SF) or liquid nitrogen immersed (N2).

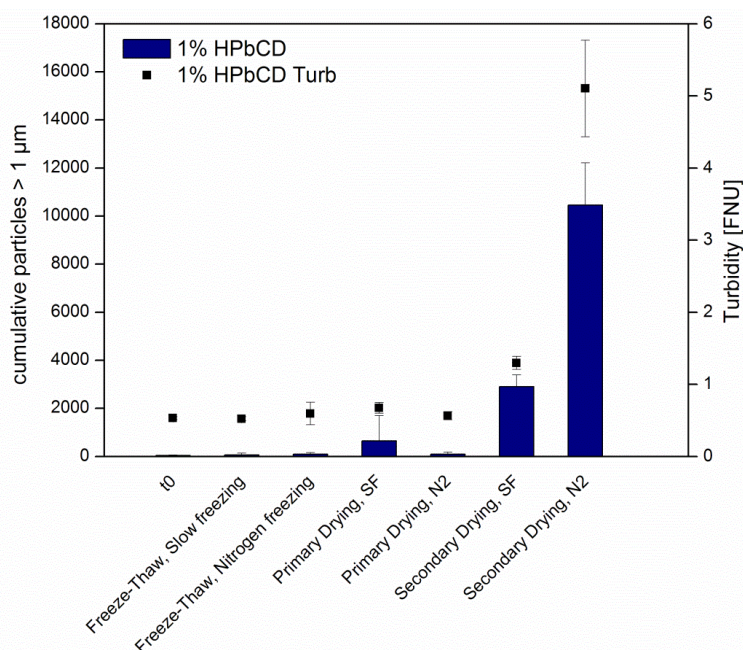


Figure II-124: Subvisible particles and turbidity for formulations with 1.0 % HP β CD. Samples were analysed after preparation (t0), freeze-thawing, primary drying or secondary drying and were either ramp frozen (SF) or liquid nitrogen immersed (N2).

II.3.14.6 INFLUENCE OF RESIDUAL MOISTURE

The formation of subvisible particles during the freeze-drying process was observed after secondary drying only, in which, among other product quality attributes, the residual moisture is decreased from 20 -5 % to a desired level of around 1 % (w/v) or below [83]. Consequently, one of the possible product quality attributes influencing particle formation is the residual moisture of the product. After secondary drying at 40 °C, residual moistures of all samples were well below 1.0 % and even below 0.5 % for the sucrose and trehalose based formulations. To see the influence of residual moisture on particle formation, a the trehalose-based formulations with no HP β CD, 0.1 % or 1.0 % was freeze-dried and extracted from the freeze-drier after 3 hours of secondary drying at 3 different temperatures (10 °C, 25 °C and 40 °C) to produce different residual moisture levels. Freezing and primary drying was carried out exactly as in the other experiments. Trehalose as bulking agent was chosen because glass transition temperatures of trehalose are higher at comparable residual moisture levels than sucrose and macroscopic collapse can be avoided. The formulations containing 5 % trehalose only, which served as a control, did not show a correlation between residual moisture and subvisible particles whereas an increase in subvisible particle concentrations was observed in the samples containing HP β CD starting at residual moistures of around 0.5 % as shown in Figure II-125 and Figure II-126. This was more pronounced with the formulation of 1.0 % HP β CD compared to the lower concentration of 0.1 %.

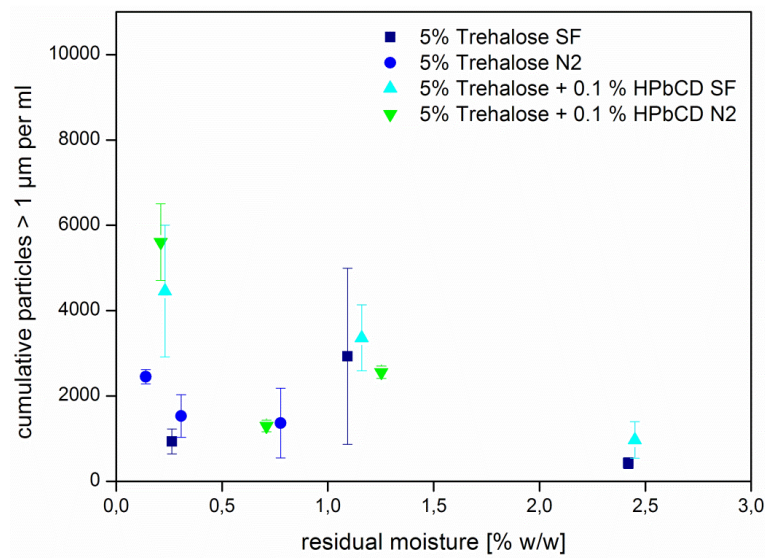


Figure II-125: Subvisible particle and formation and residual moisture of 0.1 % (w/v) HPβCD in combination with 5 % Trehalose. Samples were either ramp frozen with 0.3 °C/min (SF) or liquid nitrogen immersed (N2).

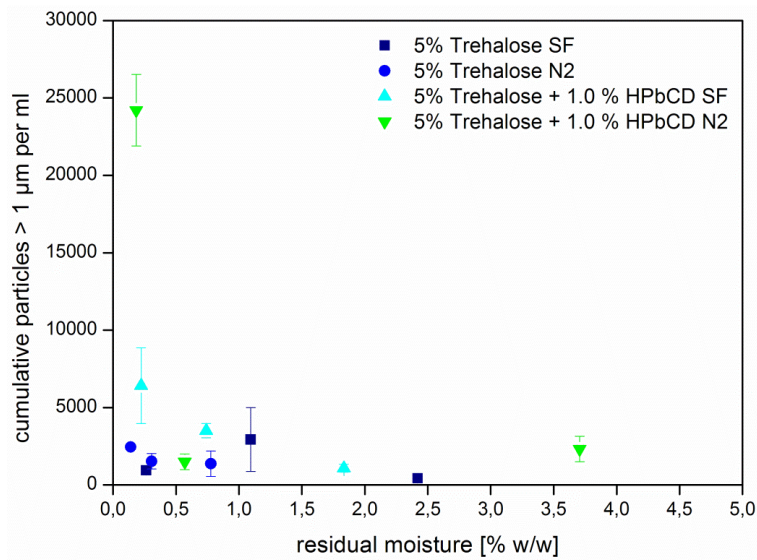


Figure II-126: Subvisible particle formation and residual moisture of 1.0 % (w/v) HPβCD in combination with 5 % Trehalose. Samples were either ramp frozen with 0.3 °C/min (SF) or liquid nitrogen immersed (N2).

II.3.14.7 INFLUENCE OF SPECIFIC SURFACE AREA

In addition to the influence of residual moisture, an influence of the freezing protocol was detected. Fast freezing with liquid nitrogen leads to super-cooling and nucleation of a small fraction of the liquid followed by directional solidification of the entire liquid. This leads to lamellar ice crystals and a comparable large specific surface area. Contrary, ramp freezing with a low speed leads to global super-cooling and nucleation with a lower specific surface area. A clear impact of those two different freezing protocols was observed with the samples containing HP β CD in both concentrations and HP β CD alone. Samples which contained HP β CD and were liquid nitrogen frozen showed a strong correlation between specific surface area and particle concentrations, as shown in Figure II-127.

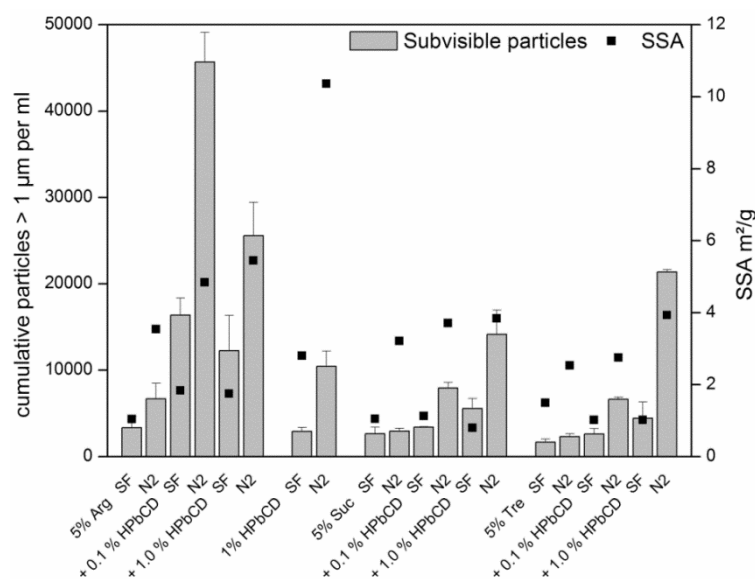


Figure II-127: Results obtained for light obscuration of all formulations and corresponding specific surface areas. Subvisible particle formation correlates with specific surface area. SF = ramp frozen, N2 = liquid nitrogen frozen.

Microflow imaging analysis (MFI) of the samples freeze-dried at 40 °C from the residual moisture study (section II.3.14.6) was performed to confirm that the particles formed are in fact in the micrometer range because it is known that for the light obscuration method, a large amount of smaller particles can be detected as less but larger particles due to coincidences in the detector. The MFI is capable to detect subvisible particles already at a size of 0.75 μm with an improved sensitivity compared to the PAMAS SVSS and hence, particle numbers are actually much more but the trends, as observed with light obscuration are the same, as shown in Figure II-128. Similar to the results from light obscuration, essentially all particles were in the lower single digit micrometer range.

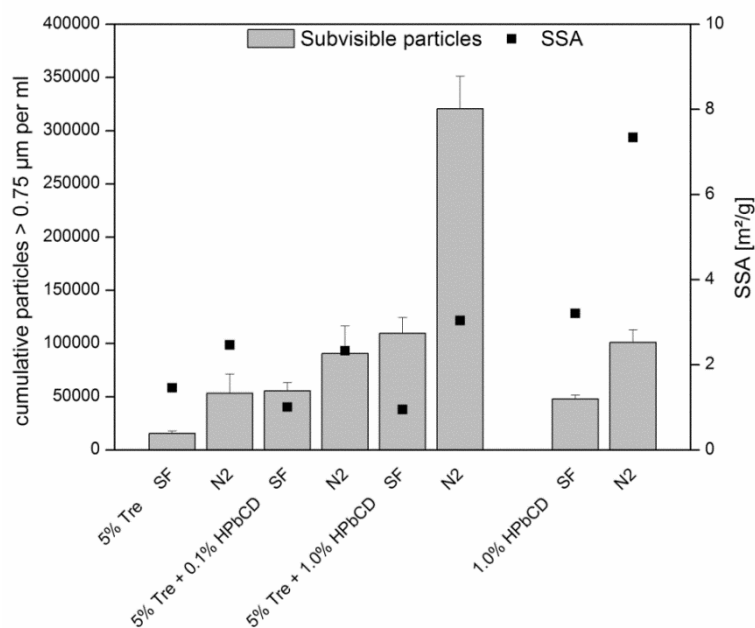


Figure II-128: Subvisible particles determined by microflow imaging and specific surface area for all formulations. SF = ramp frozen, N2 = liquid nitrogen frozen.

If an increase in SSA correlates with an increase in subvisible particles, a decrease in SSA should decrease particle formation. To test this hypothesis, collapse freeze-drying was performed with both freezing protocols. Collapse freeze-drying is primary drying at a product temperature above the collapse temperature, T_c , above which viscous flow of the amorphous matrix is occurring. Freeze-drying with macrocollapse of the matrix results in products with low specific surface area and, compared to conventional freeze-drying, to relatively high residual moistures. Collapse freeze-drying, as performed in this study, lead to a product temperature of approximately $-25\text{ }^\circ\text{C}$ for the formulation of 5 % Sucrose + 1.0 % HP β CD while the T_g' , which is usually 1-3 $^\circ\text{C}$ lower than T_c , at least for this type of formulation, is $-29.9\text{ }^\circ\text{C}$, as shown in Table II-24. Drying above T_c results in macroscopic collapse of all samples based on sucrose, however, the formulation with 1.0 % HP β CD showed no macroscopic collapse, as shown in Figure II-129. However, reconstitution times were less than 30 seconds for all formulations.

Table II-24: T_g' and ΔC_p (dCp) of the formulations based on Sucrose with no, 0.1 % or 1.0 % HP β CD and the formulation with only 1.0 % HP β CD.

Formulation	T_g' [$^\circ\text{C}$]	dCp [$\text{J}^*\text{g}/\text{K}$]
5 % Sucrose	-33.93 ± 0.29	0.16 ± 0.01
5 % Sucrose + 0.1 % HP β CD	-33.43 ± 0.38	0.15 ± 0.01
5 % Sucrose + 1.0 % HP β CD	-29.87 ± 0.23	0.17 ± 0.02
1 % HP β CD	-14.07 ± 0.21	0.09 ± 0.01

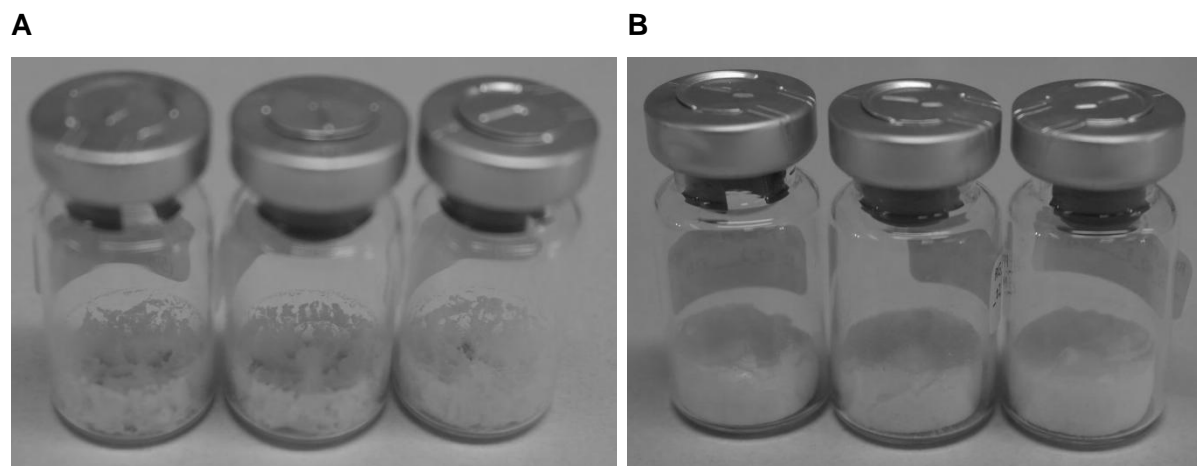


Figure II-129: Macroscopic appearance of (A) 5 % Sucrose + 1.0 % HP β CD and (B) 1.0 % HP β CD alone. The pictures show the liquid nitrogen frozen samples.

As expected, collapse of the samples lead to an immense reduction of SSA. Furthermore, no significant difference of subvisible particles concentrations could be observed after freeze-drying and rehydration compared to the reference, 5 % sucrose, as shown in Table II-25. For the non-collapsed 1.0 % HP β CD formulation, subvisible particle formation was observed with a strong correlation with SSA.

Table II-25: Subvisible particle formation as detected with light obscuration for formulations based on Sucrose with no, 0.1 % or 1.0 % HP β CD as well the formulation with 1.0 % HP β CD alone. SF = ramp frozen, N2 = liquid nitrogen immersion.

Formulation	Freezing protocol	Subv. Particles > 1 μ m	Specific surface area [m ² /g]
5 % Sucrose	SF	854 \pm 189	0.11
	N2	694 \pm 177	0.08
5 % Sucrose + 0.1 % HP β CD	SF	1310 \pm 895	0.09
	N2	885 \pm 493	0.12
5 % Sucrose + 1.0 % HP β CD	SF	1743 \pm 698	0.08
	N2	1451 \pm 321	0.12
1 % HP β CD	SF	6053 \pm 857	2.09
	N2	19646 \pm 12768	7.97

Residual moistures were, as expected, higher for the collapsed samples than the non-collapsed samples. Surprisingly, the freezing protocol showed a significant influence in residual moisture levels and the nitrogen frozen samples showed higher residual moisture than the ramp frozen samples, as presented in Table II-26.

Table II-26: Residual moisture of collapse freeze-dried samples. SF = ramp frozen, N2 = liquid nitrogen immersion.

Formulation	Freezing protocol	Residual moisture [%]
5 % Sucrose	SF	2.04 ± 0.05
	N2	2.82 ± 0.21
5 % Sucrose + 0.1 % HPβCD	SF	2.00 ± 0.04
	N2	2.70 ± 0.42
5 % Sucrose + 1.0 % HPβCD	SF	1.88 ± 0.14
	N2	3.06 ± 0.12
1 % HPβCD	SF	0.83 ± 0.14
	N2	1.01 ± 0.28

II.3.14.8 PRESENCE OF POLYSORBATE 80

In the previous sections, a strong correlation of specific surface area and the subvisible particles formed could be observed. HP β CD is a surface active derivative of β -CD and is expected to be present at the ice/liquid interface during freezing as well as the solid/void interface of the dried product. In addition, it is known that surfactants like polysorbates can displace HP β CD from these interfaces [71]. If aggregation of HP β CD is interface-driven, the addition of polysorbate is expected to interfere with this process and differences should be observable. To test this hypothesis, a formulation with 1.0 % HP β CD was compared to a formulation consisting of 1.0 % HP β CD and 0.04 % polysorbate 80 after freeze-drying and rehydration. In addition, the formulation consisting of 1.0 % HP β CD was reconstituted with a solution of 0.04 % polysorbate 80 to test, if dissolution of HP β CD aggregates can happen in the presence of this surfactant. For both formulations, the ramp freezing and the liquid nitrogen immersion freezing protocols were applied.

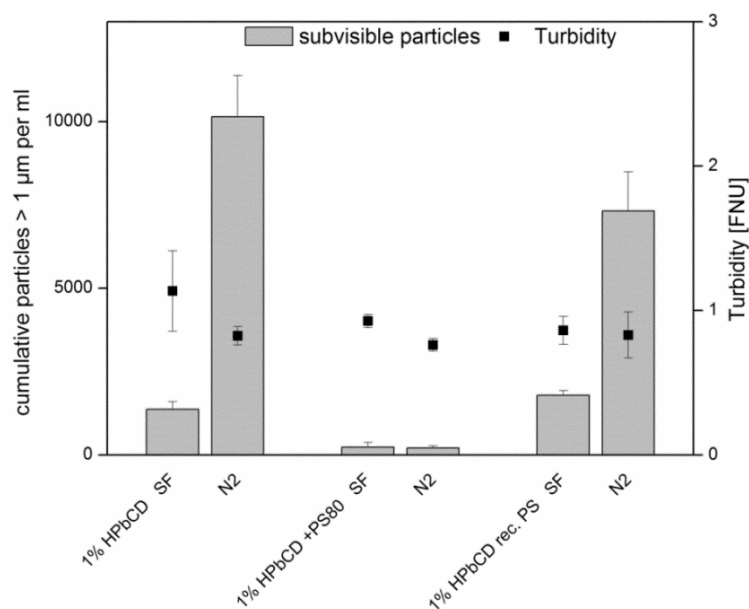


Figure II-130: Results from light obscuration and turbidity for 1.0 % HP β CD without and with 0.04 % polysorbate 80 and the formulation of 1.0 % HP β CD which was reconstituted with a solution of 0.04 % polysorbate 80. SF= ramp frozen, N2 = liquid nitrogen immersion.

The addition of 0.04 % polysorbate 80 to 1.0 % HP β CD completely prevented subvisible particle formation while the reconstitution with 0.04 % polysorbate only slightly reduced subvisible particles concentrations. Turbidity was almost unaffected for all formulations.

II.3.14.9 INFLUENCE OF IMPURITIES OF β -CD AND THE DEGREE OF SUBSTITUTION

Synthesis of HP β CD is commercially done by derivatization of the starting material β -cyclodextrin (β -CD), which is much less water soluble than the resulting derivative. However, traces of β -CD are unavoidable and are specified less than 1 % for the Wacker derivative and less than 0.1 % for the Roquette product. To test whether the subvisible particles originate from impurities of β -CD, the parent CD was added to sucrose in two concentrations of 0.001 % and 0.01 % which equals the maximum amount of impurities that can be present in both HP β CD products. The results from light obscuration and turbidity are shown in Figure II-131. The formulations with β -CD showed no significant difference to the reference 5 % sucrose independent of freezing protocol employed whereas subvisible particle concentrations and turbidity were higher with the formulations containing HP β CD.

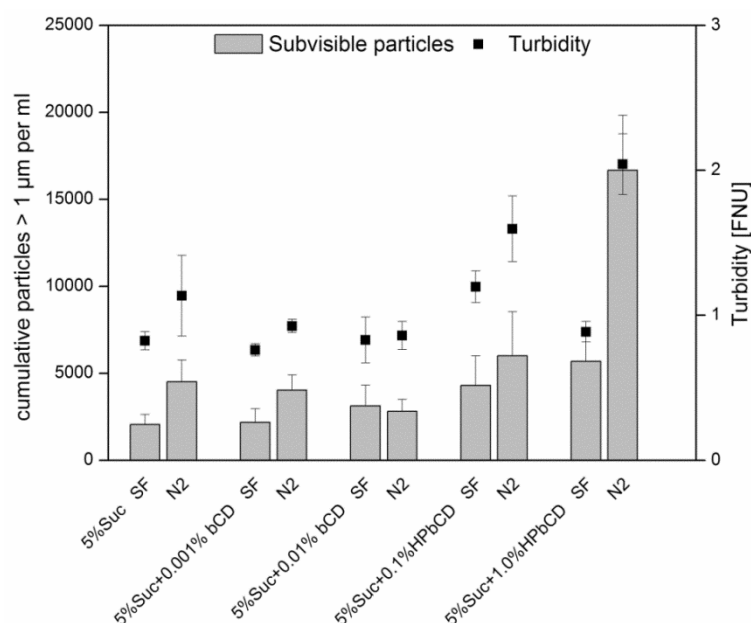


Figure II-131: Results for sucrose-based formulation with the addition of two different concentrations of β -CD. As reference, two different concentrations of HP β CD were employed. SF = ramp frozen, N2 = liquid nitrogen immersion.

HP β CD self-aggregation is most probably driven by intermolecular hydrogen bonds between hydroxyl-moieties of the glucose units and the moieties introduced by hydroxypropylation. Hence, the (molar) degree of substitution ((m)DS) is expected to influence the amount of particles after rehydration. Two different HP β CD derivatives from Wacker and Roquette were employed to test this hypothesis. Figure II-132 shows the results from light obscuration and turbidity. The product from Roquette (mDS 0.87) shows slightly higher particle counts than the derivative from Wacker (mDS between 0.59-0.73). The differences in the degree of substitution may be too small to have a noticeable impact in subvisible particle formation.

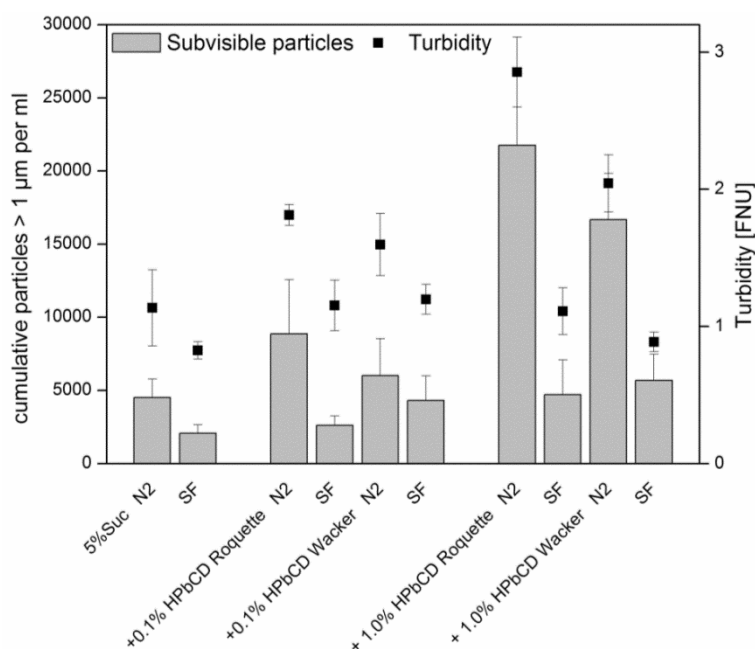


Figure II-132: Results from light obscuration and turbidity for the sucrose-based formulations of two different HPβCD derivatives in two concentrations. SF = ramp frozen, N2 = liquid nitrogen immersion.

II.3.14.10 IMPACT OF SUBVISIBLE PARTICLES OF HPβCD ON THE AGGREGATION OF A MODEL ANTIBODY

One possible problem occurring from self-aggregation of HPβCD, besides general increase in particle levels, is the potential ability of those particles to serve as heterogeneous nucleation seeds for protein aggregates formed during rehydration. To test this, reconstitution of a model antibody was performed using a solution of either 1.0 % HPβCD or a lyophilized, rehydrated solution of 1.0 % of HPβCD which contains a certain amount of particles. The antibody was freeze-dried with and without the presence of 0.04 % PS80. As depicted in Figure II-133, reconstitution of the antibody samples with HPβCD particles present did not lead to disproportional large amounts of subvisible particles. Independent of antibody formulation, the values obtained were comparable with the sums of the reference formulations, at least after reconstitution. A similar picture was observable also with Microflow imaging, where also no unproportional large number of subvisible particles could be observed. However, there are some differences when the antibody lyophilizates were reconstituted with the non-lyophilized HPβCD solutions. The amount of subvisible particles in this case was lower compared to reconstitution with water, as shown in Figure II-134. This was more pronounced in the formulation containing no polysorbate.

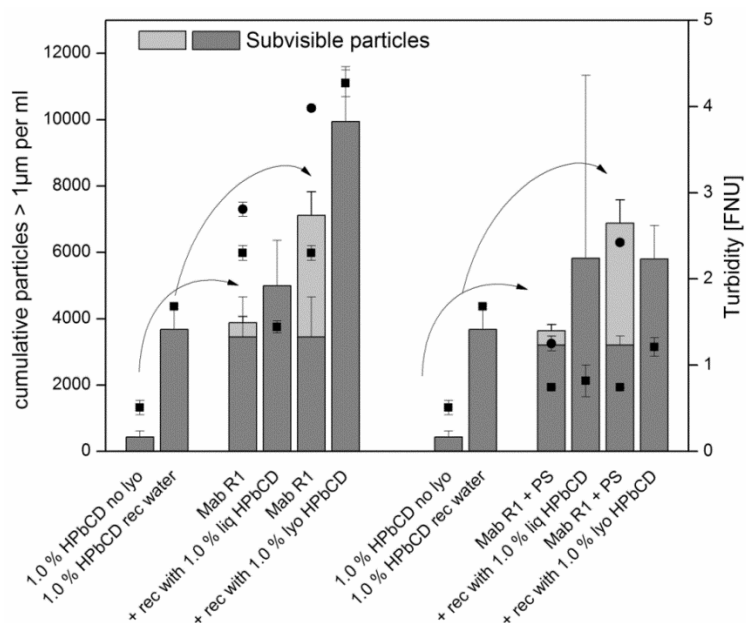


Figure II-133: Results from light obscuration for the model antibody Mab R1 which was reconstituted with solutions of 1.0 % HPβCD which were freshly prepared or lyophilized and rehydrated. The light grey bars on top of the dark grey bars represent the mathematical sum of those two samples and the dark grey bar in each case the actual particle concentration after reconstitution.

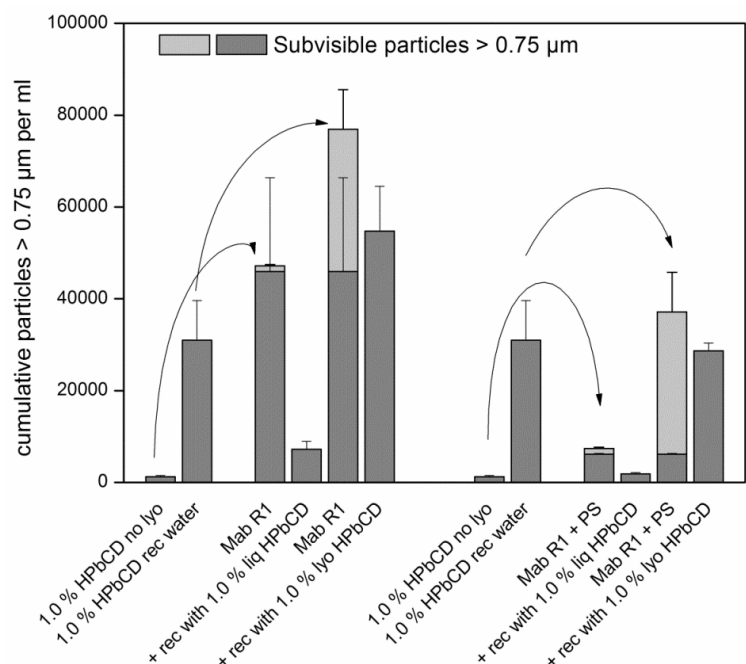


Figure II-134: Results from microflow imaging for the model antibody Mab R1 which was reconstituted with solutions of 1.0 % HPβCD which were freshly prepared or lyophilized and rehydrated. The light grey bars on top of the dark grey bars represent the mathematical sum of those two samples and the dark grey bar in each case the actual particle concentrations after reconstitution.

II.3.14.11 SUMMARY AND DISCUSSION

Our results obtained from freeze-drying of various pharmaceutically relevant formulations of HP β CD show strong evidence that subvisible particles can be formed by HP β CD after freeze-drying and rehydration. To our knowledge, this has not been reported yet in the literature. However, aggregation due to hydrogen bonds of parent CDs in the nm range has been observed by dynamic light scattering in aqueous solutions [84]. In addition, also an influence of derivatization of the glucose monomers has been observed, however, aggregation of those derivatives, including HP β CD was found to be negligible in literature [85]. Main factors influencing particle formation in our study are residual moisture and (specific) surface area. This is supported by the fact that a significant increase of subvisible particles are formed after the secondary drying step but not after the primary drying or the freeze-thawing step. The results from microflow imaging confirm that the particles detected by light obscuration are in fact subvisible particles. In addition, the freezing protocol and the freeze-drying process also greatly influence the formation of subvisible particles. It is known that, in contrast to the parent cyclodextrins α -, β -, and γ -CD, certain derivatives like methylated or hydroxypropylated decrease the surface tension of water by accumulating at the air-water interface [24], so it is no surprise that an increase in the ice-water and the solid-void interface has a certain effect on subvisible particle formation. A large specific surface area, obtained from liquid nitrogen immersion, leads to a larger amount of subvisible particles than a smaller specific surface area, obtained by ramp freezing with 0.3 °C/min or a drying process with a product temperature $T_p > T_c$ with resulting collapse of the lyophilized cake. However, in this case, also the residual moisture could not be decreased to a very low level of less than 0.5 %. Furthermore, it is known that HP β CD can be displaced from the air-water interface by the addition of polysorbate 80 [71]. Our data show that the addition of polysorbate 80 did almost completely inhibit subvisible particle formation by HP β CD. β -CD impurities seemed not to be responsible for subvisible particle formation. The concentration which could be present in our studies is at maximum 0.01 % (w/v) and therefore much lower than the solubility of β -CD in water which is approximately 1.85 % (w/v) [86] and also much lower as the concentration which has been used in the aggregation studies of parent CDs [85]. Based on the results obtained in this study, the authors speculate that formation of subvisible particles by HP β CD takes place at the solid-void interface due to close proximity of single molecules. While the residual water content is decreased, the formation of intermolecular hydrogen bonds may be the reason for aggregation of HP β CD, although this is speculative and there is no direct evidence in our data. To mitigate formation of particles of HP β CD, one could increase residual moisture of the formulations; however, this is not always applicable, because an increase in residual moisture decreases glass transition temperatures of dried products. One should also keep the surface area of a

formulation as low as possible, which can be done by using controlled ice nucleation with low degrees of super-cooling or an additional annealing step after the freezing step.

II.3.15 FINAL DISCUSSION

II.3.15.1 INFLUENCE OF SPECIFIC SURFACE AREA

As shown in the sections in chapter II, the freeze- and spray-drying processes had a significant impact on MabR1 stability. The different drying processes differed in process conditions and in product quality attributes. Table II-27 shows a short overview on the different drying processes employed in this study.

Table II-27: Overview of the different drying processes and their impact on product quality attributes.

Process	Specific surface area	Residual moisture
Conventional FD	High (> 1 m ² /g)	Low (< 1 % w/w)
Controlled-nucleation at high T _p	Low (0.5 m ² /g)	Intermediate (1 % - 2 %) ^a
Collapse FD	Very low (< 0.2 m ² /g)	High (2 % - 5 %, formulation dependent)
Spray drying	High (> 1-2 m ² /g) ^b	High (2 % - 5 %, formulation dependent)

a: can be changed if process conditions in secondary drying are changed.

b: Surface area is larger after atomization and is decreased during drying-induced shrinkage of droplets.

Figure II-135 shows an overview on the correlation of SSA generated by different freeze-drying processes and the corresponding subvisible particles formed immediately after freeze-drying and rehydration. Results from spray-drying are not included because the impact of foreign subvisible particles, which were also present in the placebos, was difficult to estimate and specific surface area measured of the dried product differs from the surface area generated by atomization. A trend towards lower subvisible particles with lower SSA can be observed for the formulations which contain HP β CD as well as for sucrose-based formulations which did not contain any surfactant. A large difference between sucrose concentrations was also observed with significantly lower subvisible particles for the 5 % formulation compared to 1 % sucrose-based formulations. The formulations which contain 0.04 % or 0.004 % polysorbate 80, both concentrations are larger than the CMC, which is 0.0014 % (w/v) (equals 0.010 mM [87]), did not show a correlation between SSA and subvisible particles. Comparing the results from freeze-thaw studies, in which HP β CD as well as polysorbate 80 were very effective stabilizers, with the results after freeze-drying and rehydration, the following conclusion can be drawn: HP β CD seems to be able to stabilize better at the ice-liquid interface formed during the freezing step as well as in the thawing step than at the liquid-air interface, which is encountered during rehydration of the dried products. HP β CD, in addition, is slowly covering the air-liquid interface and is not able to displace an antibody which has already accumulated at this interface. Hence, kinetics are also expected to influence the stabilization mechanism of HP β CD. The results from atomization experiments in the spray-drying experiment also point in this direction. When

HP β CD-containing samples were reconstituted with a solution of polysorbate 80, lower subvisible particle counts were observed, indicating that a positive effect of PS80 on subvisible particles is effective at the liquid-air interface during reconstitution which is not observed for HP β CD to this extent. With all this results in mind, HP β CD is an effective stabilizer, if the interface area is kept low.

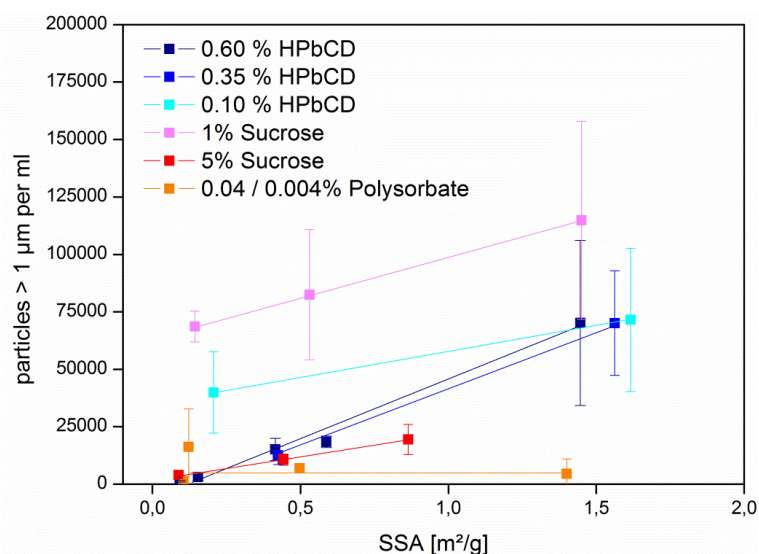


Figure II-135: Overview of specific surface area (SSA) vs. subvisible particles > 1 μm for all formulations except spray-dried formulations investigated in this study. For HP β CD and PS80, each point represents either the excipient in combination with 1 % or 5 % Sucrose.

In general, a low SSA can be considered beneficial for protein formulations independent of employing HP β CD as an excipient if one assumes that degradation of protein is the sum of degradation in the bulk and at the interface [70]. The cumulative degradation rate k can then be described using

$$k_{obs} = k_S F_{PS} + k_B F_{PB} \quad \text{Equation II-1}$$

with k_{obs} being the observed degradation constant, k_S is the rate constant of protein located at the surface of the dried product and F_{PS} is the corresponding fraction of protein at the surface; k_B is the rate constant of bulk degradation and F_{PB} is the fraction of protein in the bulk [70]. Consequently, the lower the fraction of protein at the surface is, the lower the overall degradation rate is. Furthermore, water uptake during storage may be lower for samples with lower SSA compared to samples with a higher SSA and chemical degradation, which is triggered at the surface, is expected to be slowed. There are some hints in literature that a low SSA is indeed increasing long-term storage stability of proteins, as shown for antibodies [70, 88] and interferon- γ [80]. However, it is difficult to rule out other effects which contribute to long-term storage stability of lyophilizates besides SSA, e.g. residual moisture, molecular mobility, glass transition temperatures, etc. This is even harder to accomplish if the different

SSAs are produced by different drying methods. Controlled ice nucleation may be a valuable tool to study SSAs-dependent stability effects of lyophilizates.

II.3.15.2 PLACEBO PARTICLES OF HP β CD

As presented in chapter II.3.14, placebo particles of HP β CD can be formed during freeze-drying and rehydration. These particles are formed after secondary drying and their numbers depends on residual moisture and specific surface area. With the studies performed for MabR1, one critical aspect was to control formation of those particles because their number may, in the best case and if those particles are “inert”, contribute to total number of subvisible particles or even act as heterogeneous seeds to trigger aggregation of proteins. That had been observed for an antibody in the presence of micro- and nanoparticles [89, 90]. Although we could not confirm that placebo particles of HP β CD lead to excessive aggregation of MabR1 (see section II.3.14.10), it shall be noted that subvisible particles of protein formulations were acceptable only when subvisible particles of placebo controls were also minimized. Unfortunately, we were not able to distinguish between proteinaceous and non-protein particles in antibody formulations in this study. A useful tool for this scientific challenge would be raman spectroscopy of filtered particles as available with the RapID® device. In the literature available so far on cyclodextrin and protein stability, no subvisible particle counts have been published. Subvisible particle aggregates in the μm -range have attracted protein formulations scientists’ attention quite recently [54, 91], thus formation of HP β CD placebo-particles may have been unnoticed in published literature of cyclodextrins in freeze-drying so far.

II.3.15.3 POSSIBLE STABILIZATION MECHANISM OF HP β CD

While it has been discussed that HP β CD is binding to hGH [79], we could not show an interaction of HP β CD (0.6 % and 1.0 %) with MabR1 at a concentration of 10 mg/ml at least by microcalorimetry, as shown in Figure II-136. In general, aggregates form through partially unfolded proteins (so called molten globules, which have a larger surface than the native state) and probably not by complete unfolded species [92]. The Lumry-Eyring framework [93] is a model, in which a native protein (N) reversibly transforms to a partially unfolded transition state (TS*), which is prone to aggregate to an aggregation intermediate (A_I) see (1). A_I is capable of interacting with Aggregates containing m aggregates (A_m), forming a complex A_{m+1} , see (2).



If HP β CD binds to the unfolded state of the protein TS*, this state is thermodynamically favored and a lower T_m should be observed. However, although not extensively studied, this was not the case in our studies with almost superimposing melting curves of MabR1 at 10 mg/ml, as shown in Figure II-136.

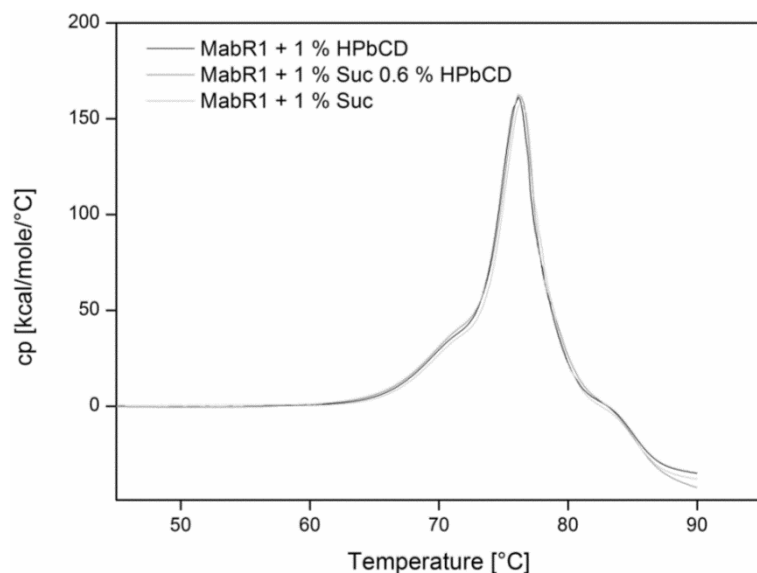


Figure II-136: Results from microcalorimetry for MabR1 formulated at 10 mg/ml.

In the case of non-interaction for MabR1, HP β CD still showed positive effects compared to sucrose alone. As shown with the results from ESCA, HP β CD is not able to displace the protein from the interface similar to polysorbate. However, HP β CD is present at the interface, and phase separation of protein and stabilizer is possibly reduced. HP β CD may then stabilize by a mechanism shown for various excipients. Sugars, like trehalose or sucrose, polyols like mannitol or sorbitol and some amino acids are assumed to stabilize proteins via the preferential hydration / exclusion mechanism in solutions [94]. These excipients are excluded from the surface of proteins; the protein is preferentially hydrated by water molecules, which is an energetically unfavorable state. Partially unfolded or dissociated proteins have a larger surface than the native state [94, 95]. According to the law of Le Chatelier, the equilibrium



is shifted to the native state (N) in the presence of an excipient stabilizing via the preferential exclusion mechanism. Whether this stabilization mechanism is also applicable to an interface is questionable, since the protein may not be fully hydrated in this case. However, protein molecules, accumulating at an interface, may still be protected by the presence of foreign molecules that can also diffuse to interfaces and reach a sufficient concentration to stabilize via the preferential exclusion mechanism and further aggregation to the aggregation intermediate A_I or A_{M+1} may be attenuated. Concluding, HP β CD might therefore exert different

stabilization mechanisms which are connected to its unique structural properties: complexation of amino acids residues by the hydrophobic cavity; accumulation at interfaces due to hydroxypropylation; carbohydrate-like stabilization due to glucose sub-units.

II.3.16 SUMMARY

In this chapter, the potential use of cyclodextrins, especially the derivative HP β CD, in freeze-drying was investigated. HP β CD was used as a potential alternative to polysorbates, which can degrade and exert a negative influence on protein stability. Three different model proteins, which are sensitive to interfacial stress conditions, were investigated: a monoclonal antibody (MabR1), human growth hormone (hGH) and granulocyte-colony stimulating factor (GCSF). In addition, HP β CD was also employed in spray-drying of MabR1. It was found that HP β CD can be an alternative to polysorbates. In drying processes, in which intermediate to high specific surface areas are obtained (conventional freeze-drying and spray-drying), polysorbate was superior to HP β CD with the studied model antibody. However, when specific surface areas are kept small, for example by employing controlled ice nucleation or collapse freeze-drying, acceptable protein stability was obtained for both excipients. The collapse freeze-drying process could also be transferred to the other two model proteins, hGH and GCSF. While hGH was very well stabilized by HP β CD and this combination was superior to polysorbate, drying of GCSF resulted in a general instability of both formulations studied. Storage stable lyophilizates of MabR1 were only obtained when sucrose concentration was increased from 1 % to 5 % (w/v). Even under accelerated stress conditions, these products exceptionally retained protein stability, which was also true for hGH. While polysorbate was superior in the spray-drying study, the present data set suggests that oxidation of MabR1 damaged protein stability, resulting in increased dimer contents after drying and subsequent storage. Thus, a reasonable formulation strategy employing HP β CD is to keep the absolute surface area low, which is based on ESCA data suggesting that HP β CD co-exists with the antibody at the solid-void interface in a similar manner than in liquid formulations. A concentration of 6 mg/ml HP β CD was found to be optimal in the studies. A side aspect of the chapter was the potential use of HP β CD as lyoprotectant. While we could show that state-of-the-art pharmaceutical formulations can be obtained with HP β CD in combination with PS for hGH, however, there was no evidence that HP β CD may be a better cryoprotectant than the much more widely used sucrose or trehalose.

II.4 REFERENCES

1. Wang, W., *Lyophilization and development of solid protein pharmaceuticals*. International Journal of Pharmaceutics, 2000. 203(1-2): p. 1-60.
2. Carpenter, J.F., et al., *Rational Design of Stable Lyophilized Protein Formulations: Some Practical Advice*. Pharmaceutical Research, 1997. 14(8): p. 969-975.
3. Chang, L. and M.J. Pikal, *Mechanisms of protein stabilization in the solid state*. Journal of Pharmaceutical Sciences, 2009. 98(9): p. 2886-2908.
4. Arakawa, T., et al., *Factors affecting short-term and long-term stabilities of proteins*. Advanced Drug Delivery Reviews, 1993. 10(1): p. 1-28.
5. Timasheff, S.N., *The Control of Protein Stability and Association by Weak Interactions with Water: How Do Solvents Affect These Processes?* Annual Review of Biophysics and Biomolecular Structure, 1993. 22(1): p. 67-97.
6. Jones, L.S., et al., *The effects of Tween 20 and sucrose on the stability of anti-L-selectin during lyophilization and reconstitution*. Journal of Pharmaceutical Sciences, 2001. 90(10): p. 1466-1477.
7. Zhang, M.Z., et al., *The Effect of the Reconstitution Medium on Aggregation of Lyophilized Recombinant Interleukin-2 and Ribonuclease A*. Pharmaceutical Research, 1996. 13(4): p. 643-646.
8. Sarciaux, J.-M., et al., *Effects of buffer composition and processing conditions on aggregation of bovine IgG during freeze-drying*. Journal of Pharmaceutical Sciences, 1999. 88(12): p. 1354-1361.
9. Serno, T., et al., *Inhibition of agitation-induced aggregation of an IgG-antibody by hydroxypropyl-beta-cyclodextrin*. Journal of Pharmaceutical Sciences, 2010. 99(3): p. 1193-1206.
10. Katakam, M., L.N. Bell, and A.K. Banga, *Effect of surfactants on the physical stability of recombinant human growth hormone*. Journal of Pharmaceutical Sciences, 1995. 84(6): p. 713-716.
11. Crowe, J., L. Crowe, and J. Carpenter, *Preserving dry biomaterials: the water replacement hypothesis, part 1*. BioPharm, 1993. 6: p. 28-28.
12. Allison, S.D., et al., *Effects of Drying Methods and Additives on Structure and Function of Actin: Mechanisms of Dehydration-Induced Damage and Its Inhibition*. Archives of Biochemistry and Biophysics, 1998. 358(1): p. 171-181.
13. Carpenter, J.F. and J.H. Crowe, *An infrared spectroscopic study of the interactions of carbohydrates with dried proteins*. Biochemistry, 1989. 28(9): p. 3916-3922.
14. Crowe, J.H., F.A. Hoekstra, and L.M. Crowe, *Anhydrobiosis*. Annual Review of Physiology, 1992. 54(1): p. 579-599.
15. Roser, B., *Trehalose drying: a novel replacement for freeze-drying*. Biopharm, 1991. 4(9): p. 47-53.
16. Franks, F., *Long-Term Stabilization of Biologicals*. Nature Biotechnology, 1994. 12(3): p. 253-256.
17. Fox, K., *Biopreservation. Putting proteins under glass*. Science, 1995. 267(5206): p. 1922-1923.
18. Franks, F., R. Hatley, and S. Mathias, *Materials science and the production of shelf-stable biologicals*. Biopharm, 1991. 4(9): p. 38-55.
19. Slade, L. and H. Levine, *Beyond water activity: recent advances based on an alternative approach to the assessment of food quality and safety*. Critical Reviews in Food Science and Nutrition, 1991. 30(2-3): p. 115-360.
20. Chang, L., et al., *Mechanism of protein stabilization by sugars during freeze-drying and storage: Native structure preservation, specific interaction, and/or immobilization in a glassy matrix?* Journal of Pharmaceutical Sciences, 2005. 94(7): p. 1427-1444.
21. Allison, S.D., et al., *Hydrogen Bonding between Sugar and Protein Is Responsible for Inhibition of Dehydration-Induced Protein Unfolding*. Archives of Biochemistry and Biophysics, 1999. 365(2): p. 289-298.
22. Carpenter, J.F. and J.H. Crowe, *Modes of stabilization of a protein by organic solutes during desiccation*. Cryobiology, 1988. 25(5): p. 459-470.

23. Hancock, B.C. and G. Zografi, *Characteristics and significance of the amorphous state in pharmaceutical systems*. J Pharm Sci, 1997. 86(1): p. 1-12.
24. Yoshida, A., et al., *Pharmaceutical evaluation of hydroxyalkyl ethers of [beta]-cyclodextrins*. International Journal of Pharmaceutics, 1988. 46(3): p. 217-222.
25. Del Valle, E.M.M., *Cyclodextrins and their uses: a review*. Process Biochemistry, 2004. 39(9): p. 1033-1046.
26. Izutsu, K.-i., S. Yoshioka, and S. Kojima, *Increased Stabilizing Effects of Amphiphilic Excipients on Freeze-Drying of Lactate Dehydrogenase (LDH) by Dispersion into Sugar Matrices*. Pharmaceutical Research, 1995. 12(6): p. 838-843.
27. Anchordoquy, T.J., et al., *Maintenance of Quaternary Structure in the Frozen State Stabilizes Lactate Dehydrogenase during Freeze-Drying*. Archives of Biochemistry and Biophysics, 2001. 390(1): p. 35-41.
28. Santagapita, P.R., et al., *Structure/Function Relationships of Several Biopolymers as Related to Invertase Stability in Dehydrated Systems*. Biomacromolecules, 2008. 9(2): p. 741-747.
29. Chefson, A., J. Zhao, and K. Auclair, *Sugar-mediated lyoprotection of purified human CYP3A4 and CYP2D6*. Journal of Biotechnology, 2007. 130(4): p. 436-440.
30. Millqvist-Fureby, A., M. Malmsten, and B. Bergenståhl, *Surface characterisation of freeze-dried protein/carbohydrate mixtures*. International Journal of Pharmaceutics, 1999. 191(2): p. 103-114.
31. Millqvist-Fureby, A., M. Malmsten, and B. Bergenståhl, *Spray-drying of trypsin -- surface characterisation and activity preservation*. International Journal of Pharmaceutics, 1999. 188(2): p. 243-253.
32. Izutsu, K.-i., S. Yoshioka, and T. Terao, *Stabilization of [beta]-galactosidase by amphiphilic additives during freeze-drying*. International Journal of Pharmaceutics, 1993. 90(3): p. 187-194.
33. Izutsu, K.-i., S. Yoshioka, and T. Terao, *Stabilizing effect of amphiphilic excipients on the freeze-thawing and freeze-drying of lactate dehydrogenase*. Biotechnology and Bioengineering, 1994. 43(11): p. 1102-1107.
34. Branchu, S., et al., *Hydroxypropyl- β -cyclodextrin inhibits spray-drying-induced inactivation of β -galactosidase*. Journal of Pharmaceutical Sciences, 1999. 88(9): p. 905-911.
35. Rensing, M., et al., *The Influence of Sucrose, Dextran, and Hydroxypropyl- β -cyclodextrin as Lyoprotectants for a Freeze-Dried Mouse IgG2a Monoclonal Antibody (MN12)*. Pharmaceutical Research, 1992. 9(2): p. 266-270.
36. Hora, M.S., R.K. Rana, and F.W. Smith, *Lyophilized Formulations of Recombinant Tumor Necrosis Factor*. Pharmaceutical Research, 1992. 9(1): p. 33-36.
37. Iwai, J., et al., *Effects of various cyclodextrins on the stability of freeze-dried lactate dehydrogenase*. Journal of Pharmaceutical Sciences, 2007. 96(11): p. 3140-3143.
38. Prestrelski, S.J., K.A. Pikal, and T. Arakawa, *Optimization of Lyophilization Conditions for Recombinant Human Interleukin-2 by Dried-State Conformational Analysis Using Fourier-Transform Infrared Spectroscopy*. Pharmaceutical Research, 1995. 12(9): p. 1250-1259.
39. Brewster, M.E., et al., *Use of 2-Hydroxypropyl- β -cyclodextrin as a Solubilizing and Stabilizing Excipient for Protein Drugs*. Pharmaceutical Research, 1991. 8(6): p. 792-795.
40. Hora, M., et al., *Development of a lyophilized formulation of interleukin-2*. Developments in biological standardization, 1992. 74: p. 295.
41. Jalalipour, M., et al., *Effect of dimethyl-beta-cyclodextrin concentrations on the pulmonary delivery of recombinant human growth hormone dry powder in rats*. Journal of Pharmaceutical Sciences, 2008. 97(12): p. 5176-5185.
42. Jovanovic, N., et al., *Stabilization of IgG by supercritical fluid drying: Optimization of formulation and process parameters*. European Journal of Pharmaceutics and Biopharmaceutics, 2008. 68(2): p. 183-190.

43. Tavornvipas, S., et al., *Effects of Hydrophilic Cyclodextrins on Aggregation of Recombinant Human Growth Hormone*. *Pharmaceutical Research*, 2004. 21(12): p. 2369-2376.
44. Allison, S.D., et al., *Optimization of storage stability of lyophilized actin using combinations of disaccharides and dextran*. *Journal of Pharmaceutical Sciences*, 2000. 89(2): p. 199-214.
45. Chang, B.S., et al., *Physical factors affecting the storage stability of freeze-dried interleukin-1 receptor antagonist: glass transition and protein conformation*. *Archives of Biochemistry and Biophysics*, 1996. 331: p. 249-258.
46. Shalaev, E.Y. and F. Franks, *Changes in the Physical State of Model Mixtures during Freezing and Drying: Impact on Product Quality*. *Cryobiology*, 1996. 33(1): p. 14-26.
47. Izutsu, K., S. Yoshioka, and T. Terao, *Effect of mannitol crystallinity on the stabilization of enzymes during freeze-drying*. *Chemical & Pharmaceutical Bulletin*, 1994. 42(1): p. 5.
48. Franks, F., *Solid aqueous solutions*. *Pure and Applied Chemistry*, 1993. 65(12): p. 2527-2538.
49. Bam, N.B., et al., *Tween protects recombinant human growth hormone against agitation-induced damage via hydrophobic interactions*. *Journal of Pharmaceutical Sciences*, 1998. 87(12): p. 1554-1559.
50. Serno, T., *Inhibition of therapeutic protein aggregation by cyclodextrins*. *Dissertation written in English, Department for Pharmaceutical Technology and Biopharmaceutics, Ludwig-Maximilians-Universität, Munich, Germany*. 2010.
51. Geidobler, R., S. Mannschedel, and G. Winter, *A new approach to achieve controlled ice nucleation of supercooled solutions during the freezing step in freeze-drying*. *Journal of Pharmaceutical Sciences*, 2012. 101(12): p. 4409-4413.
52. Arakawa, T., et al., *The critical role of mobile phase composition in size exclusion chromatography of protein pharmaceuticals*. *Journal of Pharmaceutical Sciences*, 2010. 99(4): p. 1674-1692.
53. Prestrelski, S.J., T. Arakawa, and J.F. Carpenter, *Separation of Freezing- and Drying-Induced Denaturation of Lyophilized Proteins Using Stress-Specific Stabilization : II. Structural Studies Using Infrared Spectroscopy*. *Archives of Biochemistry and Biophysics*, 1993. 303(2): p. 465-473.
54. Singh, S.K., et al., *An industry perspective on the monitoring of subvisible particles as a quality attribute for protein therapeutics*. *Journal of Pharmaceutical Sciences*, 2010. 99(8): p. 3302-3321.
55. van den Berg, L. and D. Rose, *Effect of freezing on the pH and composition of sodium and potassium phosphate solutions: the reciprocal system KH_2PO_4 --- Na_2HPO_4 --- H_2O* . *Archives of Biochemistry and Biophysics*, 1959. 81(2): p. 319-329.
56. Anchordoquy, T.J. and J.F. Carpenter, *Polymers Protect Lactate Dehydrogenase during Freeze-Drying by Inhibiting Dissociation in the Frozen State*. *Archives of Biochemistry and Biophysics*, 1996. 332(2): p. 231-238.
57. Schersch, K., et al., *Systematic investigation of the effect of lyophilizate collapse on pharmaceutically relevant proteins I: Stability after freeze-drying*. *Journal of Pharmaceutical Sciences*, 2010. 99(5): p. 2256-2278.
58. Schersch, K., et al., *Systematic investigation of the effect of lyophilizate collapse on pharmaceutically relevant proteins, part 2: Stability during storage at elevated temperatures*. *Journal of Pharmaceutical Sciences*, 2012. 101(7): p. 2288-2306.
59. Webb, S.D., et al., *A new mechanism for decreasing aggregation of recombinant human interferon- γ by a surfactant: Slowed dissolution of lyophilized formulations in a solution containing 0.03% polysorbate 20*. *Journal of Pharmaceutical Sciences*, 2002. 91(2): p. 543-558.
60. Webb, S.D., et al., *Surface adsorption of recombinant human interferon-gamma in lyophilized and spray-lyophilized formulations*. *Journal of Pharmaceutical Sciences*, 2002. 91(6): p. 1474-1487.

61. Pikal, M.J., et al., *The secondary drying stage of freeze drying: drying kinetics as a function of temperature and chamber pressure*. International Journal of Pharmaceutics, 1990. 60(3): p. 203-207.
62. Nema, S. and E.A. Kenneth, *Freeze-Thaw Studies of a Model Protein, Lactate Dehydrogenase, in the Presence of Cryoprotectants*. PDA Journal of Pharmaceutical Science and Technology, 1993. 47(2): p. 76-83.
63. Schneider, H.A., *The Gordon-Taylor equation. Additivity and interaction in compatible polymer blends*. Die Makromolekulare Chemie, 1988. 189(8): p. 1941-1955.
64. Schersch, K., et al., *Systematic investigation of the effect of lyophilizate collapse on pharmaceutically relevant proteins III: Collapse during storage at elevated temperatures*. European Journal of Pharmaceutics and Biopharmaceutics, 2013. 85(2): p. 240-252.
65. Abdul-Fattah, A.M., D.S. Kalonia, and M.J. Pikal, *The challenge of drying method selection for protein pharmaceuticals: Product quality implications*. Journal of Pharmaceutical Sciences, 2007. 96(8): p. 1886-1916.
66. Hancock, B., S. Shamblyn, and G. Zografi, *Molecular Mobility of Amorphous Pharmaceutical Solids Below Their Glass Transition Temperatures*. Pharmaceutical Research, 1995. 12(6): p. 799-806.
67. Abdul-Fattah, A.M., et al., *The effect of annealing on the stability of amorphous solids: Chemical stability of freeze-dried moxalactam*. Journal of Pharmaceutical Sciences, 2007. 96(5): p. 1237-1250.
68. P. Fäldt, B.B., G. Carlsson, *The surface coverage of fat on food powders analyzed by ESCA (electron spectroscopy for chemical analysis)*. Food Structure, 1993. 12(2): p. 225-234.
69. Angell, C.A., *Formation of Glasses from Liquids and Biopolymers*. Science, 1995. 267(5206): p. 1924-1935.
70. Abdul-Fattah, A.M., et al., *Drying-induced variations in physico-chemical properties of amorphous pharmaceuticals and their impact on stability (I): Stability of a monoclonal antibody*. Journal of Pharmaceutical Sciences, 2007. 96(8): p. 1983-2008.
71. Serno, T., et al., *The Role of Polysorbate 80 and HP β CD at the Air-Water Interface of IgG Solutions*. Pharmaceutical Research, 2013. 30(1): p. 117-130.
72. Otzen, D.E., et al., *Structural basis for cyclodextrins' suppression of human growth hormone aggregation*. Protein Science, 2002. 11(7): p. 1779-1787.
73. Bam, N.B., J.L. Cleland, and T.W. Randolph, *Molten Globule Intermediate of Recombinant Human Growth Hormone: Stabilization with Surfactants*. Biotechnology Progress, 1996. 12(6): p. 801-809.
74. Wang, W., Y.J. Wang, and D.Q. Wang, *Dual effects of Tween 80 on protein stability*. International Journal of Pharmaceutics, 2008. 347(1-2): p. 31-38.
75. Kishore, R.S.K., et al., *Degradation of polysorbates 20 and 80: Studies on thermal autoxidation and hydrolysis*. Journal of Pharmaceutical Sciences, 2011. 100(2): p. 721-731.
76. Kerwin, B.A., *Polysorbates 20 and 80 used in the formulation of protein biotherapeutics: Structure and degradation pathways*. Journal of Pharmaceutical Sciences, 2008. 97(8): p. 2924-2935.
77. Donbrow, M., R. Hamburger, and E. Azaz, *Surface tension and cloud point changes of polyoxyethylene non-ionic surfactants during autoxidation*. Journal of Pharmacy and Pharmacology, 1975. 27(3): p. 160-166.
78. Ha, E., W. Wang, and Y.J. Wang, *Peroxide formation in polysorbate 80 and protein stability*. Journal of Pharmaceutical Sciences, 2002. 91(10): p. 2252-2264.
79. Serno, T., R. Geidobler, and G. Winter, *Protein stabilization by cyclodextrins in the liquid and dried state*. Advanced Drug Delivery Reviews, 2011. 63(13): p. 1086-1106.
80. Webb, S.D., et al., *Surface adsorption of recombinant human interferon- γ in lyophilized and spray-lyophilized formulations*. Journal of Pharmaceutical Sciences, 2002. 91(6): p. 1474-1487.
81. Kishore, R.S.K., et al., *Degradation of polysorbates 20 and 80: Studies on thermal autoxidation and hydrolysis*. Journal of Pharmaceutical Sciences, 2010: p. n/a-n/a.

82. Mahler, H.-C., et al., *Protein aggregation: Pathways, induction factors and analysis*. Journal of Pharmaceutical Sciences, 2009. 98(9): p. 2909-2934.
83. Tang, X. and M. Pikal, *Design of Freeze-Drying Processes for Pharmaceuticals: Practical Advice*. Pharmaceutical Research, 2004. 21(2): p. 191-200.
84. Coleman, A.W., et al., *Aggregation of cyclodextrins: An explanation of the abnormal solubility of beta-cyclodextrin*. Journal of Inclusion Phenomena and Macrocyclic Chemistry, 1992. 13(2): p. 139-143.
85. González-Gaitano, G., et al., *The Aggregation of Cyclodextrins as Studied by Photon Correlation Spectroscopy*. Journal of Inclusion Phenomena and Macrocyclic Chemistry, 2002. 44(1): p. 101-105.
86. Szejtli, J., *Introduction and General Overview of Cyclodextrin Chemistry*. Chemical Reviews, 1998. 98(5): p. 1743-1754.
87. Wan, L.S.C. and P.F.S. Lee, *CMC of polysorbates*. Journal of Pharmaceutical Sciences, 1974. 63(1): p. 136-137.
88. Sane, S.U., R. Wong, and C.C. Hsu, *Raman spectroscopic characterization of drying-induced structural changes in a therapeutic antibody: Correlating structural changes with long-term stability*. Journal of Pharmaceutical Sciences, 2004. 93(4): p. 1005-1018.
89. Bee, J.S., et al., *Monoclonal antibody interactions with micro- and nanoparticles: Adsorption, aggregation, and accelerated stress studies*. Journal of Pharmaceutical Sciences, 2009. 98(9): p. 3218-3238.
90. Tyagi, A.K., et al., *IgG particle formation during filling pump operation: A case study of heterogeneous nucleation on stainless steel nanoparticles*. Journal of Pharmaceutical Sciences, 2009. 98(1): p. 94-104.
91. Carpenter, J.F., et al., *Overlooking subvisible particles in therapeutic protein products: Gaps that may compromise product quality*. Journal of Pharmaceutical Sciences, 2009. 98(4): p. 1201-1205.
92. Chi, E.Y., et al., *Physical Stability of Proteins in Aqueous Solution: Mechanism and Driving Forces in Nonnative Protein Aggregation*. Pharmaceutical Research, 2003. 20(9): p. 1325-1336.
93. Lumry, R. and H. Eyring, *Conformation Changes of Proteins*. The Journal of Physical Chemistry, 1954. 58(2): p. 110-120.
94. Arakawa, T. and S.N. Timasheff, *The stabilization of proteins by osmolytes*. Biophysical Journal, 1985. 47(3): p. 411-414.
95. Krishnan, S., et al., *Aggregation of Granulocyte Colony Stimulating Factor under Physiological Conditions: Characterization and Thermodynamic Inhibition†*. Biochemistry, 2002. 41(20): p. 6422-6431.

III. CONTROLLED ICE NUCLEATION IN PHARMACEUTICAL FREEZE-DRYING

III.1 INTRODUCTION

Controlled ice nucleation is a new upcoming technology in pharmaceutical freeze-drying. The term “controlled” refers to the ability to not accept the random nature of spontaneous water-to-ice conversion but to actually influence ice nucleation during the freezing step in the freeze-drying process. In this chapter, a review on ice nucleation and crystallization is given and methods to achieve controlled ice nucleation as well as other modifications of the freezing step are presented. Further, we developed a method to achieve controlled ice nucleation and also investigated its applicability in a pilot-scale freeze-drier. Finally, the developed method was used to study ice nucleation effects on protein and placebo formulations. Finally, the Mpemba effect, a surprising phenomenon that hot water freezes faster than cold water, was investigated using lyophilization equipment.

III.2 CONTROLLED ICE NUCLEATION IN THE FIELD OF FREEZE-DRYING: FUNDAMENTALS AND TECHNOLOGY REVIEW²

III.2.1 INTRODUCTION

Lyophilization, the most important drying process for biologicals, usually consists of three process steps. An aqueous solution is frozen and subsequently, water is removed by sublimation during primary drying. Non-frozen water is removed by diffusion and desorption during secondary drying. Although the importance of the freezing step has long been known in literature, the transformation of water to ice could not be controlled directly. The need to control the temperature at which the super-cooled aqueous solution spontaneously forms ice (T_n) can improve primary drying times and product uniformity. These benefits, saving process time, energy and money have recently led to the development of several methods to actively control ice nucleation in pharmaceutical drug solutions. The goal of this review is to supply the reader with background information about ice nucleation, impact on product quality attributes and to present the different technical solutions to induce ice nucleation.

III.2.2 FUNDAMENTALS OF ICE NUCLEATION AND IMPACT ON THE FREEZE-DRYING PROCESS

III.2.2.1 THE ICE NUCLEATION PROCESS

Freezing of water is a highly complex process which becomes even more complex with pharmaceutical formulations used in freeze-drying. In general, freezing of water includes the following steps: (1) cooling of the solution below its equilibrium freezing temperature with a defined cooling rate; (2) primary nucleation which is the formation of an ice nucleus; (3) secondary nucleation which instantly follows primary nucleation and describes the growth of the nucleus to ice crystals; (4) completion of the liquid-to-solid phase transition by further growth of ice crystals [1]. The nomenclature is adopted from to the work of Searles and co-workers [1]; the term secondary nucleation refers to ice crystallization only; the authors want to point out that the term secondary nucleation or secondary crystallization is also used in the literature for crystallization of solutes [2]. While lowering the temperature below the equilibrium freezing temperature, ice nucleation is usually not observed in pharmaceutical formulations with low particle levels and samples are super-cooled up to -20 °C [1]. Pure water can even

² The section in the thesis was part of the publication Geidobler, R. and G. Winter, Controlled ice nucleation in the field of freeze-drying: Fundamentals and technology review. *European Journal of Pharmaceutics and Biopharmaceutics*, 2013. The text was written by R. Geidobler and was corrected for publication by G. Winter.

be super-cooled to $-48\text{ }^{\circ}\text{C}$ in the absence of particulates or other impurities [3]. It is important to distinguish between global super-cooling (the whole solution is homogeneously super-cooled) and local super-cooling (only a fraction of the liquid is super-cooled). Slow cooling rates usually lead to global super-cooling whereas local super-cooling is observed above a critical cooling rate, e.g. with liquid nitrogen immersion [1, 4]. In the super-cooled, liquid state, many different possibilities to form networks of hydrogen bonds are possible. Only by the formation of a nucleus of water molecules with relatively long-lasting hydrogen bonds, growth of this initial nucleus, and rapid, homogeneous crystallization of ice is possible [5]. The appearance of the initial nucleus is called primary nucleation. The number of those nucleation sites is increased with a higher degree of super-cooling [6]. Secondary nucleation, which is the growth of the nuclei proceeds with a certain interface velocity in the range of cm/s [7]. During crystallization, the temperature of the ice-liquid mixture rises close the equilibrium freezing temperature and crystallization stops. Consequently, not the entire liquid freezes instantly during secondary nucleation. With continuous heat removal, crystallization proceeds until all crystallisable water is transformed from the liquid to the solid state [8]. The speed of ice crystal growth and complete solidification is determined by the removal of generated heat [8]. After complete solidification, the temperature of the sample drops. Figure III-1 shows typical thermocouple readings for standard, ramp frozen samples.

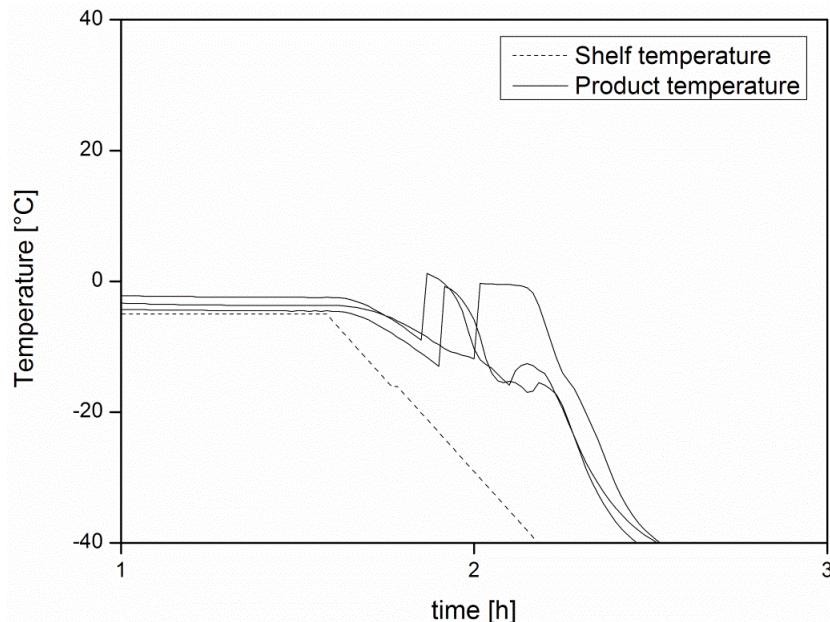


Figure III-1: Typical thermocouple readings for shelf ramp freezing.

In the field of pharmaceutical freeze-drying, heterogeneous nucleation of ice is reality [4]. In contrast to homogeneous nucleation in pure water, ice nucleation is triggered by impurities, which can act as foreign ice nucleation sites [1]. Such impurities hence increase the average ice nucleation temperature in a batch [1]. Still, super-cooling of pharmaceutical formulations

up to -20 °C or -30 °C could be observed. The amount of sub-micron particles is expected to be higher in lab-scale environment and may decrease dramatically in a manufacturing environment. It may be concluded that in production scale, ice nucleation temperatures are in average lower than in early development and therefore modifications of the freeze-drying process are necessary [9].

III.2.2.2 THE IMPORTANCE OF THE DEGREE OF SUPER-COOLING

Based on the aforementioned physics, there are some implications concerning the degree of super-cooling. First, the degree of super-cooling influences the fraction of ice formed after secondary nucleation and temperature rise since crystallization stops when the equilibrium freezing temperature is reached. The higher the degree of super-cooling, the more crystallization heat can be absorbed by the super-cooled solution and the more water instantly freezes. The fraction of ice initially frozen can be calculated according to Searles et al [1]:

$$x = \frac{m_{wn}}{m_{wf}} = \frac{(T_f - T_n)C_{pw}}{\left(1 - \frac{C}{C_g}\right)\Delta H_m}$$

Equation III-1: Fraction of water crystallized dependent on nucleation temperature.

With the mass of water crystallized at nucleation m_{wn} , and the mass of freezable water m_{wf} . T_f is the equilibrium freezing temperature of water and T_n is the nucleation temperature. C_{pw} is the heat capacity of water (around 4.2 J/g*K), and C is the mass fraction of solutes. C_g is the mass fraction of solutes in the maximally freeze-concentrated state. ΔH_m is the crystallization heat of ice [1] (334 J/g [10]). The equation is simplified and does not take into account minor changes of equilibrium freezing temperature depression, crystallization heat and heat capacity of water. To give an estimate, 7 % – 27 % of water crystallized at nucleation temperatures from -5 °C to -19 °C [1]. The amount of total crystallisable water and unfrozen water is mainly determined by the composition of the formulation and is not influenced by the ice nucleation temperature.

Second, due to a colder environment, e.g. a cold freeze-dryer shelf, ice crystal growth is also faster with low ice nucleation temperatures since heat is removed relatively fast via the cold shelf. Contrary, with a lower degree of super-cooling, resulting in a higher nucleation temperature, a smaller fraction of ice is instantly frozen and also ice crystal growth is slower since the freeze-dryer shelf is warmer and thus the driving force of heat removal is lower. The difference between a low and a high nucleation temperature is illustrated in Figure III-2.

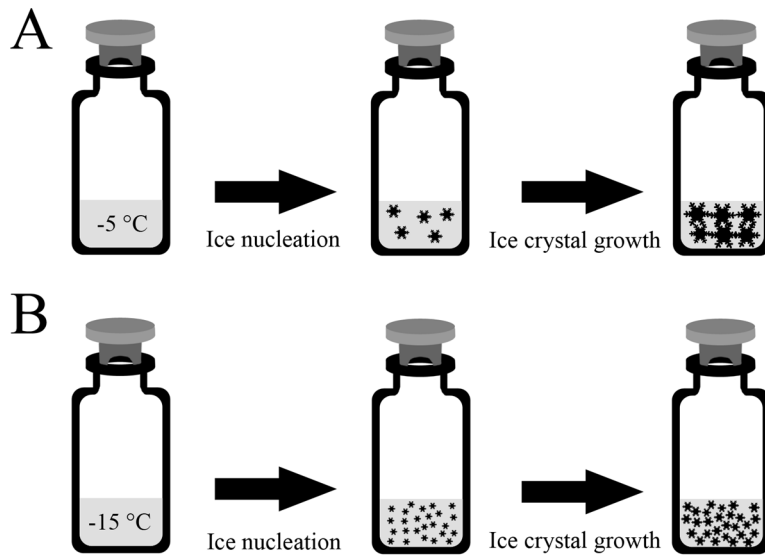


Figure III-2: Exemplary description of ice nucleation at different product temperatures. A: Ice nucleation at a high product temperature of around $-5\text{ }^{\circ}\text{C}$. Fewer but larger ice crystals are generated which grow to larger ice crystals. Also, a smaller fraction of ice is instantly formed. B: Many small ice crystals are formed by large super-cooling and a larger fraction of total freezable water instantly freezes. These ice crystals also grow but their average size will be smaller than those from a higher T_n .

The differences in number of nuclei, fraction of instantly frozen water and ice crystallization growth rate leads to a lot of different morphologies of ice [11]. For example, with a super-cooling of around $-1.5\text{ }^{\circ}\text{C}$, dendritic ice crystals are formed whereas different needle-like crystals or platelets are formed with lower nucleation temperatures [11]. For a given ice nucleation temperature T_n , more than one ice crystal morphology can exist, indicating that T_n is probably the most important but not the only parameter influencing ice morphology [11]. Obviously, different solutes in various concentrations can affect ice crystal morphology [12] and also the presence of tertiary butyl alcohol (TBA) can change ice morphology [13]. Directional solidification can lead to chimney-like [14] or lamellar ice crystals [8].

III.2.2.3 THE INITIATION OF ICE NUCLEATION AND SIMILARITIES TO ANNEALING

Any method that allows for a control of the nucleation temperature T_n results in several degrees of freedom for the freeze-drying scientist. In principle, there are three parameters which can directly be controlled. First, the nucleation temperature T_n ; second, the isothermal hold time post nucleation (which can be zero in the case of nucleation control during shelf ramping); third, the cooling rate of the shelf post nucleation. In the literature, different methods have been used for ice nucleation. In one approach, ice nucleation was induced at several product temperatures and subsequently, the shelf temperature was held for 15 additional minutes and cooled down after that time span [15]. In another approach, the shelf was immediately cooled down after ice nucleation in all vials to complete solidification [9]. Also, ice nucleation during shelf ramping has been performed. In this case, nucleation has been

triggered when a special vial, monitored using a thermocouple, was cooled below a specific temperature [16-19]. However, in larger freeze-dryers, cooling of all shelves may show some variations, and not all vials may show the same temperature during the shelf ramping [17]. Figure III-3 shows an example of controlled ice nucleation after equilibration of the vials on the freeze-dryer shelf.

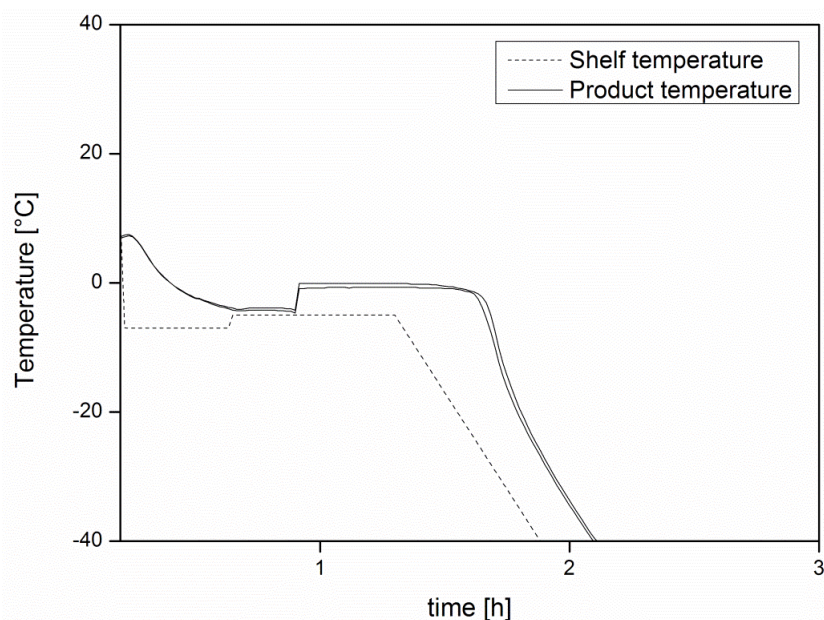


Figure III-3: Thermocouple readings for controlled nucleation at approximately -5 °C followed by 20 minutes of isothermal hold (unpublished data by the authors).

While the link between T_n and primary drying time is already well established (see also following chapters), there are no systematic investigations on the relevance of the speed of final solidification which is controlled by the isothermal hold time and the cooling rate of the shelf ramp. There are some aspects which may favour a long isothermal post nucleation hold time. First, crystallization and complete solidification proceeds quite slow due to slow heat removal. It can be speculated that this may result in very large ice crystals yielding large pores with a low tortuosity. Furthermore, at an ice nucleation temperature far above T_g' , annealing or devitrification is simultaneously taking place and the extent is dependent on post nucleation isothermal hold time and the following shelf ramp. Annealing is usually performed after ramp freezing at elevated temperatures above T_g' to allow crystallization of initially amorphous excipients [20] and Ostwald ripening of ice crystals to improve sample homogeneity and primary drying speed [21]. With annealing, the ice/water interface is initially large and is reduced due to Ostwald ripening process in which smaller ice crystals melt in favour of larger ice crystals while the interfacial free energy is decreased [21]. It can be considered as an advantage for interfacial-sensitive drugs that during controlled ice nucleation and isothermal hold, the ice/water interface area remains smaller compared to ramp freezing followed by annealing. Of course, also the downsides have to be considered. For active ingredients, which

are sensitive to freeze-concentration, a long isothermal hold time may be detrimental and a fast ramp cooling may result in better process stability of those drugs. Unwanted crystallization, for example of buffer components may also occur and result in pH shifts [22]. Furthermore, annealing may lead to phase separation of polymer-containing formulations [23, 24].

III.2.2.4 IMPACT OF ICE CRYSTAL SIZE ON PRIMARY AND SECONDARY DRYING

A link between ice nucleation temperature and ice crystal size has been established quite early [25] and this correlation has been confirmed by several publications from the field of food science and freeze-drying. An early correlation between ice nucleation temperature and primary drying speed was established by Roy and Pikal [26]. They observed that the presence of a thermocouple probe in a vial increased T_n and those vials finished primary drying earlier than the other vials without thermocouples. A strong correlation between T_n and sublimation rates was also observed by Searles et al [1]. Samples, which nucleated at high product temperatures also showed higher primary drying rates as determined by mass loss. Direct analysis of ice crystal size and distribution by optical microscopy in a cold chamber was correlated to sublimation rates by Hottot et al [27, 28]. They found that larger ice crystals, generated by annealing of ramp-frozen samples increased sublimation rates whereas small ice crystals, prepared by liquid nitrogen immersion, resulted in rather low sublimation rates. The link between ice nucleation, temperature and sublimation rates is therefore considered as well-understood.

Large ice crystals provide less resistance to water vapour flow during sublimation because they leave behind larger pores [9, 15]. Freeze-dried cake pore size is interrelated to its specific surface area (SSA) by assuming a capillary tube model [9].

$$SSA \left[\frac{\text{m}^2}{\text{g}} \right] = \frac{2\varepsilon}{\rho_s(1-\varepsilon)} \cdot \frac{1}{r}$$

Equation III-2: Specific surface area and pore radius.

With ε being the sample porosity, ρ_s the sample density and r is pore radius [9]. The specific surface area is therefore inversely connected to the radius of pores.

Furthermore, dry layer resistance of freeze-dried cakes can be connected to pore size radius [9]:

$$\hat{R}_p = \sqrt{\frac{\pi RT}{2M} \cdot \frac{3}{4} \cdot \frac{\tau^2}{\varepsilon} \cdot \frac{1}{r}}$$

Equation III-3: Product resistance and pore radius.

With \hat{R}_p equals product resistance, R is the gas constant, T is the absolute temperature, M is the molecular weight of water, ε is cake porosity and r is pore size radius. τ is a parameter describing the tortuosity of the cake by taking into account the length of the channels and the thickness of the porous system [9]. Consequently, by increasing pore size, dry layer resistance is decreased which decreases primary drying time. Furthermore, product temperature during steady state heat and mass transfer during primary drying is slightly lower due to lower product resistance. This allows for further fine-tuning of shelf temperature, hence additional reduction of primary drying time.

However, the specific surface area determines the speed of desorption of water in the secondary drying stage [29, 30]. A rate limiting step in secondary drying kinetics is the diffusion of water from the amorphous solid solution to the solid/void interface [29]. A lower specific surface area therefore decreases secondary drying kinetics for two reasons: first, the surface area for evaporation of water is reduced; second, the path of diffusion becomes longer due to thicker walls of the lyophilized cake. Of course, this is only valid if cake porosity and density are constant. A given freeze-drying process therefore leads to different residual moistures depending if ice nucleation occurs at higher or lower product temperatures. In fact, it has been shown that the higher the nucleation temperature, the higher the residual moisture of water develops [31]. This has also been experimentally confirmed by Konstantinidis et al [15]. Hence, modification of a freeze-drying cycle applying controlled nucleation may also involve extension of secondary primary drying time, or, more preferably, an increase in secondary drying temperature to achieve sufficiently low residual moisture. Another interrelated aspect is the shelf temperature ramp between primary and secondary drying. In this dynamic situation, the glass transition temperature T_g is increased while the water content is simultaneously decreased. For fully amorphous products, it is important that T_{shelf} is at least lower than T_g to avoid structural collapse of the lyophilized cake by exceeding the actual glass transition temperature. Heating rates of approximately 0.15 °C/min are suggested in the literature [30]. This is also true for mixtures of crystalline bulking agents and amorphous co-stabilizers; however, structural collapse may not be macroscopically visible.

III.2.2.5 HOMOGENEITY ASPECTS

Controlling the ice nucleation temperature not only allows selecting ice nucleation temperature, but it is claimed that also homogeneity of those samples may be improved because variations in random ice nucleation temperatures are reduced. Recent studies mainly focus on the benefits of ice nucleation at elevated temperatures, at which samples normally do not nucleate. Indeed, reduction in standard deviations for certain product characteristics have been observed, e.g. for specific surface area [32] as well as freeze-drying process parameters, e.g. the slope of the pirani gauge indicating the end of sublimation [33]. However, slightly increased standard deviations of controlled nucleated samples at -5 °C compared to random nucleated samples with respect to residual moisture and specific surface area were also observed [15]. Comparison of controlled-nucleated samples with uncontrolled, random nucleated samples is currently biased by the different product properties these two populations have, e.g. different residual moistures and specific surface areas. So far, no comparison of controlled nucleated samples with a T_n similar to that of random nucleation has been published. In addition, standard deviations usually observed in random-nucleated samples are not that high as one would expect looking at the distribution of ice nucleation temperatures [15]. Furthermore, controlled nucleated samples will certainly also show certain variability in product properties. These differences may not result from initial ice crystal distribution but from different freezing rates post nucleation due to variations in intra shelf temperature distribution, variations of vial heat transfer coefficients, various heat input during primary and secondary drying, pressure inhomogeneity during primary drying, the edge-vial effect and product temperature variations. Finally, currently marketed lyophilized products are produced without control of ice nucleation temperature and are accepted by the authorities and the scientific community. Homogeneity is not yet a striking argument for controlled ice nucleation.

III.2.3 METHODS TO INDUCE AND CONTROL ICE NUCLEATION

The main scope of this review is to present methods which allow free selection of the ice nucleation temperature T_n . Besides that, also other methods, which increase the average ice nucleation temperature, are presented. Additives like silver iodide or *Pseudomonas syringae* suspensions are beyond the scope of the review due to regulatory reasons; their effect on ice nucleation in the field of freeze-drying was reported by Searles et al [1]. An overview of all the methods is presented in Table III-1.

Chapter III: Controlled ice nucleation in pharmaceutical freeze-drying

Table III-1: Overview of methods that allow to control the ice nucleation temperature or to increase average ice nucleation temperature. Please note that the column "Repeatability" somewhat conflicts with the requirement to induce ice nucleation very fast. During repetitions, heterogeneity of samples may originate.

Method	Ability to select T_n	Scalability	Positive / negative pressures used	Usable in aseptic environments	Efficiency	Repeatability	Retro-fit needed	Ref.
Ice fog (original)	Yes	Difficult	Negative, 67 mbar	Yes *	Up to 100 % (after 5 minutes)	Yes	Yes	[9, 32]
Ice fog (commercial scale)	Yes	Yes	No	Yes	Up to 100 %	Yes (circulation)	Yes	[16, 17]
Ice fog (ice seed generator)	Yes	Yes	Negative, 67 mbar	Yes	No data published	Not proven, difficult *	Yes	[34, 35]
Ice fog (ventilation through cold condenser)	Yes	Not yet proven	Negative, 3.7 mbar	Not yet proven	~99 %	Not proven, difficult *	No	[36]
Depressurization technique	Yes	Yes	Positive, up to 2 bar over-pressure	Yes	Up to 100 %	Yes	Yes	[15, 37]
Ultrasound ice crystallization	Yes	Difficult *	No	Difficult *	Up to 80 %	Yes	Yes	[18, 33]
Vacuum induced surface freezing	No	Difficult *	Negative (~1 mbar)	Yes	No data published	No	No	[14, 31]
Gap freezing	No	Yes	No	Yes	-	No	Yes (Thermal insulators)	[38]
Temperature quench freezing	No	Yes	No	Yes *	Up to 100 %	Yes	Yes	[39]
Electro-freezing	Yes	Difficult *	No	Difficult, invasive	High, up to ~96 %	Yes	Yes	[40, 41]
Pre-cooled shelf method	No	Difficult *	No	Yes	-	No	No	[1, 28]
Mechanical agitation	Yes*	Difficult *	No	Yes	-	Yes *	Yes	[42]

*: expectation by the author

III.2.3.1 REQUIREMENTS FOR A METHOD INDUCING ICE NUCLEATION

For any method which is employed to induce ice nucleation in freeze-drying processes, there are several requirements which need to be fulfilled:

Success of nucleation: Most important, of course, is the ability to induce ice nucleation in super-cooled solutions. Furthermore, ice nucleation should be independent of freeze-drying equipment, vial type and size, fill volume, formulation and lyophilization stopper geometry.

Robustness and controllability: Any method needs to be robust and should allow for ice nucleation in a reproducible and well controllable way and nucleation success should be 100 %. Beyond that, ice nucleation should take place immediately to ensure homogeneity in product temperatures. The method should be scalable to allow its use both in early development and production units. Since many methods have increased technical needs, the software controlling the freeze-drying process should be as flexible as possible. An optimal method should control the product temperature prior to ice nucleation to actually control T_n and not just a specific time after process start.

Product quality: Product quality is not allowed to be altered in any negative way by the method of choice, sterility and aseptic conditions must be maintained throughout the nucleation process. Operational qualification of the method must be possible and the method should not have a negative impact on media fill freeze-drying runs.

III.2.3.2 MONITORING OF THE NUCLEATION EVENT

One of the greatest challenges faced by any method employed in a freeze-drying process is the ability to achieve 100 % nucleation success and the monitoring of the nucleation event. Up to now, monitoring of ice nucleation is performed using thermocouples, preferably attached to the outside of the vial to not induce ice nucleation by the temperature sensors itself. For the ice fog method, vials were chosen for which ice nucleation was expected to be difficult [17]. However, only a limited amount of vials can be monitored this way. Monitoring was also done visually using a camera which was built into the freeze-dryer [15]. However, up to now, there is no technology available which is able to monitor ice nucleation of all vials simultaneously and can be retrofitted to freeze-dryers of all sizes. Samples nucleated at higher temperatures differ from samples with lower nucleation temperatures and show different residual moistures and specific surface areas. By that, identification of differently nucleated vials can be carried out after the drying process has been finished. While BET SSA measurements are time-consuming and destructive, residual moisture of lyophilized samples can be determined non-invasively by near-infrared spectroscopy [43].

III.2.3.3 THE ICE FOG TECHNIQUE

As first proposed by Rowe [44], the obviously easiest way to induce ice nucleation of super-cooled solutions is by using ice crystal as seeds. It was first applied in the field of freeze-drying by Rhambhatla and co-workers [9]. Nitrogen gas is transported at slightly increased pressure through copper coils which were immersed in liquid nitrogen, thus cooling the gas stream to temperatures less than -40°C . Subsequently, the gas enters the product chamber as shown in Figure III-4, method A. Water vapour, already present in the chamber, is cooled by the cold gas and forms ice crystals. The gas enters the chamber at minimum overpressure and the ice crystals pass into the pre-cooled vials inducing ice nucleation. Despite the striking concept, it is difficult to distribute ice crystals fast and homogeneously throughout the product chamber. The first approach was successful at various product temperatures ranging from -1°C to -12°C and a partial freeze-dryer load of one shelf [9]. However, complete ice nucleation for all vials containing 5 % (w/v) sucrose took up to 30 minutes and during this relatively long time span, annealing for the earlier nucleated samples took place while remaining at a temperature far above T_g' , which impacted homogeneity in the samples [9]. By improving the technical setup, the temperature of the gas could be lowered to less than -50°C . Further, distribution of the cold gas within the freeze-dryer could be optimized by employing a circular tube with holes. Ice nucleation of all samples was completed within five minutes [9]. To reduce the time needed for nucleation and improving product homogeneity, a follow-up study by Patel and co-workers [32] was conducted. The ice-fog was introduced in the product chamber after depressurizing the product chamber to approximately 66 mbar. Higher pressures (above 66 mbar) required several repetitions of the process. By this optimization, ice nucleation of all vials was achieved in around one minute for one shelf, but for a full loaded freeze-dryer, the process had to be repeated four times to achieve complete ice nucleation in all samples within five minutes. Inhomogeneous Ostwald ripening is likely to happen during this time span and may cause heterogeneity in the samples. To circumvent the problem, the authors proposed to use the CIP/SIP equipment in a manufacturing freeze-dryer to optimize distribution of ice crystals [32].

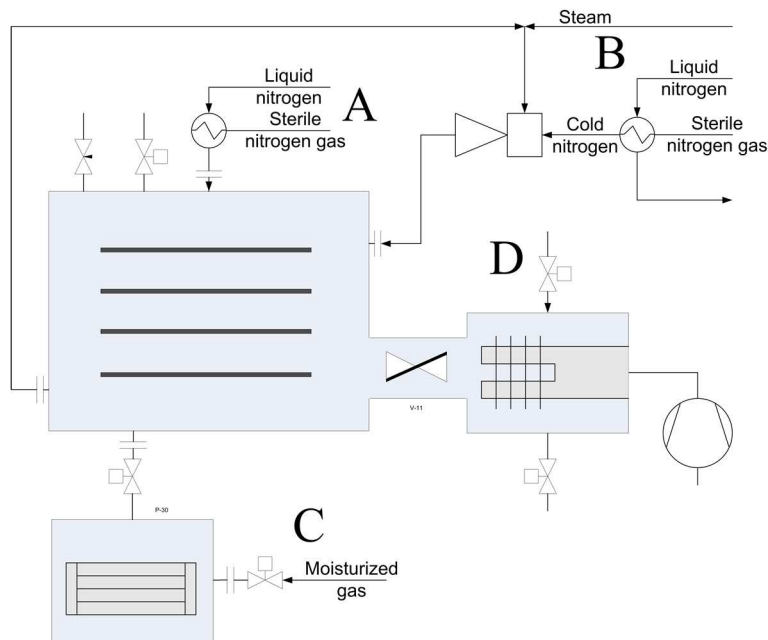


Figure III-4: Overview of the various ice fog methods. A: Original ice fog method, B: improved ice fog method with circulation (adapted from [17]), C: ice fog generation in an external condenser, D: re-pressurization method through cold condenser.

Currently, development of the ice fog method continues to ensure fast and uniform distribution of ice crystals. One approach taken by the companies Linde and IMA to address this problem is to mix sterile water vapour with liquid nitrogen cooled nitrogen gas in an ejector [16, 17, 19]. The hardware setup is illustrated in Figure III-4, method B. Water vapour will freeze upon contact with the cold gas and is brought into the product chamber, subsequently inducing ice nucleation. The ejector allows selecting the density of the ice fog and also serves as a pump for the ice fog without the need for mechanical parts, which is beneficial for steam sterilization. The ice fog mixture is removed from the product chamber through a second connection, is mixed with steam and enters the ejector again [17, 19]. This circulation of the ice fog allows for sufficient distribution and ice nucleation was achieved in 30 to 50 seconds by this method in lab- and pilot scale freeze-dryers of 1.1 m² and 2.5 m² shelf area [17, 19]. With the use of steam and sterile-filtered nitrogen gas, sterility of the process is maintained [17, 19].

Liquid nitrogen is necessary to successfully apply the ice fog technique in the methods above; however, handling of liquid nitrogen requires a certain effort and continuous supply. Hence, there are also approaches to create an ice fog without the need for liquid nitrogen. For example, an ice fog can be generated in an external product chamber or condenser, separated by an isolation valve by injection of moisturized gas with adjustable humidity [34, 35]. First, the whole system is depressurized to approximately 67 mbar similar to the approach of Patel et al [32]. Depending on the setup, either an external, second condenser as shown in Figure III-4, method C or the condenser of the freeze-drying unit is used to create an ice fog by injection of humidified gas. The ice crystals are then released into the product chamber by opening the

isolation valve, driven by the pressure difference between the product chamber and the ice fog compartment [35]. According to the manufacturer, the method could be scaled up to freeze-dryers with a shelf area of 3 square meters [34]. Ice nucleation is fast in the time scale of seconds [35] and works with vials, syringes and microtiter well plates [34].

In another method recently published, ice nucleation could be induced by first depressurizing the entire freeze-dryer, followed by immediately re-pressurization of the system via the cold condenser [36]. It was speculated that, by depressurizing the chamber to approximately 3.7 mbar, a large enough batch will create enough water vapour which is transported onto the condenser. During re-pressurization through the condenser, as shown in Figure III-4, method D, these ice crystals could be blown back into the product chamber. The hypothesis is supported by the fact that small batches could only be nucleated when the condenser had certain ice pre-load. Re-pressurization via the product chamber did not lead to ice nucleation, so the sudden increase in pressure alone was not responsible for successful ice nucleation. Ice nucleation was achieved almost instantly [36]. An advantage of this method is that no hardware modifications of the freeze-dryer are required; however, the depressurization step needs to be well controlled to avoid boiling of solutions.

III.2.3.4 HIGH PRESSURE SHIFT FREEZING / DEPRESSURIZATION TECHNIQUE

High pressure shift freezing [45-47] and high pressure assisted freezing [45, 46] has been known for several years from food science. The thermodynamic freezing temperature of water can be lowered to approximately -20 °C by an increase of pressure to approximately 2000 bar, because the system evades the volume expansion of ice [45]. The sample is then cooled to sub-zero temperatures, and pressure is released [45]. During pressure release to atmospheric pressure, the equilibrium freezing point of water is increased and ice nucleation takes place. With this technique, a high degree of super-cooling can be achieved because product temperature is above the melting curve and small ice crystals are obtained [45]. The concept of pressurizing and depressurizing the product chamber which contains the product vials was adopted by Gasteyer et al and transferred to the field of freeze-drying [37, 48]. However, product chambers of freeze-dryers are not able to withstand high pressure of 2000 bar, and pressurization was performed at approximately 2.9 bar with argon. The shelf-temperature is then lowered to the desired product temperature and ice nucleation is induced by depressurizing the product chamber to 1 bar [15]. The pressure difference for successful application is at least 0.48 bar and de-pressurization needs to be sufficiently fast with a rate of at least 0.014 bar/sec [37]. Having a closer look at the phase diagram of water, the original concept of high pressure shift freezing is only partly applicable. With a comparably low pressure of around 2.9 bar, the product is constantly super-cooled and in metastable state during lowering of the shelf temperature and with pressure release, the melting curve is not

crossed. Consequently, the mode of action of the depressurization technique is not completely understood and the authors speculated that cooling of the liquid product surface by expansion of the gas would be inducing ice nucleation [15]. This theory is supported by the fact that ice nucleation proceeds from the top to the bottom of the liquid. Local evaporation and self-cooling of the product or a pressure wave, mechanically disturbing the liquid surface, are also imaginable [15]. Furthermore, under pressurized conditions, gas is dissolved in the super-cooled aqueous liquid. During depressurization, bubbles may be formed which could induce ice nucleation [15]. One or more of these mechanisms may contribute to successful nucleation.

The depressurization technique has been shown to be effective from 1 m² shelf area up to 5 m² shelf area [49]. A freeze-dryer, capable of using the depressurization technique needs to be able to handle the high pressures involved, which most production scale, steam-sterilizable freeze-dryers do. Furthermore, the calibration status of manometers needs to be maintained in such systems. To quickly pressurize and depressurize the product chamber, the freeze-dryer needs to be retrofitted with manifolds. Lab-scale freeze-dryers are usually not designed to withstand high positive pressures, so there are difficulties to use the depressurization technique in early development.

III.2.3.5 VACUUM INDUCED SURFACE FREEZING

As first presented by Kramer et al, formation of ice can also be achieved by evaporative self-cooling of the sample [14]. The product is placed on the lyophilizer shelf and equilibrated at 10 °C. For pure water, the chamber is then depressurized to approximately 1 mbar and the pressure is held for 5 minutes, until a thin layer of ice is formed due to local super-cooling which will serve as nucleation seeds. To avoid boiling and puff-off of the product, the pressure is then increased rapidly to 1 bar and simultaneously the shelf temperature is reduced to temperatures of 3-4 K below the onset of ice melting temperatures to avoid melting of the ice layer. Large chimney like ice crystals were obtained by directional solidification. The shelf temperature is held for 1 hour at this set-point to allow for Ostwald ripening and complete solidification. The samples are vitrified by lowering the shelf temperature to -40 °C with 2 °C/min [14]. A modification of this method for highly concentrated, large fill volume formulations was published by Liu et al [31]. The shelf temperature was set to -10 °C and pressure was set to 0.8 mbar. After creation of the ice layer, pressure was increased and the shelves were cooled to -45 °C. Unfortunately, there are several drawbacks of this method. It is questionable if the technology can be scaled to large scale freeze-dryers, because massive evaporation of water may induce choked flow in the freeze-dryer and chamber pressures of 1 mbar or even 0.8 mbar may not be controllable. Furthermore, it is important that, after formation of the ice layer, pressure is rapidly increased and shelf-temperature is lowered, as discussed above. This is only possible with a thorough monitoring of the nucleation process as discussed in

section III.2.3.1 and can only be executed if nucleation is induced in all vials in a short time period. Furthermore, the pressure which is needed to form ice on the surface is formulation dependent [14] and needs to be experimentally determined for every batch. Although large ice crystals were obtained with this method [14], it was also observed by Liu et al that two-layer solidification occurred when the shelf temperature was lowered quickly, because a second ice nucleation front also started from the bottom [31]. In this case, a broken cake was observed after freeze-drying [31]. Macroscopic defects of the cake could lead to rejection of those samples.

III.2.3.6 ULTRASOUND INDUCED FREEZING

It has been known for many years that in super-cooled water, nucleation of ice can be achieved by ultrasonic vibration [50], which is also called sonocrystallization. The impact of ultrasonic waves on liquids leads to cavitation, the formation of gas-filled bubbles. Cavitation produces a locally complex situation of pressure and temperature and both influence vapour pressure and equilibrium freezing temperature [50, 51]. It is assumed that, by collapse of a cavitation bubble, ice starts to form if a correct cavitation intensity is used; however, this intensity is quite difficult to determine [52]. Nakagawa et al have shown that ultrasound-induced nucleation is also possible in glass vials by attaching an ultrasound generator and transducer to a temperature controllable aluminium plate on which the glass vials were placed. By triggering the ultrasonic wave at a defined temperature for 1 second, ice nucleation was observed. However, up-scaling of this technique is quite difficult. In order to efficiently propagate the ultrasonic waves, silicon oil had to be used to ensure good contact of the vial with the aluminium plate. With changing geometries of different vial types, a series of trial-and-error tests are necessary to find the correct ultrasonic frequency and the frequency is also dependent on the resonance frequency of the aluminium plate [18]. Furthermore, ice nucleation fails if vials are placed on so-called nodal points with minimum ultrasonic intensity [18]. In addition, also fragmentation of larger ice crystals in was observed after already nucleated sucrose samples were treated with ultrasound [53]. Nevertheless, a prototype freeze-dryer has been built to test ultrasound-induced ice nucleation [33]. The efficiency of ice nucleation was somewhat dependent on the product temperature with favourable lower temperatures. Unfortunately, only around 80 % of the vials could be nucleated by the protocol used [33].

III.2.3.7 ELECTROFREEZING

It has been reported early that super-cooled water can be nucleated by electric current. [54]. Development of appropriate electrodes in fact lead to successful ice nucleation in super-cooled solutions, however, these approaches are invasive and therefore not practical in pharmaceutical freeze-drying. In addition, care has to be taken to select the right electrode

material [55] and success of ice nucleation is also somewhat dependent on formulation composition, for example the presence of ionic substances [40, 41]. For difficult to nucleate formulations, indirect nucleation, that is separate nucleation of water and growing ice crystals proceeds into the super-cooled formulation. Phase transformation was induced by repeated pulses of 4 kV for 2.5 ms with a gold wire electrode [40]. Hydroxyethyl starch (HES) could be nucleated at temperatures as high as $-1.5\text{ }^{\circ}\text{C}$ using this method. However, the impact of electric current on sensitive drug molecules like proteins was not tested. Since every vial needs an electrode with accompanying cable connections, scale-up is considered impossible.

III.2.3.8 PRE-COOLED SHELF METHOD

A modification of the ice nucleation temperature was observed by placing the vials on a pre-cooled shelf in the lyophilizer. The shelves are cooled to around $-44\text{ }^{\circ}\text{C}$ and the vials are placed on those cold shelves. While cooling from room temperature to the shelf set point, it was observed that the average nucleation temperature was increased compared to standard ramp freezing but also heterogeneity in T_n was still heterogeneous [1]. The initial set-point plays a role as the effect was less pronounced with a temperature of $-40\text{ }^{\circ}\text{C}$ [1]. In another study, only small differences between the pre-cooled shelf method and ramp freezing with $0.6\text{ }^{\circ}\text{C}/\text{min}$ were observed with respect to ice crystal size and sublimation rates [28]. With the pre-cooled shelf method, also the filling volume and vial geometry plays an important role resulting in differences in cooling rates and subsequent freezing rates [28, 56]. In production scale, the use of pre-cooled shelves has already been established. Care has to be taken that the cold shelves do not mist over with ice due to contact with humid air. Slight positive inert gas pressure in the freeze-drier may prevent icing of the shelves and the use of a slot door with movable shelves is recommended.

III.2.3.9 TEMPERATURE QUENCH FREEZING

As recently introduced in a patent, ice nucleation can be induced and also to a certain extent controlled by temperature quench freezing [39]. Although described for a controlled rate freezer, this technique is applicable to freeze-drying. Temperature control is provided by mixing liquid nitrogen with gaseous nitrogen and the cryogen mixture is passed through a heater to control its temperature. The vials are placed on a porous metal plate, through which uniform and laminar distribution of the cryogen is ensured. The gas is collected and removed through an exhaust manifold above the vials. This system allows for very fast cooling and heating rates. Samples are first cooled and equilibrated at a temperature below the equilibrium freezing temperature, e.g. at $-5\text{ }^{\circ}\text{C}$ for several minutes. Subsequently, the temperature of the cryogenic liquid nitrogen is rapidly decreased to $-80\text{ }^{\circ}\text{C}$ within approximately 2 minutes, which results in a fast temperature drop in the vials to $-10\text{ }^{\circ}\text{C}$ followed by uniform ice nucleation. The gas

temperature may then be adjusted to a specific temperature to permit Ostwald ripening or fast solidification. Currently, there are no literature reports on temperature quench freezing used in lyophilization. However, implementation of this method is limited by high cooling and heating rates of the shelves which are usually not even achievable with liquid nitrogen boosters. To circumvent this problem, vials could be frozen in a controlled rate freezer and transported to the freeze-drying unit subsequently. The nucleation temperature cannot be controlled directly by this method and it is expected that nucleation temperatures are in general lower compared to other ice nucleation methods.

III.2.3.10 GAP FREEZING

Gap freezing was recently published in a patent, introducing a concept of thermally insulating the samples from the lyophilizer shelves by the use of a spacer with low thermal conductivity [38]. Cooling of the samples is then mainly provided by radiation. The goal of this setup is to ensure that the samples freeze from the bottom and the top simultaneously to avoid formation of a highly concentrated amorphous layer on top of the vial which may decrease primary drying time by its high resistance. By employing different spacers, the average nucleation temperature could be increased. However, since the spacers are difficult to remove, changes to the freeze-drying process have to be made, for example higher shelf temperatures throughout primary and secondary drying. Development and up-scaling of those processes is expected to be difficult.

III.2.3.11 AGITATION INDUCED ICE NUCLEATION

In an early patent, a special construction of a freeze-dryer is described [42]. The shelves are connected to the hydraulic unit of the freeze-dryer which is mounted on swing-metal connections on top of the product chamber. A vibrator is able to agitate the whole shelf package via the hydraulic piston and the vibrator can be adjusted in frequency [42]. This setup was originally designed to improve unloading of vials from the freeze-dryer if sticking of vials with the stopper to the corresponding upper shelf occurs [42]. However, this setup may be suitable to induce ice nucleation by mechanical agitation of the vials. Both lab-scale and production-scale freeze-dryers can be equipped with the vibrator. Up to now, there are no literature reports on this concept and the equipment, including vibrator, swing metal connectors and seals is probably quite expensive.

III.2.4 SUMMARY AND OUTLOOK

A lot progress has been made to control ice nucleation temperature in pharmaceutical formulations, resulting in various, well-engineered techniques which allows for further control

of the freeze-drying process. The ability to control and select T_n is another step towards a better understanding of the resulting product and perfectly fits in the quality by design approach of the authorities by eliminating another variable in the freeze-drying process. Control of T_n can lead to less out-of-specification samples and may reduce failures and trial-and-error approaches in up-scaling of freeze-drying processes. Primary drying times can be massively shortened when T_n is selected at lower super-cooling. However, new questions have to be answered. Although a variety of methods allow to freely select T_n , it is unknown if different methods, although inducing ice nucleation at the same product temperature, will result in a similar product with comparable ice crystal size and distribution. Ice crystal morphology, although documented in many studies, is very heterogeneous and description of ice crystals is not always uniform. More studies on the significance of ice crystal morphology (and not only size) may be useful. Furthermore, little is known about the impact of ice nucleation on relaxation times and long-term stability. In addition, the plurality of excipients may pose a challenge when T_n is comparably high and the state of freeze-concentration is prolonged. The freeze-drying process needs to be adapted regarding temperature/pressure conditions in primary and secondary drying to make best use of the controlled features of the frozen product. With potentially smaller specific surface area, increased secondary drying temperatures have to be considered. The near future will certainly bring up some interesting new experimental work which will further illuminate the freezing process of pharmaceuticals.

III.2.5 REFERENCES

1. Searles, J.A., J.F. Carpenter, and T.W. Randolph, *The ice nucleation temperature determines the primary drying rate of lyophilization for samples frozen on a temperature-controlled shelf*. Journal of Pharmaceutical Sciences, 2001. 90(7): p. 860-871.
2. Akers, M., et al., *Glycine Crystallization During Freezing: The Effects of Salt Form, pH, and Ionic Strength*. Pharmaceutical Research, 1995. 12(10): p. 1457-1461.
3. Moore, E.B. and V. Molinero, *Structural transformation in supercooled water controls the crystallization rate of ice*. Nature, 2011. 479(7374): p. 506-508.
4. Kasper, J.C. and W. Friess, *The freezing step in lyophilization: Physico-chemical fundamentals, freezing methods and consequences on process performance and quality attributes of biopharmaceuticals*. European Journal of Pharmaceutics and Biopharmaceutics, 2011. 78(2): p. 248-263.
5. Matsumoto, M., S. Saito, and I. Ohmine, *Molecular dynamics simulation of the ice nucleation and growth process leading to water freezing*. Nature, 2002. 416(6879): p. 409-413.
6. Burke, M., et al., *Freezing and injury in plants*. Annual Review of Plant Physiology, 1976. 27(1): p. 507-528.
7. Lindenmeyer, C.S., et al., *Rate of Growth of Ice Crystals in Supercooled Water*. The Journal of Chemical Physics, 1957. 27(3): p. 822-822.
8. Patapoff, T.W. and D.E. Overcashier, *The importance of freezing on lyophilization cycle development*. Biopharm, 2002. 15(3): p. 16-21.

9. Rambhatla, S., et al., *Heat and mass transfer scale-up issues during freeze drying: II. Control and characterization of the degree of supercooling*. AAPS PharmSciTech, 2004. 5(4): p. 54-62.
10. Kumano, H., et al., *Study on latent heat of fusion of ice in aqueous solutions*. International Journal of Refrigeration, 2007. 30(2): p. 267-273.
11. Shibkov, A.A., et al., *Morphology diagram of nonequilibrium patterns of ice crystals growing in supercooled water*. Physica A: Statistical Mechanics and its Applications, 2003. 319(0): p. 65-79.
12. Luyet, B. and G. Rapatz, *Patterns of ice formation in some aqueous solutions*. Biodynamica, 1958. 8(156): p. 1-68.
13. F. Franks, T.A., *Freeze-Drying of Pharmaceuticals and Biopharmaceuticals*. 2007, Cambridge: RSC Publishing.
14. Kramer, M., B. Sennhenn, and G. Lee, *Freeze-drying using vacuum-induced surface freezing*. Journal of Pharmaceutical Sciences, 2002. 91(2): p. 433-443.
15. Konstantinidis, A.K., et al., *Controlled nucleation in freeze-drying: Effects on pore size in the dried product layer, mass transfer resistance, and primary drying rate*. Journal of Pharmaceutical Sciences, 2011. 100(8): p. 3453-3470.
16. Brower, J., *Presentation: Ice fog induced nucleation, CPPR Conference on Freeze Drying of Pharmaceuticals and Biologicals*. 2012: Breckenridge.
17. Kaltenecker, J.C., P.; Lee, R.; DeMarco, F.; Renzi, E., *Neuartiges Verfahren zur Steuerung der Eiskeimbildung*. Technopharm, 2012. 2(6): p. 420-424.
18. Nakagawa, K., et al., *Influence of controlled nucleation by ultrasounds on ice morphology of frozen formulations for pharmaceutical proteins freeze-drying*. Chemical Engineering and Processing: Process Intensification, 2006. 45(9): p. 783-791.
19. Chakravarty, P., et al., *Ice Fog as a Means to Induce Uniform Ice Nucleation During Lyophilization*. BioPharm International, 2012. 25(1): p. 33-38.
20. Wang, W., *Lyophilization and development of solid protein pharmaceuticals*. International Journal of Pharmaceutics, 2000. 203(1-2): p. 1-60.
21. Searles, J.A., J.F. Carpenter, and T.W. Randolph, *Annealing to optimize the primary drying rate, reduce freezing-induced drying rate heterogeneity, and determine Tg' in pharmaceutical lyophilization*. Journal of Pharmaceutical Sciences, 2001. 90(7): p. 872-887.
22. van den Berg, L. and D. Rose, *Effect of freezing on the pH and composition of sodium and potassium phosphate solutions: the reciprocal system $\text{KH}_2\text{PO}_4\text{---Na}_2\text{HPO}_4\text{---H}_2\text{O}$* . Archives of Biochemistry and Biophysics, 1959. 81(2): p. 319-329.
23. Heller, M.C., J.F. Carpenter, and T.W. Randolph, *Manipulation of Lyophilization-Induced Phase Separation: Implications For Pharmaceutical Proteins*. Biotechnology Progress, 1997. 13(5): p. 590-596.
24. Izutsu, K.-i., et al., *Effect of salts and sugars on phase separation of polyvinylpyrrolidone[dash]dextran solutions induced by freeze-concentration*. Journal of the Chemical Society, Faraday Transactions, 1998. 94(3): p. 411-417.
25. Fennema, O.R., W.D. Powrie, and E.H. Marth, *Low temperature preservation of foods and living matter*. 1973: Marcel Dekker, Inc.
26. Roy, M.L. and M.J. Pikal, *Process Control in Freeze Drying: Determination of the End Point of Sublimation Drying by an Electronic Moisture Sensor*. PDA Journal of Pharmaceutical Science and Technology, 1989. 43(2): p. 60-66.
27. Hottot, A., S. Vessot, and J. Andrieu, *A Direct Characterization Method of the Ice Morphology. Relationship Between Mean Crystals Size and Primary Drying Times of Freeze-Drying Processes*. Drying Technology, 2004. 22(8): p. 2009-2021.
28. Hottot, A., S. Vessot, and J. Andrieu, *Freeze drying of pharmaceuticals in vials: Influence of freezing protocol and sample configuration on ice morphology and freeze-dried cake texture*. Chemical Engineering and Processing: Process Intensification, 2007. 46(7): p. 666-674.

29. Pikal, M.J., et al., *The secondary drying stage of freeze drying: drying kinetics as a function of temperature and chamber pressure*. International Journal of Pharmaceutics, 1990. 60(3): p. 203-207.
30. Tang, X. and M. Pikal, *Design of Freeze-Drying Processes for Pharmaceuticals: Practical Advice*. Pharmaceutical Research, 2004. 21(2): p. 191-200.
31. Liu, J., et al., *A Study of the Impact of Freezing on the Lyophilization of a Concentrated Formulation with a High Fill Depth*. Pharmaceutical Development and Technology, 2005. 10(2): p. 261-272.
32. Patel, S., C. Bhugra, and M. Pikal, *Reduced Pressure Ice Fog Technique for Controlled Ice Nucleation during Freeze-Drying*. AAPS PharmSciTech, 2009. 10(4): p. 1406-1411.
33. Passot, S., et al., *Effect of controlled ice nucleation on primary drying stage and protein recovery in vials cooled in a modified freeze-dryer*. Journal of biomechanical engineering, 2009. 131(7): p. 074511.
34. Thompson, T.N., *Personal Communication: The FreezeBooster technique*. 2012.
35. Weija, L., *Controlled nucleation during freezing step of freeze drying cycle using pressure differential ice fog distribution*, Patent US2012/02722544 A1. 2012.
36. Geidobler, R., S. Mannschedel, and G. Winter, *A new approach to achieve controlled ice nucleation of supercooled solutions during the freezing step in freeze-drying*. Journal of Pharmaceutical Sciences, 2012. 101(12): p. 4409-4413.
37. Gasteyer, T.H., et al., *Method of inducing nucleation of a material*, Patent US20070186567A1. 2007.
38. Kuu, W.-Y., Doty, Mark J., Hurst, William S., Rebbeck, Christine L., *Optimization of nucleation and crystallization for lyophilization using gap freezing*, Patent US 20120192448A1, B. Healthcare, Editor. 2012: US.
39. Zhou, Y.G., Theodore H.; Grinter, Nigel J.; Cheng, Alan T.; Ho, Yeu-Chuan Simon; Sever, Robert R., *Method and System for nucleation control in a controlled rate freezer (CRF)*, Patent US 20120102982A1. 2012.
40. Petersen, A., G. Rau, and B. Glasmacher, *Reduction of primary freeze-drying time by electric field induced ice nucleus formation*. Heat and Mass Transfer, 2006. 42(10): p. 929-938.
41. Petersen, A., et al., *A new approach for freezing of aqueous solutions under active control of the nucleation temperature*. Cryobiology, 2006. 53(2): p. 248-257.
42. Hof, H.-G., *Gefriertrocknungsanlage*, European Patent EP0777092B1. 1998.
43. Last, I.R. and K.A. Prebble, *Suitability of near-infrared methods for the determination of moisture in a freeze-dried injection product containing different amounts of the active ingredient*. Journal of Pharmaceutical and Biomedical Analysis, 1993. 11(11-12): p. 1071-1076.
44. Rowe, T., *A technique for the nucleation of ice*. International Symposium on Biological Product Freeze-Drying and Formulation. Geneva, Switzerland, 1990.
45. Fernández, P.P., et al., *High-pressure shift freezing versus high-pressure assisted freezing: Effects on the microstructure of a food model*. Food Hydrocolloids, 2006. 20(4): p. 510-522.
46. Sanz, P.D., et al., *Freezing processes in high-pressure domains*. International Journal of Refrigeration, 1997. 20(5): p. 301-307.
47. Kalichevsky, M.T., D. Knorr, and P.J. Lillford, *Potential food applications of high-pressure effects on ice-water transitions*. Trends in Food Science & Technology, 1995. 6(8): p. 253-259.
48. Gasteyer, T.H., et al., *Lyophilization system and method*, Patent US20070186437A1. 2007.
49. Bursac, R., R. Sever, and B. Hunek, *A practical method for resolving the nucleation problem in lyophilization*. BioProcess International, 2009. 7(9): p. 66-72.
50. Hickling, R., *Nucleation of Freezing by Cavity Collapse and its Relation to Cavitation Damage*. Nature, 1965. 206(4987): p. 915-917.
51. Ohsaka, K. and E.H. Trinh, *Dynamic nucleation of ice induced by a single stable cavitation bubble*. Applied Physics Letters, 1998. 73(1): p. 129-131.

52. Inada, T., et al., *Active control of phase change from supercooled water to ice by ultrasonic vibration 1. Control of freezing temperature*. International Journal of Heat and Mass Transfer, 2001. 44(23): p. 4523-4531.
53. Chow, R., et al., *The sonocrystallisation of ice in sucrose solutions: primary and secondary nucleation*. Ultrasonics, 2003. 41(8): p. 595-604.
54. Rau, W., *Eiskeimbildung durch Dielektrische Polarisierung*. Z. Naturforsch., 1951. 6: p. 649–657.
55. Hozumi, T., et al., *Effects of electrode materials on freezing of supercooled water in electric freeze control*. International Journal of Refrigeration, 2003. 26(5): p. 537-542.
56. Jiang, S. and S.L. Nail, *Effect of process conditions on recovery of protein activity after freezing and freeze-drying*. European Journal of Pharmaceutics and Biopharmaceutics, 1998. 45(3): p. 249-257.

III.3 A NEW APPROACH TO ACHIEVE CONTROLLED ICE NUCLEATION OF SUPER-COOLED SOLUTIONS DURING THE FREEZING STEP IN FREEZE-DRYING³

III.3.1 INTRODUCTION

Controlled ice nucleation of super-cooled solutions has recently attracted a lot of interest in the field of freeze-drying [1-4]. Ice nucleation is a stochastic event and the probability of spontaneous ice crystal formation is, among others, dependent on the presence of foreign particles [5]. Thus, ice nucleation becomes a major issue during scale-up from lab-scale to almost particle-free clean room production environment [6]. Controlling ice nucleation at a certain product temperature is expected to lead to a more uniform product since the degree of super-cooling and nucleation temperature is influencing product parameters, for example cake resistance [5], specific surface area and residual moisture [2]. Reduction of cake resistance is greatly reducing primary drying time [6] and therefore saves energy, time and money since primary drying usually is the longest step in a freeze-drying cycle.

However, ice nucleation of super-cooled aqueous solutions is difficult to achieve. One method to achieve controlled nucleation is the “ice-fog” technology, introduced by Pikal et al [5]. A stream of cold nitrogen gas is released into the product chamber to freeze present water vapor. Ice crystals, passing into the super-cooled solution, induce ice nucleation. However, it takes up to five minutes until all vials are frozen. Currently, this technique is improved by depressurizing the product chamber before releasing the cold nitrogen into the chamber, resulting in a faster freezing of vials [3].

Another recently published technique involves pressurizing the product chamber with an inert gas up to 2 bar over-pressure and quickly release the overpressure by evacuation, inducing instant ice nucleation [2]. However, the mechanism of ice nucleation is not fully understood. Moreover, this technique is rather expensive and is only applicable for freeze-driers which are capable to resist around 2 bars over-pressure and requires major technical changes to the freeze-drier.

Besides those two methods there are further methods of minor commercial interest, for example electro-freezing [7], vacuum-induced surface freezing [8] and nucleation by ultrasound [9]. A review recently published summarizes all of the abovementioned techniques [4].

³ This section was published as Geidobler, R., S. Mannschedel, and G. Winter, A new approach to achieve controlled ice nucleation of supercooled solutions during the freezing step in freeze-drying. *Journal of Pharmaceutical Sciences*, 2012. 101(12): p. 4409-4413.

In this article, we want to present a cheap and easy way to instantly induce ice nucleation that can be used in lab-scale and large-scale equipment without the use of liquid nitrogen and without any need for technical changes or hardware modifications. The procedure involves first a well-controlled depressurizing step and secondly, a re-pressurization through the venting valve of the condenser. With a condenser, having some water load, immediate nucleation in the vials takes place.

III.3.2 MATERIALS AND METHODS

III.3.2.1 MATERIALS

Type 1 glass vials (DIN 2R and DIN 10R) were used throughout the study. Stoppers were provided by West Pharmaceuticals. High purified water (Purelab Plus, USF Elga, Celle, Germany) which is filtered through a 0.2 μm filter at the dispenser, was either used alone to be frozen or to prepare a 5 % (w/v) sucrose formulation (Boehringer Ingelheim, Germany). Experiments were carried out using a FTS Lyostar II (SP Scientific, Stone Ridge, USA) lab-scale freeze-drier. To show transferability to other freeze-driers, an Epsilon 2-6D (Martin Christ, Osterode am Harz, Germany) lab-scale freeze-drier was also employed. Various amounts of vials were loaded into the freeze-driers to test scalability. The amounts of vials ranged from 9 to around 600 vials.

III.3.2.2 INDUCTION OF ICE NUCLEATION

The vials are loaded on to the freeze-dryer and are equipped with thermocouples (Type T, Newport Electronics, Deckenpfronn, Germany for the Lyostar II and PT100 temperature sensors, provided by Martin Christ for the Epsilon 2-6D) to monitor product temperature invasively. The shelves of the lyophilizer are cooled and the product is equilibrated to the desired product temperature. The freeze-dryer is then depressurized to a specified vacuum set point and immediately brought to atmospheric pressure using either the release valve of the Lyostar II or the drain valve of the Epsilon 2-6D which ventilates both systems via the cold condenser. During the re-pressurization, almost instant nucleation of the product takes place. The re-pressurization took place with an over-pressure of 0.8 bar of gaseous nitrogen which passed through a sterile 0.2 μm gas filter (Merck Millipore GmbH, Schwalbach, Germany) before entering the freeze-drier and takes around 5 minutes. The success of nucleation was determined by drawing the vials onto a Plexiglas pane and visual inspection. No additional nucleation could be induced by this method, as tests with super-cooled and agitated samples showed.

III.3.3 RESULTS

III.3.3.1 INFLUENCE OF VACUUM SET-POINT

During the experiments, a vacuum set-point of around 3.7 mbar (appr. 2.8 Torr) turned out to be the optimal vacuum set point to induce ice nucleation because on the one hand side it lead to successful nucleation of the super-cooled solutions and on the other hand did not significantly decrease product temperature, as lower vacuum set-points did, e.g. 1.87 mbar.

It is also worth noting that, with this vacuum setting, we never accidentally performed vacuum-induced surface freezing, for which chamber pressure needs to be much lower (1 mbar [8]). Furthermore, we found that product temperature massively dropped by applying such low pressures as 1 mbar, which would result in non-controlled nucleation due to random evaporative cooling and warming due to nucleation, as shown in Figure III-5.

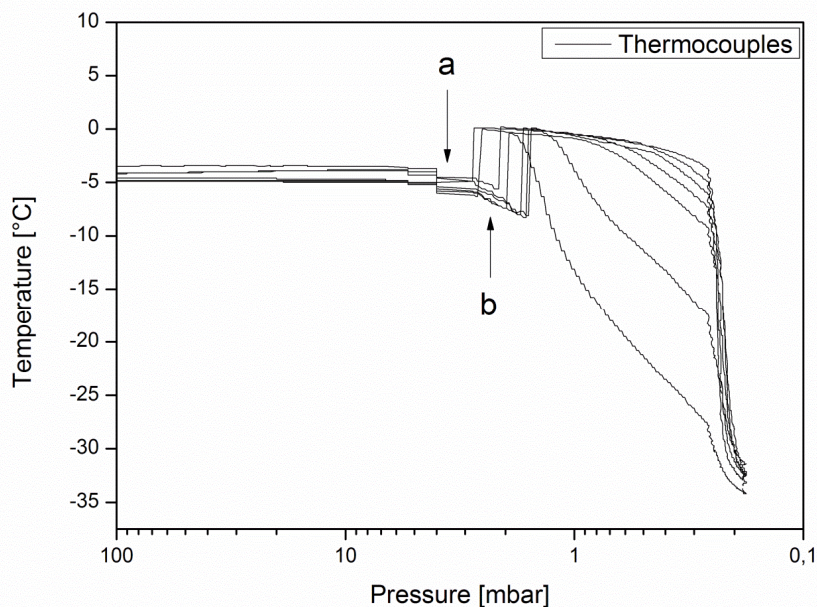


Figure III-5: Temperature profile of 7 thermocouples during vacuum pull-down, placed inside 3 ml of water in DIN 10R vials. (a) Set-point of our method (3.7 mbar), (b) random ice-nucleation due to evaporative self-cooling.

III.3.3.2 INFLUENCE OF CONDENSER ICE PRE-LOAD AND BATCH SIZE

Loosely attached ice from the condenser, which is then blown into the product chamber during re-pressurization, is most likely the predominant mechanism by which ice nucleation is induced in our method. Ice loaded on the condenser is therefore an important parameter.

Freezing of larger batches (more than ~ 300 ml, DIN 10R vials) could be performed starting with a defrosted, empty condenser. It is obvious that a large batch of vials and volume creates a large amount of water vapor in the product chamber which is transported to the condenser due to temperature and pressure gradients. During re-pressurization, in-situ generated ice

crystals from the condenser may be transferred back into the product chamber, inducing ice nucleation.

Successful and reproducible nucleation even of very small batches (~10 vials 2R filled with 1 ml solution) could be obtained by opening the condenser to the outside via a venting valve and a sterile filter and collecting ice from humid air. It is worth noting that without a cold condenser, nucleation of the vials was not possible. A rapid change in pressure alone hence is not responsible for ice nucleation. Furthermore, placement of a tray filled with 100 ml water into the drying chamber during vacuum pull down resulted also in successful, reproducible freezing of a small amount of vials (9 2R vials filled with 1 ml water).

III.3.3.3 SUCCESS OF NUCLEATION

While nucleation of very small batches was 100 % successful using the aforementioned methods, we could also scale up the method to 115 DIN 10R vials filled with 3 ml of water and 594 DIN 2R vials filled with 1 ml of water or sucrose solution and achieved almost 100 % nucleation (see Table III-2).

Figure III-7 shows a batch of 111 vials DIN 10R filled with 3 ml water which is nucleated at a product temperature of around -4.5 °C with a vacuum set-point of 3.7 mbar. Ice nucleation is fast and is finished within 4-5 seconds. Figure III-6 shows the pressure gauge readings and temperature profiles of 8 thermocouples placed in 5% Sucrose solution which was nucleated at around -5 °C.

Table III-2: Nucleation rates for different loadings of the freeze-drier. All experiments were carried out with the aforementioned settings: vacuum set-point 3.7 mbar, re-pressurize through condenser chamber. Product temperature varied between -4 °C and -6 °C.

#	Freeze-dryer loading	Fill volume per vial [ml]	Nucleation success [%] (n=3)
1	9 Vials (2R) of water, pre-loaded condenser	1	100.00 ± 0.00
2	115 Vials (10R) of water	3	99.43 ± 1.00
3	594 Vials (2R) of 5 % sucrose	1	99.04 ± 1.67

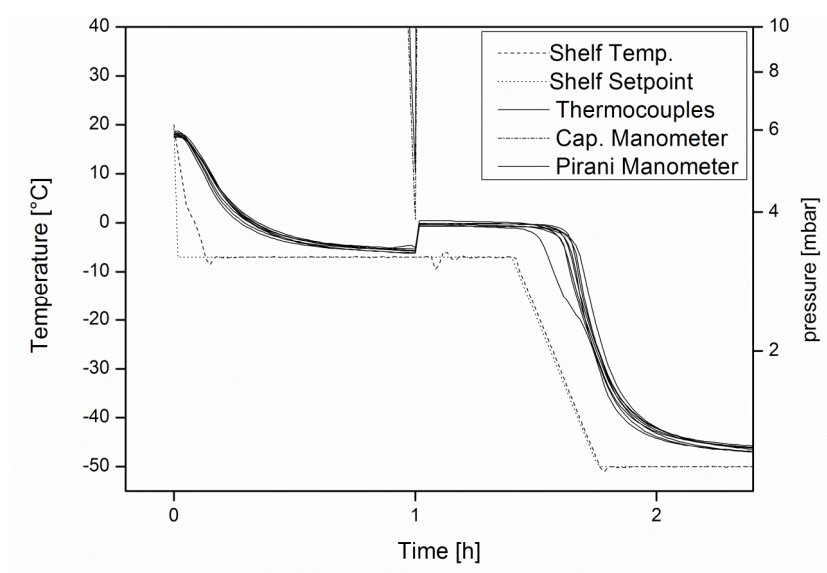


Figure III-6: Temperature profile of 8 thermocouples placed inside a 5 % sucrose solution in the Lyostar II. Nucleation was induced at around -5 °C to -6 °C

A:
0s



B:
2s



C:
4s



Figure III-7: Ice nucleation in 111 vials 10R filled with 3 ml water, placed in the Lyostar II. Ice nucleation took place at around -4.5 °C and is finished after 4-5 seconds.

III.3.4 DISCUSSION

The presented method allows to achieve successful and reproducible ice nucleation, independent of freeze-drier, vial size or fill volume. However, the mechanism is not yet fully understood. One theory is that the water vapor stream, generated during evacuation of the system, is frozen by cold nitrogen gas and blown back into the product chamber. However, our results point towards the assumption that loosely attached ice crystals, blown from the condenser during re-pressurizing the system via the condenser, are transported into the product chamber and lead to instant nucleation in all vials. Ice crystals can either be provided by allowing water to freeze on the condenser or by in-situ generation during vacuum pull down. At first glance, the transfer of ice crystals into all vials containing the product is expected to be quite difficult, however, due to the quick expansion of the gas and the resulting fast gas flow entering the chamber, it was no problem to nucleate 2R vials with a very small opening of the stopper. Another important variable during vacuum release is product chamber temperature. In theory, ice crystals cannot exist at a temperature warmer than 0.01 °C, according to the phase diagram of water. The product chamber in our freeze-drier, as measured with thermocouples, was approximately 8 °C even when shelves were equilibrated at -7 °C. However, since the gas entering the system has to pass the cold condenser of around -80 °C, it is significantly cooled down. Tests with a thermometer, placed at the opening of the drain valve with closed isolation valve showed that the condenser-exiting gas stream had a temperature of around -8 °C at atmospheric pressure. It is expected that the situation during re-pressurizing the system is far more complex, involving expansion of the gas, warming of gas due to emissivity of drier components and temperature changes due to possible melting of ice crystals. Furthermore, it is expected that also the condenser temperature is an important parameter; however, we could not test the method yet with a condenser temperature of around -50 °C.

Another important factor is the vacuum set-point when using in-situ ice crystal generation. We found that 3.7 mbar (appr. 2.8 Torr) was successful for a product temperature of around -3 to -5 °C at the moment of nucleation, but it is expected that this needs to be re-adjusted if lower product temperatures (e.g., -10 °C) are desired. It is important to keep the balance between generating enough water vapour in the chamber and accompanying product temperature drop by evaporative self-cooling during vacuum pull down to avoid vacuum induced surface freezing. In addition, no boiling or bubbling of the solutions was observed with our method; however, as by pulling vacuum, a certain de-gassing of the samples is likely to happen. Re-pressurization of the samples did not blow up the solution in the vials.

III.3.5 OUTLOOK

For successful application of this very simple method in large-scale production, it is necessary to validate and fix batch size and total volume to ensure that enough water vapor is generated, frozen and reproducible nucleation of all vials is achieved. It is easily possible to allow sterile, water vapor saturated air from the outside to freeze on the condenser. Of course, it is necessary to ensure that no contaminants are transferred into the product chamber when the gas stream is reversed during re-pressurization via the condenser compared to the regular use of the unit. Mass spectroscopy could be a valuable tool to check for contaminants like silicon oil droplets in the gas stream. At least for development purpose, we provide a very elegant and simple tool for everyone who wants to assure immediate and homogeneous nucleation in the entire batch during development or in the context of basic research on nucleation effects.

III.3.6 REFERENCES

1. CPPR. *Freeze-drying of pharmaceuticals and biologicals, Conference program*, available at <http://nipte.org/docs/FreezeDrying%20Revised%20Program.pdf>. 2012; Available from: <http://nipte.org/docs/FreezeDrying%20Revised%20Program.pdf>.
2. Konstantinidis, A.K., et al., *Controlled nucleation in freeze-drying: Effects on pore size in the dried product layer, mass transfer resistance, and primary drying rate*. *Journal of Pharmaceutical Sciences*, 2011. 100(8): p. 3453-3470.
3. Patel, S., C. Bhugra, and M. Pikal, *Reduced Pressure Ice Fog Technique for Controlled Ice Nucleation during Freeze-Drying*. *AAPS PharmSciTech*, 2009. 10(4): p. 1406-1411.
4. Kasper, J.C. and W. Friess, *The freezing step in lyophilization: Physico-chemical fundamentals, freezing methods and consequences on process performance and quality attributes of biopharmaceuticals*. *European Journal of Pharmaceutics and Biopharmaceutics*, 2011. 78(2): p. 248-263.
5. Rambhatla, S., et al., *Heat and mass transfer scale-up issues during freeze drying: II. Control and characterization of the degree of supercooling*. *AAPS PharmSciTech*, 2004. 5(4): p. 54-62.
6. Roy, M.L. and M.J. Pikal, *Process Control in Freeze Drying: Determination of the End Point of Sublimation Drying by an Electronic Moisture Sensor*. *PDA Journal of Pharmaceutical Science and Technology*, 1989. 43(2): p. 60-66.
7. Rau, W., *Eiskeimbildung durch Dielektrische Polarisierung*. *Z. Naturforsch.*, 1951. 6: p. 649-657.
8. Kramer, M., B. Sennhenn, and G. Lee, *Freeze-drying using vacuum-induced surface freezing*. *Journal of Pharmaceutical Sciences*, 2002. 91(2): p. 433-443.
9. Inada, T., et al., *Active control of phase change from supercooled water to ice by ultrasonic vibration 1. Control of freezing temperature*. *International Journal of Heat and Mass Transfer*, 2001. 44(23): p. 4523-4531.

III.4 TRANSFERABILITY TO A PILOT-SCALE FREEZE-DRYER

III.4.1 INTRODUCTION

After development of the method to induce ice nucleation (see section III.3) in a laboratory scale freeze-dryer, we wanted to find out if the method is also scalable to larger freeze-dryers. We got access to use a pilot scale freeze-dryer with 2.5 m² shelf area.

III.4.2 MATERIALS AND METHODS

III.4.2.1 PREPARATION AND FILLING OF 5 % SUCROSE

Sucrose (Suedzucker, AG, Mannheim, Germany) was dissolved in highly-purified water and filtered using a 0.2 µm PVDF sterile filter (Steritop, Merck Millipore, Darmstadt, Germany). An Inova VFVM 3031S (Optima Pharma, Schwaebisch Hall, Germany) was used to fill either 3 ml of the sucrose solution in 10R Vials or 1 ml in DIN 2R vials (Schott, Mainz, Germany). 1540 vials (10R) and 3540 vials (2R) were prepared, resulting in a load of approximately 10 l. Approximately one third of each vial type was used without stopper, the rest was semi-stoppered with lyophilization stoppers (West Pharmaceuticals, Lionville, PA, USA).

III.4.2.2 LOADING OF THE FREEZE-DRIER AND INDUCTION OF ICE NUCLEATION

The vials were loaded into a pilot-scale freeze-drier (Hof Sonderanlagen, Lohra, Germany) with a shelf area of 2.5 m² and a condenser capacity of 30 kg and were equilibrated at 1 °C overnight. Before nucleation, the shelf temperature was reduced to -5 °C to obtain approximately the same product temperature. The product temperature was monitored using built-in PT100 temperature probes. On each of the 4 shelves, one thermocouple was placed into a vial without stopper. Table III-3 shows the loading of the freeze-dryer shelves with the different types of vials as well as the placement of the temperature probes.

Table III-3: Schematics of loading of the freeze-dryer with two different vial types and use of stopper. TP=temperature probe was used in one vial of this tray. The cell values indicate tray number / vial type (2R, 10R) / use of stopper (yes, no).

Shelf	Pos.	left	middle	right
1	back	1 / 2R / yes	12 / 2R / no / TP 1	4 / 2R / yes
	front	2 / 2R / yes	3 / 2R / yes	11 / 2R / yes
2	back	5 / 2R / yes	7 / 2R / yes	6 / 2R / yes
	front	8 / 2R / yes	13 / 2R / no / TP 2	10 / 2R / yes (3 rows no)
3	back	2 / 10R / yes	3 / 10R / yes	5 / 10R / yes
	front	1 / 10R / yes	11 / 10R / no / TP3	6 / 10R / yes
4	back	7 / 10R / yes	4 / 10R / yes	9 / 10R / no / TP4
	front	8 / 10R / yes/no (50:50)	14 / 2R / no, not full	10 / 10R / no

Ice nucleation was induced by evacuation of the product and condenser chamber to 6.44 mbar which took approximately 10 minutes followed by re-pressurization via the cold condenser, which had a temperature of -58.4 °C and -50.6 °C, measured at two different positions. The product chamber was monitored using a Samsung NX100 digital camera and the condenser chamber was monitored using a Logitech Quickcam Pro 9000. After induction of nucleation, the vials were allowed to stand for additional 15 minutes on the lyophilizer shelves before unloading. After unloading, each tray was analysed visually and a picture was taken of the vial bottom by placing each tray on a transparent acrylic glass pane.

III.4.3 RESULTS

III.4.3.1 INDUCTION OF NUCLEATION

After incubation of the samples over night at 1 °C, water condensed in the chamber which froze on the shelves when those were cooled to -5 °C. It was also observed that the vials without stoppers froze whereas only few samples with stoppers froze when they were equilibrated at -5 °C. In previous experiments, when only a partial load of the freeze-drier was employed, we found that a vacuum set-point of 3.7 mbar was a good compromise between product temperature drop and high success rates of the method. However, with a full load in the pilot scale freeze-drier, this set-point could not be reached within a short period of time, indicating massive generation of water vapour in the product chamber. Thus, re-pressurization

was performed at 6.44 mbar. The videos showed a dense ice fog with many small ice crystals for a period of approximately 4 seconds. Snapshots of the videos from condenser and product chamber are shown in Figure III-8 and Figure III-10.

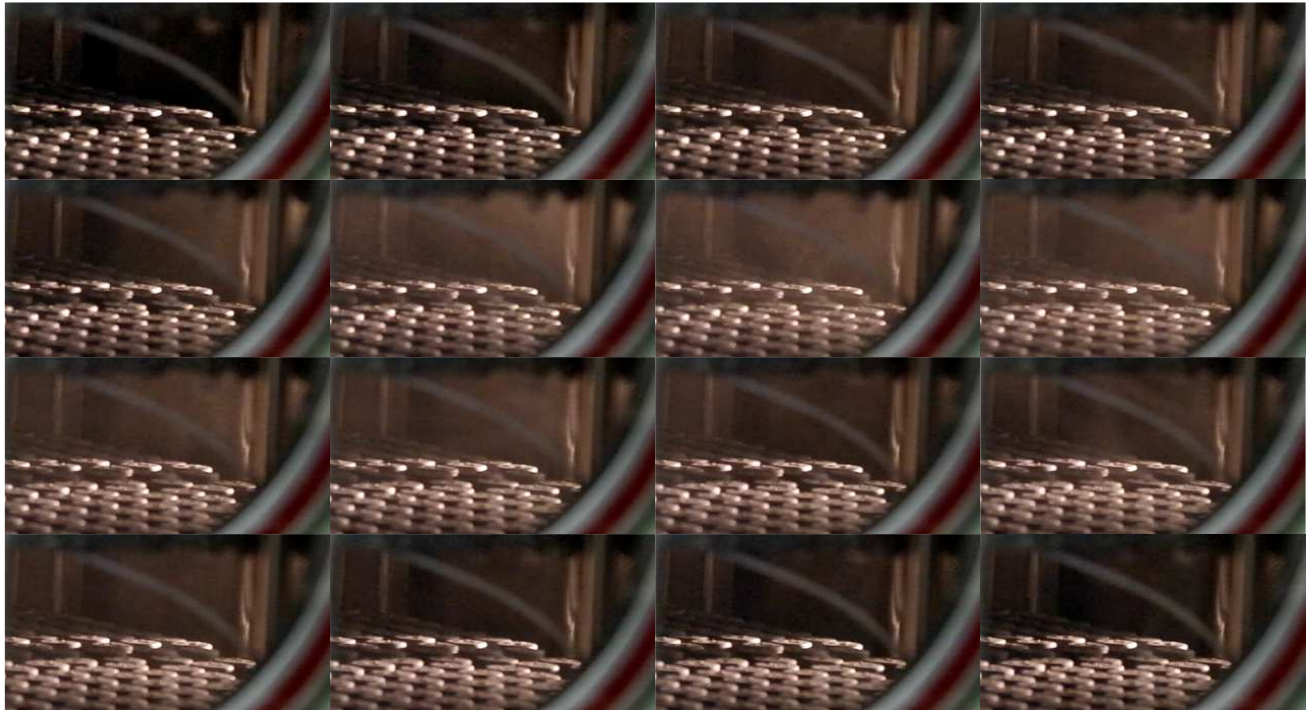


Figure III-8: Snapshots of the video taken from the product chamber. A very fine, dense ice fog is observable immediately after re-pressurization. The images represent a total time of approximately 4 seconds.

The thermocouples employed to monitor product temperature showed that ice nucleation was successful, as shown in Figure III-9. However, thermocouple 3 showed earlier freezing during equilibration and is therefore not shown in the figure. The other sensors 1, 2 and 4 showed nucleation during the ice nucleation procedure. Usually, no nucleation takes place during equilibration at $-5\text{ }^{\circ}\text{C}$, this may be due to different particle loads of the non-washed vials employed or the presence of frozen water on the shelves.

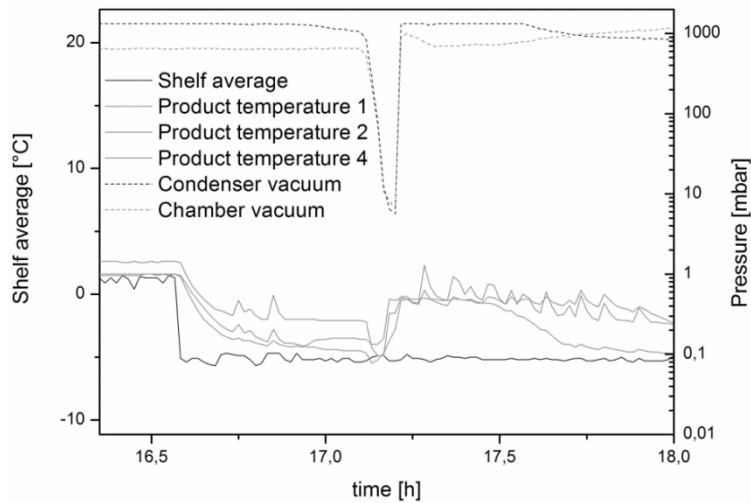


Figure III-9: Thermocouple and pressure traces of the nucleation induction in the pilot-scale freeze-dryer. The increase in product temperature simultaneous with pressure drop indicates ice nucleation.

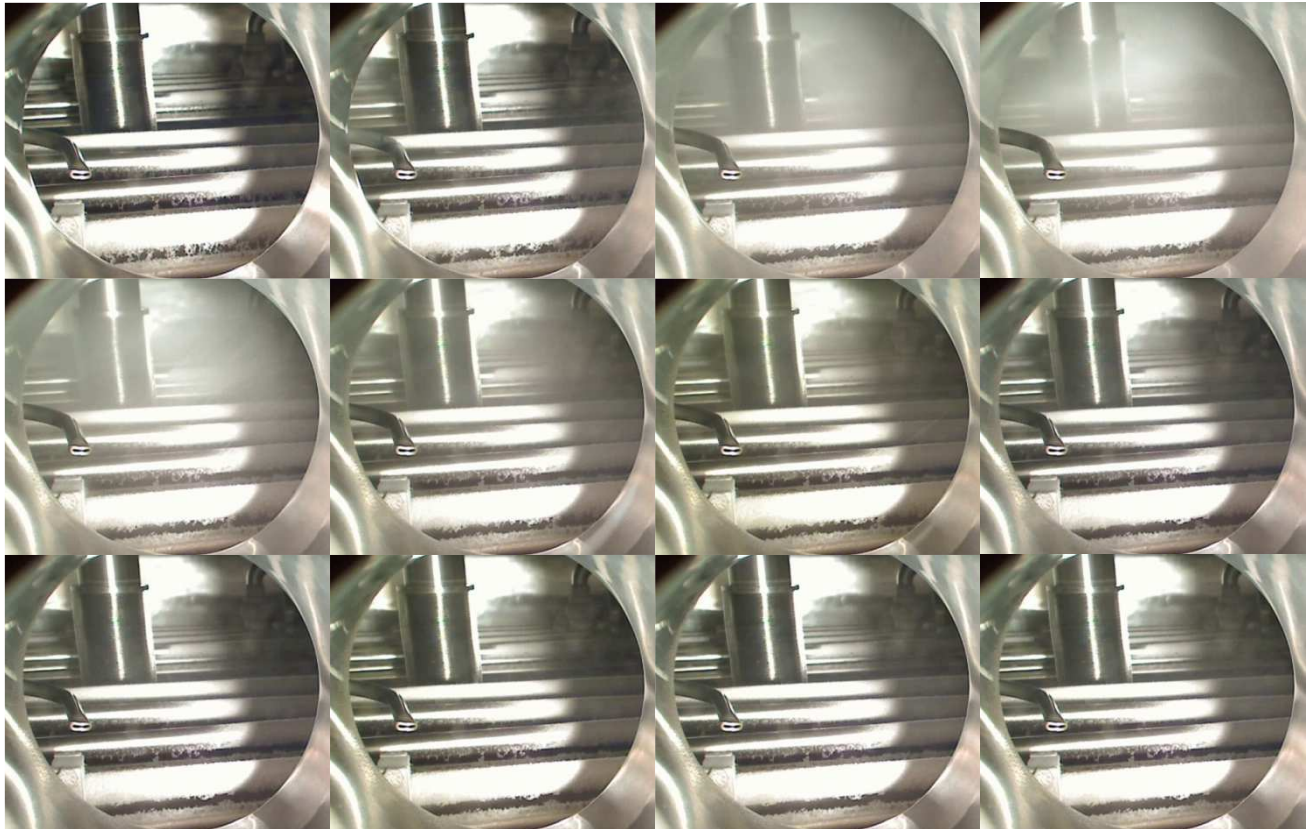


Figure III-10: Snapshots of the video taken from the condenser. At the time of re-pressurization, a fine and dense ice fog is visible which is blown upwards into the product chamber. The ice fog is visible for approximately 2 seconds.

III.4.3.2 SUCCESS OF NUCLEATION

All vials except 19 vials of the 2R type with stoppers from shelf 3 and 2 were frozen when they were unloaded from the freeze-dryer. Vials, which are nucleated with the method employed, usually show turbidity due to ice crystals formed but the appearance of the surface of the ice/water mixture is almost the same as in solution. It could be observed that, especially with

the larger 10R vials without stoppers which froze earlier, a defective ice structure was formed due the vacuum pull down, as shown in Figure III-11. Some of the 10R vials with stoppers also froze earlier, and a defective ice structure could be observed. In tray 4, only 5 of 170 vials (appr. 3 %) and in tray, 14 of 172 vials (appr. 8 %) showed this defective ice structure. For the 2R vials, almost all vials looked the same with no defective ice structures, indicating that probably all of the vials were nucleated with the method and did not freeze before or during the vacuum pull down. A representative picture of those vials is shown in Figure III-12.



Figure III-11: Normal ice structure in 10R vials (left) and defective ice structure of the vials which were frozen before vacuum pull down (right).



Figure III-12: Ice structure of DIN 2R vials with and without stoppers after ice nucleation.

III.4.4 DISCUSSION AND OUTLOOK

We experienced some problems with earlier freezing of the vials during equilibration which was unexpected because usually, no ice nucleation is observable during equilibration at this rather high temperature. However, ice nucleation temperature can be increased by higher amount of particles present in the solution. Possible reason for earlier nucleation of the vials may be the use of non-washed vials, particles present in sucrose solution after filling in a non-classified environment and transferral to the freeze-dryer. However, these sources of contamination can easily be excluded in class A clean rooms and no pre-nucleation is expected to be observable in those environments. These already nucleated vials showed a defective ice structure when the pressure was reduced to induce nucleation. Nevertheless, we could determine visually that only a small fraction of vials were frozen earlier and also most of the vials containing temperature probes did not nucleate during equilibration. Our results show that the method developed with lab-scale freeze-dryers (Martin Christ Epsilon 2-6D, 0.21 m² shelf area and SP Scientific Lyostar 3, 0.43 m² shelf area) is also transferrable to a larger pilot-scale freeze-dryer with a shelf area of 2.5 m². We observed that, for a fully-loaded freeze-dryer, the vacuum set-point to generate enough water vapour in the chamber can be set higher than for partial loads. On the one hand, a higher vacuum set-point is beneficial to avoid boiling or puff-off of the liquid, on the other hand, for partial loads, the vacuum set-point needs to be determined depending on load of the freeze-dryer. With the fully-loaded freeze-dryer and the vacuum set-point of 6.44, we were able to create a very dense ice fog, which is important because in every vial at least one ice crystal has to be blown to induce ice nucleation. Furthermore, we also confirmed that, also with a slightly higher condenser temperature of approximately -54 °C, our method can be used. We therefore propose that, if not only shelf area is scaled but also other dimensions of the freeze-dryer, especially vacuum pull down rate, re-pressurization gas flow, ventilation cross-sections and valve sizes, our method may be used also in those larger freeze-dryers. Since the condenser chamber of those freeze-dryers is also cleaned and steam sterilized using the same CIP/SIP system as the product chamber and the ventilation gas is the same as used for backfill of the chamber after freeze-drying, we do not expect difficulties regarding sterility of the nucleated samples.

III.5 FREEZE-THAW STUDIES OF A MONOCLONAL ANTIBODY

III.5.1 INTRODUCTION

One of the stresses involved in freeze-drying is the generation of an ice-liquid interface which is transferred to an ice-glass interface. It is long known that proteins can denature at this interface during freezing and it is also known that, by increasing this interface, more protein can degrade (e.g. [1]). Controlled ice nucleation is known to change SSA and pore sizes, therefore also ice-liquid interfaces are expected to be changed. Hence, controlled nucleation can be a valuable tool to check protein degradation at these interfaces, since controlled ice nucleation allows not only selection of the nucleation temperature but also the post-nucleation hold time. In this study, the impact of different nucleation temperatures and post-nucleation temperatures on the stability of the model protein MabR1 was investigated. MabR1 was formulated at 1 mg/ml and 1.0 % Sucrose was added as a cryoprotectant. As controls, also formulations containing 0.6 % HP β CD and 0.004 % PS80 were added, because they already showed to protect MabR1 from interfacial degradation.

III.5.2 MATERIALS AND METHODS

III.5.2.1 MATERIALS

A monoclonal antibody MabR1 was used as a model protein because it is sensitive to freezing-associated stresses. The antibody was formulated in a 10.5 mM sodium-phosphate buffer at pH=6.4. Sodium phosphate monobasic and dibasic were bought from Merck, Darmstadt, Germany or Applichem, Darmstadt, Germany; Sodium chloride was purchased from BDH Problao (VWR, Ismaning, Germany) and sucrose was kindly provided from Suedzucker, Plattling, Germany. Polysorbate 80 was obtained from Sigma Aldrich Chemicals. Hydroxypropyl-beta-cyclodextrin (Cavasol HP Pharma) was kindly provided by Wacker Chemie AG, München, Germany. All chemicals were of analytical grade.

III.5.2.2 PREPARATION OF FORMULATIONS

Formulations were prepared by mixing concentrated stock solutions of excipients and protein and final dilution with buffer. For Sucrose, HP β CD, 10 % solutions were prepared and for polysorbate 80, a 1 % (w/v) solution was used. The final solutions were filtered through 0.22 μ m PVDF filters (Pall Acrodisc) which were pre-rinsed with at least 5 ml of buffer to remove extractables, particularly surfactant residuals. 2.3 ml of filtered solutions were pipetted into DIN 6R vials which were semi-stoppered and transferred to the freeze-dryer.

III.5.2.3 INDUCTION OF ICE NUCLEATION AND THAWING EXPERIMENT

The experiments were performed in an FTS Lyostar 2 (SP Scientific, Stone Ridge, NY, USA). The vials were loaded into the freeze-drier and equilibrated to the desired product temperature and ice nucleation was induced with our published method [2]. Due to only a small amount of samples which were subjected to the nucleation procedure, the condenser had to be pre-loaded with 10 ml of high-purified water. Subsequently, the freeze-drier was depressurized to 3.7 mbar and re-pressurized via the cold condenser. The samples were held for the desired amount of time at the shelf temperature and after that time span, the shelf temperature was reduced to -50 °C with a ramp speed of 2 °C/min. Samples were equilibrated for at least 1 h at -50 °C and then thawed in a water bath of 25 °C.

III.5.2.4 TURBIDITY

The turbidity of samples was measured using a Hach Lange Nephla nephelometer (Hach Lange GmbH, Düsseldorf, Germany). Scattered light of $\lambda = 860$ nm laser is detected at an angle of 90 ° and the result is given in FNU (Formazine nephelometric units). 1.9 ml were pipetted in pre-rinsed turbidity glass cuvettes with a flat bottom and placed into the device. Measurement was performed twice with a 90 ° turn between measurements.

III.5.2.5 LIGHT OBSCURATION

Subvisible particles were determined using a PAMAS SVSS-35 particle counter (PAMAS - Partikelmess- und Analysesysteme GmbH, Rutesheim, Germany) equipped with an HCB-LD-25/25 sensor which has a detection limit of approximately 120,000 particles > 1 μm per ml. The rinsing volume was 0.5 ml and was followed by three measurements of 0.3 ml. Before each measurement, the system was rinsed with highly purified water until the total particle concentration was less than 100 per ml and no particles larger than 10 μm were present in the measurement cell. The samples were analyzed in the turbidity cuvettes. Data collection was done using PAMAS PMA software and particle diameters in the range of >1 μm to 200 μm were determined. All results are given in cumulative particles per milliliter.

III.5.2.6 ASYMMETRICAL FLOW-FIELD-FLOW FRACTIONATION (AF4)

An orthogonal method to size exclusion chromatography is asymmetrical flow-field-flow fractionation. Protein fragments, monomer as well as higher molecular aggregates are separated by a liquid cross flow combined with a parabolic channel flow. A Postnova AF2000 system (Postnova GmbH, Landsberg am Lech, Germany) was used for separation equipped with a PN 1122 pump, a PN 5300 autosampler. A Shimadzu SPD 10 UV detector was used to monitor protein absorption at $\lambda = 280$ nm. Furthermore, the system is equipped with a PN 3150 refractive index detector and a PN 3620 or a Wyatt miniDawn MALLS detector. A spacer of

500 μm was used. For MabR1, A buffer with 10 mM sodium phosphate and 150 mM sodium chloride was used. Approximately 30 μg were injected into the separation channel equipped with a regenerated cellulose membrane (RC) with a cut off of 10 kDa and focused for 4 min with an injection flow of 0.2 ml/min and a cross flow of 2.0 ml/min. Subsequently, protein species were separated with a constant cross-flow of 2.0 ml/min and a detector flow of 1.0 ml/min for 25 minutes. The cross flow is reduced to 0 ml/min within 5 minutes and elution is continued for additional 20 minutes at a detector flow of 1.0 ml/min.

III.5.3 RESULTS

III.5.3.1 SUBVISIBLE PARTICLES AND TURBIDITY

The nucleation temperature T_n and also the isothermal hold time post-nucleation had an impact on subvisible particle formation and turbidity of MabR1. Subvisible particles and turbidity increased with decreasing nucleation temperature from -4°C and -6°C to -10°C and decreased with prolonged isothermal hold from 5 minutes to 2h. When polysorbate 80 or HP β CD was added, no increase in subvisible particles and turbidity was observed. The ramp frozen MabR1 showed the highest amount of subvisible particles and turbidity, as shown in Figure III-13.

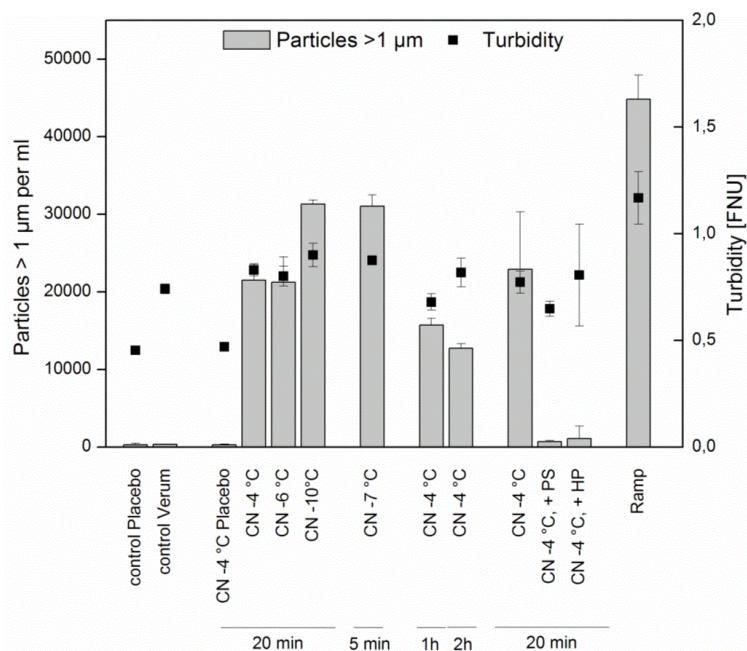


Figure III-13: Results from light obscuration and turbidity for nucleation experiments of MabR1 formulated with sucrose. The $^\circ\text{C}$ value indicates the nucleation temperature and the time span indicates post-nucleation isothermal hold.

III.5.3.2 ASYMMETRICAL FLOW-FIELD-FLOW FRACTIONATION

It was further checked if the various freezing protocols had an impact on the relative amount of protein species, which were detected with AF4. As shown in Figure III-14, only minor changes were detectable for protein species as detected with AF4 for MabR1.

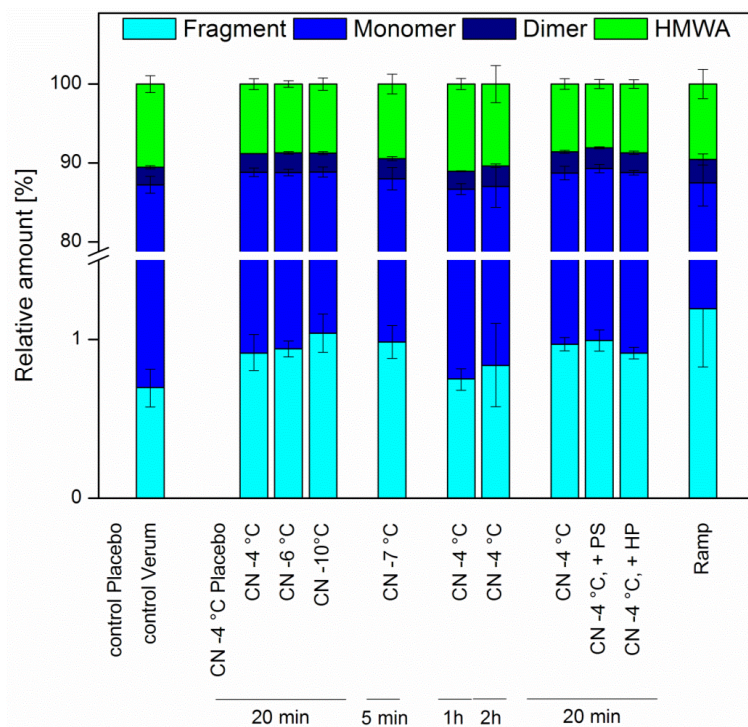


Figure III-14: Results from AF4 for nucleation experiments of MabR1 formulated with sucrose.

III.5.4 DISCUSSION

Since both, nucleation temperature and isothermal hold time, had a small influence on subvisible particle concentrations, controlled nucleation may be a valuable tool to study protein aggregation at the ice-liquid interface. While the nucleation temperature influences ice crystal size and distribution, the rate of ice crystal growth, influenced by the shelf temperature and hold time, seems also to affect protein degradation. Furthermore, the long isothermal hold post-nucleation also allows Ostwald ripening of ice crystals. Interestingly, the slower the ice crystal growth, the lower the subvisible particles were. These findings suggest that protein unfolding takes place at the end, when crystal growth is complete and the amount is determined by final interface area. However, it has to be further investigated if a freezing procedure, at which the protein is held for a long period of time at a high temperature above T_g' is negatively influencing protein stability with respect to physical and chemical degradation.

III.5.5 REFERENCES

1. Webb, S.D., et al., *Surface adsorption of recombinant human interferon-gamma in lyophilized and spray-lyophilized formulations*. *Journal of Pharmaceutical Sciences*, 2002. 91(6): p. 1474-1487.
2. Geidobler, R., S. Mannschedel, and G. Winter, *A new approach to achieve controlled ice nucleation of supercooled solutions during the freezing step in freeze-drying*. *Journal of Pharmaceutical Sciences*, 2012. 101(12): p. 4409-4413.

III.6 INFLUENCE OF THE FREEZING STEP ON THE PROPERTIES OF TWO PLACEBO MODEL FORMULATIONS

III.6.1 INTRODUCTION

As stated in the literature, the ice nucleation temperature is the most important parameter influencing ice crystal size, primary drying time and product quality attributes like residual moisture or specific surface area [1]. However, as observed in the previous chapter, also the isothermal hold time post-nucleation has an impact on protein stability. This study was conducted to elucidate the influence of nucleation temperature and isothermal hold time on the specific surface area, residual moisture, solid state properties (amorphous vs. crystalline) and reconstitution time of two model formulations, 5 % Sucrose and 3.75 % Mannitol + 1.25 % Sucrose.

III.6.2 MATERIALS AND METHODS

III.6.2.1 MATERIALS

Sucrose was kindly provided by Suedzucker (Suedzucker, Plattling, Germany) and Mannitol was purchased from Boehringer Ingelheim (Ingelheim am Rhein, Germany).

III.6.2.2 PREPARATION OF FORMULATIONS

5 % Sucrose or 3.75 % Mannitol and 1.25 % Sucrose were dissolved in highly-purified water (USF Elga) and filtered through 0.22 µm celluloseacetate syringe filters (VWR, Ismaning, Germany). 2.3 ml of each formulation was transferred into DIN 6R vials (MGlas AG, Muennerstadt, Germany) and subjected to the different freezing variations.

III.6.2.3 INDUCTION OF ICE NUCLEATION AND FREEZE-DRYING PROCESS

The vials were equilibrated at the desired nucleation temperature and ice nucleation was induced using our previously published method [2]. Due to the small batch size of approximately 24 vials for each freezing procedure, the condenser was pre-loaded with water by spraying 10 ml of highly-purified water on the condenser coils before pulling of vacuum. The product temperature was monitored using Type T thermocouples (Newport electronics, Deckenpfronn, Germany) throughout the whole process. After induction of nucleation, the shelf temperature was held for various time spans and then cooled to -50 °C with 1 °C/min. Samples were unloaded from the freeze-drier using a pre-cooled shelf and transferred to a deep-freezer

with -80 °C on dry ice. Table III-4 shows the freezing procedures for both investigated formulations.

Table III-4: Freezing procedures for both formulations of 5 % Sucrose and 3.75 % Mannitol + 1.25 % Sucrose.

Nucleation temperature	Isothermal hold post-nucleation
-4	5 minutes / 30 minutes / 90 minutes
-7	5 minutes / 30 minutes / 90 minutes
-10	5 minutes / 30 minutes / 90 minutes
Ramp	1 °C/min
Ramp + Annealing	Increase of temperature to -19 °C; hold for 6 h; cool temperature to -50 °C

After all vials had been treated with the respective freezing procedure, they were transferred to the freeze-drier, a FTS Lyostar 3. Primary drying was carried out at a pressure of 0.067 mbar and a shelf temperature of -27 °C. These rather conservative drying conditions were chosen to avoid any changes in ice crystals or pore volume due to microcollapse in the samples during drying. After primary drying was finished, the shelf temperature was increased to 30 °C with a ramp of 0.1 °C/min and this temperature was held for 6 h.

III.6.2.4 RESIDUAL MOISTURE

To determine residual moisture of collapsed freeze-dried and spray-dried samples, the Karl-Fischer direct injection method with methanol was used. Between 10 and 50 mg of sample aliquots were prepared in a glove box with a relative humidity of less than 10 %, filled into DIN 2R Vials and crimped. Approximately 2.5 ml of methanol with very low water content was added to the sample for extraction of water. Subsequently, the sample was placed in an ultrasonic bath for 10 minutes. An aliquot of 1 ml was injected into a coulometric Karl Fischer titrator (737 KF Coulometer, Metrohm, Filderstadt, Germany). The results are calculated in relative water content (m/m).

III.6.2.5 SPECIFIC SURFACE AREA

Specific surface area of lyophilizates was determined using Brunauer-Emmet-Teller krypton gas adsorption in a liquid nitrogen bath at 77.3 K (Autosorb 1, Quantachrome, Odelzhausen, Germany). Samples were gently crushed with a spatula and weighed into glass tubes. Outgassing was performed at least for 2 h at room temperature and an outgassing test was performed before every measurement. An eleven point gas adsorption curve was measured,

covering a p/p_0 ratio of appr. 0.05 to 0.30. Data evaluation was performed according to the multipoint BET method fit of the Autosorb 1 software.

III.6.2.6 X-RAY POWDER DIFFRACTION

X-Ray diffraction (XRD) measurements of lyophilized powders were performed on a STOE powder diffractometer in transmission geometry (Cu $K\alpha_1$, $\lambda = 1.5406 \text{ \AA}$) equipped with a bent image plate detector. Samples were placed on a multi-sample holder on cellulose filter paper. A blank run was subtracted from every sample.

III.6.2.7 SCANNING ELECTRON MICROSCOPY

The lyophilized powder was gently crushed and placed on Leit-Tabs (Plano GmbH, Wetzlar, Germany), carbon sputtered under vacuum and visualized by a Joel JSM-6500F field emission scanning electron microscope (Joel Inc., Peabody, USA).

III.6.2.8 RECONSTITUTION TIME

Water was added to the lyophilized product and the time needed to obtain a clear solution was noted.

III.6.3 RESULTS

III.6.3.1 LYOPHILIZATION PROCESS

For the different formulations and freezing protocols, the product temperature (T_p) during steady-state sublimation was determined by thermocouples. The product temperature allows to qualitatively estimate the product resistance. A lower product resistance leads to higher sublimation rates and lower product temperatures. As shown in Table III-5, controlled nucleation at any temperature lead to slightly lower product temperatures compared to ramp-frozen samples and ramp-frozen samples but annealed samples. This tendency is more pronounced for the sucrose formulations whereas with the mannitol-sucrose combinations, the differences were smaller. Furthermore, it can be observed, that an increase in post-nucleation hold time could further lower T_p . This is also more pronounced for the formulation of 5 % sucrose.

Table III-5: Product temperature (T_p) during steady state primary drying of both formulations for various freezing protocols.

Nucleation temperature [°C]	Isothermal hold post nucleation	T_p 5 % Sucrose	T_p 3.75 % Mannitol + 1.25 % Sucrose
-4	5	-40.8	-40.3
	30	-	-
	90	-42.0	-39.6
-7	5	-	-
	30	-39.8	-40.1
	90	-	-
-10	5	-40.5	-40.3
	30	-40.5	-40.5
	90	-42.5	-41.3
Ramp		-37.5	-39.1
Ramp + Annealing		-38.0	-39.7

III.6.3.2 X-RAY POWDER DIFFRACTION

As shown in Figure III-15, 5 % sucrose remained fully amorphous with no peaks in x-ray diffractogram, independent of freezing protocol. In contrast, the mannitol-sucrose combinations showed distinct peaks in the diffractograms, independent on freezing procedure,

which indicates crystallization of mannitol (see Figure III-16). The sample which was nucleated at a product temperature of $-10\text{ }^{\circ}\text{C}$ and held for 5 minutes (orange line) showed peaks at 9.6 and $17.9\text{ }^{\circ}2\text{-theta}$ which both can be attributed to mannitol hydrate [3]. The other formulations showed distinct peaks at 9.7 and 20.4 but no peaks at 9.6 and only a very small peak at $17.9\text{ }^{\circ}2\text{-theta}$. These results suggest that in most cases, δ -mannitol is the predominant form, but small amounts of mannitol-hydrate are still present.

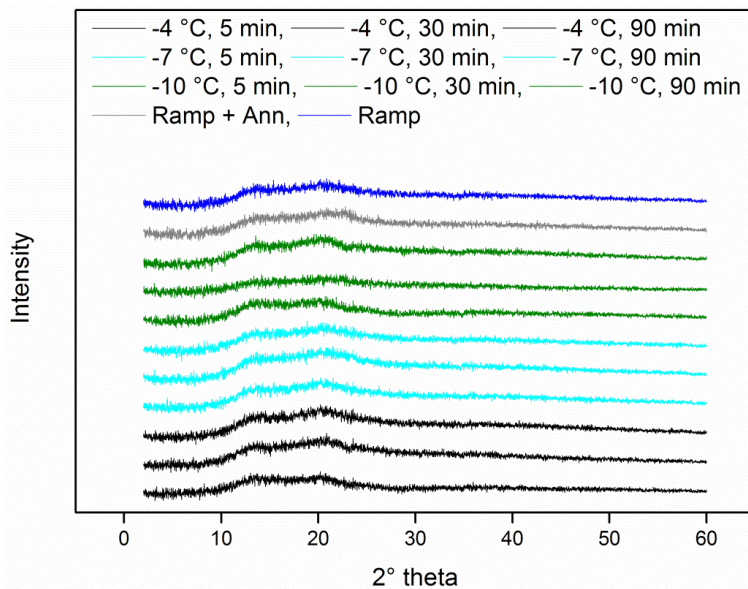


Figure III-15: X-ray-powder diffraction patterns for 5 % Sucrose formulations.

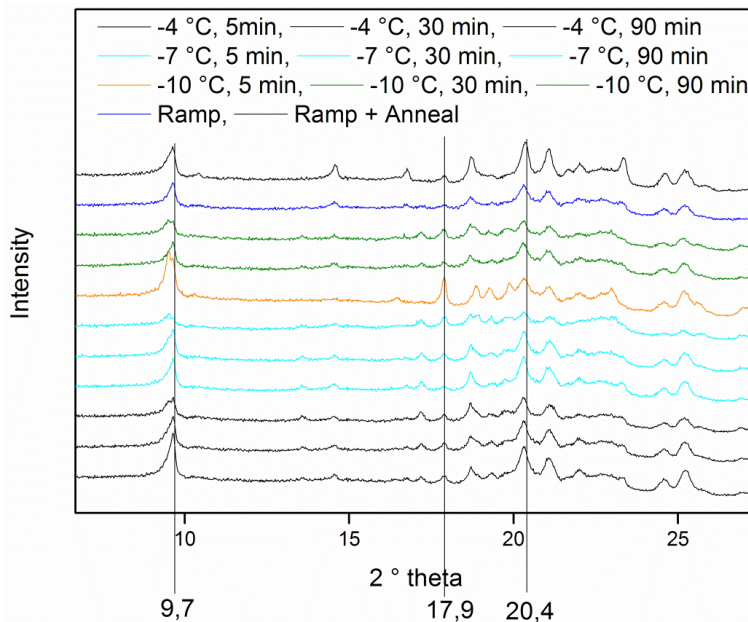


Figure III-16: X-ray-powder diffraction patterns for Mannitol-Sucrose formulations.

III.6.3.3 SPECIFIC SURFACE AREA AND RESIDUAL MOISTURE

Figure III-17 shows the specific surface area (SSA) and residual moisture of the 5 % Sucrose formulation with the different freezing protocols. Different SSAs and residual moistures were obtained for the freezing protocols; however, some combinations of nucleation temperature and isothermal hold post-nucleation lead to similar residual moisture values and SSAs. In general, SSAs were lower for all controlled-nucleation samples compared to ramp-frozen samples and ramp-frozen and annealed samples. A trend to lower SSAs and higher residual moistures could be observed for one nucleation temperature and increasing hold time. This is true for all nucleation temperatures; however, with decreasing nucleation temperatures, higher SSAs and lower residual moistures were obtained. Consequently, the lowest SSA obtainable was with the highest nucleation temperature of -4 °C and the longest hold time of 90 min. Ramp frozen samples, with or without annealing, showed the highest SSAs, however, the annealed samples showed slightly higher residual moistures.

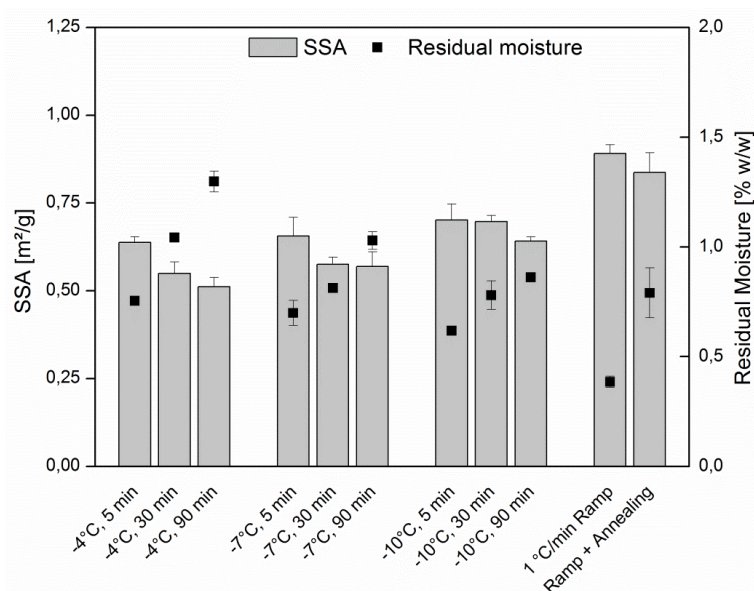


Figure III-17: Specific surface area and residual moisture for 5 % Sucrose formulations and the performed freezing protocols.

A different picture was obtained for the combination of Mannitol and Sucrose. While SSAs were in general higher than with the sucrose formulation, standard deviations for SSA and residual moisture were quite high for those formulations and trends were not easily visible. Controlled nucleation lead to slightly smaller SSAs than ramp or ramp followed by annealing. The results imply that by crystallization of mannitol, some of the effects of controlled nucleation can be mitigated. At least, homogeneity of those samples as indicated by standard deviations is not as good as with the fully amorphous sucrose formulation.

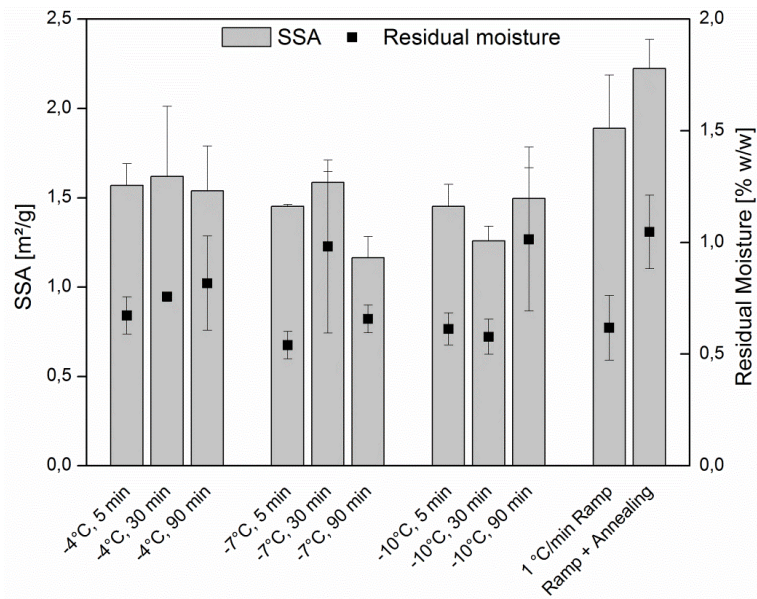


Figure III-18: Specific surface area and residual moisture for 3.75 % Mannitol + 1.25 % Sucrose formulations and various freezing protocols.

III.6.3.4 SCANNING ELECTRON MICROSCOPY

Differences in scanning electron microscopy were observed for both samples and freezing protocols. Whereas with both formulations, small pores and a quite dense structure was observed for ramp frozen as well as ramp frozen and annealed samples, the samples which were nucleated at higher temperatures showed bigger pores. This was most pronounced for the amorphous samples of sucrose, as shown in Figure III-19. Figure III-20 shows SEM-pictures of Mannitol/Sucrose mixtures. Differences in pore sizes of ramp frozen and controlled nucleated samples are also visible, however, these differences were less pronounced than with sucrose based formulations, further indicating that, by mannitol crystallization, the impact of freezing protocol is slightly mitigated.

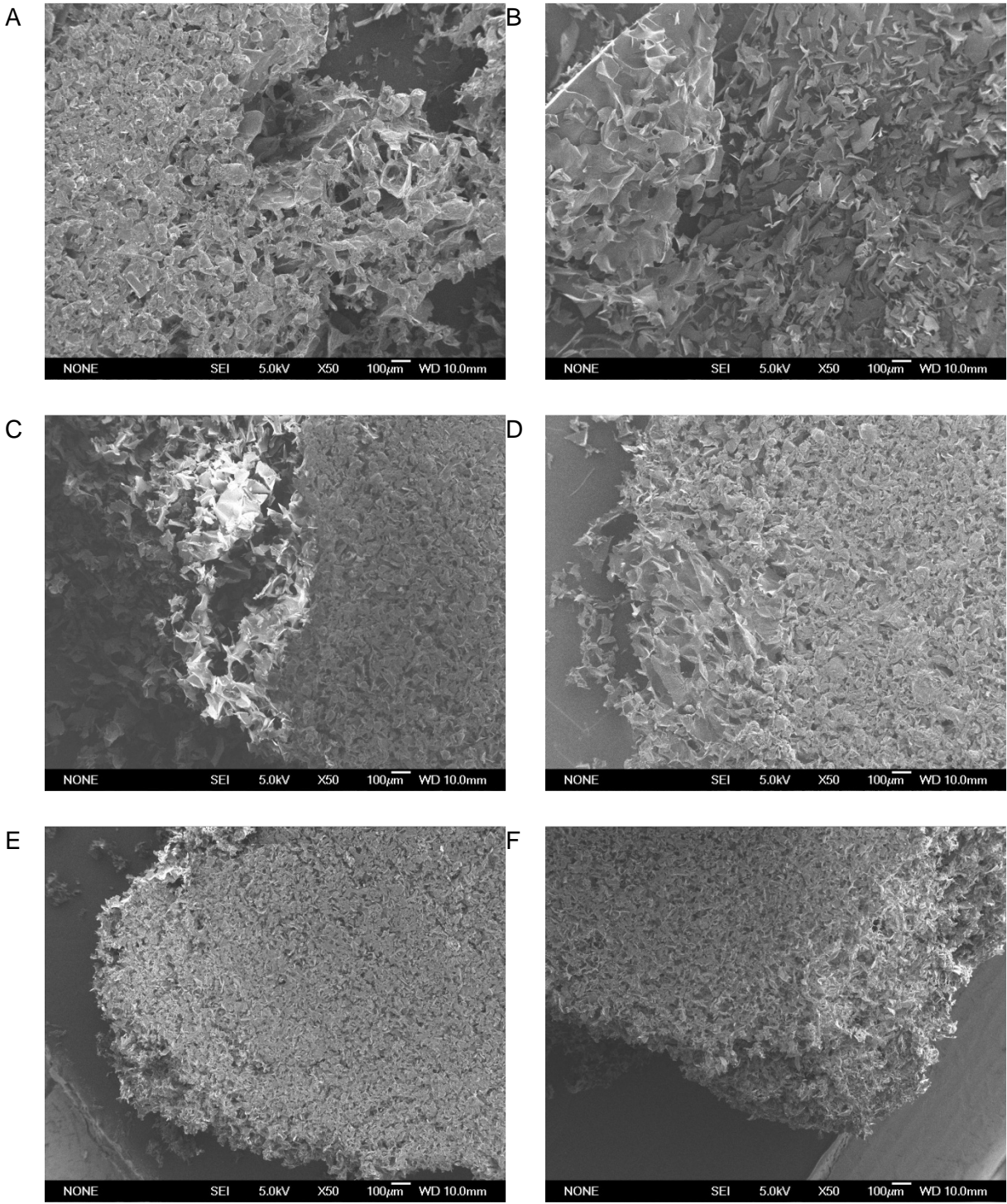


Figure III-19: SEM pictures of various sucrose samples. All pictures were taken with a magnification of 50 x. -4 °C, 5min (A); -4 °C, 90 min (B); -10 °C, 5 min (C); -10 °C, 30 min (D); Ramp-frozen (E); Ramp + Annealing (F).

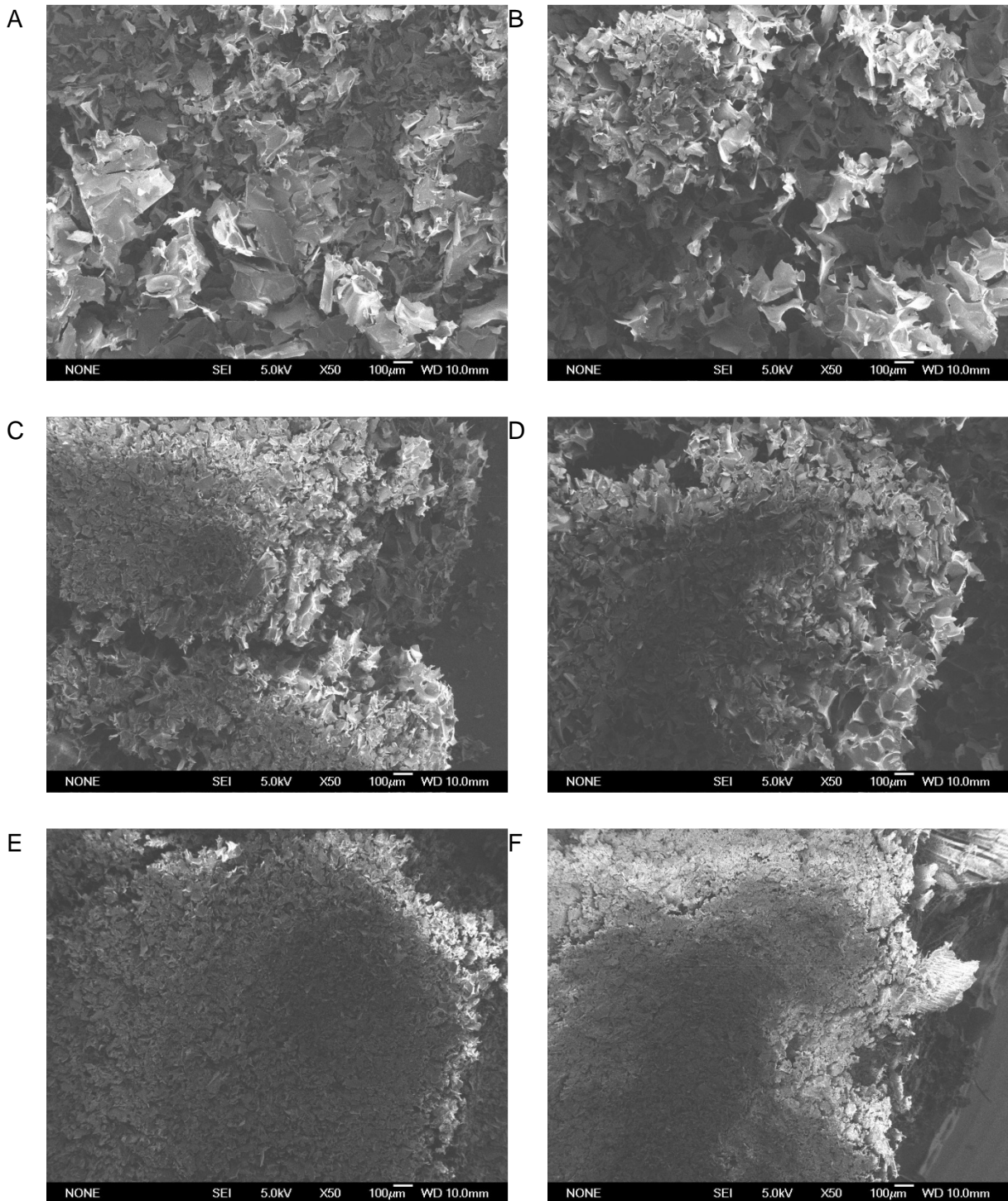


Figure III-20: SEM pictures of various mannitol/sucrose samples. All pictures were taken with a magnification of 50 x. -4 °C, 5 min (A); -4 °C, 90 min (B); -10 °C, 5 min (C); -10 °C, 90 min (D); Ramp-frozen (E); Ramp + Annealing (F).

III.6.3.5 RECONSTITUTION TIME

All samples were fully reconstituted within 10 seconds and no differences between the samples were observable. The changes in SSA generated by controlled nucleation did not, at least not in this scale, influence reconstitution time.

III.6.4 DISCUSSION

As observed, both, the ice nucleation temperature and the isothermal hold time had an influence on SSA and residual moisture as well as on crystallinity of the solid. The Mannitol/Sucrose mixture, with crystalline mannitol and amorphous sucrose showed bigger standard deviations than the fully amorphous formulation of sucrose. Furthermore, during the freezing process as conducted in our study, mannitol hydrate was obtained, which is usually avoided in freeze-drying [3]. Neither T_n nor isothermal hold time had an influence on reconstitution times. No evidence of increased homogeneity of controlled nucleated samples was observed compared to ramp frozen samples.

III.6.5 CONCLUSION

By making use of controlled ice nucleation, not only the ice nucleation temperature can be selected but also the post-nucleation hold time, if desired, can be controlled as well as the ramp post nucleation. In this study, the impact of the post-nucleation hold time was investigated for two model formulations, 5% Sucrose and a mixture of mannitol and sucrose 3:1 with 5 % solids in total. It was found that for sucrose a long post nucleation hold time further decreased SSA compared to a short period, possibly by fostering Ostwald ripening of ice crystals. Basically, this trend was observed for all nucleation temperatures studied. For the mannitol mixtures, no distinct correlations were observed, indicating that mannitol crystallization somehow interferes with ice crystallisation. To our knowledge, this is the first study which shows that also the post-nucleation hold time can influence the final product quality attributes and not only the ice nucleation temperature itself, which is often stated in literature. However, as stated in section III.5, freeze-concentration takes place after nucleation and an API must withstand this stress if a long post-nucleation isothermal hold is desired.

III.6.6 REFERENCES

III.7 CAN CONTROLLED ICE NUCLEATION IMPROVE FREEZE-DRYING OF HIGHLY-CONCENTRATED PROTEIN FORMULATIONS?⁴

⁴ This section was published as R. Geidobler, I. Konrad and G. Winter, Can Controlled Ice Nucleation Improve Freeze-Drying of Highly-Concentrated Protein Formulations? *Journal of Pharmaceutical Sciences*, 2013. The text was written by R. Geidobler and was corrected for publication in the journal by I. Konrad and G. Winter. The lab-work was shared between R. Geidobler and I. Konrad.

III.7.1 INTRODUCTION

Controlled ice nucleation in the field of freeze-drying has become of major interest in the scientific and industrial community because of the recent advancements of methods [2, 4-6] and the ability to control the ice nucleation temperature, T_n . The ice nucleation temperature affects the average ice crystal size and distribution; higher nucleation temperatures lead to larger ice crystals [7]. During sublimation, these large ice crystals generate large pores which reduce the water vapour resistance of the cake, also called product resistance, R_p [8]. Hence, primary drying times are greatly reduced with high nucleation temperatures [1]. Furthermore, the ice nucleation temperature interrelated ice crystal size not only influences primary drying times but affects also other product quality attributes, for example residual moisture and specific surface area [9].

Some freeze-dried protein pharmaceuticals, especially monoclonal antibodies, require administration of high doses > 100 mg [10]. These APIs are usually formulated at high concentrations and will be freeze-dried if an acceptable shelf-life time cannot be achieved with a liquid formulation. Freeze-drying has also been used as a simple method to create even higher concentrated antibody solution by reconstituting the lyophilized cake in e.g. the half of the volume. Upon administration, a diluent is added and the lyophilized cake dissolves. One of the challenges of those highly-concentrated freeze-dried products is their comparable long reconstitution time [10] which can last for up to 1 hour, whereas lower concentrated formulations yield an injectable solution within less than 1 minute [11], even for collapsed lyophilizates [12].

Rehydration of a lyophilized cake includes the following steps: (1) wetting of the lyophilized cake with displacement of gas in pores, (2) hydration of the solid. These steps are expected to be influenced by product attributes, e.g. pore sizes and specific surface area [10].

The aim of our study was to use our previously developed method to induce ice nucleation in highly concentrated protein solutions. Furthermore, we want to study if controlled nucleation of highly concentrated protein formulations of bovine serum albumin and a monoclonal antibody also shows positive effects on primary drying time and on reconstitution time of these lyophilizates.

III.7.2 MATERIALS AND METHODS

III.7.2.1 MATERIALS AND PREPARATION OF FORMULATIONS

Bovine serum albumin (BSA) was purchased from Fluka chemicals (Sigma-Aldrich, Munich, Germany) as a lyophilized powder. A monoclonal antibody (mAb) was kindly provided by

Roche Diagnostics (Penzberg, Germany). Sucrose was kindly provided from Suedzucker (Suedzucker, Plattling, Germany). BSA was formulated at 10 mg/ml, 100 mg/ml and 193.9 mg/ml with 5% sucrose (w/v) in a 10 mM sodium-phosphate buffer, pH=7.4. The antibody was formulated in 20 mM histidine buffer with 5 % trehalose at a concentration of 10 mg/ml and 40 mM histidine buffer and 10 % trehalose at a concentration of 161.2 mg/ml, both at pH=5.4. The concentration of all formulations was checked after filtration through 0.22 µm PVDF membrane filters (Millipore, Schwalbach, Germany) using a Nanodrop 2000 UV photometer (Thermo Scientific, Wilmington, USA). 1.0 ml of all BSA formulations, 0.8 ml of the low-concentrated mAb and 0.370 ml of the high-concentrated mAb were filled in DIN 2R tubing vials (MGLas AG, Muennerstadt, Germany) and semi-stoppered with lyophilization stoppers (kindly provided by West Pharmaceuticals, Eschweiler, Germany). The vials were arranged on a lyophilization tray and surrounded with two rows of 5% (w/v) sucrose shielding vials.

III.7.2.2 FREEZING PROTOCOL AND FREEZE-DRYING PROCESS

The samples were subjected to one of the following freezing protocols in a FTS Lyostar 3 (SP Scientific, Stone Ridge, USA):

Controlled nucleation (CN): Controlled ice nucleation was performed as previously published by our group [2]. To increase water vapour amount in the chamber and condenser coils, a tray of 100 ml high-purified water was placed into the lyophilizer and in addition, 10 ml of water was sprayed on the condenser coils before triggering nucleation at a product temperature of -5 °C. After nucleation, the samples were thermally treated at -5 °C for 120 minutes. Complete solidification was achieved by ramping down to -60 °C with a ramp of 1°C/min. The product temperatures were monitored with type T thermocouples (Newport Electronics, Deckenpfronn, Germany).

Ramp-freezing (Ramp): The samples were equilibrated at 5 °C for 30 minutes followed by ramping down the shelf with 1°C/min to -60 °C.

Pre-cooled-shelf method (PCS): The freeze-dryer shelves were pre-cooled to -60 °C and the samples were placed on the cool shelves. The enormous temperature difference between liquid and shelf leads to nucleation of a small fraction of liquid at the bottom of each vial and crystallization proceeds from bottom up (directional solidification). Due to lack of material, this freezing method was not performed with the mAb formulation.

T-type thermocouples were used to determine primary drying times during the freeze-drying process which was carried out at a pressure of 0,066 mbar and a shelf temperature of -22 °C. These rather conservative process conditions with low product temperatures were chosen to avoid changing the ice crystal size and distribution by an aggressive drying process

with possible microcollapse of the amorphous samples. Secondary drying was carried out at 30 °C for 6h with a 0.1 °C/min ramp. After completion of secondary drying, samples were stoppered at approximately 700 mbar nitrogen atmosphere.

III.7.2.3 DETERMINATION OF RECONSTITUTION TIMES

For determination of reconstitution times, no generally accepted protocol is available. Therefore, we subjected the samples to one of the two protocols:

Setup 1: Add the desired amount of water with a pipette to the lyophilized cake and let the sample sit without agitation.

Setup 2: Add the desired amount of water to the lyophilized cake and put the vial on an orbital shaker (VWR, Ismaning, Germany) at a speed of 400 rpm.

The time until a clear solution was obtained was recorded as the reconstitution time.

III.7.2.4 RESIDUAL MOISTURE

To determine residual moisture of the high concentration samples, the Karl-Fischer direct injection method with methanol was used. Approximately 2.5 ml of anhydrous methanol was added to the sample for extraction of water. Subsequently, the sample was placed in an ultrasonic bath for 10 minutes. An aliquot of 1 ml was injected into a coulometric Karl Fischer titrator (737 KF Coulometer, Metrohm, Filderstadt, Germany). The results are calculated in relative water content (m/m).

III.7.2.5 SPECIFIC SURFACE AREA

Specific surface area of high-concentrated lyophilizates was determined using Brunauer-Emmet-Teller krypton gas adsorption in an liquid nitrogen bath at 77.3 K (Autosorb 1, Quantachrome, Odelzhausen, Germany). Approximately 100 mg to 200 mg of each sample was gently crushed with a spatula and weighed into glass tubes. Outgassing was performed at least for 2 h at room temperature and an outgassing test was performed before every measurement. An eleven point gas adsorption curve was measured, covering a p/p_0 ratio of appr. 0.05 to 0.30. Data evaluation was performed according to the multipoint BET method fit of the Autosorb 1 software.

III.7.3 RESULTS

III.7.3.1 LYOPHILIZATION PROCESS

Controlled ice nucleation at high product temperatures followed by a long isothermal hold post-nucleation has shown to yield the lowest achievable specific surface area (unpublished data by the authors). With a constant porosity of the freeze-dried cake, this freezing procedure results in large ice crystals and pores. Due to the resulting low product resistance, R_p , the product temperature during primary drying is slightly lower for the controlled nucleation samples compared to the other two sets of samples as shown in Figure III-21 and Table III-6. The differences in product temperatures become larger when higher concentrations of protein and excipient are employed. Furthermore, primary drying is finished earlier for the controlled-nucleated samples, as shown in Table III-6.

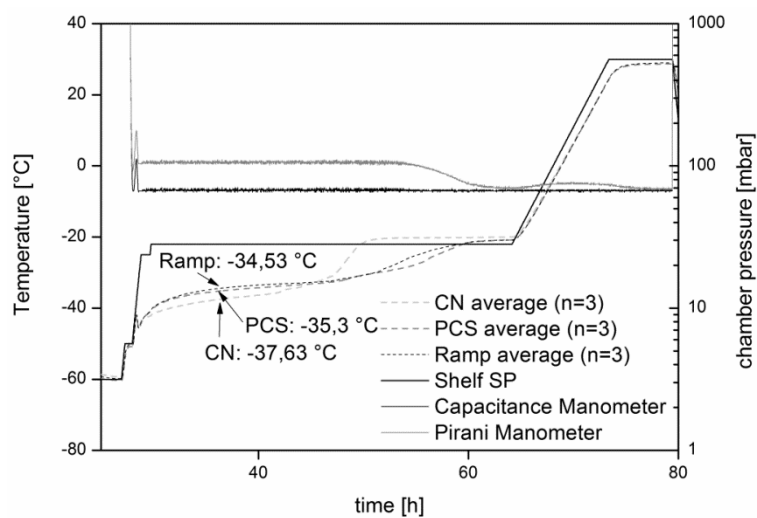


Figure III-21: Thermocouple and pressure readings from the freeze-drying run of samples with 100 mg/ml of BSA. The arrows indicate the product temperature at 7 h of primary drying. CN = controlled nucleation, PCS = pre-cooled shelf.

Table III-6: Product temperatures (Tp) and primary drying duration (d) of the three different freezing protocols for all protein concentrations.

	Controlled nucleation		Ramp freezing		Pre-cooled shelf	
	Product temperature (Tp)	Primary drying duration (d)*	Tp	d	Tp	d
BSA 10 mg/ml	-39.8 °C	23.4 h	-37.57 °C	27.6 h	-	-
BSA 100 mg/ml	-37.63 °C	25.0 h	-34.53 °C	34.5 h	-35.30 °C	34.5 h
BSA 193.9 mg/ml	-38.65 °C	24.2 h	-35.15 °C	32.6 h	-33.73 °C	32.6 h
mAb 10 mg/ml	-37.63 °C	22.9 h	-35,03 °C	27,6 h	-	-
mAb 161.2 mg/ml	-33.21 °C	20.0 h	-30.50 °C	25.0 h	-	-

*: Primary drying time was determined from thermocouple readings. Tp was determined after 7 h of primary drying.

III.7.3.2 SPECIFIC SURFACE AREA AND RESIDUAL MOISTURE

It was found that residual moisture depends mainly on specific surface area and drying temperature in the secondary drying step [13]. As expected, the controlled nucleated samples showed a significant lower specific surface area than the ramp frozen samples, which also translates into higher residual moistures after secondary drying. The pre-cooled shelf method leads to similar specific surface areas and residual moistures than the ramp freezing protocol, as shown in Figure III-22. This is true for both concentrations of BSA. All samples had residual moistures of less than 1 %. As expected, the controlled nucleated samples with the lower SSA have higher residual moistures (0.5-0.8 %) compared to the samples processed differently (0.2-0.4 %). Those small differences on an overall very low level are not considered to be relevant for stability and reconstitution time.

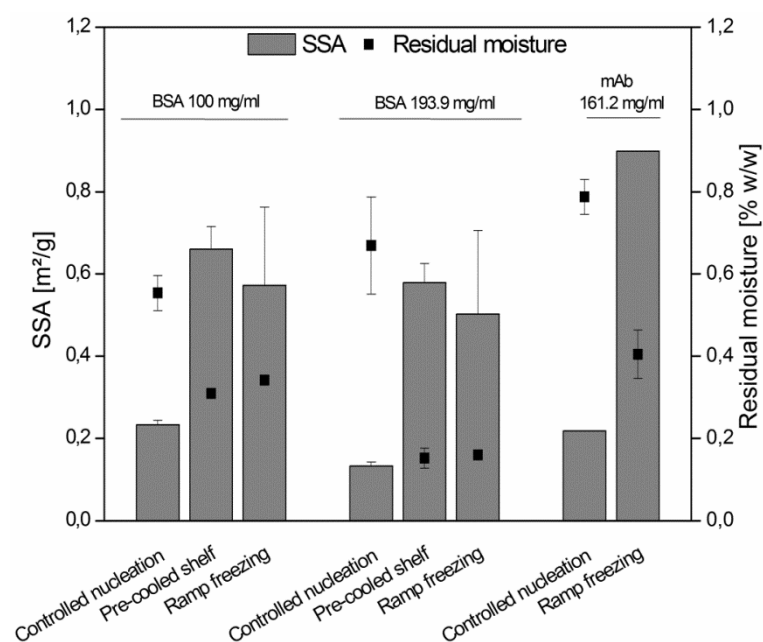


Figure III-22: Specific surface area and residual moisture for BSA at both concentration and the monoclonal antibody. All experiments were performed in triplicates except for the mAb formulation where SSA was $n=1$ and residual moisture was determined $n=2$.

III.7.3.3 RECONSTITUTION TIME AND BEHAVIOUR

For both proteins, no measurable difference was observed when they were formulated at 10 mg/ml and reconstitution was finished within 10 seconds. When BSA was formulated at 100 mg/ml, the reconstitution times were all below 10 minutes with a reconstitution volume of 0.91 ml and a clear impact of the freezing protocol was detectable, as shown in Figure III-23. Throughout all experiments, the samples which were nucleated at -5°C showed faster cake dissolution than the ramp frozen samples. Also, the pre-cooled shelf samples in average showed faster reconstitution times independent of the reconstitution protocol. It is also important to note that the controlled nucleated samples showed much less foaming during rehydration than the samples with the other two freezing protocols, which simplifies identification of complete dissolution. It can be speculated that larger pores are beneficial for gas displacement from the cake. Slightly different results were obtained with BSA at 193.9 mg/ml. When those samples were rehydrated with 0.80 ml of water and were subjected to reconstitution setup 2 with constant agitation, it was observed that the controlled nucleation cakes seemed to have a head start, indicated by a faster yellowing of the liquid, however, in the end, reconstitution were only slightly shorter with controlled nucleation and pre-cooled shelf than with ramp freezing. When the double amount of water was added to the lyophilized cakes, a distinct difference was observable between the different freezing protocols. Dissolution of controlled nucleated samples was almost two-fold faster than ramp frozen samples, and also pre-cooled shelf samples showed slightly shortened reconstitution times. Finally for the

monoclonal antibody, the controlled nucleation method lead to a remarkable and drastic reduction in reconstitution times compared to the ramp frozen samples.

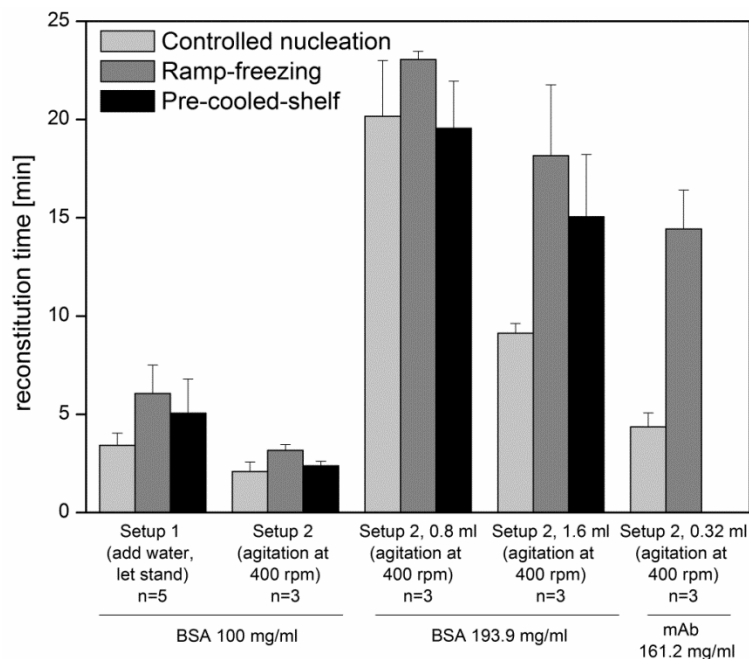


Figure III-23: Reconstitution times determined for the different freezing protocols and reconstitution setups for all formulations.

III.7.4 DISCUSSION AND OUTLOOK

With this study, we could show that controlled ice nucleation with our previously published simple method is also applicable to highly concentrated protein formulations. Our results show that controlled ice nucleation can speed up primary drying of high-concentrated protein formulations and can have a positive impact on reconstitution times of such lyophilizates. While the reduction of reconstitution times was observable already at 100 mg/ml of the model protein BSA, the absolute reduction in reconstitution times was approximately 2 minutes. At the high concentration of 193.9 mg/ml, the effect was only visible when 1.6 ml instead of 0.8 amount of water was added which results in a final concentration of approximately 120 mg/ml. For the antibody formulation, the reduction in reconstitution time was significant and a total reconstitution time of less than 5 minutes instead of 15 minutes was observed. As a consequence, it is proposed that controlled nucleation may improve wetting of the cake and displacement of gas due to the larger pores and therefore speeds up dissolution of the solid cake. However, if protein concentrations approach the solubility limit, hydration of protein molecules is the velocity-determining step and wetting of the cake becomes less important for complete dissolution. In this case, reconstitution times may not be affected much by the freezing protocol. The pre-cooled shelf method also showed a positive influence on reconstitution times for BSA but was inferior to controlled nucleation.

Controlled ice nucleation has the potential to become an even more important method in freeze-drying because of the applicability on highly-concentrated protein formulations. Furthermore, for these formulations, not only economic benefits are possible but also product quality with respect to reconstitution times can be improved. In a next step, controlled nucleation can be combined with aggressive short primary drying for highly-concentrated mAb solutions, leading most likely to drastic economic savings that go along not with compromised but even improved product features.

III.7.5 REFERENCES

1. Searles, J.A., J.F. Carpenter, and T.W. Randolph, *The ice nucleation temperature determines the primary drying rate of lyophilization for samples frozen on a temperature-controlled shelf*. Journal of Pharmaceutical Sciences, 2001. 90(7): p. 860-871.
2. Geidobler, R., S. Mannschedel, and G. Winter, *A new approach to achieve controlled ice nucleation of supercooled solutions during the freezing step in freeze-drying*. Journal of Pharmaceutical Sciences, 2012. 101(12): p. 4409-4413.
3. Hawe, A. and W. Friess, *Impact of freezing procedure and annealing on the physico-chemical properties and the formation of mannitol hydrate in mannitol-sucrose-NaCl formulations*. European journal of pharmaceutics and biopharmaceutics : official journal of Arbeitsgemeinschaft fur Pharmazeutische Verfahrenstechnik e.V, 2006. 64(3): p. 316-325.
4. Konstantinidis, A.K., et al., *Controlled nucleation in freeze-drying: Effects on pore size in the dried product layer, mass transfer resistance, and primary drying rate*. Journal of Pharmaceutical Sciences, 2011. 100(8): p. 3453-3470.
5. Weija, L., *Controlled nucleation during freezing step of freeze drying cycle using pressure differential ice fog distribution*, Patent US2012/02722544 A1. 2012.
6. Chakravarty, P., et al., *Ice Fog as a Means to Induce Uniform Ice Nucleation During Lyophilization*. BioPharm International, 2012. 25(1): p. 33-38.
7. Hottot, A., S. Vessot, and J. Andrieu, *A Direct Characterization Method of the Ice Morphology. Relationship Between Mean Crystals Size and Primary Drying Times of Freeze-Drying Processes*. Drying Technology, 2004. 22(8): p. 2009-2021.
8. Rambhatla, S., et al., *Heat and mass transfer scale-up issues during freeze drying: II. Control and characterization of the degree of supercooling*. AAPS PharmSciTech, 2004. 5(4): p. 54-62.
9. Patel, S., C. Bhugra, and M. Pikal, *Reduced Pressure Ice Fog Technique for Controlled Ice Nucleation during Freeze-Drying*. AAPS PharmSciTech, 2009. 10(4): p. 1406-1411.
10. Shire, S.J., Z. Shahrokh, and J. Liu, *Challenges in the development of high protein concentration formulations*. Journal of Pharmaceutical Sciences, 2004. 93(6): p. 1390-1402.
11. Lewis, L., et al., *Characterizing the Freeze-Drying Behavior of Model Protein Formulations*. AAPS PharmSciTech, 2010. 11(4): p. 1580-1590.
12. Schersch, K., et al., *Systematic investigation of the effect of lyophilizate collapse on pharmaceutically relevant proteins I: Stability after freeze-drying*. Journal of Pharmaceutical Sciences, 2010. 99(5): p. 2256-2278.
13. Pikal, M.J., et al., *The secondary drying stage of freeze drying: drying kinetics as a function of temperature and chamber pressure*. International Journal of Pharmaceutics, 1990. 60(3): p. 203-207.

III.8 THE MPEMBA EFFECT IS NOT APPLICABLE TO VIAL FREEZE-DRYING

III.8.1 INTRODUCTION

While making ice cream out of sugared milk in a refrigerator, Erasto Mpemba noticed that the milk, that had been boiled before in a container froze faster than when cooled from ambient temperature [1]. Later, he and Dr. Osbourne experimented with water and obtained similar results, which were published in 1969, thus establishing the term “Mpemba effect” [1]. Today, many possible explanations for this phenomenon are discussed. First, due to initial preheating, evaporation of water is increased, causing both mass loss and surface cooling [2]. Although the extent of evaporation is not sufficient for a full explanation, the exclusion of evaporation by covering the water surface led to elimination of the Mpemba effect [1]. Theoretical approaches [3], different behavior of either gaseous [4] or solid impurities [5] inside the cold and hot tap water are also discussed as possible explanations. For D. Auerbach [6] and J. Brownridge [7] however, the Mpemba effect occurred because of a lower degree of super-cooling for initially preheated water. Super-cooling in aqueous solutions describes the temperature difference between the thermodynamic freezing point and the actual ice nucleation temperature [8]. For pure water, super-cooling of 20 K is often observed [8]. Although the effect has long been known, it was never resolved completely and thus, a price of 1000 pounds was offered by the royal society of chemistry in England last year.

Controlled nucleation and the possibility to induce ice nucleation with a low degree of super-cooling has recently become a focus of investigations in the field of freeze-drying [9]. A lyophilization cycle consists of three steps: freezing, primary drying and secondary drying, whereas primary drying is the most time-consuming step [9]. Investigations have shown the importance of ice nucleation temperature during the freezing step and its influence on the primary drying time and product characteristics [10-12]. A low degree of super-cooling leads to the formation of large ice crystals. Large ice crystals decrease product resistance during primary drying and thus reduce primary drying time. Another parameter, which influences the resulting ice morphology, is the nature of freezing. One can distinguish between global super-cooling and directional solidification [8], whereas with global super-cooling, the entire volume reaches the same stadium of super-cooling, and with directional solidification, a smaller fraction is super-cooled whereas other parts have already nucleated. Nucleation and solidification then slowly proceeds through the whole solution during further cooling.

Different modifications of the freezing step can be applied in order to obtain a lower degree of super-cooling and an optimized ice morphology. The ice fog technique [10, 11, 13], the

depressurization technique [12], vacuum induced surface freezing [14], annealing [15] and different ice nucleating agents [8] are described in literature to achieve “controlled nucleation”.

In our study we want to find out whether the Mpemba effect might be considered when super-cooling and nucleation shall be controlled for freeze-drying processes to modify ice crystal structure and, finally, product properties.

III.8.2 MATERIALS AND METHODS

Throughout the study, highly purified water (Purelab Plus, ELGA LabWater, Celle, Germany) was used which was filtered on the outlet port. Water was filled in pre-rinsed 10 R glass vials Type I (MGlas AG, Muennerstadt, Germany). Type T thermocouples (SP Scientific, Stone Ridge, NY USA) were used to determine product temperature non-invasively on the outside. To ensure good contact with the vial, the thermocouples were dipped into Keratherm® Type KP97 thermal grease (KERAFOL, Eschenbach, Germany) and fixed on the vial outside about a millimeter over the bottom with a piece of adhesive tape. Filling volumes were 2.5 ml, 5.0 ml and 7.5 ml for different experiments. Each experiment was performed with three replicates.

For preheating, vials were first filled and closed with lyophilization stoppers. Then, the thermocouples were attached. Reference samples, were prepared similarly at room temperature and closed until transfer into the freeze-dryer (FTS LyoStar III, SP Scientific, Stone Ridge, NY USA). For the analysis of the evaporation mass loss, all the vials and corresponding stoppers were weighed before and after the experiment. The preheating process was controlled with a data logger thermometer (Omega Engineering, INC, Connecticut, USA). The closed vials were heated outside of the LyoStar III, completely opened by removal of the stopper and subsequently placed onto the pre-cooled freeze-dryer shelf. The non-heated reference vials were also opened and simultaneously positioned onto the pre-cooled freeze-dryer shelves. The temperature measurement was performed by the software of the LyoStar III.

The temperature difference between the initial product temperature and the shelf temperature was varied. Samples remained at ambient room temperature (20 °C) or were preheated to 45 °C, 65 °C and 85 °C. The freeze-dryer shelf was pre-cooled to -20 °C, -40 °C and -60 °C.

For certain experiments, the chamber pressure in the freeze-dryer was reduced and adjusted manually by switching the vacuum pump on and off during the cooling/freezing process. The pressure was determined with a pirani gauge.

To mimic lyophilization conditions, one of the experiments was performed with semi-stoppered vials. The experiment was carried out at ambient pressure and the vials were preheated to 85 °C. The shelf temperature was set to -20 °C and the filling volume was 7.5 ml.

III.8.3 RESULTS

III.8.3.1 IMPACT OF THE INITIAL PREHEATING AND THE SHELF TEMPERATURE

A main objective of this study was to examine whether the preheated samples freeze differently compared to the samples loaded at room temperature. Hence, the preheating temperature and the shelf-temperature were varied.

The samples with a fill volume of 7.5 ml, starting at 20 °C and placed on a -20 °C shelf, showed the same behavior throughout all experiments. Ice nucleation took place at temperatures between -11 °C and -19 °C. However, the preheated samples with same water volumes behaved differently with increasing initial temperatures. With a starting temperature of 65 °C, one sample out of three super-cooled only to -4.6 °C. With a preheating temperature of 85 °C, the ice nucleation started at approximately -5 °C for all samples. Consequently, a lower degree of super-cooling was observed with increasing preheating temperatures (Figure III-24).

Figure III-25 shows the nucleation temperatures for samples with different pre-heating temperatures and pre-cooled shelf temperature setpoints. The difference between pre-heating temperature and shelf was kept constant at 105 K. A significant increase in nucleation temperature was observed compared to samples which were not pre-heated, independent of fill volume. However, with decreasing shelf-temperature but 105 K temperature difference, the measured ice nucleation temperatures were also shifted to lower values. The temperature measurement on the outside of the vial is measuring the glass temperature. Although a good agreement between invasive and non-invasive temperature measurement was obtained for warmer shelf temperatures, a very low shelf temperature of -60 °C is quickly cooling the glass and this influences the nucleation temperature measured. However, measured ice nucleation temperatures were still significantly higher than for reference samples with a higher degree of super-cooling.

Interestingly, the effect was not observable when a lyophilization stopper was put on top of the vial at 85 °C/ -20 °C. It is therefore obvious, that evaporation from the vials must have an effect.

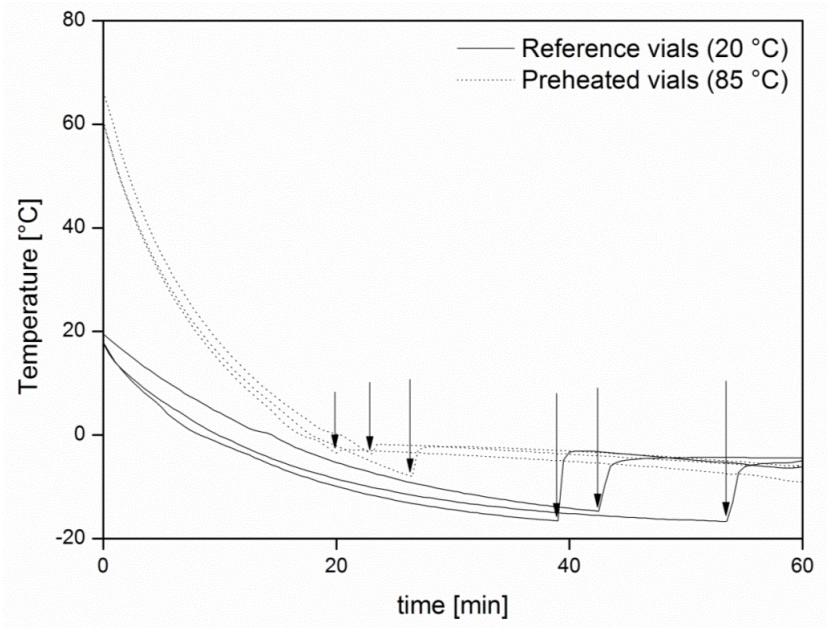


Figure III-24: With an initial preheating of 80 °C, an effect of elevated ice nucleation temperature was observed on a pre-cooled shelf of -20 °C. The arrows mark the ice nucleation event.

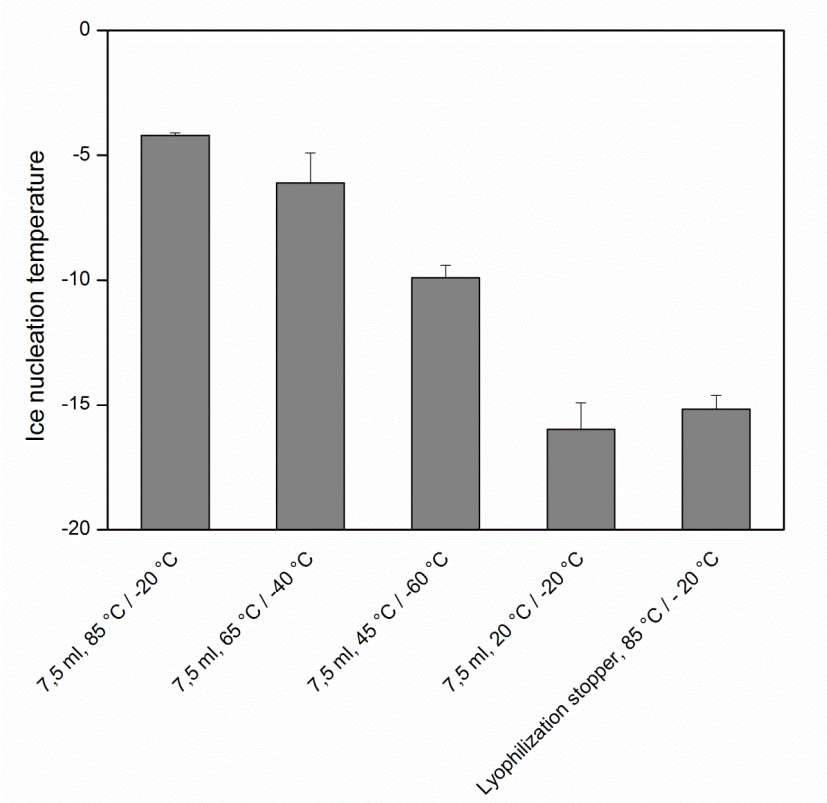


Figure III-25: The volume given indicates fill volume of the vials and the first temperature is the pre-heating temperature and the negative temperature is the pre-cooled shelf temperature. The phenomenon of a lower degree of super-cooling occurred in open samples with sufficient initial preheating or shelf cooling (three columns on the left) but was not observed after the performed covering method. Please note that ice nucleation temperatures are becoming slightly lower with lower pre-cooling of the shelves because the non-invasive temperature measurement on the outside of the vial is influenced by the lower shelf temperatures.

III.8.3.2 VISUAL OBSERVATION OF THE FREEZING PROCESS

During the processes, unexpected freezing behavior was observed. Usually, globally super-cooled liquid turns opaque as it freezes. With pre-heated samples of 105 K temperature difference between pre-heating and shelf temperature however, an ice front inside of the sample could be observed, which moved from the bottom to the upper layers. Air bubbles assembled on the water surface, thus forming ice structures shown in Figure III-26. Throughout the freezing process, the main ice structure remained translucent. The ice/water phase conversion hence is driven by directional solidification.

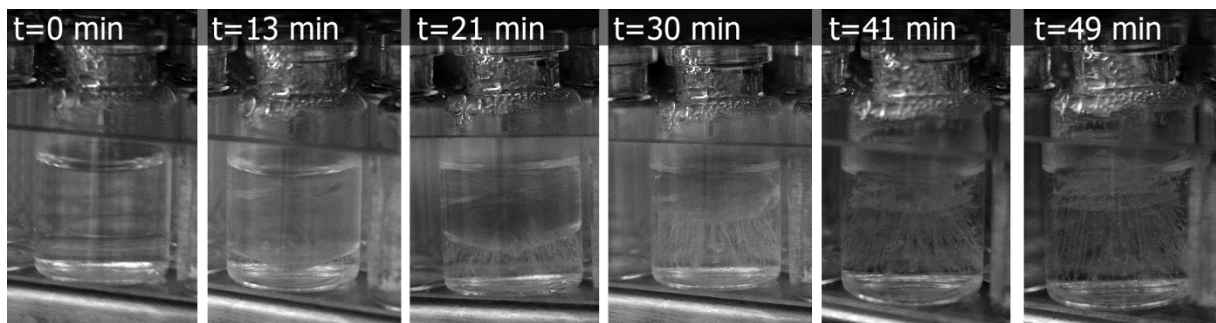


Figure III-26: Instead of the expected freezing behavior, when samples instantly appear turbid (global super-cooling), an ice front moving from the bottom up was observed (directional solidification).

III.8.3.3 REDUCED PRESSURE EXPERIMENTS

If enhanced evaporative self-cooling or the mass loss due to evaporation were the critical factors influencing the ice nucleation temperature, depressurizing the product chamber to 60 mbar should increase the probability of nucleation at elevated temperatures. The measured mass loss due to evaporation rose after depressurizing the product chamber from 0.1 % to 1.3 % of the fill volume. Surprisingly, the experiments showed no differences to atmospheric pressure conditions.

III.8.4 DISCUSSION

III.8.4.1 FREEZING AT ELEVATED TEMPERATURES

Experiments, inspired by the Mpemba effect, showed that the phenomenon of nucleation at elevated temperatures occurred in preheated vials. The temperature difference between product and shelf of approximately 105 °C constantly provoked a lower super-cooling effect, independently of the filling volume. This included the measurements for preheating/shelf temperature settings of 85 °C/-20 °C, 65 °C/-40 °C and 45 °C/-60 °C, respectively. The initial temperature value of the water therefore is less important for the lower degree of super-cooling than the temperature difference between the solution and the shelf temperature.

By reducing the chamber pressure, the influence of evaporation increases but neither the cooling rates nor the ice nucleation temperatures changed from the results at ambient air pressure experiments. The evaporative self-cooling and enhanced mass loss through plain evaporation at ambient conditions therefore seem to not to be critical for the ice nucleation at higher temperatures.

Although reduced chamber pressure did not affect the evaporation effect, restrictions of the opening for the gas phase on top of the vials by freeze-dry stoppers set to the drying position changed the situation dramatically. Semi-stoppered vials are not affected anymore and showed same super-cooling as “regular” ones.

III.8.4.2 APPLICABILITY TO LYOPHILIZATION

This study could show that the initial preheating of the samples actually results in lower degrees of super-cooling in full accordance with the Mpemba effect. As lyophilization is, among others, a stabilization technique for temperature-sensitive protein formulations [16], preheating temperatures much above 40 °C cannot be applied. However, a 105 K difference between the initial sample and shelf temperature can be achieved with 45 °C samples and -60 °C shelf and results in a lower degree of super-cooling comparable to controlled ice nucleation at rel. high temperatures. Different from the pre-cooled shelf method [8], which is already described in literature, samples were not only placed onto pre-cooled shelves but also preheated. The standard deviations for nucleation temperatures we found were relatively low compared to the temperature distribution described in literature [8].

The ice structure was not explicitly analyzed, but the solidification process was observed visually. Ice nucleation and solidification started from the bottom and the nucleation front moved slowly up to the water surface. The ice remained translucent throughout the freezing process. It is concluded that ice nucleation and freezing proceeds by directional solidification [8]. The relevance of this observation for product characteristics is subject to future investigations.

In order to preserve the purity and sterility of the formulations, the vials are usually put into the freeze-dryer, covered with stoppers in the drying position with an opening for removal of water vapor. However, by placement of a lyophilization stopper, the effect of increased nucleation temperatures was eliminated.

Consequently, the application of the Mpemba effect for controlled nucleation of state of the art freeze-drying processes for sterile dosage forms in vials or cartridges is not possible. But bulk freeze-drying processes on shelf trays or e.g. in Goretex Lyo Guard® and similar containers

might very well take advantage of the concept. The “Mpemba process” could be considered as an improvement on the pre-cooled shelf method.

III.8.5 REFERENCES

1. Mpemba, E.B. and D.G. Osborne, *Cool?* Physics Education, 1969. 4(3): p. 172.
2. Jeng, M., *The Mpemba effect: When can hot water freeze faster than cold?* American Journal of Physics, 2006. 74(6): p. 514-522.
3. Vynnycky, M. and N. Maeno, *Axisymmetric natural convection-driven evaporation of hot water and the Mpemba effect.* International Journal of Heat and Mass Transfer, 2012. 55(23–24): p. 7297-7311.
4. Wojciechowski, B., I. Owczarek, and G. Bednarz, *Freezing of aqueous solutions containing gases.* Crystal Research and Technology, 1988. 23(7): p. 843-848.
5. Katz, J.I., *When hot water freezes before cold.* American Journal of Physics, 2009. 77(1): p. 27-29.
6. Auerbach, D., *Supercooling and the Mpemba effect: When hot water freezes quicker than cold.* American Journal of Physics, 1995. 63(10): p. 882-885.
7. Brownridge, J.D., *When does hot water freeze faster than cold water? A search for the Mpemba effect.* American Journal of Physics, 2011. 79(1): p. 78-84.
8. Searles, J.A., J.F. Carpenter, and T.W. Randolph, *The ice nucleation temperature determines the primary drying rate of lyophilization for samples frozen on a temperature-controlled shelf.* Journal of Pharmaceutical Sciences, 2001. 90(7): p. 860-871.
9. Kasper, J.C. and W. Friess, *The freezing step in lyophilization: Physico-chemical fundamentals, freezing methods and consequences on process performance and quality attributes of biopharmaceuticals.* European Journal of Pharmaceutics and Biopharmaceutics, 2011. 78(2): p. 248-263.
10. Rambhatla, S., et al., *Heat and mass transfer scale-up issues during freeze drying: II. Control and characterization of the degree of supercooling.* AAPS PharmSciTech, 2004. 5(4): p. 54-62.
11. Patel, S., C. Bhugra, and M. Pikal, *Reduced Pressure Ice Fog Technique for Controlled Ice Nucleation during Freeze-Drying.* AAPS PharmSciTech, 2009. 10(4): p. 1406-1411.
12. Konstantinidis, A.K., et al., *Controlled nucleation in freeze-drying: Effects on pore size in the dried product layer, mass transfer resistance, and primary drying rate.* Journal of Pharmaceutical Sciences, 2011. 100(8): p. 3453-3470.
13. Geidobler, R., S. Mannschedel, and G. Winter, *A new approach to achieve controlled ice nucleation of supercooled solutions during the freezing step in freeze-drying.* Journal of Pharmaceutical Sciences, 2012. 101(12): p. 4409-4413.
14. Kramer, M., B. Sennhenn, and G. Lee, *Freeze-drying using vacuum-induced surface freezing.* Journal of Pharmaceutical Sciences, 2002. 91(2): p. 433-443.
15. Searles, J.A., J.F. Carpenter, and T.W. Randolph, *Annealing to optimize the primary drying rate, reduce freezing-induced drying rate heterogeneity, and determine Tg' in pharmaceutical lyophilization.* Journal of Pharmaceutical Sciences, 2001. 90(7): p. 872-887.
16. Wang, W., *Lyophilization and development of solid protein pharmaceuticals.* International Journal of Pharmaceutics, 2000. 203(1-2): p. 1-60.

III.9 SUMMARY OF CHAPTER III

Controlled nucleation in freeze-drying is a new technology which has a high potential to improve freeze-drying processes with regard to economic benefits. The methods available require hardware modifications and/or retrofits and some of them are quite expensive. We developed a method that works in lab-scale and we could transfer this method also to a pilot-scale freeze-drier. This allows everyone to study effects on controlled ice nucleation already in lab-scale. However, benefits of controlled ice nucleation besides more economic processes have not yet been shown, although this benefit is already quite important thinking on other ideas scientists had to improve primary drying. In addition, we found that not only nucleation temperature influenced final product quality attributes but also the post nucleation hold time, as shown for two placebo model formulations. Further, a longer post-nucleation hold time was also beneficial for subvisible particle formation of the model antibody MabR1 in freeze-thawing experiments. In this chapter, a first answer to the question “do we obtain a better product” was given. For highly-concentrated protein formulations, we obtained faster reconstitution times for the dried product compared to a conventional drying process. These formulations also profited from controlled nucleation regarding drying kinetics.

IV. FINAL SUMMARY

The present thesis is divided into two parts. The first part, as described in chapter II, is about the potential use of cyclodextrins in drying of proteins and the second part (chapter III) evaluates controlled ice nucleation in freeze-drying.

I. The objective of the first part was to assess the potential use of cyclodextrins in freeze-drying and its ability to provide an alternative to polysorbates. In section II.1, the literature on cyclodextrins in protein drying was reviewed as well as the potential protein stabilization mechanisms of cyclodextrins. The most important derivative of β -cyclodextrin is Hydroxypropyl-beta-cyclodextrin, which is a surface active molecule and has shown its ability to stabilize proteins in liquid protein formulations. In addition, HP β CD is approved by authorities and is considered safe from a toxicological perspective. Hence, this thesis clearly focused on HP β CD as excipient in freeze-drying. The freeze-drying process, although considered as gentle and activity-retaining, poses several stresses to proteins. To study protein degradation during the freeze-drying process, a model protein, MabR1 was used in the first screening study in section II.3.1. To further create challenging conditions, the amount of sucrose added was kept low and a mass ratio of sucrose to protein of 1:1 was chosen. It was found that MabR1 is sensitive to the formation of an ice-water interface as well as dehydration and the air-liquid interface present during reconstitution, rendering the model protein a good candidate to study excipient effects in the freeze-drying process. However, the gold standard to protect proteins at interfaces, surfactants of the polysorbate group combined with sucrose, showed better results and could more effectively suppress formation of subvisible particles than HP β CD, when employed as single excipient or in combination with sucrose. This was confirmed by using different concentrations of HP β CD and two different lots of the model antibody MabR1 in section II.3.2 for conventional freeze-drying. However, it was shown that HP β CD is a very effective stabilizer in freeze-thaw studies even at very low concentrations of 1 mg/ml and the addition of HP β CD decreased subvisible particles compared to a formulation with sucrose only (no surfactant). With conventional freeze-drying, at least in our studies, we could observe stabilizing effects of HP β CD, but our goal, to provide an alternative to polysorbates, could not be reached. It could be shown that, especially during reconstitution of the freeze-dried cakes polysorbate was superior to HP β CD.

Freeze-dried products can differ in their characteristics depending on the freeze-drying process. With the data in mind from the first studies, collapse freeze-drying was performed to intentionally decrease the specific surface area (SSA) of the dried product. Although

considered to be inelegant, it has been shown that collapse freeze-drying does not necessarily harm protein activity but can even improve stability of the dried product. In our case, the reduction of specific surface area at which proteins can possibly degrade and form aggregates during rehydration, lead to acceptable and comparable protein stability with HP β CD and polysorbate, as was shown in section II.3.3.

Furthermore, by creating lyophilizates with intermediate specific surface area by employing the new technology of controlled ice nucleation at low super-cooling of the aqueous liquid in section II.3.4, a SSA between conventional freeze-drying and collapse freeze-drying could be obtained and also the number of subvisible particles formed for the formulation containing the model antibody and HP β CD were intermediate. Hence, a correlation between specific surface area and particulate matter could be established. This correlation was also true for the negative control of MabR1 when freeze-dried without surfactant. However, when both formulations of MabR1 formulated with sucrose + HP β CD or sucrose + polysorbate 80 were subjected to storage stability in section II.3.5, both formulations showed temperature-dependent degradation with formation of soluble and insoluble aggregates. Thus, sucrose concentration was increased to a mass ratio of 5:1 sucrose:protein. In preliminary experiments, this formulation was freeze-dried with controlled nucleation (section II.3.6) and with a collapse freeze-drying process (section II.3.7). Collapse of the freeze-dried cake reduced SSA to a minimum and showed lowest subvisible particle numbers for the formulations of sucrose with HP β CD or PS80, as already observed in the study with 1 % sucrose, while MabR1 stability was preserved. Controlled ice nucleation again showed higher subvisible particle concentrations and SSAs than collapse freeze-drying.

A storage stability study of MabR1 was performed with the formulations based on 5 % sucrose in section II.3.8 and excellent storage stability of MabR1 was observed at 40 °C as well as 25 °C and 2-8 °C for approximately 150 days.

The formulation and process concept was then transferred to two other, structurally different model proteins which are sensitive to interfacial degradation, GCSF and hGH. Both proteins are also stable in liquid formulations and do not necessarily need to be dried; however, they are very suitable model proteins to study excipient effects on process stability. For hGH, collapse freeze-drying with HP β CD and polysorbate lead to acceptable formulations with an advantage for HP β CD with respect to subvisible particles and dimer formation, as shown in section II.3.10. In addition, storage stable lyophilizates of hGH were obtained for 3 months at 2-8, 25 and 40 °C. Polysorbate 80 was superior to HP β CD for the model protein GCSF as detected with subvisible particle formation and monomer content, however, with both formulations, visible particles appeared in the subsequent storage stability study of GCSF, as

described in section II.3.11. The appearance of visible particles points into the direction of a general instability of GCSF in the dried state, thus, the storage stability study was cancelled.

With the positive effects of a low SSA observed in the collapse freeze-drying studies in mind, we performed a control experiment with higher SSAs and spray-dried MabR1. While the stability immediately after spray-drying was better for polysorbate than for HP β CD, the dimer content of MabR1 was increased immediately after drying and further increased during storage of the spray-dried powder. These results suggest that the antibody was damaged and oxidation may have occurred during the spray-drying process and the following storage study.

While most of the work focused on the ability of HP β CD to protect proteins at interfaces, another possibility of the cyclodextrin derivative is the ability to act as bulking agent in a carbohydrate-like manner. Due to its high glass transition temperatures, very economic, fast processes can be designed. However, we could not show an advantage in storage stability of MabR1 when using HP β CD compared to sucrose, as presented in section II.3.13.

By using electron spectroscopy for chemical analysis (ESCA), we could gain insight into the situation at the interface of the freeze-dried products (see section II.3.9). It could be shown that for conventional freeze-drying a co-existence of the model antibody with HP β CD at the interface is supposedly the case and HP β CD is exerting a different stabilization mechanism on proteins compared to classical surfactants, which displace proteins from the interface. This finding was in good agreement with studies conducted at the liquid-air interface by other members of our research group.

Another side aspect of the thesis was the surprising finding that HP β CD is forming subvisible placebo particles in the lower one-digit micrometer range when freeze-dried and rehydrated. The amount of particles formed was dependent on SSA and residual moisture and could also be reduced by employing controlled nucleation or collapse freeze-drying with the latter completely eliminating the formation of placebo particles. For the protein formulations, it remains unclear if, and to which extent, placebo particles contribute to total particle amounts.

Finally, the goal of providing an alternative for polysorbates could be achieved for certain formulations; if the specific surface area is kept low, cyclodextrins may be a valuable alternative to the degradation-prone polysorbates.

II. The second part of the thesis was focused on a new technology in freeze-drying, which is called controlled ice nucleation. Besides the parameters time, temperature and pressure, a new option to tune the freeze-drying process is possible with this technology: control of super-cooling and the ice nucleation temperature as well as the post-nucleation thermal treatment. With commercial methods for all scales emerging for industrial freeze-drying, there is also a

need for a laboratory method to study effects of controlled ice nucleation on products in early development. In section III.2, we gave a general introduction into the topic of controlled ice nucleation and presented available methods as well as other modifications of the freezing step. In section III.3, we developed a method to induce ice nucleation in laboratory-scale freeze-driers. So far, it is the only method without the need for hardware modifications and can be used in any freeze-dryer with external condenser. Water vapour is generated from the product vials in a controlled way by depressurization of the freeze-drier and is frozen on the cold condenser coils. Upon re-pressurization of the condenser compartment, the ice crystals are blown into the super-cooled solutions and induce ice nucleation. In lab-scale, success rates were larger than 99 %, and we were curious if this method can also work in larger freeze-driers. Thus, in section III.4, we tested the method in a pilot-scale freeze-drier with 2.5 m² shelf area. Similar to the lab-scale equipment, we obtained a success rate of more than 99 %. We conclude that, if all components of a freeze-drier are scaled, the method is potentially also applicable to production-scale freeze-driers.

In the following section III.5, the impact of nucleation temperature and post-nucleation hold time is evaluated for the model protein MabR1 in freeze-thaw studies. These investigations were performed to support the controlled ice nucleation sections in chapter II. It was found, that besides the ice nucleation temperature, also the post-nucleation hold time, which influences the velocity of ice crystallization had an impact on protein stability observed after freeze-thawing.

The impact of the ice nucleation temperature as well as the post-nucleation hold time was further elucidated for two placebo model formulations in section III.6, confirming the importance of both variables for the final product quality attributes, e.g. the residual moisture and the specific surface area.

In section III.7, we could show that controlled ice nucleation not only improves primary drying duration but can also improve reconstitution times of highly-concentration freeze-dried formulations by increasing wetting of the freeze-dried cake. If wetting of the solid is the velocity-determining step, controlled ice nucleation can greatly improve rehydration and hence product quality of these pharmaceuticals.

The Mpemba effect, an interesting observation that warm water freezes faster than cold, was investigated in section III.8 using freeze-drying equipment. Interestingly, it was found that pre-heating of water influenced super-cooling of the liquid and, compared to cold water, nucleation and freezing occurred faster. The Mpemba effect was under investigation for several years and many possible explanations for this effect were proposed. Our observation with super-

cooling differences of hot and cold water is in agreement with a study of the winner of the 2012's science competition advertised by the Royal Chemistry Society in London.

V. APPENDIX

V.1 PUBLICATIONS

Serno, T., R. Geidobler, and G. Winter, Protein stabilization by cyclodextrins in the liquid and dried state. *Advanced Drug Delivery Reviews*, 2011. 63(13): p. 1086-1106.

Geidobler, R., S. Mannschedel, and G. Winter, A new approach to achieve controlled ice nucleation of supercooled solutions during the freezing step in freeze-drying. *Journal of Pharmaceutical Sciences*, 2012. 101(12): p. 4409-4413.

Geidobler, R. and G. Winter, Controlled ice nucleation in the field of freeze-drying: Fundamentals and technology review. *European Journal of Pharmaceutics and Biopharmaceutics*, 85, (2), p. 214–222

Geidobler, R., I. Konrad, and G. Winter, Can Controlled Ice Nucleation Improve Freeze-Drying of Highly-Concentrated Protein Formulations? *Journal of Pharmaceutical Sciences*, 2013, 102, (11): p. 3915–3919

HP β CD as an alternative to polysorbate in drying of proteins. Geidobler R, Winter G, manuscript in preparation

The Mpebma Effect is not applicable to vial freeze-drying. Geidobler R, Ilyukhina E, Hirschmann A, Winter G, ready for submission.

V.2 POSTER PRESENTATIONS

R. Geidobler, E. Härtl, T. Serno, A. Besheer, G. Winter: Cyclodextrins as stabilizing excipients in protein formulation, *Forum Life Science*, Munich, Germany (March 2011)

Geidobler R, Winter G: Subvisible particle formation by freeze-dried Hydroxypropyl- β -cyclodextrin, 8th World meeting on Pharmaceutics, Biopharmaceutics and Pharmaceutical Technology Istanbul, Turkey, March 2012

Geidobler R, Winter G, Stabilization of a monoclonal antibody by freeze-drying in the presence of cyclodextrins, 8th World meeting on Pharmaceutics, Biopharmaceutics and Pharmaceutical Technology Istanbul, Turkey, March 2012

Geidobler R, Mannschedel S, Winter G, How to simply achieve controlled ice nucleation during the freezing step in freeze-drying, *CPPR Freeze-Drying of Pharmaceuticals & Biologicals*, Breckenridge, August 2012

V.3 ORAL PRESENTATIONS

Geidobler R: Controlled nucleation in pharmaceutical freeze-drying: Fundamentals and Methods; Lyophilization for Biologicals 2013, München

Geidobler R: Controlled ice nucleation method applied at the LMU - Application and experience with biopharmaceutical formulations; Lyosummit 2013, Rottach-Egern